

The Roles of Conserved Dbf4 Motifs in DNA Replication and  
Checkpoint Responses in *Saccharomyces cerevisiae*

by

Ajai Anand Prasad

A thesis  
presented to the University of Waterloo  
in fulfillment of the  
thesis requirement for the degree of

Doctor of Philosophy

in

Biology

Waterloo, Ontario, Canada, 2009  
© Ajai Anand Prasad 2009

## **AUTHOR'S DECLARATION**

I, hereby, declare that I am the sole author of this thesis. This is a true copy of the thesis, including any required final revisions, as accepted by my examiners.

I understand that my thesis may be made electronically available to the public.

## **Abstract**

The Dbf4 protein is involved in the initiation of DNA replication, in complex with Cdc7 kinase, and also plays a role in the intra-S-phase checkpoint response via an interaction with Rad53 in *Saccharomyces cerevisiae*. The Dbf4 protein has three highly conserved motifs, called the N, M and C motifs. In view of the fact that a comprehensive analysis of the roles of the three motifs in the initiation of DNA replication and checkpoint response was not previously available, this study was, therefore, conducted. The objectives of the study were: (1) to assess the function of the three conserved motifs, with respect to their essentiality for cell viability, (2) to determine their roles in mediating interactions with other proteins (i.e. Cdc7, Orc2, Mcm2) involved in the initiation of DNA replication and with Rad53 in the intra-S-phase checkpoint response, and (3) to obtain the three-dimensional structure of the Dbf4 N-motif by X-ray crystallography.

The Dbf4 N-motif was found to be nonessential for cell viability, mediates the interaction between Dbf4 and Rad53, and as well as the interaction with Orc2. A mutant lacking the N-motif (*dbf4ΔN*), was found to have a growth defect and was hypersensitive to the genotoxic agents: hydroxyurea (HU) and methyl methane sulfonate (MMS), suggesting that a disruption in the intra-S-phase checkpoint occurred because of an abrogated Dbf4-Rad53 interaction. Double point mutation of two threonine residues of the N-motif (threonines 171 and 175) to alanines also caused an abrogated Dbf4-Rad53 FHA1 domain interaction.

The Dbf4 M-motif was found to be essential for cell viability and mediates the interaction between Dbf4 and Mcm2. A single proline to leucine point mutation at amino acid residue 277 conferred resistance to HU and MMS and caused disrupted Dbf4-Mcm2

and Dbf4-Orc2 interaction, while Dbf4-Rad53 interaction was maintained. Thus, the alteration of the M-motif may facilitate the role of Dbf4 as a checkpoint target.

The Dbf4-C motif was also found to be essential for cell viability. Deletion and point mutations to the C-motif affected the interactions between Dbf4 and Rad53, Orc2, Mcm2 and also with Mcm4.

Attempts were also made to obtain the three-dimensional structure of Dbf4, using X-ray crystallography methods.

The work presented here represents a thorough functional analysis of the three conserved domains of Dbf4 in *Saccharomyces cerevisiae*. These results can be used as a baseline for further research involving higher eukaryotic organisms, including humans. This is particularly of relevance in light of recent evidence demonstrating an overexpression of the human Dbf4 orthologue overexpression as a cancer phenotype in human cancer cells.

## Acknowledgements

Firstly, I would like to express my sincere gratitude and appreciation to Dr. B. Duncker for his support in this work, for his advice in preparing the manuscript, and for giving me the opportunity to pursue graduate research in his laboratory. I always thought of this opportunity as a privilege that I valued a lot. I appreciate his guidance, help and supervision throughout the project. He has been very generous with his knowledge and experience. I would also like to thank Dr. R.P. Bird and Dr. B. Dixon for serving as my committee members and for their encouragement and helpful suggestions over the years.

I am also very grateful to Dr. A. Guarné for her enthusiasm, generous spirit and genuine interest in the Dbf4 crystallography collaboration. It was a real pleasure being involved in this collaboration. There were several contributors to this collaborative project: Lindsay Matthews, Melanie Gloyd, Monica Pillon and Andrew Duong. I thank them all for their cooperation during the summer I spent at McMaster and also during my visits over the years. Always helpful and attentive, no matter how busy they were.

Of course, I must acknowledge my two apprentices: Darryl Jones and Phil Chan. Their contribution to the Dbf4 project is much appreciated. I enjoyed meeting and working with them both. I learned a lot from them, and, hopefully, I was able to share some useful knowledge and wisdom with them.

It is with great nostalgia that I acknowledge my other lab mates: Rohan Gidvani, Shanna Cutting, Matt Ramer, Michelle Liu and Dong Ryoung Kim. It was a very pleasant atmosphere in the latter years of my PhD studies and that is because of the humour and genuine friendliness that they all brought to the lab with them every morning. Yes, I enjoyed “the comraderie” too. Coping with the stresses and challenges of graduate

research is definitely easier in the presence of good company. I enjoyed their company very much. I should also mention Lance Da-Silva, whose technical experience and organization was a very important in early days of the lab.

I would also like to express my appreciation to my wife, Amita, for her patience, support and resilience during this challenging time. This accomplishment would not have been possible without her backing and sustenance. I would also like to express my sincere gratitude to my parents for a lifetime of unconditional support and encouragement. Their value for education and knowledge has fueled my desire to learn. They have been the invisible champions of this degree and all of my previous education. My father was especially helpful, using his vast experience, in assisting me with the editing process of this manuscript preparation.

I have come to realize, over the years, that it takes an army of people to produce one Ph.D. It is not just the work of one individual. Those people that I mentioned above and some that I did not mention have all contributed to this accomplishment.

## Table of Contents

<b>Author's Declaration.....</b>	<b>ii</b>
<b>Abstract.....</b>	<b>iii</b>
<b>Acknowledgements.....</b>	<b>v</b>
<b>Table of Contents.....</b>	<b>vii</b>
<b>List of Tables.....</b>	<b>xi</b>
<b>List of Figures.....</b>	<b>xii</b>
<b>List of Abbreviations and Acronyms.....</b>	<b>xvi</b>
<b>CHAPTER 1: Literature Review and Research Objectives.....</b>	<b>1</b>
<b>1.0. Literature Review.....</b>	<b>2</b>
<b>1.1. The Yeasts.....</b>	<b>2</b>
<b>1.2. Genetics and Life Cycle.....</b>	<b>6</b>
<b>1.3 .<i>Saccharomyces cerevisiae</i> As A Model Organism.....</b>	<b>10</b>
<b>1.4. The Cell Cycle and The Initiation of DNA Replication.....</b>	<b>14</b>
<b>1.5. Cell Cycle Phases.....</b>	<b>16</b>
<b>1.5.1 <i>G1 Phase (Gap 1 Phase)</i>.....</b>	<b>16</b>
<b>1.5.2. <i>S-Phase</i>.....</b>	<b>20</b>
<b>1.5.3. <i>G2 Phase (Gap 2 Phase)</i>.....</b>	<b>24</b>
<b>1.5.4. <i>M-Phase</i>.....</b>	<b>24</b>
<b>1.6. Cell Cycle Checkpoint Responses.....</b>	<b>26</b>
<b>1.6.1. <i>DNA Damage</i>.....</b>	<b>26</b>
<b>1.6.2. <i>The Intra-S-Phase Checkpoint Response</i>.....</b>	<b>28</b>
<b>1.7. Cdc7/Dbf4 Complex.....</b>	<b>33</b>

<b>1.8. Dbf4 N, M and C-motifs.....</b>	<b>34</b>
<b>1.9. Rad 53.....</b>	<b>41</b>
<b>1.10. Dbf4/Rad 53 and the Intra-S-Phase Checkpoint Response.....</b>	<b>46</b>
<b>1.11. Research Objectives.....</b>	<b>49</b>
<b>1.12 Relevance to Biomedical Sciences and Cancer.....</b>	<b>51</b>
<b>CHAPTER 2: Materials and Methods.....</b>	<b>53</b>
<b>2.1. Cloning.....</b>	<b>54</b>
<b>2.2. Quickchange Mutagenesis.....</b>	<b>61</b>
<b>2.3. Bacterial Transformation.....</b>	<b>62</b>
<b>2.4. Yeast Transformation .....</b>	<b>62</b>
<b>2.5. Genomic DNA Isolation.....</b>	<b>63</b>
<b>2.6. Protein Analysis.....</b>	<b>64</b>
<b>2.6.1. Preparation of Whole Cell Extracts.....</b>	<b>64</b>
<b>2.6.2. Western Blotting.....</b>	<b>65</b>
<b>2.6.3. Protein Solubility Assay.....</b>	<b>66</b>
<b>2.7. Genomic Integration .....</b>	<b>69</b>
<b>2.8. Yeast Strain Sporulation and Tetrad Dissection.....</b>	<b>72</b>
<b>2.9. Plasmid Shuffle Assay and Creation of a Plasmid Shuffle Strain.....</b>	<b>73</b>
<b>2.9.1. Creation of Plasmid Shuffle Strain.....</b>	<b>74</b>
<b>2.9.2. Plasmid Shuffle Assay.....</b>	<b>75</b>
<b>2.10. Two-Hybrid Assay .....</b>	<b>76</b>
<b>2.11. One-Hybrid Assay.....</b>	<b>79</b>
<b>2.12. Co-immunoprecipitation.....</b>	<b>79</b>

<b>2.13. Growth Spotting Assay.....</b>	<b>80</b>
<b>2.14. Complementation Assay.....</b>	<b>81</b>
<b>2.15. Short-Term Viability Assay.....</b>	<b>82</b>
<b>Chapter 3: A Mutation in Dbf4 M-Motif Impairs Interactions with DNA Replication Factors and Confers Increased Resistance to Genotoxic Agents. ....</b>	<b>92</b>
<b>3.1. Introduction.....</b>	<b>93</b>
<b>3.2. Results.....</b>	<b>96</b>
<b>3.3. Discussion.....</b>	<b>117</b>
<i>3.3.1. The M and N motifs of Dbf4 mediate specific interactions with replication and checkpoint factors.....</i>	<b>117</b>
<i>3.3.2. A single amino acid change within Dbf4 motif M confers resistance to genotoxic agents.....</i>	<b>120</b>
<i>3.3.3. Conservation of eukaryotic DDK function.....</i>	<b>122</b>
<b>CHAPTER 4:Mutagenesis of Dbf4 N-motif and the effect of Dbf4 N-motif mutations on Dbf4-Rad53 interactions.....</b>	<b>123</b>
<b>4.1. Introduction.....</b>	<b>124</b>
<b>4.2. Results.....</b>	<b>126</b>
<b>4.3. Discussion.....</b>	<b>150</b>
<i>4.3.1. Removal of Dbf4 N-motif causes a growth defect.....</i>	<b>150</b>
<i>4.3.2.The Rad53 binding site of Dbf4 lies within amino acids 168-178 of the N-motif.....</i>	<b>151</b>
<b>CHAPTER 5: Characterization of the Dbf4 C-motif.....</b>	<b>155</b>
<b>5.1. Introduction.....</b>	<b>156</b>
<b>5.2. Results.....</b>	<b>160</b>
<b>5.3. Discussion.....</b>	<b>196</b>

<b>5.3.1. Deletion of the Dbf4 C-motif results in a loss of cell viability.....</b>	<b>196</b>
<b>5.3.2. Point mutations to the Dbf4 C-motif Zinc-finger confer resistance to genotoxic agents.....</b>	<b>203</b>
<b>CHAPTER 6: X-Ray Crystallography of the Dbf4 N-motif.....</b>	<b>212</b>
<b>6.1. Introduction.....</b>	<b>213</b>
<b>6.2. Results.....</b>	<b>220</b>
<b>6.3. Discussion.....</b>	<b>233</b>
<b>CHAPTER 7: General Discussion and Conclusions.....</b>	<b>235</b>
<b>7.1. Dbf4 Motifs (N, M, and C).....</b>	<b>236</b>
<b>7.2. Essentiality of Motifs N, M and C .....</b>	<b>236</b>
<b>    7.2.1. <i>Dbf4 N-motif</i>.....</b>	<b>236</b>
<b>    7.2.2. <i>Dbf4 M-motif</i>.....</b>	<b>238</b>
<b>    7.2.3. <i>Dbf4 C-motif</i>.....</b>	<b>238</b>
<b>7.3. <i>Saccharomyces cerevisiae</i> Does Not Have a Dbf4-Related Protein.....</b>	<b>240</b>
<b>7.4. The Role of Dbf4 in the Intra-S-Phase Checkpoint Response.....</b>	<b>241</b>
<b>7.5. Resistance To Genotoxic Agents.....</b>	<b>245</b>
<b>7.6. Relevance to Cancer.....</b>	<b>247</b>
<b>7.7. Future Directions.....</b>	<b>251</b>
<b>7.8. Summary.....</b>	<b>254</b>
<b>APPENDIX.....</b>	<b>256</b>
<b>REFERENCES.....</b>	<b>271</b>

## List of Tables

<b>Table 2.1. List of Plasmids.....</b>	<b>84</b>
<b>Table 2.2. List of Primers.....</b>	<b>87</b>
<b>Table 2.3. List of Strains.....</b>	<b>90</b>
<b>Table 2.4. A List of Antibodies and the Concentrations used.....</b>	<b>91</b>

## List of Figures

### CHAPTER 1

<b>Figure 1.1. Diagram of <i>Saccharomyces cerevisiae</i>, including its organelles.....</b>	<b>5</b>
<b>Figure 1.2. Transition in the life cycle of <i>S.cerevisiae</i>.....</b>	<b>7</b>
<b>Figure 1.3. The life cycle of heterothallic and homothallic strains of <i>Saccharomyces cerevisiae</i>.....</b>	<b>9</b>
<b>Figure 1.4. <i>Saccharomyces cerevisiae</i> cell cycle phases.....</b>	<b>15</b>
<b>Figure 1.5. Assembly of the Pre-Replicative Complex at an origin of DNA replication.....</b>	<b>19</b>
<b>Figure 1.6. Eukaryotic DNA replication fork.....</b>	<b>23</b>
<b>Figure 1.7. Rad17-Ddc1-Mec3 pathway of the intra-S-phase checkpoint response..</b>	<b>30</b>
<b>Figure 1.8. S-phase checkpoint response.....</b>	<b>31</b>
<b>Figure 1.9. Conserved motifs of Dfp1/Dbf4.....</b>	<b>40</b>
<b>Figure 1.10. Rad 53 protein kinase.....</b>	<b>45</b>
<b>Figure 1.11. A model in which Cdc7/Dbf4 is an important target of Rad53 regulation during the checkpoint response to HU.....</b>	<b>48</b>

### CHAPTER 3

<b>Figure. 3.1. Dbf4 mutants.....</b>	<b>97</b>
<b>Figure 3.2. Two hybrid analysis of Dbf4 variant interactions with replication and checkpoint factors.....</b>	<b>101</b>
<b>Figure 3.3. Dbf4 M-motif is required for interaction with Mcm2 and for normal cell growth, while N-motif mediates association with Rad53 and confers resistance to both HU and MMS.....</b>	<b>106</b>
<b>Figure 3.4. Dbf4ts-FL has weakened interactions with both Orc2 and Mcm2.....</b>	<b>110</b>
<b>Figure 3.5. Dbf4ts-FL confers resistance to both MMS and HU.....</b>	<b>114</b>

<b>Figure 3.6. Cells expressing Dbf4ts-FL are resistant to short-term exposure to either MMS or HU.....</b>	<b>116</b>
-------------------------------------------------------------------------------------------------------------	------------

## CHAPTER 4

<b>Figure 4.1. Growth rate of the <i>dbf4ΔN</i> mutant (DY-78) relative to an isogenic wild type (DY-77) strain. ....</b>	<b>129</b>
---------------------------------------------------------------------------------------------------------------------------	------------

<b>Figure 4.2. Schematic diagram of Dbf4.....</b>	<b>131</b>
---------------------------------------------------	------------

<b>Figure 4.3. The Dbf4Δ168-178 mutation abrogates interaction with Rad53.....</b>	<b>133</b>
------------------------------------------------------------------------------------	------------

<b>Figure 4.4. Schematic flow diagram of attempted construction of a <i>dbf4Δ168-178</i> mutant strain.....</b>	<b>139</b>
-----------------------------------------------------------------------------------------------------------------	------------

<b>Figure 4.5. Genomic integration of Dbf4Δ168-178 mutation.....</b>	<b>142</b>
----------------------------------------------------------------------	------------

<b>Figure 4.6. Two-hybrid analysis of Dbf4 N-motif point mutant and Rad53 FHA1 domain interactions.....</b>	<b>146</b>
-------------------------------------------------------------------------------------------------------------	------------

<b>Figure 4.7. Growth spotting assay of N-motif point mutant plasmid shuffle strains.....</b>	<b>149</b>
-----------------------------------------------------------------------------------------------	------------

## CHAPTER 5

<b>Figure 5.1. Analysis of Dbf4ΔN, Dbf4ΔM and Dbf4ΔC in a one-hybrid assay.....</b>	<b>166</b>
-------------------------------------------------------------------------------------	------------

<b>Figure 5.2. Dbf4 C-motif deletion mutants are not able to complement a Dbf4 temperature sensitive mutant strain at the non-permissive temperature of 37°C.....</b>	<b>168</b>
-----------------------------------------------------------------------------------------------------------------------------------------------------------------------	------------

<b>Figure 5.3. Schematic representation of Dbf4 and its highly conserved motifs (motif N, M and C).....</b>	<b>169</b>
-------------------------------------------------------------------------------------------------------------	------------

<b>Figure 5.4. The Dbf4 C-motif point mutants are able to complement the Dbf4 temperature sensitive strain at the non-permissive temperature of 37°C.....</b>	<b>171</b>
---------------------------------------------------------------------------------------------------------------------------------------------------------------	------------

<b>Figure 5.5. The Dbf4 C-motif point mutants have an increased interaction with Rad53 relative to wild type (Dbf4), in the two-hybrid assay.....</b>	<b>176</b>
-------------------------------------------------------------------------------------------------------------------------------------------------------	------------

<b>Figure 5.6. The Dbf4 C-motif point mutants have decreased interactions with Mcm2 relative to the wild type Dbf4-Mcm2 interaction in the two-hybrid assay..</b>	<b>178</b>
-------------------------------------------------------------------------------------------------------------------------------------------------------------------	------------

<b>Figure 5.7. The Dbf4 C-motif point mutants have an increased interaction with Orc2 relative to wild type (Dbf4), in the two-hybrid assay.....</b>	<b>180</b>
<b>Figure 5.8. The Dbf4 C-motif point mutants have interactions with Cdc7 that are similar to that with wild type (Dbf4) in the two-hybrid assay.....</b>	<b>182</b>
<b>Figure 5.9. The Dbf4 C-motif point mutants have an increased interactions with Mcm4 in the two-hybrid assay relative to the wild type Dbf4-Mcm4 Interaction.....</b>	<b>184</b>
<b>Figure 5.10. The Dbf4 C-motif point mutants have a decreased interaction with ARS1 in the one-hybrid assay relative to the wild type interaction.....</b>	<b>186</b>
<b>Figure 5.11. Growth spotting assay testing <i>rad53-11</i> Dbf4 C-motif point mutants for sensitivity/resistance to genotoxic agents.....</b>	<b>189</b>
<b>Figure 5.12. Bleomycin short-term survival assay.....</b>	<b>190</b>
<b>Figure 5.13. The Dbf4 C-motif point mutants have an increased interaction with the <i>rad53-11</i> mutant in the two-hybrid assay.....</b>	<b>192</b>
<b>Figure 5.14. The Dbf4 C-motif point mutants do not confer resistance to genotoxic agents in plasmid shuffle strains, in which the <i>DBF4</i> allele has been disrupted.....</b>	<b>195</b>
<b>Figure 5.15. Model proposing the mechanism by which Dbf4-C motif mutants confer resistance to genotoxic agents.....</b>	<b>211</b>

## CHAPTER 6

<b>Figure 6.1. Phase diagram for protein crystallization.....</b>	<b>219</b>
<b>Figure 6.2. Plasmid map of pET15b expression vector.....</b>	<b>223</b>
<b>Figure 6.3. SDS-PAGE of Protein Solubility Assay for the pET15b Dbf4FL construct in STAR pRARE cells.....</b>	<b>226</b>
<b>Figure 6.4. SDS-PAGE of Protein Solubility Assay for the pET15b Dbf4-396 construct in BL21 (DE3) pRARE cells.....</b>	<b>230</b>
<b>Figure 6.5. SDS-PAGE for the pET15b Dbf4-248 construct in STAR pRARE cells.....</b>	<b>231</b>
<b>Figure 6.6. Comparison of Dbf4 truncations that were cloned into pET15b expression vector and tested for solubility.....</b>	<b>232</b>

## **APPENDIX**

<b>Figure A-1. SDS-PAGE and Western Blot for BL21 (DE3) pET15bDbf4-FL.....</b>	<b>257</b>
<b>Figure A-2. SDS-PAGE and Western Blot for BL21 (DE3) pLySs pET15bDbf4-FL.....</b>	<b>260</b>
<b>Figure A-3. SDS-PAGE and Western Blot for STAR pET15bDbf4-FL.....</b>	<b>262</b>
<b>Figure A-4. SDS-PAGE and Western Blot for STAR pLySs, pET15b Dbf4-FL.....</b>	<b>264</b>
<b>Figure A-5. SDS-PAGE and Western Blot for STAR pRARE pET 15bDbf4-FL.....</b>	<b>266</b>
<b>Figure A-6. SDS PAGE for A. STAR, pET15b Dbf4-396 15bDbf4-FL. B. STAR pRARE, pET15b Dbf4-396. C. STAR pLySs, pET15b Dbf4-396.....</b>	<b>268</b>
<b>Figure A-7. SDS PAGE for BL21 (DE3) pET15b Dbf4-248.....</b>	<b>270</b>

## **List of Abbreviations and Acronyms**

APC/C-Anaphase promoting complex (cyclosome)

ARS-Autonomously Replicating Sequence

BLEO-Bleomycin

BRCT- *BRCA1* C-terminus

BRDF-BRCT and DBf4 similarity

CCHH-Cysteine Cysteine Histidine Hisitidine-type zinc-finger motif

Cdc-Cell Division Cyclin

Co-IP-Coimmunoprecipitation

CSE-Cigarette smoke extract

DDK-Dbf4 Dependent Kinase

ddH<sub>2</sub>O- Double distilled water

DNA-Deoxyribonucleic Acid

dNTP-deoxynucleotide phosphate

DSB-Double strand break

DTT- Dithiothreitol

EDTA- Ethylenediaminetetraacetic acid

EMS-Ethylmethyl sulfate

ES-Embryonic stem

FHA-Fork-head Homology Associated

For-Forward

FACS-Fluorescence Activated Cell Sorting

5'FOA- 5-Fluoroorotic Acid

GAL/RAF-Galactose/Raffinose  
G1-Gap 1  
G2-Gap 2  
HIS-Histidine  
HA-Hemagglutinin  
HU-Hydroxyurea  
IPTG- Isopropyl  $\beta$ -D-1-thiogalactopyranoside  
IR-Ionizing radiation  
kb-Kilobases  
kD-Kilodalton  
LDAO- Lauryldimethylamine oxide  
MCM-Minichromosome Maintenance  
MMS-Methylmethane sulfonate  
MYC-Myelocytomatosis  
NLS-Nuclear Localization Signal  
NMR-Nuclear Magnetic Resonance  
ONPG- 2-Nitrophenyl- $\beta$ -D-galactopyranoside  
ORC-Origin Recognition Complex  
PCR-Polymerase Chain Reaction  
PMSF- Phenylmethylsulphonyl fluoride  
Pre-RC- Pre-Replicative Complex  
Rev-Reverse  
RNA-Ribonucleic Acid

RNR-Ribonucleotide reductase

ROS-Reactive Oxygen Species

SC-Synthetic complete

SDS-Sodium dodecyl sulfate

SDS-PAGE-Sodium dodecyl sulfate-Polyacrylamide gel electrophoresis

TRP-Tryptophan

URA-Uracil

UV-Ultraviolet

WCE-Whole Cell Extract

WT-Wild Type

YPD-Yeast Extract/Peptone/Dextrose

## **CHAPTER 1: Literature Review and Research Objectives**

This section deals, briefly, with the general characterization of yeasts, and their use as a model organism in the areas of cell cycle and checkpoint research. It also includes a review of literature concerning the *Saccharomyces cerevisiae* Dbf4 (dumbbell former) protein, its involvement in the initiation of DNA replication through interactions with various cell cycle proteins (Cdc7, Orc2, Mcm2) and its role in the intra-S-phase checkpoint response through an interaction with the effector checkpoint kinase, Rad53 (Radiation repair protein 53).

## **1.0 LITERATURE REVIEW**

### **1.1 The Yeasts**

Yeast, collectively, are included in the Ascomycota group of fungi that have lost the mycelial mode of growth and are now limited to a unicellular form. These organisms are facultative, with optimum pH ranging from 3.8 to 5.6 and optimum temperature ranging from 25 to 28°C (Kockova-Kratochilova, 1990). Some yeasts grow better at 37°C, and there are a number of strains of psychrophilic yeasts that have an optimum temperature below 20°C for growth (Considine and Considine, 1983). Some strains grow at the low temperatures of 4 to 5°C and others at a highest temperature of 40°C (Kackova-Kratochilova, 1990). They are usually small oval-shaped cells (Figure 1.1.), but some appear elongated and some are spherical. They can vary in size from 1 to 5 µm in width and from 5 to 30µm or more in length (Pelczar and Chan, 1981). Yeasts are heterotrophic organisms, requiring organic compounds for nutrition. In nature, they are found adapted to environments with a high sugar content, such as the surface of fruits, the nectar of flowers and the slime flux from trees. They are also present in soil, water, wastewaters, sewage sludge and aquatic sediments (Alexopoulos and Bold, 1967; APHA,1995).

*Saccharomyces cerevisiae*, also known as budding yeast, has for centuries, been used in various fermentation processes (brewing, wine-making, baking) (discussed in Landry *et al.*, 2006). The first archaeological evidence of *S. cerevisiae* being used in wine fermentation, dates back to 3150 B.C. in ancient Egypt (discussed in Landry *et al.*, 2006). The first laboratory strain was derived from a heterothallic strain found on rotting figs and presented to Carl Lindgren by Emril Mrak in 1938 (discussed in Landry *et al.*, 2006). Lindgren's laboratory published the first genetic maps of *S. cerevisiae* (Lindgren, 1949; Lindgren and Lindgren, 1951; Lindgren *et al.*, 1959).

*S. cerevisiae*, is comprised of a cell wall and a cell membrane that encapsulate a network of organelles and microbodies (mitochondria, peroxisomes, nucleus, endoplasmic reticulum, vacuoles, cytoplasm, lipid and glycogen storage bodies). A cross-sectional diagram of *S. cerevisiae*, including its organelles, is shown in Figure 1.1. The cell wall serves to protect the cell, maintains its shape, mediates cellular interactions, reception and attachment. The cell wall is 100 to 200 nm thick and consists of an inner and an outer layer. The cell walls of *S. cerevisiae* also have bud scars and birth scars. Bud scars are chitin rich, convex protrusions that remain on the mother cell surface after budding. Birth scars are concave indentations on the daughter cell wall surface that are the result of budding (discussed in Walker, 1998). The fundamental component of the yeast cells is the protoplasm which is differentiated into the nucleus and the cytoplasm.

The yeast nucleus is approximately 1.5  $\mu\text{m}$  in diameter and is located at the centre of the cell. The nucleus contains the yeast genome. It is noteworthy that the nuclear membrane of yeast does not break down during mitosis, unlike what occurs with most other eukaryotic cells. Mitochondria, in yeast, are structurally similar to those in higher

eukaryotes, consist of an outer membrane, a matrix and an inner membrane. Yeasts usually contain one or very few large, occasionally branched, mitochondria. The Endoplasmic reticulum and the Golgi apparatus are involved in the secretory system, as in higher eukaryotes. In yeasts, vacuoles are lysosome-like acidic compartments that are involved in intracellular protein trafficking and non-specific intracellular proteolysis. Yeast vacuoles may exist as a single large compartment, or as several smaller compartments. Yeast microbodies include peroxisomes and glyoxysomes. Peroxisomes contain catalase and several oxidases. Glyoxysomes contain catalase and enzymes involved in the glyoxylate cycle and amine metabolism (discussed in Walker, 1998).

*S. cerevisiae* reproduces sexually by conjugation and asexually by forming a bud that increases in size, followed by a nuclear division. One daughter nucleus migrates into the bud and a cross-wall forms between the mother and daughter cell. Eventually, the daughter cell becomes detached from the mother cell. Some yeasts, for example *Schizosaccharomyces pombe*, also reproduce sexually by conjugation and reproduce asexually by transverse binary fission (discussed in Stanier *et al.*, 1965). In this study, *Saccharomyces cerevisiae* was used as a model organism.

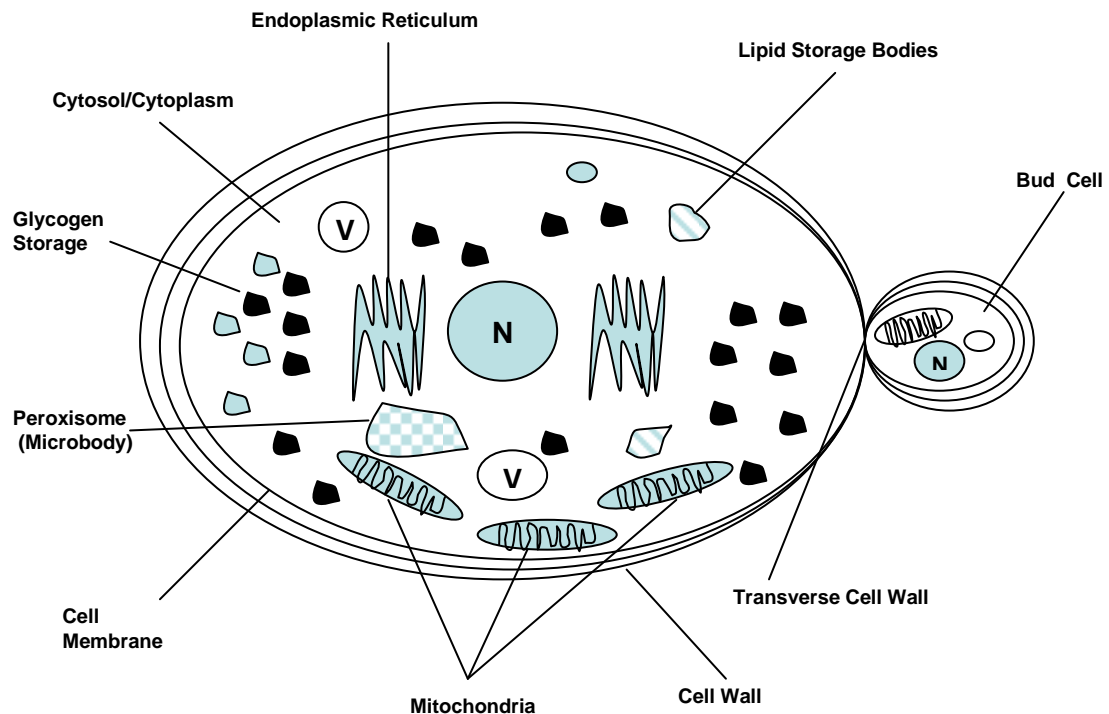


**Figure 1.1. Diagram of *Saccharomyces cerevisiae*, including its organelles.**  
N=nucleus, V=vacuole. (Adapted from Ratledge, 1991)

## **1.2 Genetics and Life Cycle:**

*S.cerevisiae* can exist as a haploid or diploid organism. A haploid genome organized into 16 chromosomes, consists of  $1.2 \times 10^7$  base pairs (bp) and includes approximately 6200 genes (discussed in Game, 2002; Bjornsti, 2002). Genes represent 72% of the total genomic sequence (Guthrie and Fink, 2002).

In general, the term life cycle of *S. cerevisiae* refers to two aspects of its life (reviewed in Herskowitz, 1988). The first aspect pertains to how a single cell divides into two identical cells. The second aspect involves how the ploidy of a cell can change (reviewed in Herskowitz, 1988). Diploid cells, under conditions of starvation, are able to undergo sporulation (meiosis) resulting in an ascus containing four haploid spores (Codon, *et al.*, 1995) (Figure 1.2.). Haploid spores can reproduce vegetatively and can be one of two possible mating types (MAT $\alpha$  or MAT $\alpha$ ) (reviewed in Landry *et al.*, 2006). It is possible for two haploid cells of opposite mating type to fuse and form a diploid cell (reviewed in Landry *et al.*, 2006) (Figure 1.3).

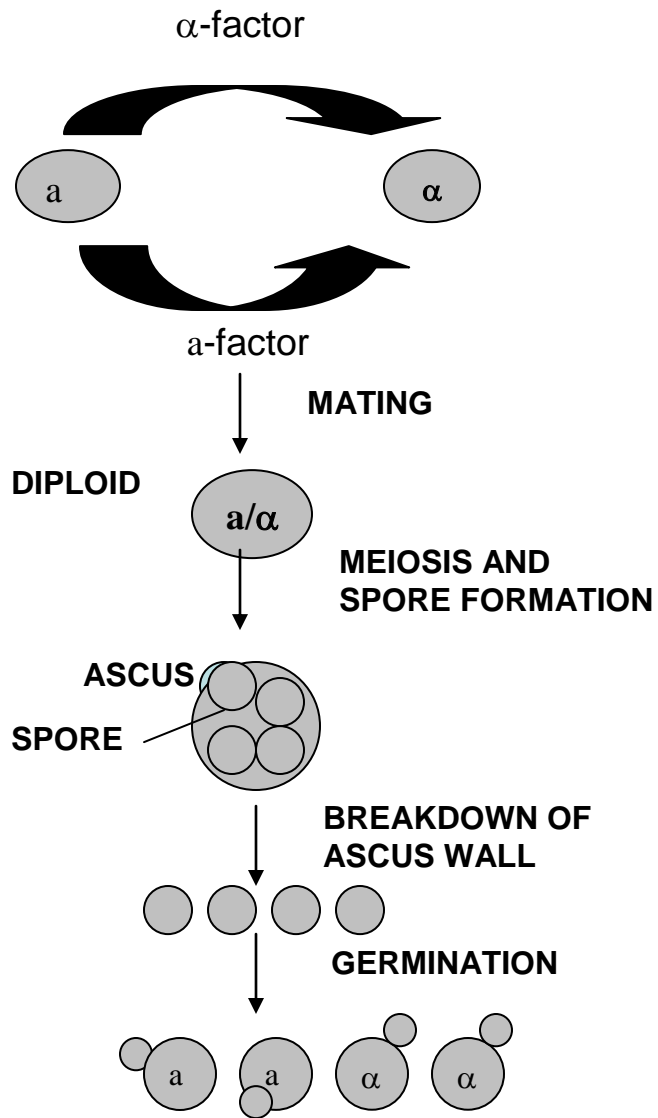


**Figure 1.2. Transition in the life cycle of *Saccharomyces cerevisiae*.** Diagram depicts the mating of MAT $\alpha$  and MAT $a$  cells resulting in a diploid MAT  $a/\alpha$ . The diploid cell undergoing meiosis (sporulation) results in an ascus containing four spores (two MAT $a$  and two MAT $\alpha$ ). (adapted from Herskowitz *et al.*, 1988).

MAT $\alpha$  cells produce  $\alpha$ -factor, which is a pheromone, consisting of a peptide composed of 13 amino acids (reviewed in Herskowitz, 1988). MATa cells produce a-factor, which is also a pheromone, made of 12 amino acids (reviewed in Herskowitz, 1988). The mating factors act to halt cells of opposite mating type in G1 phase of the cell cycle, inhibiting cell growth before the onset of the initiation of DNA replication (reviewed in Herskowitz, 1988). This prepares the cells for sexual reproduction by conjugation with a cell of the opposite mating type.  $\alpha$ -factor is often used, experimentally, to synchronize liquid cultures of MATa cells at the G1 phase of the cell cycle.

Heterothallic strains have a fixed mating type (either a or  $\alpha$ ) (discussed in Landry *et al.*, 2006). Most laboratory strains are heterothallic. Homothallic strains, which include most naturally occurring strains, are able to switch mating type (reviewed in Landry *et al.*, 2006) (Figure 1.3). Homothallic strains possess the *HO* (homothallism) gene that encodes a site-specific endonuclease that promotes mating type switching from a to  $\alpha$  or from  $\alpha$  to a (reviewed in Landry *et al.*, 2006) (Figure 1.3). Only the mother cell transcribes the *HO* gene, undergoes mating type switching and fuses with the newly produced daughter cell, resulting in a diploid cell. (reviewed in Landry *et al.*, 2006). Thus, the haploid phase is transient or only temporary in homothallic strains (reviewed in Landry *et al.*, 2006) (Figure 1.3).

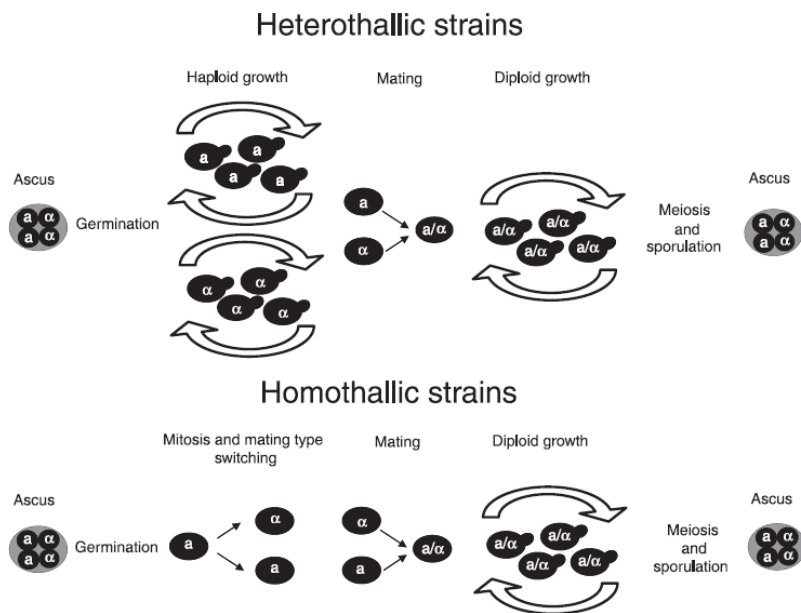


**Figure 1.3. The life cycle of heterothallic and homothallic strains of *Saccharomyces cerevisiae*.** Diagram compares the life cycle of heterothallic and homothallic strains, starting from an ascus containing four spores (two  $a$  and two  $\alpha$ ). Note that the haploid state of homothallic strains is very transient and temporary following germination. They exist in a diploid state most of the time. They can also undergo mating type switching. Heterothallic strains have fixed mating types and can exist as haploids for extended periods of time and will undergo mating with a haploid of the opposite mating type, in response to mating pheromones. This figure is from Landry *et al.* (2006) reproduced with permission.

### **1.3 *Saccharomyces cerevisiae* As A Model Organism**

A model organism is often employed by researchers to address various research questions and hypotheses that yield results which can be further attributed and extrapolated to other more complex organisms. An ideal model organism should be biologically relevant and reasonably easy to culture and maintain (discussed in Ballatori and Villalobos, 2002). Furthermore, an ideal model organism will be easy to manipulate and should not be prohibitively expensive (discussed in Ballatori and Villalobos, 2002). Ideally, a model organism can be used to produce rapid, reliable and reproducible results (discussed in Hohmann, 2005). It is of interest to note that there appears to be a trend moving away from the rodent models and shifting towards the use of non-mammalian species that have some experimental advantages and homology to humans and other higher eukaryotes (Ballatori and Villalobos, 2002). The unicellular eukaryote, *S. cerevisiae* has had a positive impact on many areas of eukaryotic cell biology research (Trotter, 2001). For example, the use of *S. cerevisiae*, as a model organism, has led to advancements in cancer-related cell cycle studies. Moreover, *S. cerevisiae* has also been used in fatty acid metabolism research (Trotter, 2001).

*S. cerevisiae* has several virtues that make it an ideal model organism for cell cycle research. It grows rapidly and is inexpensive to culture. Furthermore, the fully sequenced genome has allowed yeast researchers to make great pioneering strides that have amounted to significant contributions to various areas of eukaryotic cell biology, as mentioned above (discussed in Dolinski and Botstein, 2005). Moreover, numerous public databases, with a variety of information pertaining to *S. cerevisiae* yeast genomics, proteomics, morphology and molecular mechanism, are available to researchers

(discussed in Dolinski and Botstein, 2005). It is also possible, in some cases, for human and other eukaryotic genes to be expressed and studied in *S. cerevisiae* (reviewed in Hohmann, 2005). An example of this includes expression of apoptotic Bax (Bcl-2 associated X) protein in yeast (Li and Harris, 2005). Overexpressing the mammalian pro-apoptotic protein Bax in *S.cerevisiae* conferred a lethal phenotype (Li and Harris, 2005). Interestingly, this conferred phenotype could be suppressed by the expression of mammalian prion proteins (Li and Harris, 2005). Another example of expressing a human gene in yeast was the expression of the human Blm (Blooms) protein in yeast, which, when mutated, causes Bloom syndrome in humans (reviewed in Hohmann, 2005). Lillard-Wetherell *et al.* (2005) demonstrated that Blm expression was able to rescue the disrupted telomere lengthening phenotype of the *S. cerevisiae* mutant *sgs1* strain.

In addition to the advantageous features discussed above, *S. cerevisiae* is very amenable to genetic manipulation. Firstly, most laboratory strains have mutations in, or deletions of, genes encoding enzymes that are involved in the biosynthesis of certain amino acids or nucleotide bases. These mutations or deletions allow for the use of selective markers for maintaining plasmid DNA and can also be used for the genomic integration of mutant alleles or sequences encoding epitope-tags. Some common selectable markers include: *TRP1*, *HIS3*, *URA3* and *ADE2* (Guthrie and Fink, 2002). These selectable markers are wild type copies of genes that encode for biosynthetic enzymes that are involved in the biosynthesis of an amino acid or a nucleic acid. Specific mutations in these genes of the laboratory yeast strains allow for these genes to be used as selectable markers. *trp1-1* and *his3-1* are mutated alleles of genes encoding enzymes involved in the biosynthesis of the amino acids tryptophan and histidine, respectively.

*ura3-1* and *ade2-1* are mutant alleles of genes that encode enzymes involved in the biosynthesis of nucleotide bases, uracil and adenine, respectively. Strains carrying these mutant alleles will require the specific amino acid bases or nucleotide bases as supplements to compensate for the mutation, in order to support growth and viability. Alternatively, transformed plasmid DNA (containing the wild type gene) can supply the biosynthetic enzyme, thereby supporting growth. Alternatively, a linear piece of DNA consisting of a gene fused to the wild type gene of the biosynthetic enzyme (that is involved in the biosynthesis of an amino acid or nucleic acid) can also be transformed into the cells, and integrate into the cell's genome. The biosynthetic enzyme gene product supports cell viability by allowing the cell to grow in media lacking that particular amino acid or nucleic acid.

There are many previously characterized temperature-sensitive (*ts*) yeast strains, having mutations in a certain essential gene that cause the cells to be nonviable at a non-permissive temperature. These *ts* strains are useful tools for performing complementation assays. Plasmids expressing the essential protein, when transformed into a *ts* strain, can support cell viability at the nonpermissive temperature of a strain, which is usually 37°C. Plasmids expressing mutant variants of the same essential protein can also be transformed into the *ts* strain to determine whether a particular mutation is lethal to the cell or not. Another attractive feature of the *S. cerevisiae* model is that there are relatively simple techniques, by which genes can be tagged with a sequence encoding an epitope, that will create a fusion protein (i.e. *Myelocytomatosis (MYC)* or *Hemagglutinin (HA)*) (Guthrie and Fink, 2002). Antibodies against these epitopes, that are commercially available, facilitate easy detection in Western Blotting applications. Moreover, genetic

manipulations, in which the endogenous promoters are replaced by inducible or repressible promoters (i.e. Galactose (GAL) inducible promoters), are also quite feasible (Longtine *et al.*, 1998). These promoters facilitate the repression or induction of gene transcription which are the basis of protein depletion or overexpression experiments involving essential and important genes.

The areas of cell cycle and checkpoint research have benefited tremendously from the use of the *S. cerevisiae* model. Many yeast genes that are involved in cell cycle control, meiosis, DNA repair and checkpoints have human homologues (discussed in Game, 2002). In the late 1960s and early 1970s, Leland Hartwell's laboratory initiated pioneering cell cycle studies, in which approximately 400 temperature sensitive strains were isolated by subjecting a parental strain to a mutagen (nitrosoguanidine) (reviewed in Barnett, 2007). Hartwell's laboratory then used time-lapse photomicroscopy to identify temperature sensitive mutants that were defective in gene function at specific stages of the cell cycle (Hartwell *et al.*, 1970). Essentially, they observed the morphological development of yeast budding and progress through the cell cycle in these temperature sensitive mutants (Hartwell *et al.*, 1970). Leland Hartwell was the first person to use the term 'checkpoint' to define "the controlling mechanism that enforces the interdependency of the events of the cell cycle" (reviewed in Barnett, 2007). This groundbreaking work has led the way for all of the cell cycle research that has followed. Leland Hartwell was awarded the Nobel Prize for Medicine or Physiology in 2001, along with Paul Nurse and R.Timothy Hunt. It is important to note that cell cycle studies, using the *S. cerevisiae* model, have contributed profoundly to our fundamental understanding of cancer biology

as many of the molecular mechanisms that are the basis of cancer development have been studied in *S. cerevisiae* first.

The *S. cerevisiae* model is very suitable for studying the role of Dbf4 and Rad53 in the intra-S-phase checkpoint response, which is a main focus of this research. Both Dbf4 and Rad53 are conserved, having orthologues in higher eukaryotes, including humans. Moreover, there is a series of Dbf4 temperature-sensitive mutants that have been previously isolated. There are also various Rad53 deletion and point mutant strains that are available for experiments exploring the role of Rad53 in checkpoint responses.

#### **1.4. The Cell Cycle and The Initiation of DNA Replication**

The cell cycle is, essentially, a regulated series of events by which the cell duplicates its genetic material, ultimately resulting in two genetically identical cells (Lukas and Bartek, 2004). There are four main phases that broadly comprise the cell cycle: genome duplication (S-phase) and nuclear division (mitosis or M-phase), separated by two gap phases (G1 and G2) (Bahler, 2005) (Figure 1.4). The cell cycle, including DNA replication, is a highly conserved process in eukaryotic biology, with genome replication occurring once per cell cycle (DePamphilis, 2005).

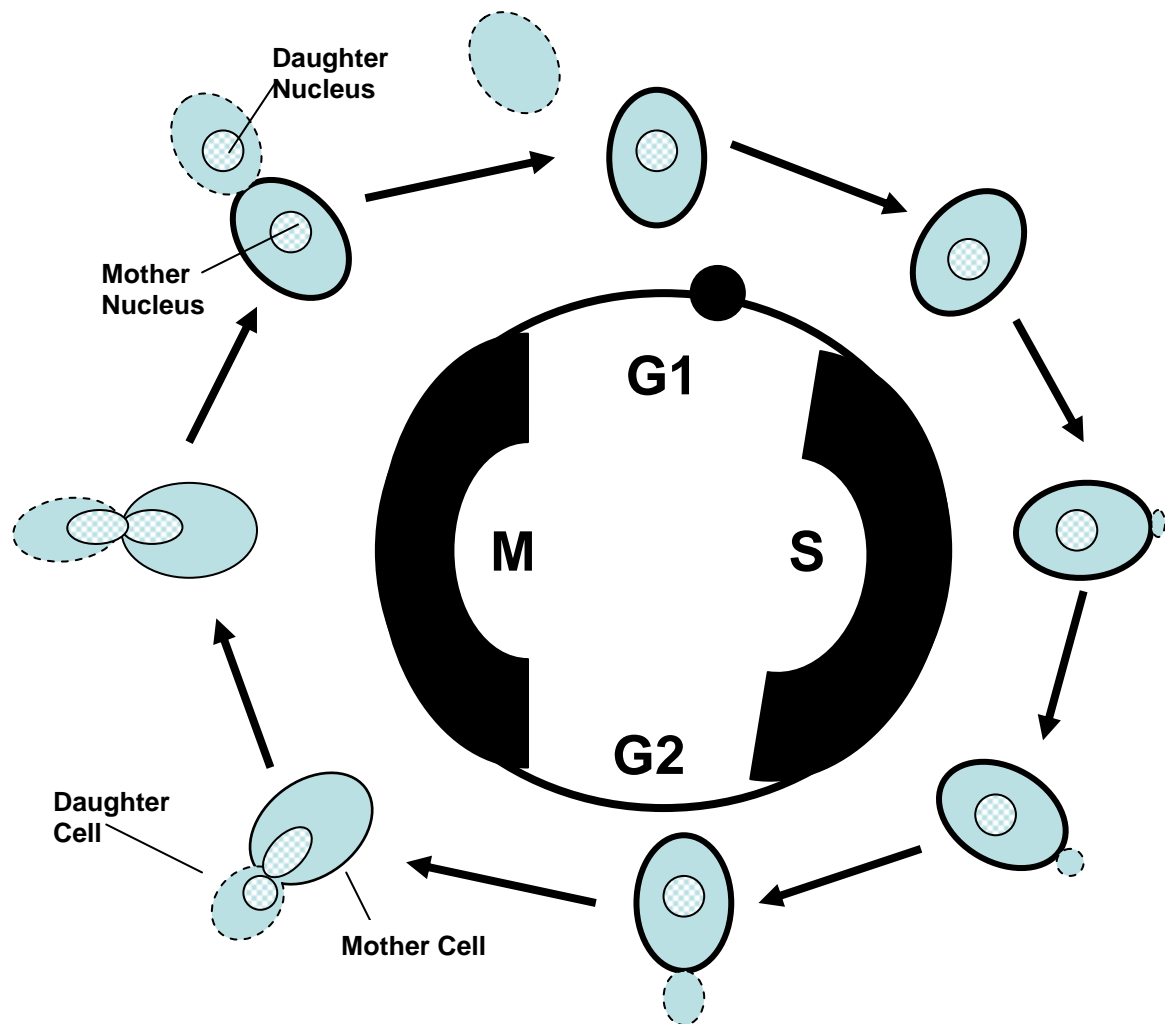


**Figure 1.4. *Saccharomyces cerevisiae* cell cycle phases.** The daughter bud formation is depicted as the cell progresses through the cell cycle phases, starting from G1, into S-phase, followed by G2 and then into M-phase (mitosis and cytokinesis). The black circle in G1 represents START. (Adapted from Herskowitz, 1988)

## **1.5. Cell Cycle Phases**

### **1.5.1 G1 Phase (Gap 1 Phase)**

During G1 phase, the cell grows and synthesizes RNA, proteins and other cellular constituents and a haploid division plane is determined (reviewed in Webster and Weber, 2007). A bud neck starts to form adjacent to the previous site of cell division (known as the bud scar) (reviewed in Wolfe and Gould, 2005). The G1 phase of *S. cerevisiae* is known to be relatively long and variable and the G2 phase is very short. Furthermore, the G1 phase of *S. cerevisiae* is variable in the sense that it is a point in the cell cycle which can result in different outcomes (described below) based on different environmental conditions, such as nutrient starvation.

START is the point near the end of G1, where the cell monitors internal and external environmental conditions before committing itself to S-phase. The environmental conditions can include nutritional deprivation, temperature and the presence of experimental chemicals, such as sodium azide or sodium fluoride. At START, the cell has three choices. Firstly, it can proceed through the cell cycle, eventually undergoing mitosis. The second option is to enter stationary phase, if it is nutritionally deprived. A stationary phase cell is resistant to heat and chemical treatment (reviewed in Forsburg and Nurse, 1991). The third option is available to haploid cells which can undergo sexual reproduction and mate with a cell of the opposite mating type (Figure 1.3) (reviewed in Forsburg and Nurse, 1991). The resulting diploid cells are able to undergo meiosis and sporulation (reviewed in Forsburg and Nurse, 1991).

At the molecular level, the pre-replicative complex (pre-RC), which forms during the M/G1 transition, remains at origins of replication throughout G1 (reviewed in

DePamphilis, 2005). Pre-RC formation involves the ordered assembly of a number of replication factors, including ORC (Origin Recognition Complex), Cdc6 (Cell division cycle protein 6), Cdt1 (Chromatin licensing and DNA replication factor 1) and the MCM (Minichromosome Maintenance) complex (Mcm2 to Mcm7) (Bell and Dutta, 2002) (Figure 1.5). ORC recognizes and binds origins of replication and serves as a “landing pad” for other proteins that, collectively, form the pre-RC (reviewed in Sclafani and Holzen, 2007). Together, Cdc6 and Cdt1 serve as helicase clamp loaders and facilitate the binding of the Mcm DNA helicase complex (Mcm2-7) to the origin. It is believed that the Clb/Cdc28 kinase complexes (also known as cyclin dependent kinases (Cdks)) target Sld2 and Sld3 to trigger the initiation of DNA replication (Zegerman, and Diffley, 2007; Tanaka *et al.*, 2007). Cdks are also, subsequently, involved in the prevention of pre-RC reassembly by targeting Cdc6, ORC and the MCM complex (Honey and Futterer, 2007; Nguyen *et al.*, 2000). The Mcm10 protein is recruited to the pre-RC, facilitating the loading of Cdc45 (Cell division cycle protein 45) (which is essential for the subsequent unwinding and for the loading of the replicative polymerases). Mcm10 has also been implicated in promoting Dbf4/Cdc7 phosphorylation of the Mcm2-7 complex (Homesly *et al.*, 2000). Results, recently obtained, *in vitro*, have revealed that a protein complex, consisting of Cdc45, the GINS (Go, Ichi, Nii, San) tetramer and Mcm2-7 may function as an “unwindosome” at the replication fork (Moyer *et al.*, 2006; Pacek *et al.*, 2006). The unwinding of the DNA is further stimulated by the binding of RPA (Replication protein A), which binds to single-stranded DNA (reviewed in Sclafani and Holzen, 2007). RPA serves to recruit DNA polymerase  $\alpha$ -primase (DNA Pol  $\alpha$ -primase) which is involved in

synthesizing short RNA primers at early origins that are used by DNA polymerases to create the lagging and leading strands during S-phase (Garg and Burgers, 2005).

The origins of replication are well characterized in *S. cerevisiae* (discussed in Cvetic and Walter, 2005), and have been classified as early-firing, mid-firing and late-firing, based on when they fire (relative to each other) during S-phase (Friedman *et al.*, 1996; Raghuraman *et al.*, 2001). Origins consist of an A element and B elements (B1, B2, B3, B4), which are nonredundant sequence elements (Theis and Newlon, 1997). Combinations of B elements vary from one Autonomous Replicating Sequence (ARS) origin of replication to another. The A element contains the ARS consensus sequence (ACS), which is half of the ORC binding site (discussed in Cvetic and Walter, 2005). The other half of the ORC binding site is the B1 element (discussed in Cvetic and Walter, 2005). The B2 element was originally thought to be a DNA unwinding element and is now believed to be important for the binding of Cdc6 (discussed in Cvetic and Walter, 2005). Abf1 (autonomously replicating sequence binding factor 1), which is a transcription factor, binds to the B3 element. Abf1 has been identified as an essential DNA replication factor that is required for normal activity of ARS elements by direct interaction with its specific DNA binding motif (discussed in Schlect *et al.*, 2008).

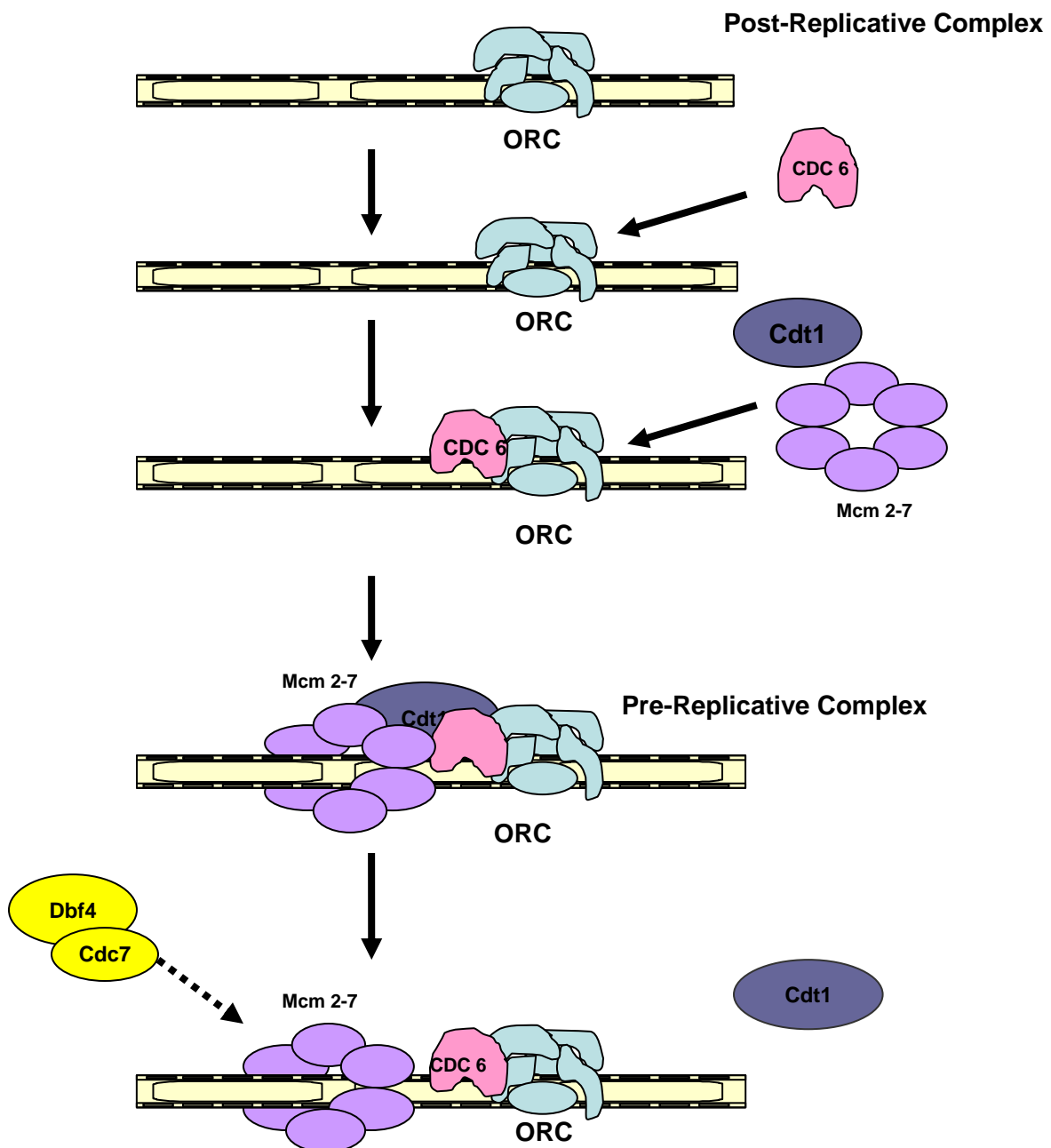


**Figure 1.5. Assembly of the Pre-Replicative Complex at an origin of DNA replication.** ORC complex assembles, followed by Cdc6 and Cdt1, which facilitates the loading of the MCM complex. The Dbf4/Cdc7 kinase complex targets Mcm2 and Mcm4 to trigger the initiation of DNA replication. The Cdc28/Clb kinase complexes also trigger the initiation of DNA replication by targeting Sld2 and Sld3 (not shown). Adapted from Sheu and Stillman (2006).

### **1.5.2. S-Phase**

S-phase is the point in the cell cycle where DNA is synthesized and the genome is duplicated. The transition into S-phase is, essentially, the conversion of pre-RCs into replication forks (reviewed in Takeda and Dutta, 2005). This process involves origin unwinding, the stabilization of single-stranded DNA and loading of the replicative polymerases. Cdc45 is thought to associate with origins in a CDK (cyclin-dependent kinase) and DDK (Dbf4-dependent kinase)-dependent manner in early S-phase for early-firing origins and late S-phase for late-firing origins. Takeda and Dutta (2005) have proposed a model in which the MCM helicase complex is inactive unless it is bound to a polymerase by an association with Cdc45. This ensures that helicase unwinding does not begin without a trailing polymerase. Sheu and Stillman (2006) have reported that Cdc7/Dbf4 (DDK) promotes a stable Cdc45/MCM complex exclusively on chromatin in S-phase in which Mcm4 is hyperphosphorylated at its N-terminus.

Unwinding of DNA at replication origins results in the emergence of (Y-shaped) replication forks. The replication fork progression exposes two complementary strands with opposing orientation. One strand has a 3' to 5' orientation and the other has a 5' to 3' orientation. The synthesis of DNA occurs, essentially, as a process by which each of these strands is utilized as a template for polymerase activity. At the replication fork, a set of proteins assemble and perform a succession of functions (Figure 1.6). Since DNA polymerase activity can only occur in a 5' to 3' direction, two different modes of polymerase activity are employed. The resulting strands that are synthesized are termed the leading and lagging strands.

The leading strand results from a 5' to 3' directed assembly of nucleotides in a complementary manner to the 3' to 5' oriented template strand. This process involves a series of events. Firstly, there is a synthesis of short RNA primers (about 8 to 12 nucleotides) by the DNA polymerase $\alpha$ -primase complex. The DNA pol $\alpha$ -primase is a 4-subunit complex. Following the RNA primer synthesis, the DNA pol $\alpha$  subunit extends the primer by approximately 20 nucleotides. On the leading strand, the DNA pol $\alpha$  is then replaced by DNA pol $\delta$ , in a polymerase switch, and then polymerase activity resumes by DNA pol $\delta$  and the polymerase activity resumes. The DNA pol $\delta$  associates with Proliferating Cell Nuclear Antigen (PCNA), a ring-shaped processivity factor, which encircles the DNA (Figure 1.6). PCNA loading onto the primed DNA template is facilitated by Replication Factor C (RFC), which is a clamp loader protein.

The lagging strand DNA replication is thought to occur in discrete stages by the synthesis of Okazaki fragments. Okazaki fragments are segments of DNA strand synthesis that are 100-200 bases in length. The Okazaki fragments are synthesized because the template strand has a 5' to 3' orientation and DNA polymerase activity can only occur in a 5' to 3' direction (requiring a 3' to 5' template). Firstly, the initiation stage is carried out by DNA pol $\alpha$ -primase which involves the synthesis of a series of short RNA primers, as mentioned above. The DNA pol $\alpha$ -subunit then extends the primers about 20 nucleotides. This is followed by a PCNA loading, thereby dissociating DNA pol $\alpha$  and recruiting DNA polymerase  $\delta$  (DNA pol  $\delta$ ) and Flap Endonuclease 1 (FEN1) to perform the elongation and maturation of the Okazaki fragments on the lagging strand (Figure 1.6) (reviewed in Garg and Burgers, 2005). It has been proposed that the DNA pol  $\alpha$  to DNA pol $\delta$  switch is mediated by the binding of Replicating factor

c (RFC). In an alternate, more likely scenario, the inhibition and dissociation of pol  $\alpha$ -primase is coupled to the loading of PCNA in complex with RFC (Garg and Burgers, 2005). The second scenario is more likely because it has been shown that only RFC complexed with PCNA is able to productively bind DNA and load PCNA. Nonetheless, the Okazaki fragments are then elongated by DNA pol  $\delta$  (in complex with PCNA and FEN1). The RNA primers are degraded by FEN1 and the resulting gaps are then filled in by the ligation activity of DNA ligase I.

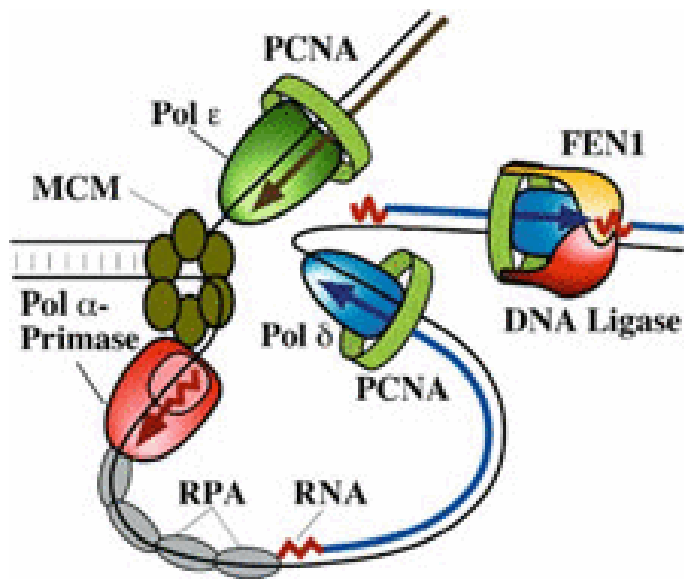


**Figure 1.6. Eukaryotic DNA replication fork.** The minimal set of proteins for fork propagation are indicated. The MCM complex at the replication fork performs a helicase function (unwinding the DNA). RPA serves to recruit DNA polymerase  $\alpha$ - primase which is involved in synthesizing short RNA primers at origins that are used by other DNA polymerases to create the lagging and leading strand during S-phase. On the lagging strand, eventually, PCNA is loaded, thereby dissociating the DNA pol $\alpha$  and recruiting DNA pol  $\delta$  and FEN1 (a flap endonuclease) to perform the elongation and maturation of the Okazaki fragments on the lagging strand. On the leading strand, the DNA pol $\alpha$  is replaced by DNA pol  $\epsilon$ , (in association with PCNA) in a polymerase switch. PCNA is a ring-shaped processivity factor-which encircles the DNA. The RNA primers are degraded by FEN1 and the gaps are then ligated by DNA ligase I. This figure is from (Garg and Burger, 2005), reproduced with permission.

### **1.5.3. G2 Phase (Gap 2 Phase)**

In *S. cerevisiae*, the G2 phase is not well defined (Novak *et al.*, 2002). During G2 phase, the nucleus moves to the constriction (neck) between the mother cell and the newly emerged bud (Carlile *et al.*, 2001) (Figure 1.4).

### **1.5.4. M-Phase**

M-phase consists of two major events: mitosis and cytokinesis (Lebedeva *et al.*, 2004). Mitosis is a continuous process. However, it is often described as several stages that occur in a consecutive sequence: prophase, prometaphase, metaphase, early anaphase, anaphase and telophase (discussed in Lebedeva *et al.*, 2004). The events of mitosis, ultimately, result in a precise chromosome segregation between the mother and daughter cell. In *S. cerevisiae*, during mitosis, the polar bodies (which are analogs of centrosomes of higher eukaryotes) separate and one positions itself near the entrance of the bud, while the other remains with the mother cell (Lebedeva *et al.*, 2004).

At the molecular level, the metaphase-anaphase transition is regulated by the anaphase promoting complex/cyclosome (APC/C), which is a ubiquitin ligase, consisting of 13 subunits. The large multisubunit nature of the APC/C complex allows for it to bind to various different substrates. APC/C targets mitotic cyclins and other factors for proteolysis by the 26S proteasome (Lindon, 2008; discussed in Pesin and Orr-Weaver, 2008). Proteolysis is an important mechanism that regulates the events of mitosis (reviewed in Pesin and Orr-Weaver, 2008).

The protein factors Cdc20 and Cdh1 are non-core subunits of APC/C. They are involved in the activation of APC/C and also confer substrate specificity to the APC/C

complex. This activation of APC/C and the conferring of substrate specificity occur by various means, including targeted protein degradation, phosphorylation and direct binding of inhibitory proteins. The protein factor Cdc20 is involved in the ubiquitination of mitotic cyclins, and other substrates for the onset of anaphase. Cdc20 is also indirectly involved in the separation of sister chromatids by ubiquitinating Securin, which in turn, causes the Separase protease to be activated. The Separase protease cleaves the cohesin complex ring that physically attaches the sister chromatids (Pesin and Orr-Weaver, 2008). Cdh1 targets mitotic cyclins and additional substrates for degradation during mitotic exit and G1 phase (reviewed in Pesin and Orr-Weaver, 2008). Essentially, the ubiquitinated proteins will subsequently undergo proteolysis.

To summarize, as cells enter mitosis, they organize microtubules into a bipolar spindle (Straight *et al.*, 1997). Kinetochores (a specialized region of the chromosome) bind to the microtubules as the sister chromatid pairs align themselves. When the linkage between the two sister chromatids is removed (as described above), the sister chromatids segregate towards opposite spindle poles (Straight *et al.*, 1997).

Cytokinesis is known to be the final stage of the cell division process and results in the complete separation of the mother and the daughter cells (Yeong, 2005) (Figure 1.4.). In *S. cerevisiae*, cytokinesis occurs when an actinomysin contractile ring and septum are formed at the mother bud neck, ultimately resulting in the separation of the mother and daughter cells (Bi, 2001; Corbett *et al.*, 2006). At the molecular level, actomyosin-ring constituents are removed progressively from the ring during contraction and disassembled completely thereafter by a process involving APC/C and Cdh1, similar to that described above for the separation of chromatids (Tully *et al.*, 2009).

## **1.6. Cell Cycle Checkpoint Responses**

Checkpoints are surveillance mechanisms that ensure that one cell cycle stage is completed before another one begins (Jares *et al.*, 2000). The function of checkpoints is to temporarily arrest the cell cycle, which allows a cell to respond to and repair damaged DNA (reviewed in Sancar *et al.*, 2004). The depletion of deoxyribonucleotide (dNTP) pools can also cause checkpoints, resulting in replication fork pausing (Bartek *et al.*, 2004). Checkpoint defects can impair a cell's resistance to genotoxic stress or replication block, which can result in genome instability (reviewed in Branzei and Foiani, 2006). There are three main checkpoints that regulate the cell cycle. The G1/S and intra-S-phase checkpoints monitor the cell's progression into and through S-phase, ensuring an error-free duplication of the DNA (reviewed in Sancar *et al.*, 2004). The G2/M checkpoint works to detect and repair damaged DNA as the cell prepares to enter mitosis as well as defects in the microtubule-kinetochore attachments (Sancar *et al.*, 2004). Since the intra-S-phase checkpoint response is a main focus of this research, a detailed description of the factors involved is provided.

### **1.6.1. DNA Damage**

DNA damage can be caused by cellular metabolic processes that include alkylation, oxidation, hydrolysis and mismatch of DNA bases (reviewed in Hakem, 2008). DNA damage can also be caused by exogenous or environmental factors, such as various chemicals, ultraviolet radiation (UV) and ionizing radiation (IR) (reviewed in Hakem, 2008). One of the most severe forms of DNA damage is DNA double-stranded breaks (DSBs) (reviewed in Cann and Hicks, 2007). Such severe DNA damage can result in

genome instability or induce apoptosis (reviewed in Cann and Hicks, 2007). However, single-stranded breaks (SSBs) and base damage, which are also caused by ionizing radiation, are much more common than DSBs (Ismail *et al.*, 2005). In addition to cell cycle checkpoints, cells have also developed DNA repair pathways that involve homologous recombination or non-homologous end-joining of chromosomes (discussed in Cann and Hicks, 2007). Checkpoint pathways can signal DNA damage and involve three main groups of proteins, namely, sensor, transducer and effector proteins. These proteins act in signalling cascades to detect DNA damage and repair the damage (reviewed in Kolodner, *et al.*, 2002). Sensor proteins recognize damaged DNA directly or indirectly and function to signal the presence of abnormalities by initiating a biochemical cascade of activity. Transducer proteins are, typically, protein kinases that relay and amplify the damage signal from sensors by phosphorylating other kinases or downstream targeting proteins. Effector proteins include the most downstream targets of transducer protein kinases and are regulated to prevent cell cycle progression. This regulation is usually mediated by a phosphorylation event. Effector proteins can serve to prevent replication fork collapse or prevent further origin firing until the DNA damage is repaired. Rad53 is an example of an effector protein in *S. cerevisiae*.

Checkpoint recovery refers to a cell that has resumed cell cycle activity following a checkpoint response that has acted to repair damaged DNA (reviewed in Harrison and Haber, 2006). Checkpoint adaptation is another, similar, but distinct, concept that is used to describe an extended cell cycle arrest caused by DNA damage. An extended cell cycle arrest can last 12-24 hours and the cells will eventually re-enter the cell cycle and continue to divide, in spite of residual DNA damage (reviewed in Harrison and Haber,

2006; Bartek and Lukas, 2007). Alternatively, cells may also experience a checkpoint malfunction, that can, ultimately, result in cell death. Each of the checkpoint response pathways involves a vast and intricate array of protein factors that are sometimes implicated in more than one pathway.

### **1.6.2. The Intra-S-Phase Checkpoint Response**

The intra-S-phase checkpoint response functions to ensure that DNA is synthesized accurately, as the cell proceeds through S-phase. Thus, the intra-S-phase checkpoint response induces a replication fork arrest or stalling, as various proteins function to detect and repair any DNA damage, before the replication fork resumes its progression towards the completion of S-phase. For the purpose of research experimentation, the intra-S-phase checkpoint is often induced by the use of hydroxyurea (HU) or methylmethane sulfonate (MMS). HU is a ribonucleotide reductase inhibitor that results in replication fork stalling, by the depletion of deoxyribonucleotide phosphate (dNTP) pools (Koc and Merril, 2007). MMS methylates DNA bases which results in a variety of lesions, including double-strand breaks (Dhillon and Hoekstra, 1994). Upon the detection of DNA damage during S-phase, in *S.cerevisiae*, two complexes, namely, Mec1-Ddc2 and Rad24-RFC, assemble at the DNA-damage site independently. (Longhese *et al.*, 2003) (Figures 1.7; 1.8). The Rad24-RFC complex may play a role in the loading of checkpoint or repair proteins, onto damaged DNA (reviewed in Longhese *et al.*, 1998) (Figure 1.7).

Mec1 is a transducer kinase, which is required to activate the effector kinase Rad53 (Radiation-repair protein 53), which in turn, phosphorylates downstream effectors of the checkpoint (Pasero *et al.*, 2003). It is believed that the accumulation of RPA at the

replication fork is the primary signal that triggers the recruitment of Mec1-Ddc2 to the replication fork during an S-phase checkpoint. The phosphorylation of Mrc1 by Mec1, subsequently, promotes the activation of Rad53. Rad53 that has been activated by Mrc1 then acts in *cis* to prevent replication fork collapse and in *trans* to block further initiation events (Pasero *et al.*, 2003). Another downstream target of Mec1 is Ddc1-Rad17-Mec3 complex that forms a structure that encircles the DNA (reviewed in Longhese *et al.*, 2003). It is often referred to as a checkpoint clamp (reviewed in Harrison and Haber, 2006). The mechanism by which this acts is not fully known, but it likely serves to recruit Mec1 substrates for phosphorylation (Harrison and Haber, 2006) (Figure 1.7).

In a distinct, but partially redundant pathway, Tel1 complexes with the MRX trimeric complex (consisting of Mre11, Xrs2 and Rad50) (reviewed in Longhese *et al.*, 2003). Tel1 and MRX have been shown to be recruited to double-strand break (DSB) ends (reviewed in Harrison and Haber, 2006). The MRX complex acts in DNA repair by a mechanism of action that isn't fully understood. However, it has been suggested that the MRX complex functions to facilitate homologous recombination (Longhese *et al.*, 2003) (Figure 1.8.). It may also control DSB processing, thereby amplifying the checkpoint signal and stimulating Mec1/Tel1 kinases (reviewed in Longhese *et al.*, 2003). Interestingly, there seems to be some overlapping function between Mec1 and Tel1 (discussed in Longhese *et al.*, 2003). Tel1 has been shown to activate Rad53 in an S-phase checkpoint in the absence of Mec1 (discussed in Harrison and Haber, 2006).

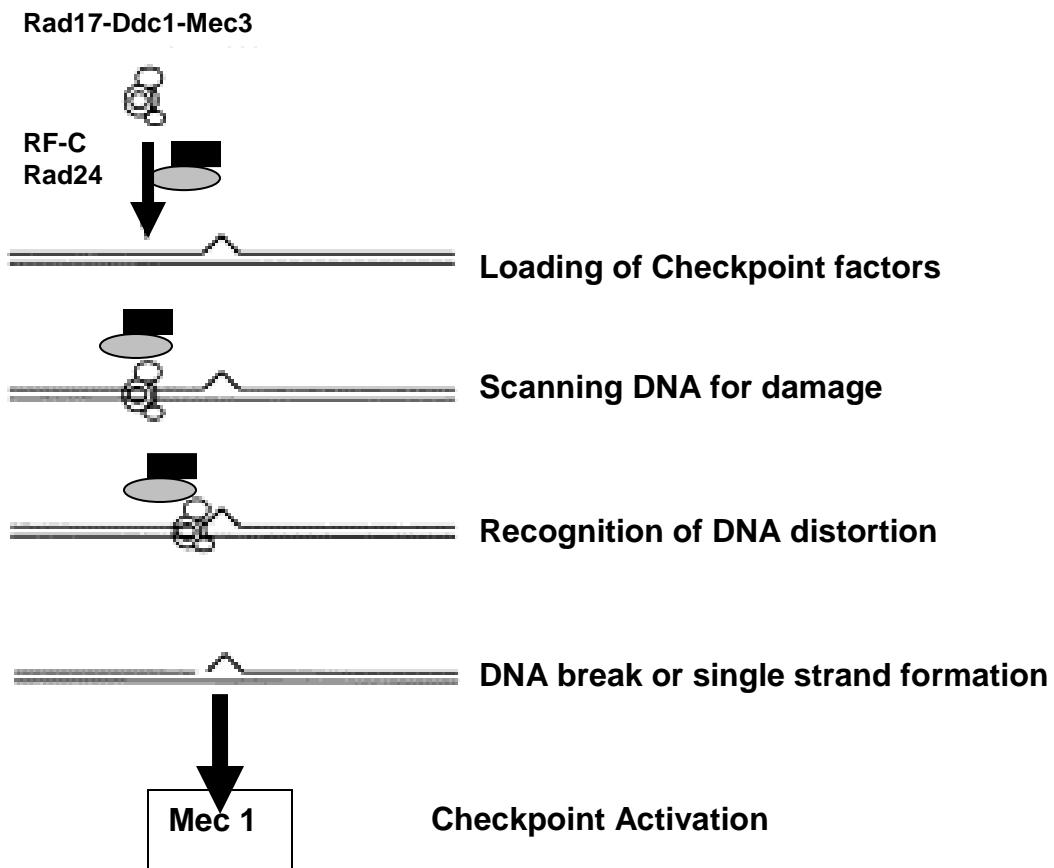


**Figure 1.7. Rad17-Ddc1-Mec3 pathway of the intra-S-phase checkpoint response.** Rad17-Ddc1-Mec3 along with RFC and Rad24 assembles onto the DNA, recognizes DNA damage and activates Mec1. This figure is adapted from Foiani *et al.* (2000) reproduced with permission.

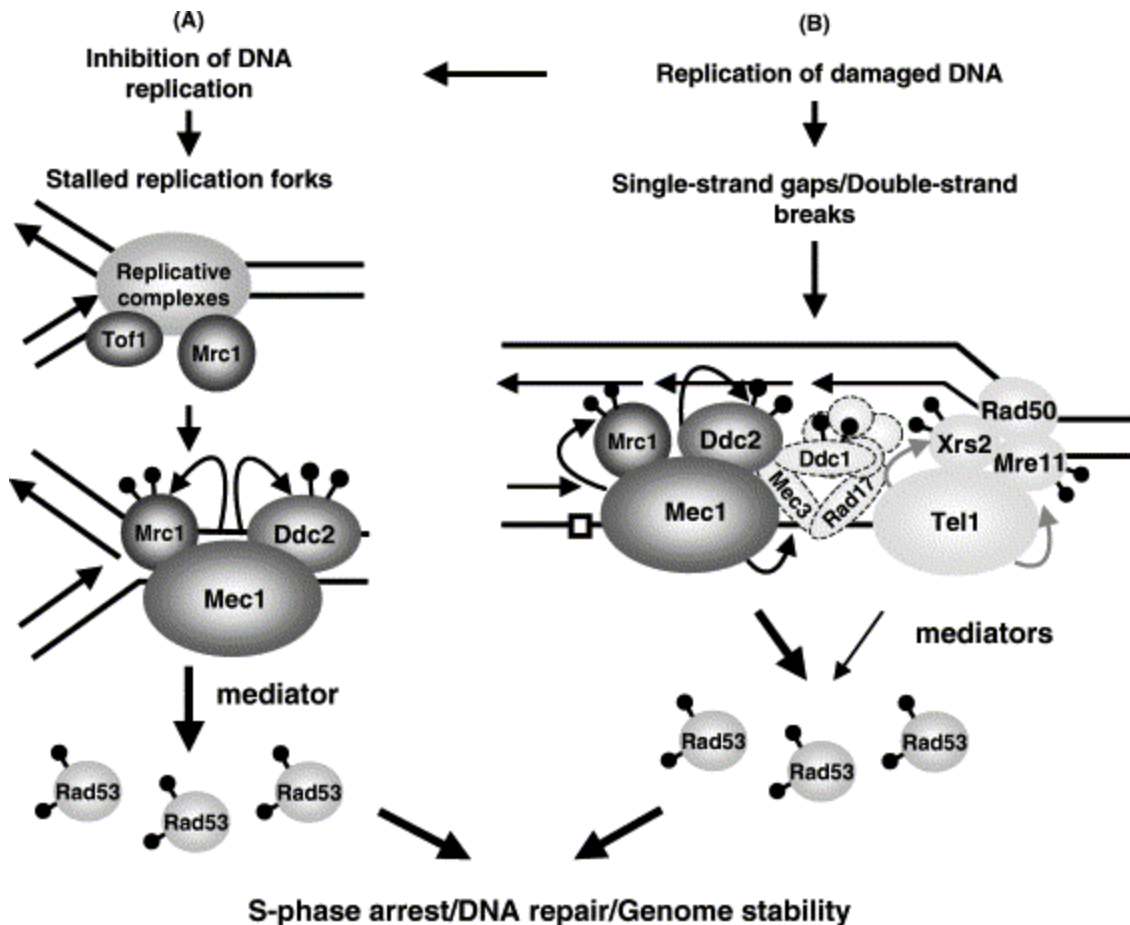


**Figure 1.8. S-phase Checkpoint Response.** **A.** S-phase checkpoint response triggered by a replication fork stalling that was induced by dNTP pool depletion. Mec-Ddc2 complexes with Tof1, Mrc1 and other factors at the replication fork resulting in the downstream activation of Rad53. **B.** Replication S-phase checkpoint induced by DNA damage (double-strand breaks). Mec-Ddc2 activates the Mec3-Ddc1-Rad17 ring-shaped complex, ultimately resulting in the downstream activation of Rad53. In an alternate pathway, Tel1 complexes with the MRX trimeric complex (consisting of Mre11; Xrs2 and Rad50) resulting in the downstream activation of Rad53 (through mediators). This figure is from (Longhese *et al.*, 2003), reproduced with permission.

Ultimately, the main effects of the intra-S-phase checkpoint response are replication fork stabilization, replication fork recovery and regulation of late-firing origins. Although, the regulation of late-firing origins *via* the interaction between Rad53 and the Dbf4/Cdc7 (DDK) was a main focus of this thesis, it is not the primary mechanism of the intra-S-phase checkpoint. Late-firing origin regulation serves to slow S-phase during the checkpoint. However, the stabilization of replication forks appears to be critical in ensuring cell survival. Tercero *et al.* (2003) treated two *mec1* mutants (*mec1-100* and *mec1Δ*) with MMS. The *mec1Δ* mutant was hypersensitive to MMS treatment but the *mec1-100* mutant was not. The *mec1Δ* mutant also had a 10-fold higher rate of replication fork breakdown than that of the *mec1-100* mutant. However, both the *mec1Δ* and the *mec1-100* mutants were defective in the regulation of late-firing origins. This result suggested that the regulation of late-firing origins and the stabilization of replication forks in the intra-S-phase checkpoint are separable functions (reviewed in Pasero *et al.*, 2003).

Nonetheless, the mechanism by which Dbf4/Cdc7 (DDK) is removed from the late-firing origins by Rad53, preventing the origins from firing has not been well studied (reviewed in Duncker and Brown, 2003). This mechanism was a main focus of this study and is discussed in detail in the text to follow. In spite of the data discussed above, which indicates that the Rad53-Dbf4 mediated regulation of origin firing is not a major mechanism by which a cell survives DNA damage, it is a conserved function among two evolutionarily divergent organisms: *S. cerevisiae* and *S. pombe*. It has been suggested that, it is likely that even this modest fitness defect can lead to the loss of a given strain from a mixed population of cells (reviewed in Duncker and Brown, 2003). Therefore, this

relatively minor protective function for surviving DNA damage could, in fact, be a significant competitive advantage within a mixed population of cells over many generations (reviewed in Duncker and Brown, 2003).

Beyond the regulation of origin firing, DDK may protect cells during the intra-S-phase checkpoint in other ways. In a recent study, Szyjka *et al.* (2008), have suggested that Rad53 deactivation is a key mechanism controlling replication fork restart following DNA damage. In fact, Szyjka *et al.* (2008) have proposed a model in which Rad53 inhibits Cdc7-Dbf4 activity in normal replication initiation at origins, while stimulating Cdc7-Dbf4 activity in replication fork restart following a checkpoint (Szyjka, *et al.*, 2008). This new model will likely provoke a renewed interest in the Dbf4-Rad53 interaction and is a good testament to the relevance of the work that has been carried out in the present study.

## **1.7 Cdc7/Dbf4 Complex**

In *S.cerevisiae*, the Cdc7 and Dbf4 proteins form an active kinase complex that is essential for the initiation of DNA replication (Dohrmann, *et al.*, 1999). Cdc7 is activated by binding the regulatory protein Dbf4 (Jackson *et al.*, 1993). Cdc7 protein levels remain constant throughout the cell cycle, with its kinase activity peaking at the G1/S transition (Jackson *et al.*, 1993). The levels of Dbf4 fluctuate throughout the cell cycle, increasing in late G1 phase, remaining at high levels throughout S-phase and into M-phase. Dbf4 is then degraded by the APC/C (Anaphase-promoting-complex/cyclosome) in M-phase (Weinreich and Stillman, 1999; Cheng *et al.*, 1999).

In *S. cerevisiae*, origins initiate replication at characteristic times, with some firing in early S-phase, most in mid S-phase and others in late S-phase (Friedman *et al.*, 1996; Raghuraman, *et al.*, 2001). The Dbf4/Cdc7 kinase complex is required for initiation to occur at each origin (reviewed by Jares *et al.*, 2000). That is, Cdc7/Dbf4 has been shown to be required in early S-phase for the initiation of early-firing origins as well as in late S-phase for the initiation of late-firing origins (Bousset and Diffley, 1998).

Two models have been put forward regarding the role of Cdc7/Dbf4 and the regulation of origin firing. One hypothesis proposes that Dbf4 targets Cdc7 kinase to the pre-RC through an association with ORC that is independent of Clb/Cdc28, resulting in replication origin firing (Pasero *et al.*, 1999; Duncker *et al.*, 2002). A second model has been proposed that suggests that Cdc7 remains at origins of replication throughout the cell cycle and Dbf4 complexes with Cdc7 during S-phase resulting in replication origin firing (Duncker and Brown, 2003).

### **1.8 Dbf4 N, M and C-motifs**

Sequence alignment comparisons between *S. cerevisiae* and other species (*Schizosaccharomyces pombe*, *Xenopus laevis*, *Drosophila melanogaster*, *Homo sapiens*) have revealed several orthologs of Dbf4 (Masai and Arai, 2000). Despite an overall poor conservation of amino acid sequence, there are three motifs that are very well conserved among the species that have been studied (Masai and Arai, 2000). These three motifs have been termed N, M and C. In *S. cerevisiae*, motif N corresponds to amino acids 129-179, motif M corresponds to amino acids 260-309 and motif C corresponds to amino acids 659-696 of Dbf4 (Masai and Arai, 2000; Duncker and Brown, 2003) (Figure 1.9). It

should be noted that there are different reports regarding which amino acid defines C-terminal boundary of the N-motif (Masai and Arai, 2000; Duncker and Brown, 2003). However, throughout this study, amino acid 179 is consistently labelled and presented as the C-terminal boundary of the N-motif. Previously, the functions associated with the three motifs had not been well studied in *S. cerevisiae*. However, in fission yeast (*Schizosaccharomyces pombe*), some interesting work has been performed by various researchers that have investigated the functions of these three motifs. These studies have revealed distinct and separable roles for these domains in DNA replication and checkpoint response functions (Fung *et al.*, 2002; Ogino, *et al.*, 2001). Also, investigations with *S. pombe* have shown that the N-motif of the Dbf4-ortholog Dfp1 is dispensible for cell cycle progression under normal conditions (Ogino, *et al.*, 2001; Fung *et al.*, 2002). In a study testing mutants with various complete and partial deletions of the N-motif in *S. pombe*, the deletion mutants were able to complement a *dfp1* null strain mutant strain. The deletions also caused sensitivity to HU treatment (Ogino *et al.*, 2001). These results suggested that the N-motif is involved in the intra-S-phase checkpoint response. A deletion of a highly conserved stretch of 8 amino acids (183-191) (containing critical threonine residues) within the N-motif in *S. pombe* resulted in a mutant strain that is sensitive to a wide-range of DNA damaging agents (Fung *et al.*, 2002). It is relevant to note that point mutations of a serine and two threonine residues (Dfp1 amino acids: serine 182 and threonines at position 187 and 191) to alanine or glutamic acid in the same region by another research group produced similar results (Ogino, *et al.*, 2001). In *S. cerevisiae*, Duncker *et al.* (2002) demonstrated that a 186 amino acid stretch of Dbf4 mediates interactions with both ORC and Rad53 and suggested a mechanism, whereby,

Rad53 binds directly to and/or phosphorylates the Dbf4 N-terminus when the S-phase checkpoint is triggered resulting in its displacement from unfired replication origins. It should be pointed out here that prior to the initiation of the present study, a detailed functional characterization of the Dbf4 conserved motifs had not been carried out in *S. cerevisiae*.

The Dbf4 C-motif is the most highly conserved of the three motifs (Masai and Arai, 2000). It contains a highly conserved GXCECX(X<sub>9</sub>)H(X)<sub>2</sub>FA region, which resembles a CCHH-type zinc finger motif (Masai and Arai, 2000). The Cys2-His2 class of zinc-finger proteins are very structurally stable in that the zinc-finger can retain its characteristic folding, in spite of changes in amino acids. In fact, studies using Nuclear Magnetic Resonance (NMR) and Crystallography have revealed that the Cys2-His2 class of zinc fingers are stable with some degree of plasticity, and have shown that a single zinc finger domain can tolerate many sequence changes while retaining its ability to fold correctly (reviewed in Hoffman *et al.*, 1993). The amino acid residues between the two cysteines and between the two histidines that compose the zinc-finger can be variable. Furthermore, the mutation of one of the histidines to alanine or tyrosine of the zinc finger protein ADR1, did not cause any structural perturbations, as was determined using NMR methods (Hoffman *et al.*, 1993). This is important because protein-induced DNA distortions can alter the positions of DNA bound proteins, relative to one another, which can affect protein-protein interactions (Shi and Berg, 1996). Thus, mutations that influence or alter protein-DNA binding can also, indirectly, influence protein-protein interactions. It is noteworthy that there are examples of zinc-finger proteins functioning to unwind DNA (Shi and Berg, 1996).

To date, there have been no published studies specifically investigating the Dbf4 C-motif in the *S. cerevisiae* model. There have, however, been some complementation assays, as well as one and two-hybrid assay studies involving C-terminally truncated Dbf4 constructs. Two-hybrid assay results revealed, for the first time, that Dbf4 physically interacts with and positively regulates the Cdc7 kinase (Dowell *et al.*, 1994). Furthermore, the one-hybrid assay results indicated that Dbf4 interacts with initiation complexes at yeast replication origins, *in vivo*, and that interaction requires a binding site for ORC. Two of five constructs that expressed Dbf4 mutant proteins truncated at the C-terminus (including the C-motif) (Dbf4 amino acids 4 to 416; Dbf4 amino acids 81 to 416) were able to complement a Dbf4 temperature sensitive strain (*dbf4-2*), which was not viable at 37°C. However, three constructs that expressed Dbf4 mutant protein truncated at the C-terminus (Dbf4 amino acids 1 to 320; 1 to 160; 241-416) were not able to complement the same temperature sensitive strain at 37°C. These variable results could suggest that the C-motif is dispensable for viability in *S. cerevisiae*. Interestingly, the truncated proteins that were expressed from the constructs that did complement were also able to bind to Cdc7 in two-hybrid assay. They also appeared to bind to ARS1 in the one-hybrid assay (Dowell *et al.*, 1994). The three truncated proteins that did not complement also did not bind to ARS1 in the one-hybrid assay. Jackson *et al.* (1993), reported that deleting the C-terminal domain of Dbf4 increases the interaction with Cdc7 in a two-hybrid assay. They explained this increase in interaction by pointing out that this region of Dbf4 has a PEST sequence, that possibly has an effect on the stability of the protein. This instability of Dbf4 could possibly be limiting Cdc7 protein kinase activity (Jackson *et al.*, 1993).

Some studies have examined the C-motif of Dbf4 orthologues in other organisms. *Aspergillus nidulans* is a filamentous fungus that can exhibit two modes of cellular morphogenesis: hyphal growth and yeast growth. Hyphal growth involves the extension of hyphae (long tubular structures, typically partitioned into individual cellular compartments by the formation of septa). During yeast growth yeast cells do not undergo sustained polarized growth; they generally cycle between periods of polarized and isotropic growth. Secondly, upon the formation of septa, yeast cells subsequently separate into individual cells (i.e. budding). Many filamentous fungi exhibit both forms of cellular morphogenesis. During their vegetative phase they proliferate as hyphae, followed by a switch to yeast-like growth upon entry into asexual development (i.e., conidiation) (Harris *et al.*, 2009).

The *Aspergillus nidulans* Dbf4 orthologue is NimO. James *et al.* (1999) reported a complementation assay involving a temperature sensitive (ts) lethal *nimO* strain. The *nimO18 ts* lethal mutant has a general defect in DNA synthesis, and at the nonpermissive temperature, it behaves as a null mutation. Interestingly, the overexpression of NimO with a C-terminal truncation (up to 244 amino acids) was able to support hyphal growth (described above) in a *ts*-lethal *nimO* strain. However, the same overexpressed truncated allele was not able to support asexual growth (James *et al.*, 1999). These findings led them to conclude that the C-terminus of the *Aspergillus nidulans* Dbf4 orthologue (NimO) is essential for viability (James *et al.*, 1999).

In the fission yeast model, in one study, mutant strains in which the Dfp1 C-motif was partially or completely deleted, were found to be viable (Fung *et al.*, 2002). However, these same mutant strains were more sensitive to MMS than wild type cells,

but were not more sensitive to treatment with HU, ultraviolet (UV) irradiation or ionizing (IR) irradiation (Fung *et al.*, 2002). It is of particular interest to note that although the *S. pombe* C-motif mutants are sensitive to MMS, they retain an intact intra-S-phase checkpoint (Fung *et al.*, 2002). It is also noteworthy that another research group has published contradictory results. Ogino *et al.* (2001) found that the C-motif is essential for viability. It was suggested that this difference could be accounted for by different methods employed in the complementation assay (Fung *et al.*, 2002). Fung *et al.* (2002) initially demonstrated that the C-motif was dispensable using a plasmid shuffle strategy and then followed-up with genomic integration of a Dbf4 mutant allele lacking the C-motif. The results published by Ogino *et al.* (2001) showed that a plasmid expressing the Dbf4 orthologue (lacking the C-terminus) was unable to support viability in a null mutant. It is possible that the expression levels of the plasmids in the Ogino *et al.*, (2001) study were not high enough to support growth.

In a study involving mammalian cell lines, a series of truncation and deletion mutants of the Dbf4 orthologue ASK were constructed as fusion proteins with Green Fluorescent Protein (GFP). These ASK mutants were tested for their ability to bind to and activate Cdc7, leading to the hyperphosphorylation of Mcm2 (Sato *et al.*, 2003). Among those ASK polypeptides tested, only those carrying both the Dbf4 M and C-motifs were able to activate wild type Cdc7 (Sato *et al.*, 2003).

In the African aquatic clawed frog model (*Xenopus laevis*), Dbf4 has been found to be a Wnt inhibitor, which is crucial for early development (Brott and Sokol, 2005). Interestingly, overexpression of the mutant Dbf4 $\Delta$ M $\Delta$ C (lacking M and C motifs) was

able to rescue heart marker expression in Dbf4 depleted explants (Brott and Sokol, 2005). Since, Dbf4 $\Delta$ M $\Delta$ C inhibits  $\beta$ -catenin signalling, Dbf4's role in heart development is



**Figure 1.9. Conserved motifs of Dfp1/Dbf4.** Amino acid residues corresponding to the conserved N, M and C motifs are indicated. Dfp1 is the *Schizosaccharomyces pombe* orthologue of Dbf4. This figure is from (Duncker and Brown, 2003) reproduced with permission.

likely to involve Wnt inhibition and seems to be a component of a pathway that is independent of its interaction with Cdc7 (Brott and Sokol, 2005). Data suggests that Dbf4 acts through physical and functional interaction with Frodo, a context-dependent regulator of Wnt signalling (Brott and Sokol, 2005). Nonetheless, this function of the Dbf4 orthologue appears to be unrelated to its cell cycle and checkpoint roles.

### **1.9. Rad 53**

In *S. cerevisiae*, Rad 53, an effector checkpoint kinase, is known to be involved in the G1/S, Intra-S-phase and G2/M checkpoints (reviewed in Elledge, 1996). Rad53 consists of a kinase or activation domain flanked by two fork-head homology associated domains (FHA1 and FHA2) (Figure 1.10). Rad53 is the only known protein that contains two FHA domains (discussed in Hammet *et al.*, 2003). The tertiary structure has been obtained for yeast Rad53 FHA1 and FHA2 (Liao *et al.*, 2000). FHA domains act as protein-protein interaction modules and tend to target phosphothreonine (Thr(P)) protein ligands. They consist of 100-180 amino acid residues that form an 11-stranded  $\beta$ -sandwich structure (Durocher and Jackson, 2002). FHA domains can be found in many proteins, functioning in organisms ranging from bacteria to mammals. It is noteworthy that although FHA domains have diverse biological function; they are commonly found in proteins that are involved in cell cycle and checkpoint pathways (discussed in Pike *et al.*, 2003; Yongkiettrakul *et al.*, 2004). Three main factors have been identified that influence the ligand specificity of FHA domains: a phosphothreonine residue target, the residues at the +1 and +3 position from the pThr and the presence of an extended binding surface (Yongkiettrakul *et al.*, 2004).

Two-hybrid assay studies have demonstrated that Rad53 binds to Dbf4 (Dohrmann, *et al.*, 1999). In a subsequent study, Duncker *et al.* (2002) demonstrated that the N-terminal domain of Dbf4 mediates the interaction with the Rad53 FHA1 and FHA2 domains using two-hybrid assay and co-immunoprecipitation methods. The Rad53 FHA1 interaction with Dbf4 is considerably stronger than the Rad53 FHA2-Dbf4 interaction. Pike *et al.* (2003) proposed a model suggesting that both FHA1 and FHA2 domains of Rad53 interact with Dbf4/Cdc7 resulting in the inhibition of late replication origins. Tam *et al.* (2008) investigated the importance of the relative position of FHA1 and FHA2 domains of Rad53. They constructed three Rad53 alleles in which FHA1 and FHA2 domains were transposed to the opposite location, either individually or simultaneously (Tam *et al.*, 2008). That is, the positions of the Rad53 FHA domains were altered relative to each other in a series of mutants. These Rad53 mutants were hypersensitive to MMS. These authors proposed that MMS sensitivity was caused by the cells inability to stabilize stalled replication forks during S-phase, which is FHA-dependent. Interestingly, the same three mutants were not hypersensitive to bleomycin treatment in a growth plate spotting assay (Tam *et al.*, 2008). Bleomycin is a drug that mimics the effects of ultraviolet radiation. They attempted to explain this difference by suggesting that there may be an alternative or redundant Rad53 activation mechanism in the response to bleomycin that is not available for the response to MMS damage (Tam *et al.*, 2008). That is, the response to bleomycin-induced DNA damage is independent of the FHA domains. It is possible that a dose of bleomycin treatment, higher than what was used in the growth spotting assay performed by Tam *et al.* (2008), might have caused increased sensitivity. As stated above, Bleomycin is a U.V. mimetic drug, which causes pyrimidine dimerization of the

DNA backbone residues. The subsequent excision and repair of the pyrimidine dimerization can lead to single and double strand breaks of the DNA. Presumably, at higher doses of Bleomycin treatment, more single and double strand breaks would occur, possibly leading to a phenotype of sensitivity in a growth spotting assay. Nonetheless, it was concluded that both FHA domains of Rad53 can only fulfill their functions when they are in their natural position. Fiorani *et al.*, (2008) demonstrated the importance of two highly conserved phosphorylatable threonine residues (T354 and T358) in the kinase domain of Rad53. Mutants in which T354 and T358 were mutated to alanines, were checkpoint impaired and hypersensitive to genotoxic agents.

Rad53 has several known targets and binding partners (Sidorova and Breeden, 2003). Smolka *et al.*, (2006) performed a biochemical screen to identify proteins with specific affinity for the two FHA domains of Rad53. Their results suggested a novel function for Rad53 in the regulation of polarized cell growth in response to DNA replication stress. The FHA1 domain was found to coordinate a complex protein interaction that includes nuclear checkpoint proteins and transcriptional regulators. In an unexpected finding, FHA1 also seems to bind to cytosolic proteins involved in cytokinesis, including septins.

In addition to its checkpoint function, Rad53 has an essential function which is believed to be the regulation of dNTP precursors (reviewed in Sclafani, 2000). This has been established by the fact that the *rad53Δ* mutant is nonviable. However, the *rad53ΔsmlΔ* double mutant is viable. Sml1 inhibits the activity of ribonucleotide reductase (RNR). RNR is a multi-subunit enzyme that catalyzes the synthesis of dNTPs from nucleotide triphosphates (NTPs). Essentially, Rad53 regulates Sml1. Thus, deletion

of the *SML1* gene can bypass the essential function of Rad53. Koc and Merril (2007) tested whether the checkpoint mutant *rad53-11* affected dNTP levels in cells exposed to ethylmethane sulfonate (EMS) (a DNA-damaging agent). They observed that following EMS treatment, the wild type cells had increased dNTP levels and the *rad53-11* mutant cells did not. This difference in dNTP levels suggests that Rad53 is involved in the dNTP pools expansion in cells that have experienced DNA damage (Koc and Merril, 2007). Recently, Dohrmann and Sclafani (2006), have proposed a novel role for Rad53 in the initiation of DNA replication that is independent of checkpoint and dNTP regulation. They suggested that Rad53 may be regulating initiation of DNA replication by controlling histone protein levels and/or by affecting origin chromatin structure (Dohrmann and Sclafani, 2006). They also showed, using the one-hybrid assay, that Rad53 is targeted to the ARS1 (early-firing origin) through its kinase domain (Dohrmann and Sclafani, 2006).

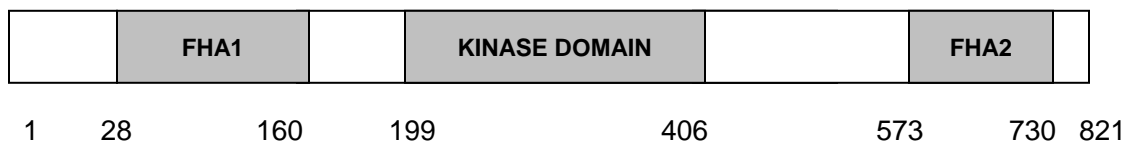


**Figure 1.10. Rad53 protein kinase.** This protein consists of a kinase domain flanked by two Fork-head Homology Domains (FHA1 and FHA2). (Adapted from Lee *et al.*, 2008). The numbers indicate the amino acid residues positions.

## **1.10. Dbf4/Rad 53 and the Intra-S-Phase Checkpoint Response**

Several reports by various research groups have led to the notion that Dbf4 plays a central role in the intra-S-phase checkpoint response (reviewed in Duncker and Brown, 2003). Weinreich and Stillman (1999) demonstrated that Dbf4 becomes phosphorylated after HU treatment and this phosphorylation is dependent on the checkpoint kinase Rad53. Moreover, this Rad53 phosphorylation reduces the Cdc7/Dbf4 kinase activity. In another study, it was observed that there is a Rad53-dependent removal of Dbf4 from chromatin following HU treatment (Pasero, *et al.*, 1999) (Figure 1.11). Recently, Travesa *et al.* (2008) demonstrated that following genotoxic stress, three phosphatases serve to return Rad53 to its basal state. Their results also suggested that there is another unidentified phosphatase that is involved in the recovery from replication stress (Travesa *et al.*, 2008).

Presently, available evidence suggests that during the S-phase checkpoint response, Rad53 is phosphorylated by the upstream kinase Mec1 during HU treatment, *via* Mrc1 (reviewed in Pasero *et al.*, 2003). The phosphorylated Rad53 binds to the N-terminus of Dbf4 and the Cdc7/Dbf4 complex is removed from late-firing origins of replication. In recent years, several studies with *S. cerevisiae* have been published further investigating the role of Rad53 in the intra-S-phase checkpoint response. Ogi *et al.* (2008) showed that the *Δcdc7mcm5-bob1* and *Δdbf4mcm5-bob1* mutants are sensitive to HU and MMS. The *mcm5-bob1* mutant carries a single point mutation in Mcm5 (P83L) causing a structural change that facilitates a bypass of the DDK (Dbf4/Cdc7) function in the initiation of DNA replication (Hoang *et al.*, 2007). Furthermore, Ogi *et al.* (2008) showed that Rad53 was hyperphosphorylated as a result of genotoxic treatment, but

autophosphorylation of Rad53 was reduced. They concluded that Cdc7/Dbf4 is involved in the activation of Rad53 during a checkpoint response. However, this needs to be studied further.

Raveendranathan *et al.* (2006) studied the origin firing of two S-phase checkpoint mutants: *mec1-1* and *rad53-1*. As expected, both the *mec1-1* and *rad53-1* cells failed to inhibit late-origin firing activities. However, they also observed that 17 early-firing origins were not replicated efficiently in the mutants. The authors classified these 17 origins as “compromised early origins”. Two-dimensional agarose gel electrophoresis and chromatin immunoprecipitation experiments confirmed that this phenotype was the result of inefficient elongation and not due to faulty initiation of DNA replication at the early-firing origins. The authors suggested that this problem was likely the result of the fact that replication forks were arrested in close proximity to these origins (Raveendranathan *et al.*, 2006). Thus, recent evidence has further established that Rad53 plays a role in conjunction with Dbf4/Cdc7 kinase complex in the intra-S-phase checkpoint response by regulating late-firing origins. Nonetheless, more work is needed to fully explore this molecular mechanism.

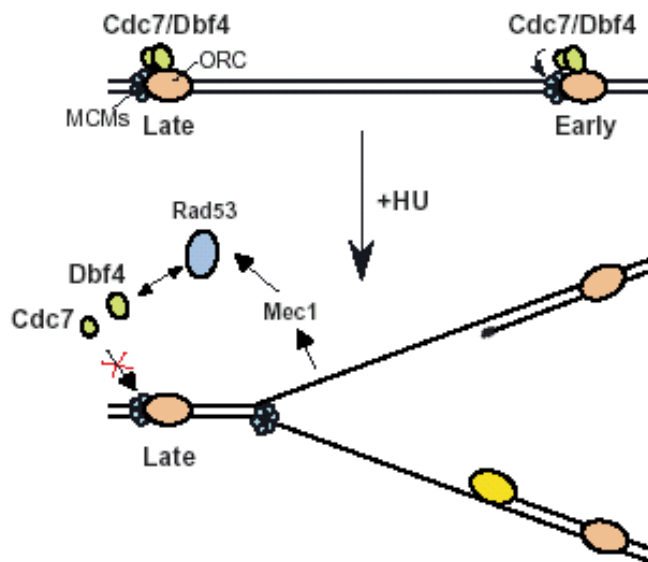


**Figure 1.11. A model in which Cdc7/Dbf4 is an important target of Rad53 regulation during the checkpoint response to HU. Rad53 binding and phosphorylation of Dbf4 prevents Cdc7/Dbf4 phosphorylation of its critical targets at late origins of DNA replication.** This figure is from (Duncker and Brown, 2003) reproduced with permission.

## **1.11 Research Objectives**

At the outset of this research, *S. cerevisiae* Dbf4 was known to play an important role in the initiation of DNA replication. However, the role of Dbf4 in the Intra-S-phase checkpoint response was still not well characterized. Dbf4 was known to be a promiscuous protein with many known binding partners. However, there were still some questions relating to the many known protein-protein interactions in which Dbf4 engages. The fact that the three Dbf4 motifs (N, M and C) are highly conserved among eukaryotes, despite an overall poor degree of conservation, made Dbf4 interesting from an evolutionary perspective. However, the importance of the three motifs had been largely unstudied, with respect to the protein-protein interactions that they were involved in mediating. Furthermore, there was no published structural data pertaining to Dbf4. Thus, there were numerous unanswered questions relating to the Dbf4's involvement in the intra-S-phase checkpoint response, the functional importance of the three conserved motifs in the initiation of DNA replication, their essentiality for cell viability and their specific involvement in various protein-protein interactions .

The role of Dbf4 in the Intra-S-phase checkpoint response was not well characterized when this research study was initiated. It had been proposed that the Dbf4-Rad53 interaction mediated the removal of Dbf4 from late-firing origins, regulating the firing of late origins (Duncker *et al.*, 2002; Duncker and Brown, 2003) (Figure 1.11). It was also hypothesized that replication fork stability and/or the replication fork recovery from the checkpoint response were important functions of Dbf4 and/or Rad53 in the intra-S-phase checkpoint response. However, the mechanisms by which these occurred were not known. Thus, in an attempt to investigate the role of Dbf4 in the intra-S-phase

checkpoint response, this research study was undertaken with an intent to first identify the Rad53 binding site in Dbf4 through mutagenesis experiments.

The roles of the conserved Dbf4 motifs in initiation of DNA replication were also investigated, in the present study. Specifically, the protein-protein interactions mediated by the conserved motifs were studied by employing a mutagenesis approach in conjunction with two-hybrid assay methods. Finally, it was thought that a successful determination of the complete or partial crystal structure of Dbf4 would provide a valuable tool for the characterization of the Dbf4-Rad53 interaction and other Dbf4 protein-protein interactions, from a structural perspective.

In summary, the research presented in this thesis is focused on the roles of Dbf4 motifs in the initiation of DNA replication and in the intra-S-phase checkpoint response. The three highly conserved motifs in Dbf4 were studied and dissected by mutational analysis to determine their involvement in the protein-protein interactions with the various known cell cycle and checkpoint protein binding targets of Dbf4 (Rad53, Mcm2, Mcm4, Orc2, Cdc7). The necessity of the motifs for Dbf4's essential function was determined, and whenever possible, *in vivo* phenotypes were also studied. Because this work constituted something of a pioneering venture, the results obtained could be used as a base-line for further research.

The three main research objectives that were investigated in this study are listed below:

1. To identify and mutate Rad53 binding site(s) in Dbf4
2. To determine the roles of the three Dbf4 motifs: Motif N, M and C, involved in the interactions with various cell cycle and checkpoint factors.

3. To determine the three-dimensional protein structure of the Dbf4 by X-Ray crystallography.

## **1.12 Relevance to Biomedical Sciences and Cancer**

Although this work was carried out from a basic research perspective, it is still of relevance to discuss this research within a context of applications to biomedical sciences. Recent data depicting the aberrant human Dbf4 orthologue expression as phenotypes of various cancer cells points to the potential of using Dbf4 as a biomarker for cancer diagnosis or, possibly, as a therapeutic target. Thus, the existing Dbf4 data derived from the *S. cerevisiae* model could be used as a foundation for such research and development. Moreover, it is also reasonable to think that these recent findings could also influence the direction of future research involving the *S. cerevisiae* model.

The most notable of recent findings involving the human system include results indicating that the human orthologue of Dbf4 has been shown to be upregulated in various cancer and tumour cell lines (Bonte *et al.*, 2008; Nambiar *et al.*, 2007). Furthermore, multiple copies of Dbf4 have been observed in tumour cell lines (Bonte *et al.*, 2008). Moreover, a high correlation between p53 loss and increased Cdc7 and Dbf4 expression in primary breast cancers and in the cancer cell lines has also been observed (Bonte *et al.*, 2008). The results summarized above lend further validity to the Dbf4 research, using the *S. cerevisiae* model, as a prelude or complement to studies carried out in the human or other mammalian model organisms. Ultimately, it is hoped that this research will contribute, directly, or, indirectly, to a greater understanding of the molecular mechanisms governing the onset and progression of cancer. Furthermore, such

knowledge could, eventually, be used to develop cancer diagnostic methods and therapeutics.

## **CHAPTER 2: Materials and Methods**

## 2.1. Cloning

Most of the cloning was done directionally, using the PCR amplification method in conjunction with forward and reverse primers along with genomic DNA or plasmid DNA as a template to generate DNA inserts which were ligated into plasmid vectors at specific restriction sites. The plasmids that were created and used are listed in Table 2.1.

The primers that were used are shown in Table 2.2.

A series of bait and prey vectors was constructed to be used for the two-hybrid assays. Some already existed in the lab stocks. The bait plasmid that was used was pEG202 (Ausubel *et al.*, 1995). Most pEG202 Dbf4 variant vectors were constructed using a forward primer (Dbf4 Eco For) containing an *EcoRI* restriction site, annealing to the start of the of the *DBF4* gene. The reverse primer (Nco Rev) contained an *NcoI* restriction site and annealed to the end of the *DBF4* gene. The pEGDbf4 N-motif point mutant plasmids (pEGDbf4T171A, pEGDbf4T175A, pEGDbf4T171AT175A, pEGDbf4T168AT169A, pEGDbf4T168AT169AT171AT175A, pEGDbf4W202E, pEGDbf4GA159LL) were constructed using QuickChange Mutagenesis kit (Stratagene) as described below using pEGDbf4wt (FL) (Duncker *et al.*, 2002) as a template plasmid. This plasmid contains the entire wild type *DBF4* sequence. The QuickChange primers were designed to anneal to the desired mutation site are listed in Table 2.2.

pEGDbf4 $\Delta$ 168-178 was created by ligating two PCR generated DNA inserts into a digested pEGDbf4wt backbone that was digested with *EcoRI* and *Kpn*21 restriction enzymes. Initially the pEGDBFwt (FL) plasmid was digested with *EcoRI* and *Kpn*21 restriction enzymes, resulting in the removal of insert DNA to prepare for the insertion of the *DBF4* $\Delta$ 168-178 mutant. As mentioned above, the *DBF4* $\Delta$ 168-178 was created by

fusing two DNA inserts into the digested backbone vector. To create the first DNA insert, the pEGDbf4wt plasmid was used as a template, along with a forward primer (Dbf4 Eco For) containing an *EcoRI* restriction site annealing to the start of the Dbf4 gene, was used in conjunction with a reverse primer (Dbf4 AatII Rev) containing an *AatII* restriction site that annealed to the *DBF4* gene at the nucleotides encoding for amino acid 168. This PCR product DNA insert was digested with *EcoRI* and *AatII*. The second PCR DNA insert was created, using the same template along with a forward primer (Dbf4 AatII For) having an *AatII* site, annealing to the Dbf4 gene at the nucleotides encoding for amino acid 178. A reverse primer (Nco Rev) annealing to the end of the *DBF4* gene in conjunction with the forward primer described above. The first PCR DNA insert was digested with *EcoRI* and *AatII* restriction endonuclease enzymes. The second PCR DNA insert was digested with *AatII* and *Kpn21*. The two PCR DNA inserts were ligated into the digested plasmid to create pEGDbf4Δ168-178.

The prey plasmid that was used in the two-hybrid assays was pJG4-6 (Duncker *et al.*, 2002). All pJG vectors were constructed using a forward primer (Dbf4 Nco For) containing an *NcoI* restriction site and a reverse primer (Eco Rev) containing an *EcoRI* restriction site.

pRSDbf4Δ168-178 was created using the pEGDBf4Δ168-178 plasmid as a template, using a forward *EcoRI* primer (Dbf4 Eco For) and a reverse *SalI* primer (Dbf4 Sal1 Rev) in a PCR reaction to create a DNA insert that was subsequently digested with *EcoRI* and *SalI*. This DNA insert was ligated into a pRS406 vector backbone that was digested with *EcoRI* and *SalI*.

pCM190Dbf4 C-motif point mutant plasmids (pCMDbf4AAHH, pCMDbf4CCAA, pCMDbf4CCHC, pCMDbf4CCHA) were constructed using the pCMDbf4wt(FL) plasmid (Duncker *et al.*, 2002) as a template using the Quickchange Mutagenesis kit (Stratagene) as described below.

The pEGDbf4 C-motif point mutant series (pEGDbf4AAHH, pEGDbf4CCAA, pEGDbf4CCHC, pEGDbf4CCHA) was created using the pCM190Dbf4 C-motif point mutant plasmids as templates for PCR reactions. A forward primer (Dbf4 Eco For) containing an *EcoRI* restriction site, annealing to the start of the Dbf4 N-terminus was used in conjunction with a reverse primer (Nco Rev) that contained an *NcoI* restriction site and annealed to the end of the *DBF4* gene. The PCR inserts were digested with *NcoI* and *EcoRI* and ligated into a pEG202 plasmid backbone digested with *NcoI* and *EcoRI*.

The pJGDbf4 C-motif point mutant series (pJGDbf4AAHH, pJGDbf4CCAA, pJGDbf4CCHC, pJGDbf4CCHA) was created using the pCM190Dbf4 C-motif point mutants as plasmid templates for PCR reactions, using forward and reverse primers. A forward primer (Dbf4 Nco For) containing an *NcoI* restriction site, annealing to the start of the *DBF4* gene was used in conjunction with a reverse primer (Eco Rev) that contained an *EcoRI* restriction site and annealed to the end of the *DBF4* gene. The PCR products were digested with *NcoI* and *EcoRI* and ligated into a pJG4-6 plasmid backbone digested with *NcoI* and *EcoRI*.

The pRSDbf4 $\Delta$ C construct was created by ligating two digested PCR product DNA inserts into a linear pRS406 vector digested with *BamHI* and *EcoRI*. The first PCR DNA insert was created using pEGDbf4wt as a template along with a forward primer (Dbf4 Eco For) containing an *EcoRI* restriction site, annealing to the start of *DBF4* gene

in a PCR reaction with a reverse primer. The reverse primer (Rev Dbf4 Sal1 deltaC) contained a *SalI* restriction site and annealed to the nucleotide sequence encoding the beginning portion of the C-motif of *DBF4*. It is important to note that there was a single (silent) nucleotide change of Dbf4 nucleotide 1965 A to C to create the *SalI* site. The first PCR insert was digested with *SalI* and *EcoRI*. The second PCR insert was created using pRSDbf4ΔN, as a template, along with a forward primer (For *SalI* Dbf4deltaC) containing a *SalI* restriction site, annealing to the end portion of the *DBF4* C-motif nucleotide sequence and a reverse primer (Rev upstream of pRS MCS) containing a *BamHI* restriction site annealing to plasmid sequence upstream of the multiple cloning site of the pRS406 vector. The second PCR insert was digested with *SalI* and *BamHI* restriction enzymes. It is also important to note that there was another single nucleotide change creating the *SalI* site (Dbf4 nucleotide 2094 A to C) as a consequence of the reverse primer that was used, resulting in a change of a glutamic acid to aspartic acid. The pRS406 vector digested with *EcoRI* and *BamHI* was ligated with the first and second DNA inserts described above. The two DNA inserts were ligated together at the complementary *SalI* restriction site that was created by the mutation of nucleotides 1965 and 2094 of *DBF4*. The resultant *DBF4ΔC* mutant allele had base pairs 1966 to 2091 removed from the wild type *DBF4* sequence.

The pEGDbf4ΔC plasmid was created utilizing the pRSDbf4ΔC as a template for a PCR reaction, using an *EcoRI* forward primer (Dbf4 Eco For) annealing to the start of the *DBF4* gene and a reverse primer (Rev NcoI) containing an *NcoI* restriction site, annealing to the end of the *DBF4* gene. The pCM190myc plasmid (from Duncker Lab frozen stocks) was used to create the pCMDbf4ΔC and pCMDbf4C-TERM plasmids. The

pCMDbf4ΔC plasmid was constructed using the pRSDbf4ΔC, as plasmid template, along with a forward primer (BamHI Dbf4 For) containing a *BamHI* restriction site that annealed to the start of the *DBF4ΔC* gene and a reverse primer (2Dbf4 Rev NotI) containing a *NotI* restriction site that annealed to the end of *DBF4ΔC* gene. This PCR product was then digested with *BamHI* and *NotI* restriction enzymes and ligated into the pCM190myc vector that was digested with *BamHI* and *NotI*. The pCMDbf4C-TERM plasmid was constructed using the pRSDbf4ΔC plasmid as a template for a PCR reaction. A forward primer (BamHI Dbf4 For) containing a *BamHI* restriction site, annealing to the start of the N-terminus of the Dbf4 gene and a reverse primer (C-term del NotI Rev) containing a *NotI* restriction site annealing to the position just upstream of the Dbf4 C-motif. This PCR DNA insert was digested with *BamHI* and *NotI* and ligated into the pCM190myc vector that was digested with *BamHI* and *NotI*. Thus, a construct that expresses a Dbf4 mutant protein that is truncated at the C-terminus and does not include the C-motif was created.

Restriction digests of plasmid and PCR amplified insert DNA were performed using the appropriate restriction enzymes for 1 to 3 hours in a waterbath at 37°C (55°C for *Kpn2I*). A PCR reaction was set up to amplify Dbf4 inserts and the T4 DNA Ligase Kit (Fermentas) was used to perform ligations. The ligation mixes were transformed into DH5- $\alpha$  competent *E.coli* cells and plated on LB-Amp, as described below for the bacterial transformation protocol.

pEGDbf4ts-FL (ts) was constructed by PCR amplification of the entire coding sequence of the *DBF4* allele (*dna52-1*) from DY-2 genomic DNA, using forward and reverse primers with incorporated *EcoRI* and *BamHI* restriction endonuclease sites,

respectively. The resultant PCR product was digested with these enzymes and cloned into the two-hybrid bait vector pEG202 that had also been digested with *EcoRI* and *BamHI*, creating an in-frame fusion with LexA coding sequence. pEGDbf4ΔM was created by amplifying the first 786 bp (encoding amino acids 1-262) of *DBF4* using DY-1 genomic DNA as template, a forward primer with an added *EcoRI* site, and a reverse primer with a *HindIII* site, created in part by a silent base change from adenine to guanine at position 786. Base pairs 928- 2112 (encoding amino acids 310 to 704) were then amplified using a forward primer which contained a *HindIII* restriction site, created, in part, by changing bases 928-930 from ATA to CTT. This caused a conservative amino acid change from isoleucine to leucine, and a reverse primer which included an *NcoI* restriction site. Following digestion with the appropriate restriction enzymes, the two *DBF4* fragments were ligated together at their respective *HindIII* restriction sites and cloned into pEG-202, which had been digested with *EcoRI* and *NcoI*, creating an in-frame fusion with a LexA coding sequence. pEGDbf4ΔN was created by PCR amplification of base pairs 1-405 (encoding amino acids 1-135) using a forward primer with an *EcoRI* restriction site and a reverse primer containing a *SalI* site created by a silent base change from adenine to cytosine at position 402, and a base change from guanine to cytosine, resulting in a conservative amino acid change from glutamic acid to aspartic acid at position 135 of the protein product. Base pairs 537-2112 (amino acids 179-704) were amplified using forward and reverse primers with added *SalI* and *NcoI* sites, respectively. Following digestion with the appropriate restriction enzymes, the two fragments were ligated through their respective *SalI* sites and cloned into pEG202, which had been digested with *EcoRI* and *NcoI*, creating an in-frame fusion with a LexA coding sequence.

pCM190Dbf4ts-FL, -ΔM, and -ΔN were created by excising the region between base pairs 170-1972 from pEGDbf4ts-FL, -ΔM, and -ΔN, respectively, using the natural *BglII* and *Kpn2I* sites within *DBF4*. These fragments were then cloned into pCM190Dbf4-FL vector, which had been digested with *BglII* and *Kpn2I*, thus replacing the *DBF4* region between these restriction sites. Full-length *MCM2* was PCR-amplified from DY-1 genomic DNA using forward and reverse primers with added *NcoI* and *XhoI* restriction sites, respectively, and was cloned into the pJG 4-6 two-hybrid prey vector (a derivative of pJG4-5, with an extended polylinker insert; gift of R. Brent) at these sites, resulting in an in-frame fusion with HA coding sequence and the creation of pJGMcm2. pJGCdc7 and -Rad53 were generated by PCR amplification of full-length *CDC7* and *RAD53* coding sequences using DY-1 genomic DNA as template, with forward and reverse primers incorporating *EcoRI* and *BglII* sites, respectively. Following digestion with *EcoRI* and *BglII*, the PCR products were cloned into the pJG-4-6 vector at these sites, resulting in an in-frame fusion with HA coding sequence.

*DBF4ΔM* and *DBF4ΔN* were amplified from pEGDBF4ΔM and pEGDBF4ΔN, respectively, using a forward primer containing an *EcoRI* restriction site and a reverse primer containing a *BamHI* restriction site. pRS406 and the PCR products were digested with *EcoRI* and *BamHI* and ligated to create pRSDBF4ΔM and pRSDBF4ΔN.

The pET15b expression plasmids that were used to produce recombinant Dbf4 and truncated Dbf4 protein variants for crystallography and were constructed as described below. The pET15b vectors were created using genomic DNA as a template along with forward and reverse primers. The forward primer (Dbf4 For NdeI) that was used included an NdeI restriction site. The reverse primers (Dbf4 Rev BamHI), (Dbf4396

Rev BamHI) and (Dbf4 248 BamHI Rev) contained *BamHI* restriction sites and were used to construct the pET15bDbf4-FL, pET1bDbf4-396 and pET15bDbf4-248, respectively. For each of the pET15b constructs, a DNA PCR product was produced using the forward and reverse primers described above that was ligated into the Zero Blunt (Invitrogen) plasmid, as a preliminary step. Subsequently, the Zero Blunt plasmids containing the DNA inserts were digested with *NdeI* and *BamHI*. The DNA insert that were released, as a result of the restriction digestion, were collected, purified and then ligated into a pET15b vector that had been digested with *NdeI* and *BamHI*.

All plasmids were fully sequenced to verify the presence of the desired mutation and to ensure that no other mutations were present.

## **2.2 Quickchange Mutagenesis**

The point mutations that were made in this study were created using the QuickChange Multi Site-Directed Mutagenesis Kit (Stratagene Inc.). Template plasmids, having the wild type *DBF4* allele were used in conjunction with the kit reagents. The QuickChange Multi Site-Directed Mutagenesis Kit Instructional Manual was followed for designing primers and the PCR protocol. The primers were designed according to the specifications of the kit and annealed directly to the intended mutation site. The primers that were used are listed in Table 2.2. Template plasmids, having the wild type *DBF4* allele, were used in conjunction with the kit reagents. The following modification was made: a 4 hour *DpnI* digest of the template plasmid was performed in some cases, instead of the 1 hour prescribed by the kit protocol. Control reagents were provided by the kit and a control protocol was also provided. The control reaction was performed at least once for each set

of mutagenesis reactions involving the different plasmids to ensure that the kit reagents were functioning properly and that the protocol being followed was also working well.

### **2.3. Bacterial Transformation**

Bacterial transformations were used to propagate recently ligated plasmids. DH5 $\alpha$  cells were thawed on ice and a 50  $\mu$ l volume of cells was mixed with 20 ng plasmid and incubated on ice for 30 minutes, followed by a heat shock (42 °C) for 90 seconds. The tubes were then held on ice for 2 minutes and 1 ml of LB liquid medium (1% tryptone, 0.5% yeast extract, 1% NaCl) was added to the tubes which were incubated at 37 °C for 1 hour. Following the incubation, the cells were centrifuged and the supernatant was removed. The pellet was resuspended in 100  $\mu$ l LB medium and spread onto LB-ampicillin (1 $\mu$ g/ml) agar plates and incubated overnight at 37 °C.

### **2.4. Yeast Transformation**

Yeast transformation is a procedure that allows for plasmid DNA to be inserted into the yeast cells. Auxotrophy markers allow for selective pressure to maintain a plasmid, carrying the selective marker, when plated on selective medium. A list of the *Saccharomyces cerevisiae* yeast strain genotypes that were used for yeast transformations and the various other yeast experiments throughout this study is given in Table 2.3.

Cells were grown to log phase ( $1 \times 10^7$  cells per ml), in YPD (1% Yeast Extract, 2% BactoPeptone, 2% Dextrose) liquid culture media, as determined by counting with a hemocytometer and microscope. The entire culture (10ml) was then centrifuged (4000 rpm) and resuspended in 40 ml of 1XTE(10mM Tris-HCl pH8, 0.1mM EDTA) and then

centrifuged again at 4000 rpm. Following the removal of the supernatant, the centrifuged cells were then resuspended in 2 ml of lithium acetate buffer (100mM LiAc/0.5XTE) and incubated for 10 minutes at room temperature. An aliquot of 100 µl of the cell resuspension was then added to a sterile tube for each transformation and 1 µg of plasmid DNA was added to the tube along with 10 µl (10 µg/ml) of salmon sperm DNA. A 300 µl volume of 100 mM LiAc/40% PEG4000/1xTE was then added to the tube and mixed. The entire mixture was then incubated for 30 minutes at 30 °C, in a waterbath. Following the incubation period, 40 µl of dimethyl sulfoxide (DMSO, 99.99%) was added to the tubes, which were then heat shocked for 7 minutes at 42 °C. Finally, the tubes were placed on ice for 2 minutes and plated onto selective media.

## **2.5. Genomic DNA Isolation**

The genomic DNA isolation procedure allows for the genomic DNA of cells to be extracted and used as template DNA for PCR amplification.

Cultures were grown to saturation and centrifuged at 4000 rpm. Supernatants were removed and the pellets were resuspended in 500 µl ddH<sub>2</sub>O and transferred to 2 ml screw cap tubes. The tubes were then briefly centrifuged and the supernatants were removed. A 200 µl volume of genomic prep buffer (2%Triton X-100, 1% SDS, 100 mM NaCl, 10 mM Tris-Cl pH8, 1 mM EDTA) was added to each tube along with 0.5 g glass beads (0.5 mm diameter) and 200 µl of phenol:chloroform:isoamylalcohol (25:24:1). The tubes were then vortexed for 4 minutes. Following the vortex procedure, 200 µl of 1xTE was added to each tube, followed by centrifugation for 5 minutes at maximum speed (14,000 rpm). After centrifugation, the top layer was collected and transferred to a 1.5 ml

Eppendorf tube and 1 ml volume of 100% ethanol was then added. The tubes were mixed by inversion and centrifuged for 2 minutes (14000 rpm). The supernatant was then removed and discarded. The pellet was resuspended in 400  $\mu$ l of TE (pH 8). A 10  $\mu$ l volume of RNase A (10mg/ml) was then added to the tubes and they were incubated at 37°C for 10 minutes. Following the incubation, 10  $\mu$ l of 4 M ammonium acetate solution along with 1 ml of 100% ethanol added and the tubes were mixed by inversion. After that, the tubes were centrifuged for 2 minutes and the supernatant was discarded. The pellets were dried at room temperature for 30 minutes to 1 hour. The pellets were then resuspended in 35  $\mu$ l ddH<sub>2</sub>O and stored at -20 °C. DNA concentration was estimated by gel electrophoresis using a 0.8% agarose gel.

## **2.6. Protein Analysis**

Protein expression levels were determined by western blot assay from whole protein cell extracts that were prepared, as described below. The proteins were quantified using the Bradford Assay method, as described below.

### ***2.6.1. Preparation of Whole Cell Extracts (WCE)***

A 10 or 20 ml volume of liquid culture was centrifuged at 4000 rpm. The pellet was then resuspended in 100-200  $\mu$ l Lysis Buffer (10 mM Tris-HCl, pH8, 140 mM NaCl, 1% Triton X-100, 1 mM EDTA, with one protease inhibitor cocktail tablet (Roche #11-836-153-001) dissolved per 20 ml). A 5 $\mu$ l volume of phenylmethylsulphonyl fluoride (PMSF) (200 mM in methanol) was also added to the Lysis Buffer, just prior to the cell lysis

procedure. This cell lysis suspension was then transferred to 2 ml screw cap tubes along with 0.3g of glass beads (0.5 mm diameter), and kept on ice.

The samples were lysed using a Mini Bead Beader (Biospec) for 8 cycles of 30 seconds on ice and 20 seconds of agitation, at 4 °C. The samples were centrifuged and the supernatant (containing the soluble protein extract), was removed with a micropipetter and placed into fresh, Eppendorf tubes. A small aliquot (20 µl) was collected to be used to determine the protein concentration using the Bradford Assay (800 µl ddH<sub>2</sub>O, 200 µl Bradford reagent from Bio-Rad, along with 2µl of protein sample). The absorbance was measured at a wavelength of 595 nm using the spectrophotometer. The remainder of the protein extracts were then prepared for future Western blotting assays by the addition of a volume of 4x loading dye that was half that of the volume of soluble protein extract. The 4x loading dye (60% 4x loading buffer (consisting of 15% SDS, 40% glycerol, 166 mM Tris Base) 0.26 M DTT, 7% Bromophenol blue) was prepared in advance. The protein extract/4x loading dye mixture was then boiled for 8 minutes and stored at -80°C for future use in the Western blotting assay.

#### ***2.6.2. Western Blotting***

Western blots were performed using boiled protein samples prepared with 4x loading dye as described above along with acrylamide gels (7.5% or 10% separating gel and a 5% stacking gel). An OWL western blot apparatus was used.

Equal amounts of the boiled protein extract/4x loading dye samples were loaded into the lanes of the acrylamide gels. A prestained marker (Fermentas) was also loaded in one of the lanes and used to measure the size of the proteins. The gels were run with

running buffer (Pierce) at 100-150 Volts for 1 to 2 hours. The proteins in the acrylamide gel were then transferred to a nitrocellulose membrane. The acrylamide gels and nitrocellulose membrane were placed in cassettes between layers of Watman paper and sponge panels and inserted into an OWL transfer apparatus containing transfer buffer (200mM Glycine; 25mM Tris Base; 20% Methanol; 0.05% SDS). The transfer was carried out overnight at 50 Volts, in a 4°C cold room. The membranes were then stained with Ponceau-S (0.1%), rinsed, briefly, with ddH<sub>2</sub>O and an image was taken using a personal computer scanner. The membranes were then destained with TEN (20mM Tris-HCl; 1mM EDTA; 0.14M NaCl) + Tween 20 (0.05%) (TENT).

The membranes were subsequently treated with blocking buffer (TENT+5% skim milk powder) for 1 hour at room temperature, or overnight at 4°C. The primary antibodies were used to detect the membranes for 1-2 hours. A list of antibodies that were used is given in Table 2.4. The membranes were then washed in TENT, 3 times (for 10 minutes), before applying the secondary antibody. The secondary antibody was applied for 1 to 2 hours. The blots were then washed 3 times (for 10 minutes) in TENT and then once in ddH<sub>2</sub>O. Detection was performed on a Typhoon 9400 Scanner using predetermined settings.

### **2.6.3. Protein Solubility Assay**

The solubility assay was carried out as a means to assess which of the *Escherichia coli* strains/transformants were most suitable for inducing the expression of recombinant protein that was appropriately soluble for crystallization. The most efficient strain/transformant was selected and then used in a large-scale protein purification

procedure to provide soluble protein for subsequent crystallization. After the plasmids (pET15b-DBF4 FL, pET15b-Dbf4 396 and pET15b-Dbf4248) were constructed they were transformed into the different strains/transformants: BL21 (DE3), BL21 (DE3) pLySs, BL21 (DE3) pRARE, STAR, STAR pLySs and STAR pRARE. A detailed description of the *E.coli* strains and transformants is given in Chapter 6.

The following procedure was performed for each of the strains/transformants in combination with the different recombinant protein expression plasmids. Initially, the transformants were grown to OD<sub>600</sub>~0.7 and three 600 µl aliquots were removed and transferred to Eppendorf tubes and centrifuged (13000 rpm for 3 minutes). After the removal of the supernatant, these aliquot samples were resuspended in 15 µl of 2x SDS and stored at -20°C. This sample represented the uninduced IPTG- control sample.

The remainder of the culture was divided into three tubes (approximately 6ml each). Each of the tubes was induced with 0.5mM IPTG. The tubes were incubated, separately, under three different conditions: for 3 hours at 37°C, for 5 hours at 25 °C or 30°C and overnight at 16°C. Following the incubation periods, a 350 µl aliquot was removed from the tubes and centrifuged for 3 minutes at 13000 rpm. The supernatant was removed and 15-25 µl of 2x SDS was added to the tubes, which were then stored at -20°C. These samples represented the induced IPTG+ samples.

The remainder of the cultures were centrifuged for 15-20 minutes at 3000-4000 rpm. The supernatant was removed and the pellet was resuspended in 200 µl of 20 mM TRIS pH=8.0, 1.4 mM β-mercaptoethanol. Lysozyme was then added to a final concentration of 1 mg/ml concentration. The tube was then incubated on ice for 30 minutes. A volume of NaCl solution was then added, giving a final concentration of 0.5

M. Subsequently, a volume of lauryldimethylamine oxide (LDAO) detergent solution was added, giving a final concentration of 0.05%. The tube was incubated on ice for another 30 minutes. Following the incubation, the tube was centrifuged for 20 minutes at 13000 rpm. A 20  $\mu$ l aliquot of the supernatant was removed and mixed with a 20  $\mu$ l volume of 2x SDS-loading dye. This sample represented the induced “Soluble” sample and was stored at -20°C.

All of the samples were thawed and then boiled for 10 minutes in ddH<sub>2</sub>O on a hot plate. Following the boiling procedure a 15  $\mu$ l volume of each of the samples (IPTG-) and (IPTG+) and (“Soluble”) was loaded onto an SDS-PAGE (10-12%) apparatus that had been previously assembled. The resulting acrylamide gel was stained with Coomasie blue and the protein banding pattern for each of the samples, described above were compared.

## 2.7. Genomic Integration

Genomic integration is a procedure that allows for the wild type allele of a given gene to be replaced by a mutant allele in the yeast genome.

The genomic integration procedure involves a series of sequential steps (see Figures 4.4; 4.5). Firstly, the *DBF4ΔI68-178* mutant allele was cloned into an integrating vector pRS406 (as described in the Cloning section). The integrating vector was then transformed into the DY-27 diploid strain and plated on SC-URA selective media plates and grown for 3 days. Any colonies that were observed were presumed to have undergone a successful integration of the mutant allele into the genome because the integrating vector carried the *URA3* gene that permitted survival on the SC-URA plates. However, it was important to confirm a successful integration of the vector. Colonies were selected from the transformation plate and restreaked onto an SC-URA plate. The restreaked growth was then used to inoculate liquid SC-URA media and grown to saturation. The saturated cultures were used to perform the genomic DNA isolation procedure. A PCR protocol was then used to confirm that the plasmid carrying the mutant allele was actually integrated, essentially, adjacent to the endogenous *DBF4* gene, as a result of a recombination event (refer to Figures 4.4 and 4.5). The integration of the vector, as a result of a recombination event, resulted in the *DBF4ΔI68-178* (mutant allele) along with the plasmid vector sequence to integrate essentially adjacent (*cis*) to the wild type *DBF4* allele. In order to confirm this, a PCR reaction was set up using forward and reverse primers that annealed to both the wild type and mutant *DBF4* alleles. Since the integrating vector sequence was situated in between the mutant and wild type alleles, the forward primer annealed to the 3' end of the *DBF4* alleles and the reverse primer

annealed to the 5' end of the alleles. Thus, a PCR product would only be produced if the integrating vector sequence, situated in between the wild type and mutant alleles, was amplified. A non-integrand would not produce a PCR product using these forward and reverse primers (refer to Figures 4.4 and 4.5). The internal primers used were:  
(forward 5'-ATGTGGCAACCTCTTGGCAATGG-3') and  
(reverse 5'-CTTGTGATAACTATTGTCACAGTAGTG-3') along with the PCR program (**1. 95°C 5min., 2. 95°C 1 min, 3. 49°C 45 secs, 4. 68°C 8min, 5. GOTO 2. repeat 35 x, 6. 68°C 15min., 7. 4°C hold**). The PCR product was approximately 5.1kb in size and was representative of the entire integrated vector sequence along with some partial *DBF4* sequence that extended from the annealing forward and reverse primers. In the absence of a successful integration of the plasmid at the desired site, a PCR product would not be produced.

Following the PCR-based confirmation that the integrating vector was integrated at the *DBF4* locus, as described above, a subsequent step was performed to essentially select for strains that have removed the integrating vector sequence and one of the two *DBF4* alleles (either the mutant or wild type). The removal of the integrating vector sequence and one of the *DBF4* alleles is called the “pop out” and occurs by a recombination event. The “pop outs” are selected for by streaking colonies that were confirmed to have successfully integrated the integrating vector along with the *DBF4Δ168-178* mutant allele onto 5'fluoroorotic acid (5'FOA) plates. The 5'FOA treatment selects against the *URA3* marker. The mechanism for selection is that the *URA3* gene product uses 5'FOA as a substrate to produce a toxic compound. Thus, any colonies that have grown on 5'FOA have “popped out” the integrating plasmid and one of the

*DBF4* alleles (either the wild type or the mutant). The colonies were then restreaked onto 5'FOA and the resulting colonies were then used to inoculate YPD liquid medium cultures, which were grown to saturation. The saturated cultures were used to prepare genomic DNA (as described earlier in this chapter). The genomic DNA was then used as a template for a PCR reaction to determine the identity of the “pop out” strain. That is, the colonies that have grown on 5'FOA, have essentially “popped-out” the integrating plasmid, including one of either the wild type or mutant Dbf4 alleles, as a result of a homologous recombination event, and the PCR reaction was set up to determine if the wild type or mutant allele remained. Primers were used that flanked the N-motif region that was to be sequenced. The forward and reverse primers that were used were: (forward 5'-GTGCGCAAATAACTAATTTTGAC-3' and reverse 5'-CGTTGGTCCATATAATTTCATTGTG-3'), using PCR program **1. 94°C 4min, 2. 94° 1min 30secs., 3. 52°C 90secs, 4. 72°C 2mins 5. GOTO 2. 20x, 6. 72°C 7mins 7. 4°C hold.** The PCR products were then subjected to agarose gel electrophoresis (1%). The PCR products identifying the *DBF4* deletion mutant alleles were 432 base pairs compared to 465 base pairs for the wild type *DBF4* allele.

## **2.8. Yeast Strain Sporulation and Tetrad Dissection**

Sporulation is, essentially, the induction of meiosis. The minimal media conditions cause diploid cells to form spores, contained in an ascus in sets of 4 (two MAT $\alpha$  and two MAT $\alpha$ ).

For the DY-27 strain, which was used for the genomic integration procedure, a single colony was used as inoculum and grown to saturation in YPD medium. A 200  $\mu$ l volume of saturated culture was added to 5 ml ddH<sub>2</sub>O in a 50 ml tube and centrifuged at 4000 rpm. The pellet was resuspended in 5 ml sporulation medium (0.3% potassium acetate, 0.02% raffinose). This sporulation culture was incubated at 23 °C for 1 to 2 weeks shaking at 200 rpm. After the extended incubation period, the cultures were examined, microscopically, to observe tetrads. When the tetrads were observed, the sporulation cultures were prepared for tetrad dissection, as described below.

For the DY-13 strain, which was used to create the plasmid shuffle strain (which is described below), a single colony was streaked onto GNA (5% D-glucose, 3% Difco nutrient broth, 1% Difco yeast extract, 2% Bacto agar) presporulation plates and grown at 30°C. A single colony was transferred to 2 ml sporulation medium (1% potassium acetate; 0.005% zinc acetate). The cultures were incubated at 23°C for 1 week at 200 rpm shake. When tetrads were observed, the sporulation cultures were prepared for tetrad dissection as described below.

A 500  $\mu$ l aliquot of sporulation culture was centrifuged at 14000 rpm for 2 minutes and the pellet was resuspended in 1 ml sterile ddH<sub>2</sub>O and centrifuged again. The pellet was then resuspended in 50  $\mu$ l of zymolyase solution (0.5 mg/ml in 1M sorbitol) and incubated for 8 minutes at 30 °C. Following the incubation, 800  $\mu$ l of ddH<sub>2</sub>O was

slowly added to the tube as it rested on ice for 5 minutes (allowing the tetrads to settle to the bottom). The ddH<sub>2</sub>O was then removed slowly, leaving only 50-100 µl in the tube. A 10 µl volume of this cellular suspension (containing tetrads) was dropped onto fully dried YPD plates. The cell suspension was then streaked out onto the plate using a flamed metal loop. This plate was used for tetrad dissection, using the MSM micromanipulator (Singer). Following the tetrad dissection procedure, the plates were then incubated at 30°C, for 5 days.

## **2.9. Plasmid Shuffle Assay and Creation of a Plasmid Shuffle Strain**

The plasmid shuffle assay is a method that allows for the comparison of the phenotype of a transformant strain expressing a mutant protein from a plasmid to a transformant strain expressing wild type protein from a plasmid, in a strain where the genomic copy of the intended gene of study has been “knocked-out”. This was performed by utilizing the plasmid shuffle strain that was created, as described below. The plasmid shuffle strain, essentially, is a strain in which the genome copy of the intended gene of study (in this case *DBF4*) has been “knocked-out” and cell viability is being supported by a plasmid carrying a wild type copy of the intended gene of study. A second plasmid (expressing either the mutant allele or wild type allele) is then introduced into the cell and eventually replaces the first plasmid as a consequence of changing the selective medium. This procedure of transferring plasmids into and out of a cell by altering the selective medium is referred to as “plasmid shuffling”. The end result is a transformant having only the second plasmid for the protein being studied. Thus, there are, essentially, two important steps: the “shuffle-in” of the second plasmid and the “shuffle-out” of the initial plasmid.

### **2.9.1. Creation of Plasmid Shuffle Strain**

A diploid strain (DY-13), having one *DBF4* allele deleted, was transformed with pCMDbf4FL plasmid (Duncker *et al.*, 2002) and selected on SC-URA plates. The DY-13 strain carries a mutation in the *URA3* gene that encodes a gene product that is involved in the biosynthesis of uracil and the pCM190 plasmid carries the wild type *URA3* gene. This diploid transformant was induced to sporulate (as described above) and tetrad dissection was performed using the MSM System Micromanipulator (Singer) (also described above). Resultant dissected spores were grown on YPD plates. Spores were restreaked on SC-URA media plates to select for transformants to retain a higher plasmid copy number of pCMDbf4wt. Colonies from the restreaked SC-URA plates were grown to saturation in SC-URA liquid medium.

Genomic DNA was extracted from the cultures, as described earlier in this chapter. PCR reactions were performed with the genomic DNA to identify which of the newly generated haploid strains had a disruption of the genomic copy of *DBF4* allele (replaced by the Kanamycin gene). The PCR reactions involved used forward primers annealing to 500 base pairs upstream and reverse primers annealing to sequence 500 base pairs downstream of the *DBF4* gene:

(forward:5'ACGGTTAGCGTCGACGTTTTAAAAAGAAAGAAATAAG-3'; reverse:5'-CTGATTGGGATCCCCGTCACTGCCAGAAC-3'); and the following PCR program (**1. 94°C 4 min, 2. 94C 45 secs.; 3. 56°C 45 secs; 4. 72° C 2 mins 5. 30 secs; 6. 72 °C 2mins, 30secs; 7.GOTO 2 repeat 30x, 8. 72 °C, 7mins, 9. 4 °C hold**) was used to confirm disruption of the genomic copy of *DBF4*. A haploid strain, having the genomic Dbf4 copy replaced by Kanamycin gene, would be confirmed to produce a single band

PCR product (approximately 2.63 kb in size, as compared to 3.1kb for a haploid carrying the *DBF4* wild type gene).

Fluorescence activated cell sorting (FACS) analysis was also performed on the strain to confirm its haploid identity by comparing the DNA content (C) between haploid and diploid control samples. A haploid FACS sample would have characteristic 1C-2C DNA content pattern and a diploid FACS sample would have a characteristic 2C-4C DNA content pattern.

#### **2.9.2. Plasmid Shuffle Assay**

The plasmid shuffle assay was performed by transforming a pEG202 plasmid (expressing a Dbf4 mutant or wild type protein) into the plasmid shuffle strain. The transformants were plated on SC-URA-HIS. The medium lacking uracil and histidine was used to retain the pCMDbf4wt plasmid carrying the *URA3* gene and to retain the pEG202 plasmid (expressing mutant or wild type Dbf4, and carries the *HIS3* gene). The DY-13 host strain has mutations in both the *HIS3* and *URA3* genes. This step is referred to as the “shuffle-in”.

Colonies were then restreaked on SC-URA-HIS medium plates. Colonies resulting from these restreaked colonies were then streaked on 5'Fluoroorotic Acid (5'FOA) –HIS. 5'FOA serves as a substrate for the *URA3* gene product, resulting in the production of a toxic compound. Thus, only cells lacking the *URA3* gene are able to grow on plates containing 5'FOA. Colonies growing on the 5'FOA-HIS plates were presumed to be lacking the initial pCMDbf4wt plasmid, with cell viability being supported by the pEGDbf4wt or a pEG202 plasmid expressing a Dbf4 mutant protein. As previously

mentioned the *URA3* gene uses 5'FOA as a substrate to produce a toxic compound. This step involving selection on 5'FOA, is referred to as the “shuffle-out” step. The resulting colonies were restreaked onto 5'FOA –HIS plates.

The “shuffle-out” transformants, bearing only pEG202 plasmids (expressing mutant or wild type Dbf4) were grown in liquid medium (SC-HIS) and were used in growth spotting assays, to test for their sensitivity to the genotoxic agents, HU and MMS.

## 2.10. Two-Hybrid Assay

The two-hybrid assay is an *in vivo* assay that is used to detect and quantify the relative strength of protein-protein interactions. The assay involves the quantification of the expression of a reporter gene plasmid that is caused by two fusion proteins interacting. Firstly, a gene that encodes a given protein (i.e. Dbf4) is cloned into a bait vector (pEG202) (Duncker *et al.*, 2002). Expression of this plasmid results in a fusion protein consisting of a LexA DNA binding domain (BD) and the bait protein (i.e Dbf4). A second gene for another protein (i.e. Rad53) is cloned into a prey vector (pJG4-6) (Duncker *et al.*, 2002). Expression of this plasmid results in a fusion protein that consists of the second protein (i.e. Rad53) fused to a B42 transcriptional activation domain (AD).

Following cloning and sequence verification of the bait and prey plasmids, the plasmids are transformed into a wild type yeast strain (DY-1 or DY-8, see list of strains for genotypes) along with the reporter plasmid (pSH18-34). This triple transformant was grown to saturation and used to perform the two-hybrid assay.

The reporter plasmid (pSH18-34) possesses the *LacZ* reporter gene. When the bait fusion protein is expressed, it will bind to the LexA DNA binding element of pSH18-34.

If the prey fusion protein interacts with the bait fusion protein, the activational domain of the prey fusion protein comes into close proximity to the promoter elements of the reporter gene, recruiting the transcription factors. This results in the expression of the *LacZ* reporter gene. The subsequent translation of the reporter gene product results in the production of the  $\beta$ -galactosidase enzyme. If the bait and prey proteins don't interact, transcription of the *LacZ* gene will not occur. If there is a weak association between the two proteins, less  $\beta$ -galactosidase enzyme will be produced. Upon the addition a substrate ONPG (2-Nitrophenyl- $\beta$ -D-galactopyranoside), the  $\beta$ -galactosidase enzyme converts the ONPG substrate into 2-nitrophenol (yellow colour) and galactose. The yellow colour of the 2-nitrophenol is quantified by spectrophotometry and the reaction strength is measured as  $\beta$ -galactosidase activity which is calculated using the formula:

$\beta$ -galactosidase activity =

$$\frac{1000 \times \text{Abs}_{420}}{(\text{OD}_{600} \text{ of cell culture})(\text{vol. of cells assayed (ml)})(\text{assay time (min.)})}$$

Transformant cells were grown to log phase ( $1 \times 10^7$  cells/ml) overnight. The cell concentrations were determined from cell counts, using a hemocytometer. The volume required for  $5 \times 10^6$  cells/ml was centrifuged for each sample of the two-hybrid assay series. The pellets were then resuspended in 20 ml of induction media (Gal/Raf-URA-HIS-TRP) in 50 ml Falcon tubes. The cells are induced in Gal/Raf-URA-HIS-TRP media because the prey plasmid (pJG4-6) has a galactose inducible promoter. The prey plasmid carries the *TRP1* gene and the bait plasmid carries the *HIS3* gene. The pSH1834 reporter

gene plasmid carries the *URA3* gene. The cells were then incubated for 6 hours at 30°C, shaking at 200 rpm.

Following the 6 hour incubation, the concentrations of cell cultures were determined using a hemacytometer and a microscope. An aliquot of cells consisting of  $5 \times 10^6$  cells was removed and put into Eppendorf tubes and centrifuged for 10 minutes at 14000 rpm. The supernatant was removed and the cells were then resuspended in 0.5 ml Z-buffer (60mM Na<sub>2</sub>HPO<sub>4</sub>, 40mM NaH<sub>2</sub>PO<sub>4</sub>, 10mM KCl, 1mM MgSO<sub>4</sub>, 0.5M β-mercaptoethanol). A blank control tube containing no cells (but all other reagents) was prepared from this step onwards.

Two drops of chloroform and one drop of 0.1% sodium dodecylsulphate (SDS) solution were then added to each sample. The tubes were then vortexed for 10 seconds, and incubated for 5 minutes at 28 °C. Following the incubation period, 100 µl of *ortho*-Nitrophenyl-β-galactoside (ONPG) solution was added to each tube and the tubes were then placed back in the 28°C heating block. During this time, the samples were observed periodically until a pale yellow colour appeared. The reaction was then stopped, by adding 250 µl of 1M Na<sub>2</sub>CO<sub>3</sub> (sodium carbonate) solution. The exact length in time of the reaction was noted and used to calculate the β-galactosidase activity. Following the reaction, the sample tubes were centrifuged for 10 minutes at 14000 rpm. The supernatants were collected and transferred to cuvettes. The absorbance of the samples was measured by spectrophotometry at a wavelength of 420 nm. The OD<sub>600</sub> of the cell cultures that were induced for 6 hours was also measured using spectrophotometry, at this time. These values were also used in the β-galactosidase activity calculation. Each two-

hybrid assay set was performed in triplicate and the averages of the sets were calculated and graphed using MS-EXCEL.

## **2.11. One-Hybrid Assay**

The One-hybrid assay was used to determine if a protein was able to bind to ARS1 origin of replication. The One-hybrid assay procedure was very similar to the Two-hybrid assay procedure, as described above. However, the cells were only transformed with the pLIARS1+ reporter plasmid that has the ARS1 origin of replication sequence and the pJG4-6 plasmid carrying the gene for the Prey Protein. The transformants were induced in GAL/RAF SC-URA-TRP media.

## **2.12. Co-immunoprecipitation**

DY-1 cells were transformed with pCM190- and pJG4-6-derived expression vectors and were initially grown to  $1 \times 10^7$  cells/ml in 10ml SC medium lacking uracil and tryptophan and supplemented with 5  $\mu$ g/ml doxycycline (Dox). Cells were then centrifuged (2,000  $\times g$ , 3min) and the pellet was resuspended in 20 mls of 2% galactose/1% raffinose medium (BD Bioscience) lacking uracil, tryptophan, and Dox, and were grown for 6 h, and the cells centrifuged (2, 000  $\times g$ , 3min). All subsequent steps were performed as described elsewhere (Duncker *et al.*, 2002).

## **2.13. Growth Spotting Assay**

The growth spotting assay was used to compare the rates of strain and transformant sensitivity to HU, MMS and bleomycin relative to wild type control strains. The colony formation that resulted from a dilution series that was spotted on agar plates (containing HU, MMS, or BLEO) was observed and compared.

DY-1 and DY-2 were transformed with pCM190, pCM-Dbf4wt or pCM-Dbf4ts-FL. Cultures of DY-1 and DY-2 transformants were grown to saturation ( $\sim 1 \times 10^8$  cells/ml) and serial 10-fold dilutions, ranging from  $1 \times 10^7$  cells/ml to  $1 \times 10^4$  cells/ml, were prepared for both strains. A 5  $\mu$ l volume from each cell suspension was spotted onto a series of plates in decreasing concentration from the top of each plate to the bottom. Synthetic complete (SC) broth lacking uracil (to select for plasmid maintenance) was supplemented with various concentrations of HU ranging from 0 – 100 mM or MMS ranging from 0 - 0.015%. Each series was spotted in duplicate, with one plate series being incubated at 23°C, and the other at 30°C for 3 days.

For the plasmid shuffle strains created as described earlier in this chapter and DY-19 transformed with the pEGDbf4 C-motif point mutant series, the growth spotting assay was done as described below.

Cells were grown in SC-HIS liquid culture to saturation for 3 to 4 days. A 100  $\mu$ l aliquot was removed and added to 500  $\mu$ l of water (1:5) dilution. The cells were counted using a hemocytometer and the concentrations of the cell suspension were determined. The concentrations were then adjusted and equalized to approximately  $2 \times 10^7$  cells/ml . The same suspensions were then used to prepare a series of dilutions (by removing 100  $\mu$ l aliquots) and placing them into 400  $\mu$ l of autoclaved, sterile water.

A 7  $\mu$ l volume of each of the cell suspensions was pipetted onto a series of SC-HIS plates, with 100, 150 and 200 mM concentrations of HU and 0.01, 0.015, and 0.02% MMS concentrations. Plates were incubated for 4 days at 30°C and digital images were taken using the Fluorochem imaging system using a dark background and an incandescent light source.

## **2.14. Complementation Assay**

Complementation assays were performed to determine if mutant Dbf4 alleles expressed from the pCM190 plasmid vector were able to complement growth of a Dbf4 temperature sensitive strain at the nonpermissive temperature of 37°C. Complementation assays were performed using the strain DY-2, which is an essential gene. In this strain, the Dbf4 allele has a mutation (*P277L*) that causes the cells to be nonviable at the nonpermissive temperature of 37°C. Any viability at 37°C would be supported by plasmid-based expression of the Dbf4 wild type or mutant alleles.

The complementation assay determining the ability of the Dbf4 $\Delta$ N and Dbf4 $\Delta$ M alleles to support viability of the the Dbf4 temperature sensitive strain at the non-permissive temperature of 37°C was performed as described below. DY-2 cells were transformed with the doxycycline repressible plasmids pCM-Dbf4-FL (wt), - $\Delta$ M, -  $\Delta$ N, -  $\Delta$ 110-296, -1-296, or unmodified pCM190 (15), and grown to saturation in SC medium lacking uracil (SC-URA), supplemented with Dox (6  $\mu$ g/ml). A total of  $5 \times 10^6$  cells of each transformant were washed in dH<sub>2</sub>O, and resuspended in SC-URA without Dox, and streaked on SC-URA plates and grown at 23, 30, or 37°C for three days. A control SC-URA plate supplemented with Dox (6 $\mu$ g/ml) was streaked with the same transformed

strains and grown at 23°C. The above yeast transformants were then transformed with pJG 4-6 and pJGCdc7 and grown to saturation in SC medium lacking uracil and tryptophan (SC-URA-TRP), supplemented with Dox (6 $\mu$ g/ml). Cells were washed twice in dH<sub>2</sub>O, and were streaked onto plates of SC-URA-TRP supplemented with Dox (6  $\mu$ g/ml) and Galactose/Rafinose lacking uracil and tryptophan (Gal/Raf-URA-TRP), and grown at 23°C.

In a separate complementation assay, DY-2 (see list of strains for genotype) was transformed with doxycycline –repressible plasmids (pCM190, pCMDbf4FL(wt) and the pCMDbf4 C-motif mutant variants). The complementation assay was performed as described above. The same procedure was repeated for the complementation assay testing the pCMDbf4 $\Delta$ C and pCMDbf4C-TERM constructs.

## **2.15. Short-Term Viability Assay**

Viability assays were performed to test for sensitivity of strains and transformants to short-term exposure to genotoxic agents. The assay is performed by treating liquid medium log-phase ( $1 \times 10^7$  cells/ml) cultures with specific concentrations of genotoxic agents HU, MMS or BLEO for a period of time (i.e. 6 hours). Alternatively, this assay can be performed for a single concentration of genotoxic agent monitoring a series of time points following exposure.

DY-1 and DY-2 cells were diluted to a concentration of  $1 \times 10^6$  cells/ml in YPD medium. Aliquots of 10 ml volumes of culture were treated with MMS (0.013, 0.0195 or 0.026%) or with HU (50, 100 or 150 mM HU) and incubated at 30°C with shaking (215 rpm) in parallel with untreated control cultures. After 4 hours of incubation, 50  $\mu$ l culture

aliquots were removed and diluted 200-fold and 50 µl of each dilution suspension was spread onto YPD plates in triplicate. Plates with DY-1 cells were then incubated for 2 days at 30°C, while those with DY-2 cells were incubated at 23°C for 2 days. The triplicated series of plates were counted using a Quebec<sup>TM</sup> colony counter. The colony counts for each triplicated series were averaged and recorded. In each case, the percentage of viable colonies was calculated relative to untreated control plate count averages. Results presented are the averages of three independent experiments along with standard deviations.

For the viability assay comparing the DY19 Dbf4 C-motif transformants, a single concentration of bleomycin (BLEO) (1µg/ml) was used and time points were taken every 2 hours for up to 8 hours. An aliquot of 50 µl cells was removed at each time point and diluted into 5 ml of water. A 50 µl volume of the diluted cells was plated in duplicate onto SC-URA plates. The plates were incubated at 30°C for 3 days. The number of colonies was counted for each plate and the percentage of colonies for each treated sample relative to the untreated control plate for each time point was determined and graphed using MS-EXCEL.

**Table 2.1 List of Plasmids.**

PLASMID	USE OF PLASMID/ORIGIN
pEG202	Two Hybrid Assay (Duncker <i>et al.</i> , 2002)
pEGDbf4FL(pEGDbf4wt)	Two Hybrid Assay (Duncker <i>et al.</i> , 2002)
pEGDbf4-296	Two Hybrid Assay (Duncker <i>et al.</i> , 2002)
pEGDbf4-Δ110-296	Two Hybrid Assay (Duncker <i>et al.</i> , 2002)
pEGDbf4 <i>ts</i> (P277L)	Two Hybrid Assay (Varrin <i>et al.</i> , 2005 (this study))
pEGDbf4 ΔN	Two Hybrid Assay (Varrin <i>et al.</i> , 2005 (this study))
pEGDbf4 ΔM	Two Hybrid Assay (Varrin <i>et al.</i> , 2005 (this study))
pEGDbf4 ΔC	Two Hybrid Assay (this study)
pEGDbf4 Δ168-178	Two Hybrid Assay (this study)
pEGDbf4 T171A	Two Hybrid Assay (this study)
pEGDbf4 T171A T175A	Two Hybrid Assay (this study)
pEGDbf4 T168AT169AT171AT175A	Two Hybrid Assay (this study)
pEGDbf4 T168A 169A	Two Hybrid Assay (this study)
pEGDbf4 T175A	Two Hybrid Assay (this study)
pEGDbf4 GA159LL	Two Hybrid Assay (this study)
pEGDbf4 W202E	Two Hybrid Assay (this study)
pEGDbf4 AAHH (C661A C664A)	Two Hybrid Assay (this study)
pEGDbf4 CCAA (H774A H780A)	Two Hybrid Assay (this study)
pEGDbf4 CCHC (H774C)	Two Hybrid Assay (this study)

**Table 2.1 List of Plasmids (continued).**

PLASMID	USE OF PLASMID/ORIGIN
pEGDbf4 CCHA (H774A)	Two Hybrid Assay (this study)
pCM190	Complementation Assay (Duncker <i>et al.</i> , 2002)
pCM190-Dbf4-296	Complementation Assay (Duncker <i>et al.</i> , 2002)
pCM190-Dbf4-Δ110-296	Complementation Assay (Duncker <i>et al.</i> , 2002)
pCM190-Dbf4FL (pCMDbf4wt)	Complementation Assay (Duncker <i>et al.</i> , 2002)
pCM190-Dbf4 <i>ts</i>	Complementation Assay (Varrin <i>et al.</i> , 2005 (this study))
pCM190-Dbf4 ΔN	Complementation Assay (Varrin <i>et al.</i> , 2005 (this study))
pCM190-Dbf4 ΔM	Complementation Assay (Varrin <i>et al.</i> , 2005 (this study))
pCMDbf4 AAHH (C661A C664A)	Complementation Assay (this study)
pCMDbf4 CCAA (H774A H780A)	Complementation Assay (this study)
pCMDbf4 CCHC (H774C)	Complementation Assay (this study)
pCMDbf4 CCHA (H774A)	Complementation Assay (this study)
pCMDbf4ΔC	Complementation Assay (this study)
pCM Dbf4 C-TERM	Complementation Assay (this study)
pJG4-6	Two Hybrid Assay (Duncker <i>et al.</i> , 2002)
pJGDbf4ΔN	One Hybrid Assay (this study)
pJGDbf4ΔM	One Hybrid Assay (this study)
pJGDbf4ΔC	One Hybrid Assay (this study)
pJG FHA1	Two Hybrid Assay (Duncker <i>et al.</i> , 2002)

**Table 2.1 List of Plasmids (continued).**

<b>PLASMID</b>	<b>USE OF PLASMID/ORIGIN</b>
pJG Rad53	Two Hybrid Assay (Duncker <i>et al.</i> , 2002)
pJG Mcm2	Two Hybrid Assay (Duncker <i>et al.</i> , 2002)
pJG Cdc7	Two Hybrid Assay (Duncker <i>et al.</i> , 2002)
pJG Mcm4	Two Hybrid Assay (this study)
pJG Rad53-11	Two Hybrid Assay (this study)
pLIARS1	One Hybrid Assay Dowell <i>et al.</i> , 1994(gift from B.Sclafani)
pJGDbf4 AAHH (C661A C664A)	One Hybrid Assay (this study)
pJGDbf4 CCAA (H774A H780A)	One Hybrid Assay (this study)
pJGDbf4 CCHC (H774C)	One Hybrid Assay (this study)
pJGDbf4 CCHA (H774A)	One Hybrid Assay (this study)
pSH18-34	Two Hybrid Assay (Duncker <i>et al.</i> , 2002)
pET15bDbf4-FL	Recombinant protein expression (this study)
pET15bDbf4-248	Recombinant protein expression (this study)
pET15bDbf4-396	Recombinant protein expression (this study)

**Table 2.2 List of Primers**

<b>Primer Name and Sequence</b>	
Dbf4 Eco For	(used for Cloning; refer to pages: 54;55;56;57)  5'-GCAATCGGAATTCATGGTTCTCCAACGAAAATG-3'
Dbf4 Nco For	(used for Cloning; refer to pages:55;56)  5'-CTGATTGCCATGGCATGGTTCTCCAACGAAAATG-3'
Eco Rev	(used for Cloning; refer to pages: 55;56)  5'-GACTTAGAATTCCCTATATTGAAATCTGAGATTTC-3'
Nco Rev	(used for Cloning; refer to pages: 54;55;56)  5'-CTGATTGCCATGGCATGGTTCTCCAACGAAAATG-3'
Dbf4 NdeI For	(used for Cloning; refer to page: 60)  5'-GCAATCGGCATATGATGGTTCTCCAACGAAAAT-3'
Rev Dbf4 Sal1 deltaC	(used for Cloning; refer to page:57)  5'-TCGCTCGTCGACCGTTCTTCTTCACCGG-3'
For Sall Dbf4 delta C	(used for Cloning; refer to page:57)  5'-GCTAGCGTCGACAATCTCAGATTCAAATA-3'
REV upstream of pRS MCS	(used for Cloning; refer to page:57)  5'-GGCACCCCAGGCTTACACTTATGC-3'
2Dbf4RevNotI	(used for Cloning; refer to page:58)  5'-GACTTAGCGGCCGCTATTGAAATCTGAGATTTC-3'
BamHI Dbf4 For	(used for Cloning; refer to page: 58)  5'-GCAATCGGGATCCATGGTTCTCCAACGAAAATG-3'
Dbf4 Aat For	(used for Cloning; refer to page: 55)  5'-GTGTCTAGACGTCGAGAACATATTTACTAAAAAG-3'
Dbf4 Aat Rev	(used for Cloning; refer to page:55)  5'-CTAGACAGACGTAAAAATTGAGTTATTGCGC-3'

**Table 2.2 List of Primers (continued)**

Primer Name and Sequence
Dbf4 SalI Rev 5'-GACTTAGTCGACCTATATTGAAATCTGAGATTTC-3'
Dbf4 NdeI For 5'-GCAATCTATAATCGCATATGATGGTTCTCCAACGAAAATG-3'
Dbf4 Rev BamHI 5'-GACTTAGGATCCCTATATTGAAATCT-3'
Dbf4 396 Rev BamHI 5'-GACTTAGGATCCCTACTTCTTAACTCGGTCTCTCAAAATT-3'
Dbf4 248 BamHI Rev 5'-GACTTAGACTTAGGATCCCTATCCGTTGGTCCATATAATTTC-3'
Dbf4T168AT169A 5'-CAATTTTGACGCTGCTGTACAATAGTTATCACAGAACGGTC-3'
Dbf4T175A 5'-GACACTACGTACAATAGTTATCGCAAGAAGGTCTGTTGAGAAC-3'
Dbf4 W202E 5'-CTACATGAAAGTTGAGAGTTACGAAAAGGCTGCCAG-3'
Dbf4GA159LL 5'-GATTTATTGAAAAGAGGGTTCTTACATTGCTTCTGCAAATAACTC-3'
QC Primer Dbf4 H680C 5'-CACTAGTTCTGAGAAGTGTGTTGCTTCGCTG-3'

QC Dbf4 C661A C664A	(used for Quickchange mutagenesis; refer to pages: 61-62)
5'-CGGTAAAAAAATTCCGGATACGCTGAAAATGCTCGTAAAATACGAATC-3'	
QC Dbf4 H674A	(used for Quickchange mutagenesis; refer to pages: 61-62)
5'-CGAATCTTAGAACAGCCATAGTTCTGAGAAGGC-3'	
DBF4 QUAD pointmutant (T168AT169AT171AT175A)	
	(used for Quickchange mutagenesis; refer to pages: 61-62)
5'-CAATTTTGACGCGTGTGCAATAGTTATCGCAAGAAGGTC-3'	
DBF4 DOUBLEpointmutant (T171AT175A)	
	(used for Quickchange mutagenesis; refer to pages: 61-62)
5'-GACACTACTGTCGCAATAGTTATCGCAAGAAGGTC-3'	

## **2.3 List of Strains**

<b>STRAIN</b>	<b>GENOTYPE</b>
DY-2	MATa, can1-11, ura3-52, <i>dna52-1</i> (dbf4)
DY-8	MATalpha, his3, trp1, ura3-52, leu2::pro, LEU2-lexAop2
DY-13	MATa/alpha, his3Δ1, leu2Δ0/leu2Δ0, .lys2Δ0, met15Δ0, ura3dΔ0/ura3Δ0; kan::Dbf4
DY-26	MATa, his3Δ200, leu2Δ0, met15Δ0, trp1Δ63, ura3Δ0
DY-27	MATa/alpha, his3Δ1, leu2Δ0/leu2Δ0, lys2Δ0, met15Δ0, ura3Δ0/ura3Δ0
DY-75	MATa/MATα, his3Δ1/ his3Δ1, leu2Δ0/leu2Δ0, lys2Δ0/+, +/met15Δura3Δ/ura3Δ, dbf4ΔM/+
DY-76	MATa/MATα, his3Δ1/ his3Δ1, leu2Δ0/leu2Δ0, lys2Δ0/+, +/met15Δ, ura3Δ/ura3Δ, dbf4ΔN/+.
DY-77	MATα, his3Δ1, leu2Δ0, ura3Δ
DY-78	MATa, his3Δ1, leu2Δ0, ura3Δ, dbf4ΔN

**Table 2.4 List of Antibodies and the Concentrations Used**

<b>Antibody</b>		<b>Company</b>	<b>Concentration</b>
1° Antibody	Anti-LexA mouse monoclonal	(Invitrogen) (2mg/ml)	1:2000
1° Antibody	Anti-Lex A mouse monoclonal	(Sigma) (2mg/ml)	1:1000
1° Antibody	Anti-HA mouse monoclonal	(Sigma) (2mg/ml)	1:3000
1° Antibody	Anti-Myc mouse monoclonal	(Sigma) (2mg/ml)	1:3000
1° Antibody	Anti-Dbf4 goat polyclonal	(Santa Cruz) (0.2mg/ml)	1:100
2° Antibody	Alexa 647 goat anti-mouse	(Sigma) (2mg/ml)	1: 3000
2° Antibody	Alexa 488 goat anti-rabbit	(Sigma) (2mg/ml)	1: 3000
2° Antibody	Alexa 488 donkey anti-goat	(Sigma) (2mg/ml)	1: 3000

**Chapter 3: A Mutation in Dbf4 Motif M Impairs Interactions with DNA Replication Factors and Confers Increased Resistance to Genotoxic Agents.**

Note: This chapter has been previously published in the following journal article.  
Permission for the reuse of this material in this thesis dissertation has been granted.

Copyright © American Society for Microbiology [Molecular and Cellular Biology, Vol.25, No.17, 2005, p.7494-7504, DOI: 10.1128/MCB.25.17.7494-7504.2005]

Varrin, A.E., Prasad, A.A., Scholz, R., Ramer, M.D., and Duncker, B.P. (2005) A Mutation in Dbf4 Motif M Impairs Interactions with DNA Replication Factors and Confers Increased Resistance to Genotoxic Agents. *Molecular and Cellular Biology*, 25:7494-7504.

Figures 3.1.; 3.2.; 3.3.A, B, C; 3.4 contributed by Angela Varrin.

## **Introduction**

The initiation of DNA replication requires both the formation of pre-replicative complexes (pre-RCs) at origins and the activity of specific protein kinases in G<sub>1</sub> phase of the cell cycle (reviewed in Bell and Dutta, 2002; Kelly and Brown, 2000). In recent years, it has been firmly established that a number of replication factors also play key roles during the S-phase checkpoint (reviewed in Longhese, *et al.*, 2003; Pasero *et al.*, 1999). Studies with the budding yeast, *Saccharomyces cerevisiae*, as well as with fission yeast, frogs and mammals have implicated one of the replicative kinase complexes, Dbf4/Cdc7, as a target of the S-phase checkpoint response to genotoxic agents (reviewed in Jares *et al.*, 2000; Kim *et al.*, 2003). Levels of the Cdc7 kinase are relatively constant throughout the cell cycle, while those of its regulatory subunit Dbf4 are low from the end of mitosis until a burst of new synthesis in late G<sub>1</sub> phase (Pasero *et al.*, 1999; Weinreich and Stillman, 1999). Work with *Xenopus laevis* cell free extracts has demonstrated that the binding of Cdc7 to chromatin requires the presence of Dbf4 (Jares *et al.*, 2004), suggesting that it targets Cdc7 to pre-RCs. Chromatin fractionation assays with *S. cerevisiae* indicate that Cdc7 is chromatin-bound throughout the cell cycle (Weinreich and Stillman, 1999), while both Dbf4 and Cdc7 have been shown to interact with ORC subunits (Duncker *et al.*, 2002). Presently it is not known whether Dbf4 relocates Cdc7 to origins in budding yeast in late G<sub>1</sub> phase, analogous to the findings with *X. laevis*, or may instead simply associate with and activate Cdc7 that is already ORC-bound. Once Dbf4/Cdc7 becomes active, it phosphorylates Mcm2, a subunit of the heterohexameric MCM complex and a pre-RC component. This phosphorylation may result in local DNA unwinding (Gari *et al.*, 1997), consistent with the putative MCM complex role as a

replicative helicase (Ishimi, 1997; Lee and Hurwitz, 2001). In budding yeast, the initiation of replication is choreographed, with individual origins categorized as early-, middle- or late-firing (Raghuraman, *et al.*, 2001). Dbf4/Cdc7 is required throughout S-phase for initiation events to occur, as inactivation of Cdc7 during this stage of the cell cycle prevents further origins from firing (Bousset and Diffley, 1998; Donaldson *et al.*, 1998). Following exposure to the ribonucleotide reductase inhibitor HU, which results in replication fork stalling and triggers the intra-S-phase checkpoint, Dbf4 is phosphorylated and removed from chromatin. Significantly, both events require the activity of the Rad53 checkpoint kinase (Pasero *et al.*, 2003; Weinreich and Stillman, 1999), and Rad53 has been shown to physically interact with Dbf4 (Dohrmann *et al.*, 1999; Duncker *et al.*, 2002). Similar mechanisms have been reported for *Schizosaccharomyces pombe* (Brown and Kelly, 1999) and *Xenopus* (Costanzo *et al.*, 2003). The preservation of unfired origins may aid in the efficient resumption of DNA synthesis once the checkpoint is lifted, while Dbf4/Cdc7 may assist in reactivating replication at stalled forks (Duncker and Brown, 2003). Additionally, Dbf4/Cdc7 has recently been shown to function in translesion synthesis, part of the checkpoint response following exposure to DNA damaging agents such as UV radiation or MMS (Pessoa-Brandao and Sclafani, 2004).

It has been previously demonstrated that a 186 amino acid Dbf4 region mediates interactions with both the origin recognition complex (ORC) and Rad53, suggesting a mechanism whereby Rad53 directly binds to and/or phosphorylates the Dbf4 N-terminus when the S-phase checkpoint is triggered, resulting in its displacement from unfired replication origins (Duncker *et al.*, 2002). This notion is supported by the finding that the

inhibition of further origin firing, characteristic of the intra-S-phase checkpoint, fails to occur in *rad53* mutant strains (Santocanale and Diffley, 1998; Shiraghe *et al.*, 1998).

Dbf4 orthologs have been identified in organisms as diverse as fruit flies, frogs, mice, and humans (Landis and Tower, 1999; Masai and Arai, 2000). Sequence comparisons between the different species have uncovered three relatively well-conserved amino acid stretches that have been termed the N- M- and C- motifs (Masai and Arai, 2000). Studies with *S. pombe* have demonstrated that both N and C motifs are involved in the response to genotoxic agents, but are not required for normal cell cycle progression (Fung *et al.*, 2002; Ogino *et al.*, 2001). Less is known about the M-motif, although it appears to be important for cell proliferation, since a mutant with combined deletions of the N and M-motifs cannot support growth in fission yeast (Ogino *et al.*, 2001).

Despite the obvious importance of these conserved regions for the replicative and checkpoint functions of Dbf4, the key interactions they mediate have not thus far been investigated. Here we show that deletion of motif M results in a disruption of the interaction between Dbf4 and Mcm2, while association with the Rad53 kinase remains intact. Similarly, a motif M point mutation in a *DBF4* allele, which is temperature-sensitive for normal growth, disrupts interactions with both Orc2 and Mcm2 while the interaction with Rad53 is preserved. Furthermore, this allele confers increased resistance to genotoxic agents. Thus, mutation of motif M may favor the association of Dbf4 with Rad53, thereby facilitating its role as an S phase checkpoint target

### 3.2. Results

Dbf4 is targeted to chromatin in late G<sub>1</sub> phase of the cell cycle when its activation of Cdc7 is required to trigger the initiation of DNA replication (reviewed in Sclafani, 2000). Earlier a 186 amino acid region of Dbf4 was identified that mediates interactions with both ORC, through the Orc2 subunit, as well as the Rad53 checkpoint kinase, via its FHA1 and FHA2 domains (Duncker *et al.*, 2002). Given the likelihood that the Dbf4-ORC interaction is important for targeting Dbf4/Cdc7 activity to origins of replication, it was decided to investigate the effect of removing a *DBF4* sequence encoding amino acids 110-296 on plasmid-based growth complementation of yeast strain DY-2 (*dna52-1*), which expresses temperature-sensitive Dbf4 (Dbf4ts-FL). DY-2 cells were transformed with doxycycline-repressible pCM190-derived (Gari *et al.*, 1997) constructs, expressing either full-length Dbf4 (pCM190 Dbf4-FL), Dbf4 lacking amino acids 110-296 (pCM190-Dbf4 Δ110-296, see Figure 3.1), or empty pCM190 vector. For both pCM190-Dbf4-FL and pCM190-Dbf4Δ110-296, a sequence encoding a C-terminal Myc<sub>18</sub> tag was incorporated into the construct. While expression of wild-type Dbf4 restored growth to DY-2 cells at 37°C, expression of Dbf4 Δ110-296 did not (data not shown). This suggests that the missing Dbf4 region (aas 110-296) is indeed required for normal cell proliferation.

### Dbf4 Cassettes

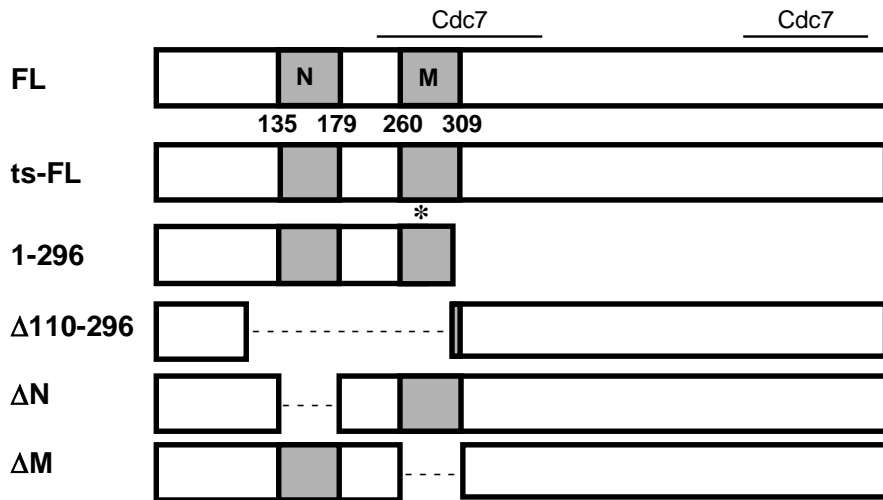
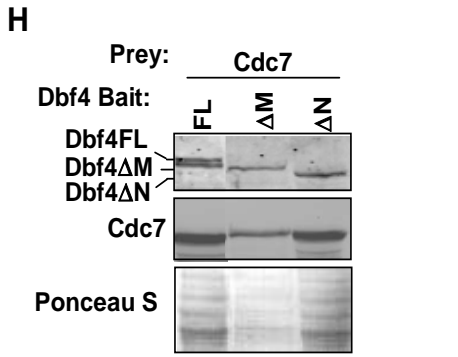
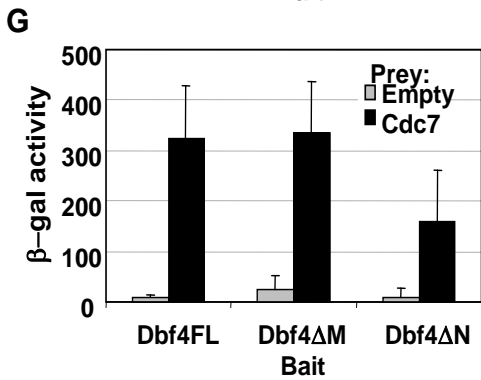
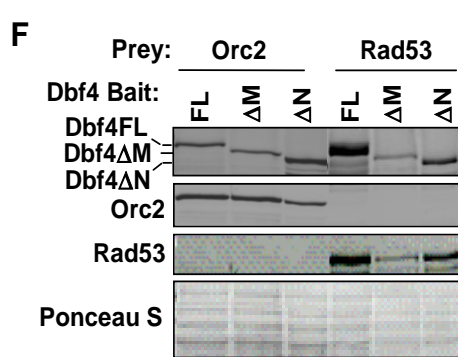
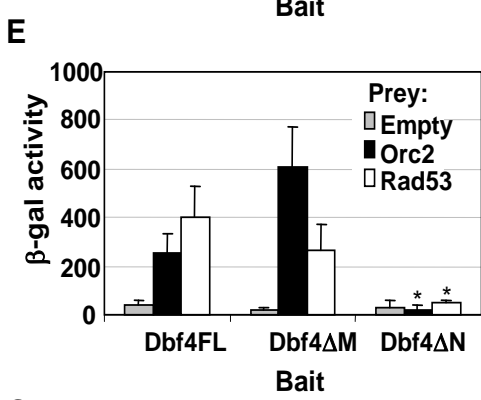
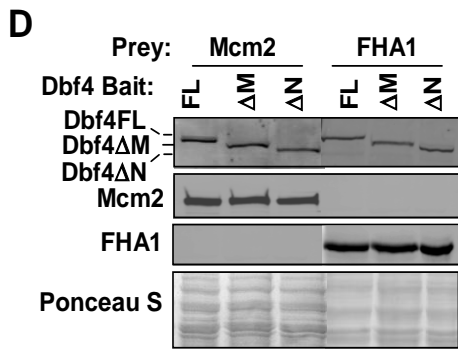
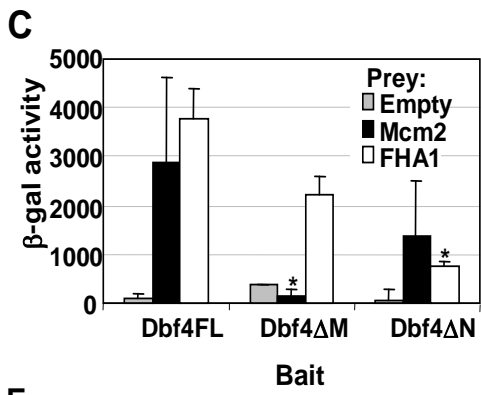
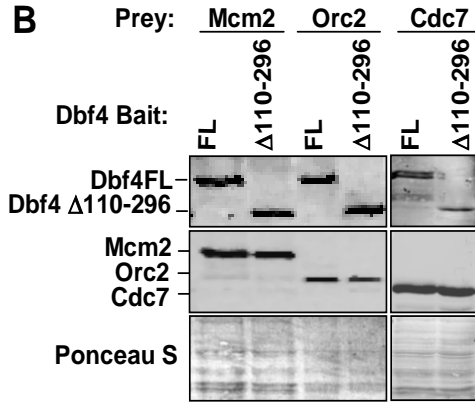
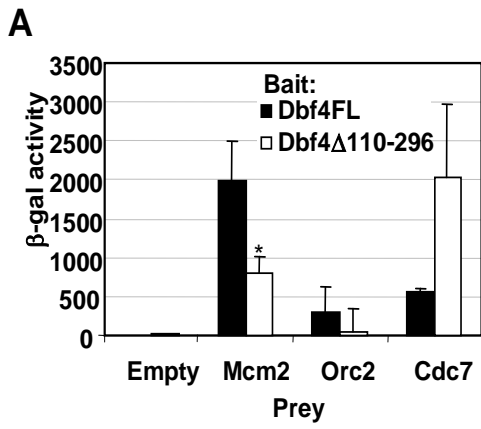


**Figure. 3.1. Dbf4 mutants.** Full length Dbf4 (Dbf4FL) and mutants used in this study are depicted. The N and M motifs, which are highly conserved among eukaryotes, are illustrated in gray. Numbers below indicate corresponding amino acid position, and the two regions that bind Cdc7 (19) are indicated by solid bars. The single amino acid change from proline to leucine at position 277 resulting from the *dna52-1* point mutation is indicated by an asterisk (Dbf4ts-FL). DNA cassettes encoding these Dbf4 variants were used for the construction of both pEG-202- (Ausubel *et al.*, 1995) and pCM190- (Gari *et al.*, 1995) based expression vectors.

The previous observation that removal of these amino acids abrogates the interaction between Dbf4 and Orc2 provides one mechanism whereby DNA replication may be inhibited (Duncker *et al.*, 2002). Nevertheless there was curiosity to determine whether this region might also mediate the previously reported physical interaction between Dbf4 and the Dbf4-dependant kinase (DDK) substrate Mcm2 (Lei *et al.*, 1997), since this would provide another explanation of how cell cycle progression is impeded by deletion of Dbf4 amino acids 110-296. In order to investigate this possibility, two-hybrid assays were conducted using pEG-202-derived (Ausubel *et al.*, 1995) bait plasmids expressing either full-length Dbf4 (pEGDbf4-FL) or Dbf4 Δ110-296 (pEGDbf4Δ110-296), in combination with pJG4-6-derived (see Materials and Methods) prey plasmids expressing full-length Mcm2 (pJGMcm2), Orc2 (pJGOrc2) or Cdc7 (pJGCdc7). As shown in Figure 3.2.A, removal of amino acids 110-296 reduces the interaction with Mcm2 to approximately half its normal level. This closely parallels what is observed with Orc2 prey, as previously reported (Figure 3.2.A and Duncker *et al.*, 2002). Immunoblot analysis indicated that levels of full-length Dbf4 and Dbf4Δ110-296 bait were comparable (Figure 3.2.B), ruling out decreased steady state levels of the latter as a cause for the weakened two hybrid signal generated by the deletion mutant with either Mcm2 or Orc2. Similarly, the levels of Mcm2 and Orc2 preys were not affected by the particular bait construct being expressed. In contrast, Dbf4Δ110-296 demonstrates a robust association with Cdc7 (Figure 3.2.A), consistent with previous data indicating that the Cdc7 interacting regions of Dbf4 span amino acids 241-416 and 573-695. The fact that the two-hybrid signal with the Cdc7 prey was higher with the Dbf4Δ110-296 bait than

with the Dbf4FL bait may indicate that residues within the deleted region partially mask one or both of the Cdc7 binding regions in the folded full-length protein.

**Figure 3.2. Two-hybrid analysis of Dbf4 variant interactions with replication and checkpoint factors.** (A) Two-hybrid assays using bait constructs pEGDBF4-FL and pEGDBF4 $\Delta$ 110-296, along with pJGMCM2, pJGORC2, pJGCDC7 and empty pJG 4-6 as prey vectors were carried out as described in Materials and Methods. Relative  $\beta$ -galactosidase activity is shown, and in each case represents the average of at least three trials. Error bars represent standard deviation. The asterisk indicates a statistically significance difference ( $p<0.05$ , Paired Student's t-Test) in the signal for Dbf4 $\Delta$ 110-296 relative to Dbf4FL. Insufficient trials were conducted to perform this analysis for the Cdc7 prey set. (B) To confirm that all baits and preys were properly expressed, culture aliquots were removed just prior the measurement of  $\beta$ -galactosidase activity, whole cell extracts were prepared and subjected to immunoblot analysis. Bait proteins were detected with rabbit polyclonal anti-LexA antibody (Invitrogen), and prey proteins were detected with mouse monoclonal anti-HA antibody (Sigma). Ponceau S staining of the membrane to confirm equal loading of whole cell extracts is shown. (C, E, G) Two-hybrid assays were carried out as above, by using pEGDBF4FL, pEGDBF4 $\Delta$ M, pEGDBF4 $\Delta$ N as bait, with pJG 4-6, -MCM2, -FHA1, -ORC2, -RAD53 and -CDC7 preys. Relative  $\beta$ -galactosidase activities are shown, and in each case represent the average of three trials. Error bars represent standard deviation. Asterisks indicate those two-hybrid interactions with significant differences at  $p<0.05$ . In each case the values obtained with Dbf4 $\Delta$ M or Dbf4 $\Delta$ N are being compared to the equivalent interactions using Dbf4FL as bait. (D, F, H) Confirmation of protein expression as above.



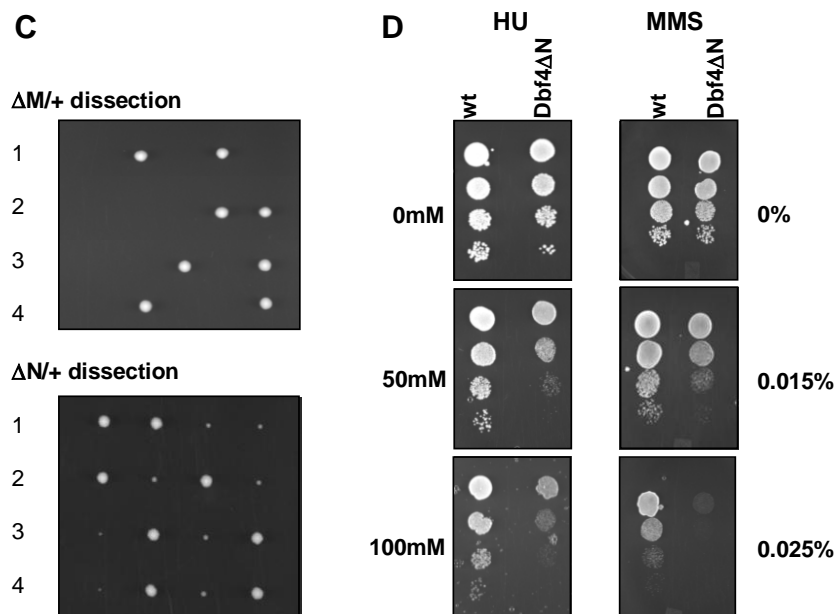
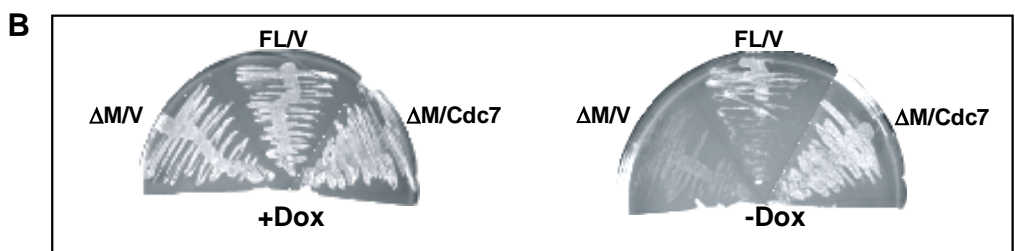
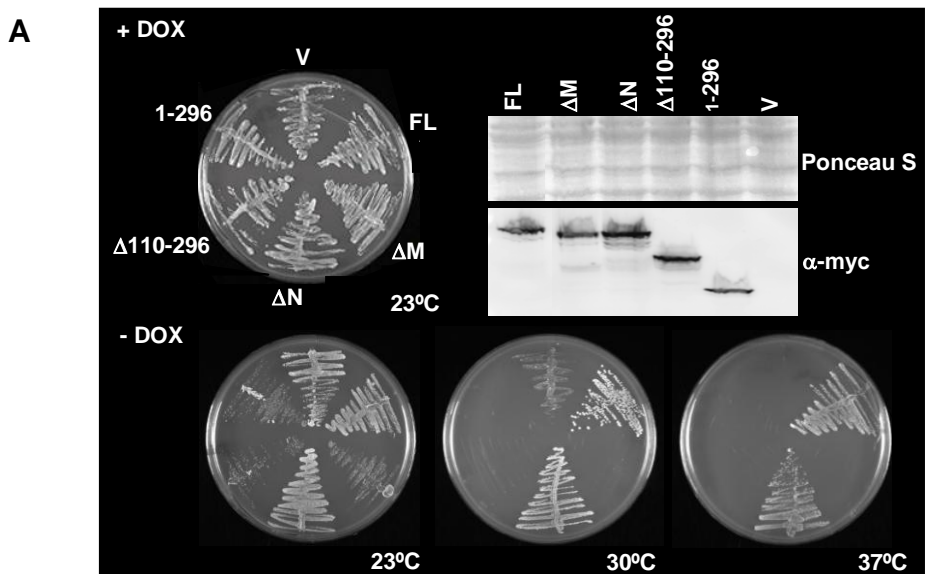
Given that the deletion of Dbf4 amino acids 110-296 eliminates all or most of the conserved N and M motifs (Figure 3.1), we decided to examine how more precise excisions of these regions would influence the ability of Dbf4 to interact with replication and checkpoint factors. Further two-hybrid bait vectors were therefore constructed, expressing Dbf4 lacking either N-motif (pEGDbf4 $\Delta$ N, amino acids 136-178 removed, Figure 3.1.) or M-motif (pEGDbf4 $\Delta$ M, amino acids 263-309 removed, Figure 3.1.). When these were tested in combination with the prey constructs pJGMcm2, pJGOrc2, pJGRad53 and pJGFHA1, a variety of deletion-dependent effects were observed. The removal of N-motif resulted in a sharp drop in the two-hybrid signal between Dbf4 and either full-length Rad53 or its FHA1 domain alone (Figure 3.2 C,E), consistent with the finding in *S. pombe* that deletion of this region from its Dbf4 ortholog, Dfp1, results in sensitivity to a broad range of genotoxic agents (Fung *et al.*, 2002). In contrast, the interaction with Mcm2 is preserved to a greater extent with Dbf4 $\Delta$ N (Figure 3.2 C), consistent with the finding that removal of N-motif does not prevent Dfp1 from carrying out its essential function (Fung *et al.*, 2002). With Dbf4 $\Delta$ M, the results were essentially reversed, the interaction with Mcm2 was completely abrogated, while removal of the M-motif had only a modest effect on the strength of the two-hybrid signal with full-length Rad53 or its FHA1 domain alone (Figure 3.2 C, E). Indeed, the modest reduction in the two-hybrid signal between Dbf4 $\Delta$ M and Rad53 may be due to lower levels of both proteins in this strain (Figure 3.2 F). Surprisingly, when Orc2 was used as prey in conjunction with Dbf4FL, Dbf4 $\Delta$ N and Dbf4 $\Delta$ M baits, the absence of N-motif rather than M-motif reduced the relative strength of interaction (Figure 3.2 E). Finally, when the interaction between the same three Dbf4 baits and Cdc7, was monitored, similar two-

hybrid signal strength in each case was found (Figure 3.2 G). For all trials, the levels of bait and prey proteins were monitored by immunoblot analysis (Figure 3.2 B, D, F, H).

In light of the fact that removal of conserved Dbf4 regions leads to reduced interactions with specific cell cycle factors, it was decided to evaluate whether one or both of the N and M motifs are required for Dbf4 to carry out its role in normal cell cycle progression. This was of particular interest given previous studies with *S. pombe* showing that removal of the N-motif does not prevent Dfp1 from fulfilling its essential function, while additional deletion of the M-motif was found to eliminate the ability of Dbf4 to support cell cycle progression (Fung *et al.*, 2002; Ogino *et al.*, 2001). In order to evaluate the requirement of these two conserved Dbf4 regions for *S. cerevisiae* growth, we prepared further doxycycline-repressible pCM190 constructs, expressing Dbf4 variants lacking either N-motif (pCM190-Dbf4 $\Delta$ N, amino acids 136-178 removed, see Figure 3.1) or M-motif (pCM190-Dbf4 $\Delta$ M, amino acids 263-309 removed, see Figure 3.1), and tested their ability to complement growth in DY-2 cells. While pCM190-Dbf4 $\Delta$ N was able to complement growth as efficiently as pCM190-Dbf4-FL at both semi-permissive (30°C) and restrictive (37°C) temperatures, pCM190-Dbf4 $\Delta$ M was not able to do so (Figure 3.3 A). Moreover, pCM190-Dbf4 $\Delta$ M acted in a dominant negative fashion, inhibiting growth at 23°C relative to cells transformed with empty vector. A plausible explanation for this phenomenon is that overexpressed Dbf4 $\Delta$ M, which is impaired for association with Mcm2, may sequester Cdc7 thereby reducing its interaction with endogenous Dbf4 and subsequent phosphorylation of Mcm2. The same effect would be expected for overexpression of pCM190- $\Delta$ 110-296, since it produces a Dbf4 variant lacking most of M-motif (Figure 3.1), while the corresponding two-hybrid bait

demonstrates a strong interaction with Cdc7 (see Figure 3.2 A), and indeed such a dominant-negative effect was observed (Figure 3.3 A). In further support of this model, it was found that co-expression of plasmid-encoded Cdc7 with Dbf4 $\Delta$ M was able to restore growth at 23°C (Figure 3.3 B). As an additional control, pCM190-Dbf4-296, expressing only the first 296 amino acids of Dbf4 also inhibited growth at 23°C, as previously reported (Duncker *et al.*, 2002). In order to establish that Dbf4 $\Delta$ N is able to support growth in the absence of any other Dbf4 variant, a +/ $\Delta$ N diploid strain was generated. Following sporulation and tetrad dissection, four viable spores were consistently obtained (Figure 3.3 C). In nearly every case, two of the four spore-derived colonies were considerably smaller than the two others. It was determined that the smaller colonies corresponded to the Dbf4 $\Delta$ N segregants (not shown). Thus, despite the fact the Dbf4 $\Delta$ N haploids are viable, they display some growth impairment relative to isogenic wildtype cells, although this was less apparent when the cells were spotted following exponential growth in liquid medium (see Figure 3.3 D). Tetrad dissection was similarly conducted with +/ $\Delta$ M diploids and in each case only two of four spores were viable (Figure 3.3 C), confirming the requirement of motif M for regular cell cycle progression.

**Figure 3.3. Dbf4 M-motif is required for interaction with Mcm2 and for normal cell growth, while N-motif mediates association with Rad53 and confers resistance to both HU and MMS.** (A) DY-2 cells were transformed with pCM190-Dbf4FL, -Dbf4 $\Delta$ M, -Dbf4 $\Delta$ N, -Dbf4 $\Delta$ 110-296, -Dbf4(1-296), or empty vector, pCM190. A complementation assay was performed as described in Materials and Methods. Cells were grown either in the presence (+Dox) or absence (-Dox, entire row) of Doxycycline which represses pCM190-based expression, at the indicated temperatures. Western blot analysis to confirm plasmid-based expression was conducted using a mouse monoclonal anti-Myc antibody (Sigma) and Alexa-Fluor 488 goat anti-mouse IgG polyclonal secondary antibody (Invitrogen). (B) DY-2 cells transformed with pCM190-Dbf4FL (FL) or pCM190- Dbf4 $\Delta$ M ( $\Delta$ M) as above, were further transformed with either pJG 4-6 (V) or pJG-Cdc7 (Cdc7), and grown in the presence or absence of Doxycycline, as indicated, at 23°C. (C) Tetrad dissection of DY -75 ( $\Delta$ M/+) and DY-76 ( $\Delta$ N/+) strains. Gene replacement, sporulation and tetrad analysis were performed as described in Materials and Methods. Growth of spores following dissection of four tetrads corresponding to each strain is shown. (D) A 10-fold dilution series of the Dbf4 $\Delta$ N and isogenic wild-type haploid strains at a starting concentration of  $1 \times 10^7$  cells/ml, were spotted onto YPD plates containing the indicated concentrations of MMS and HU. Plates were incubated at 30°C for 2 days.

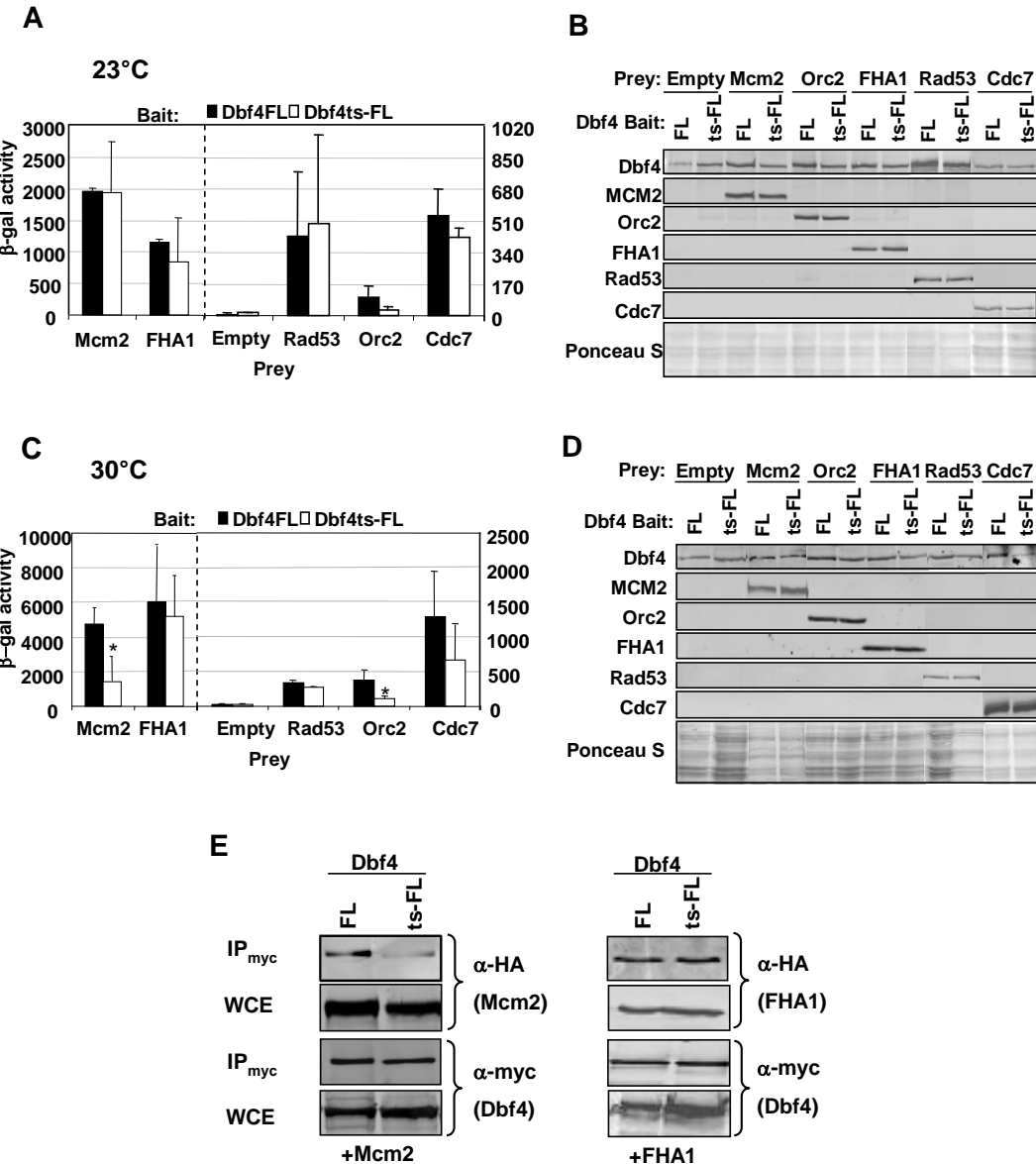


Since the removal of Dbf4 N-motif abrogates its association with Rad53 (Figure 3.2.C, E) we examined whether Dbf4  $\Delta$ N haploids are hypersensitive to agents that normally trigger the S-phase checkpoint. Growth of the Dbf4  $\Delta$ N cells relative to isogenic haploid wild type cells was inhibited in the presence of either MMS, an alkylating agent that causes DNA lesions, or HU, a ribonucleotide reductase inhibitor that causes replication fork stalling (Figure 3.3 D).

A number of temperature-sensitive (ts) *DBF4* mutant strains have been identified which demonstrate a cell cycle arrest just prior to the initiation of DNA replication at restrictive temperature (reviewed in Masai and Arai, 2000). We cloned and sequenced the Dbf4 ts allele *dna52-1* (Dumas *et al.*, 1982; Takeda *et al.*, 1999) from strain DY-2, and determined that it has a single point mutation, resulting in a change from proline to leucine at position 277 within motif M. This is identical to the previously reported sequence for the *dbf4-1* allele (Kihara *et al.*, 2000). Given the finding that the elimination of motif M disrupts the interaction between Dbf4 and the DDK target Mcm2, it was decided to test the effect of the P277L mutation on this association. Therefore, an additional two-hybrid bait construct was prepared by cloning the *dna52-1* allele into pEG202, to produce pEGDbf4ts-FL (Figure 3.1). When the assay was carried out at permissive temperature for the *dna52-1* allele (23°C), no significant difference was observed between Dbf4FL (wild-type) and Dbf4ts-FL with respect to the strength of the two-hybrid signal for interactions with Mcm2, the FHA1 domain of Rad53 or full-length Rad53, Orc2 or Cdc7 (Figure 3.4 A, B). At 30°C (semi-permissive temperature for DY-2), a sharp drop in association between Dbf4ts-FL and Mcm2 was observed, while very little difference was seen when Dbf4ts-FL or Dbf4FL was used as bait in combination

with either full length Rad53 or its FHA1 domain alone (Figure 3.4 C, D). Orc2 also had a weakened association with Dbf4ts-FL relative to Dbf4FL at 30°C. Assays at non-permissive temperature (37°C) were attempted, but regardless of whether the bait used was wild-type or mutant Dbf4, the signals were not appreciably above background values obtained with empty vectors, indicating that the assay is sub-optimal at this temperature. Finally, to confirm the effect of the Dbf4 P277L mutation on the interaction with Mcm2 at 30°C, co-immunoprecipitation experiments were carried out, and revealed that the Dbf4 mutation greatly impaired its ability to interact with Mcm2, while its association with the Rad53 FHA1 domain remained unchanged (Figure 3.4 E).

**Figure 3.4. Dbf4ts-FL has weakened interactions with both Orc2 and Mcm2.** (A, C) Two-hybrid assays were carried out as described in Materials and Methods using bait constructs pEGDbf4-FL and pEGDbf4ts-FL. pJGMcm2, -Orc2, -FHA1, -Rad53, -Cdc7 were used as prey, along with pJG 4-6 (Empty). Induction of prey expression was carried out at either 23°C (A) or 30°C (C). Relative β-galactosidase activity is shown and in each case represents the average of at least three separate trials, with the error bars indicating standard deviation. Asterisks indicate a significant difference ( $p<0.05$ , Paired Student's t-Test) in the signal for Dbf4ts-FL relative to Dbf4-FL with equivalent preys. The dashed line designates a separation of prey interactions for the left and right scales on the y-axes. (B, D) Immunoblot analysis to verify bait and prey expression was carried out as described in Fig.2. (E) Co-immunoprecipitation (co-IP) experiments were carried out as described in Materials and Methods. Shown are immunoblots of IP and input whole cell extracts (WCE) detected with either monoclonal anti-HA (for Mcm2 and FHA1 detection) or anti-Myc antibodies (for Dbf4FL and Dbf4ts-FL detection; Sigma). In each case, 20μg of the input WCE (determined by Bradford assay) and ¼ of the final bead suspension was blotted.

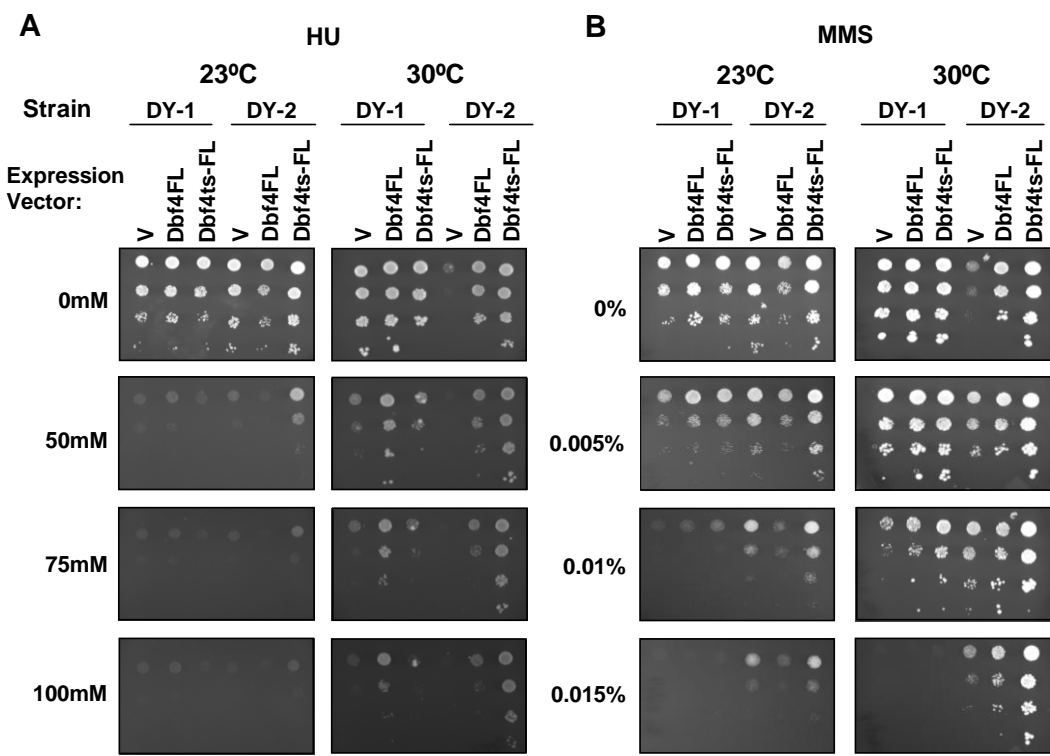


Since Dbf4ts-FL has weakened interactions with replication factors Mcm2 and Orc2 at 30°C, relative to Dbf4FL, but little change in its association with Rad53, we were interested in determining whether this mutant would be resistant to agents that normally provoke a checkpoint response. Therefore the ability of wild-type strain DY-1 and *dna52-1* strain DY-2 to withstand varying levels of either MMS or HU was compared (Figure 3.5). Serial dilutions of each strain, transformed with empty pCM190 vector, pCM190-Dbf4-FL (Figure 3.1, and Duncker *et al.*, 2002), or pCM190-Dbf4ts-FL (see Materials and Methods), were spotted on a series of SC-URA medium plates with varying concentrations of either HU or MMS. At all concentrations tested, DY-1 and DY-2 cells transformed with empty vector seemed equally sensitive to HU at 23°C (Figure 3.5 A). In contrast, at this same temperature, empty vector DY-2 transformants actually grew better on elevated concentrations of MMS than did wild-type transformants (23°C, Figure 3.5 B). Remarkably, at a semi-permissive temperature for the *dna52-1* allele, this growth advantage over the wild-type strain on MMS was maintained (30°C, Figure 3.5 B). Plasmid-based expression of Dbf4ts-FL and, to a lesser degree, Dbf4FL enhanced growth on MMS for both DY-1 and DY-2 cells at 30°C. The most dramatic effect was observed with the combination of DY-2 cells transformed with pCM190-Dbf4ts-FL (Figure 3.5 B). A particularly surprising, yet reproducible result from this analysis was that DY-2 cells transformed with empty vector actually grew better at 30°C on medium containing low concentrations of MMS than medium with no MMS. This was true for untransformed DY-2 exposed to MMS as well, but was not observed with HU or UV treatment (Figure 3.5 A and data not shown). Intriguingly, the effects of Dbf4 expression for cells spotted on HU media were allele specific, with DY-1 (wild-type) and

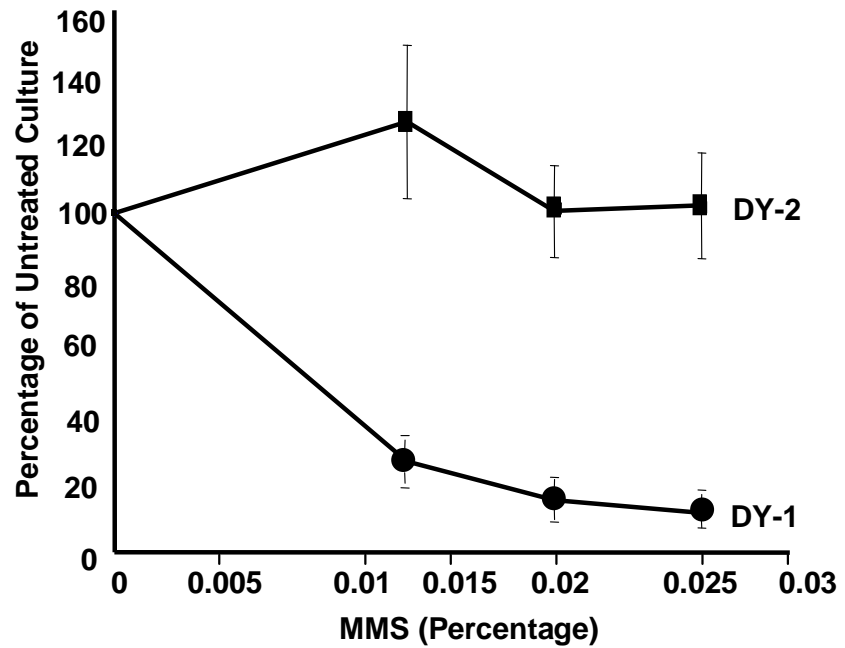
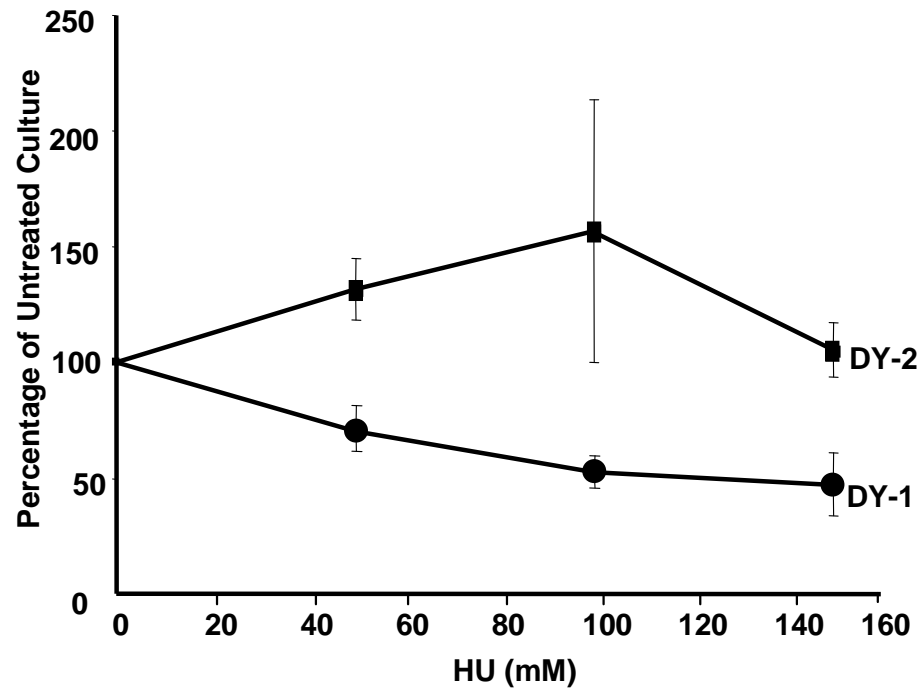
DY-2 (*dna52-1*) cells benefiting most from overexpression of Dbf4FL and Dbf4ts-FL, respectively (Figure 3.5 A).

Finally, to evaluate the viability of DY-1 and DY-2 cells following shorter HU and MMS exposures, cultures were grown in media supplemented with various concentrations of these reagents for four hours and then plated on media without the supplements. Relative to untreated controls, the DY-2 cells maintained high levels of viability at all concentrations of HU and MMS tested, whereas the DY-1 cells fared much worse, demonstrating a clear dose-dependant drop in survival (Figure 3.6).

**Figure 3.5. Dbf4ts-FL confers resistance to both MMS and HU.** DY-1 and DY-2 cells, transformed with pCM190-Dbf4-FL, pCM190-Dbf4ts-FL or empty pCM190 (V) were spotted in 10-fold dilution series onto selective media plates containing the indicated concentrations of MMS and HU, as described in Materials and Methods. Each plate series was incubated at 23 °C or 30 °C for 3 days, as indicated.



**Figure 3.6. Cells expressing Dbf4ts-FL are resistant to short-term exposure to either MMS or HU.** DY-1 and DY-2 cells were treated with three concentrations of (A) MMS (0.013, 0.0195, 0.026% MMS) or (B) HU (50, 100, 150mM) for 4 hours, plated in triplicate and incubated as described in Materials and Methods. Colonies were counted and the percentages were calculated relative to an untreated control plated cells. Each data point represents the average of three independent experiments. Error bars represent standard deviation.

**A****B**

### 3.3. Discussion

#### 3.3.1. The M and N motifs of Dbf4 mediate specific interactions with replication and checkpoint factors.

Sequence comparisons of Dbf4 and its orthologs in other eukaryotes have revealed a number of conserved regions, including the M and N motifs (Masai and Arai, 2000; Takeda *et al.*, 1999). For the first time, we have linked these motifs and their replication or checkpoint roles to previously identified physical interactions with replication and checkpoint factors. Our data demonstrates that deletion of the M-motif abolishes the essential function of Dbf4 (Figure 3.3 A, C), and strongly suggests that this is due to the abrogation of its interaction with Mcm2 (Figure 3.2 C). Interestingly, while our original deletion of Dbf4 amino acids 110-296 reduced the interaction with Mcm2 considerably (Figure 3.2 A), the excision of the M-motif (removal of amino acids 263-309) resulted in a more dramatic effect on this association (Figure 3.2 C) suggesting that residues 297-309 make an important contribution to the Dbf4-Mcm2 interaction. While Cdc7 has also been shown to interact with Mcm2, this association was much weaker than that observed for Dbf4 and Mcm2 (Lei *et al.*, 1997), thus it is very likely that disruption of Dbf4 M-motif is sufficient to prevent effective DDK interaction with its critical substrate. By extending our analysis to the Dbf4 P277L mutant encoded by the temperature sensitive *dna52-1* allele, we show that a single amino acid change within the M-motif is sufficient to dramatically impair the Dbf4-Mcm2 interaction at restrictive, but not permissive temperatures (Figure 3.4 A, C). Significantly, several other *dbf4* alleles have been sequenced from temperature-sensitive strains, including *dbf4-1* (which is identical to *dna52-1* based on our sequence data), *dbf4-2* and *dbf4-3*, all of which result in a change

of one of two conserved M-motif proline residues ( $\text{Pro}^{277}$ ,  $\text{Pro}^{308}$ ), while *dbf4-4* and *dbf4-5* produce severely truncated proteins with intact M-motifs (Kihara *et al.*, 2000). It has been shown previously that lysates from *dbf4-1* cells fail to phosphorylate Mcm2 in an *in vitro* kinase assay (Oshiro *et al.*, 1999), consistent with the notion that the Dbf4 P277L mutation impairs the Dbf4-Mcm2 association. An alternative explanation is that this mutation instead abrogates the Dbf4-Cdc7 interaction, thereby preventing kinase activation. However, our data shows that at 30°C the interaction between the mutated Dbf4 and Mcm2 is greatly impaired, whereas its interaction with Cdc7 is not significantly reduced (Figure 3.4 C). Deletion of Dbf4 N-motif produced a strongly reduced two-hybrid signal for interaction with the checkpoint kinase Rad53 (Figure 3.2 C, E), and rendered haploid cells hypersensitive to both MMS and HU (Figure 3.3 D). These results are consistent with the previously proposed role for Dbf4 as a checkpoint target (Jares *et al.*, 2000; Duncker and Brown, 2003; Pike *et al.*, 2003). Interestingly, it was the elimination of N-motif and not M-motif that had the greatest effect on the Dbf4-Orc2 interaction. It has been previously established that following exposure to HU, *S. cerevisiae* Dbf4 becomes phosphorylated and displaced from origins which are then prevented from firing, in a Rad53-dependent fashion (Pasero *et al.* 2003, Santocanale *et al.*, 1998; Weinreich and Stillman, 1999). This may be important in allowing cells to efficiently recover once the checkpoint has been lifted (see below). Therefore, it is proposed that under conditions of genotoxic stress, Rad53 interacts with and phosphorylates the Dbf4 N-motif, disrupting its interaction with Orc2 and releasing Dbf4 from origins. Consistent with this model, deletion of an eight amino acid stretch in the N-motif of *S. pombe* Dfp1 including a number of potential Ser and Thr phosphorylation

sites, or mutations of these residues, results in sensitivity to a wide range of DNA-damaging agents (Fung *et al.*, 2002; Takeda *et al.*, 1999). However, this is hard to reconcile with the fact that plasmid-based expression of Dbf4 $\Delta$ N was able to complement the growth defect in DY-2 cells at restrictive temperature as effectively as Dbf4FL (Figure 3.3 A), which suggests that the interaction between Dbf4 and Orc2 may not be essential for targeting Dbf4 to origins. While previous work has shown that the chromatin association of Dbf4 is greatly reduced in an *orc2-1* mutant at restrictive temperature, there was, nevertheless, a proportion of total cellular Dbf4 that remained associated with the chromatin pellet in cell fractionation assays (Pasero *et al.*, 1999). These two models can be reconciled if the interaction with Orc2 is only one of several that helps to efficiently tether Dbf4 to origins. This would also explain the partial growth defect observed with the *dbf4 $\Delta$ N* strain (Figure 3.3 C). Phosphorylation of Dbf4 by Rad53 may cause a conformational change that disrupts interactions with additional ligands such as other ORC subunits or MCM proteins. Interestingly, even at permissive temperature, the association of Orc2 with Dbf4ts was compromised, relative to the strength of two-hybrid signal for wild-type Dbf4-Orc2 (Figure 3.4 A). This further suggests that a tight association between the two proteins is not strictly required for cell cycle progression, which is consistent with the observed delocalization of Dbf4 foci in an *orc2-1* background at 23°C as judged by immunofluorescence (Pasero *et al.*, 1999). Given the robust Dbf4 $\Delta$ M-Orc2 association (Figure 3.2 E), the effects of the Dbf4ts Pro277Leu mutation appear to extend beyond the M-motif.

### **3.3.2. A single amino acid change within Dbf4 M-motif confers resistance to genotoxic agents.**

It has been previously shown that *cdc7ts* mutants are sensitive to genotoxic agents (Njagi and Kilbey, 1982), and this study has shown here that this is also true for the Dbf4 $\Delta$ N mutant (Figure 3.3 D). It was, therefore, interesting to observe that Dbf4 P277L (Dbf4ts-FL) encoded by the *dna52-1* allele maintains a strong interaction with Rad53, while associations with both Orc2 and Mcm2 are compromised (Figure 3.4). Furthermore, DY-2 cells are more resistant to MMS than DY-1 (wild-type) cells (Figures 3.5, 3.6), and in either strain the overexpression of Dbf4ts-FL and, to a lesser extent Dbf4FL, confers improved growth in the presence of MMS (Figure 3.5 B). What is the explanation for this effect? One possibility is that, due to its weakened interaction with replicative factors, Dbf4ts-FL is more easily displaced from origins by Rad53 during an MMS-provoked checkpoint response. This may improve the efficiency with which further origin firing is suppressed. However, the prevention of late origin firing is unlikely to lead to greater viability in the face of MMS exposure. A comparison of two *mec1* mutants that fail to suppress late origin firing revealed that *mec1* $\Delta$  cells are hypersensitive to MMS while *mec1-100* cells are not. Furthermore, the *mec1* $\Delta$  strain was found to have a ten-fold higher rate of fork catastrophe than the *mec1-100* strain (Tercero *et al.*, 2003). Thus, another explanation for the improved growth observed with the DY-2 cells is that the efficient Rad53-Dbf4 association stabilizes Dbf4 and, following checkpoint adaptation, Dbf4/Cdc7 aids in the resumption of normal replication fork progression through modification of previously identified fork-associated substrate(s) such as Mcm2 (Lei *et al.*, 1997), Cdc45 (Nougarede *et al.*, 2000) and/or the pol $\alpha$ -primase

complex (Weinreich and Stillman, 1999). Indeed, this may help to explain why DY-2 cells actually grow better at 30°C in the presence of lower concentrations of MMS (0.005 and 0.01%, but not 0.015%; Figure 3.5 B). Although clearly speculative, it is possible that the deleterious effects of the MMS are offset by the ability of Dbf4 to help to restart paused forks, mediated by its interaction with activated Rad53. Since replication fork stalling occurs even during an unperturbed S-phase (Deshpande and Newlon, 1996; Wang *et al.*, 2001) this activity of Dbf4 might aid recovery from both natural and lesion-induced impediments to fork progression. Although this effect was not observed with HU and UV exposure (Fig. 5A and data not shown), it is possible that the optimal doses of each to see such a growth enhancement were not used. Alternatively, the contrasting observations may be due to agent-specific differences in the checkpoint response (Liu *et al.*, 2003). Given that Dbf4/Cdc7 has been shown to function in translesion synthesis (Pessoa-Brandao and Sclafani, 2004), some additional candidate substrates include alternative polymerases and/or accessory proteins which are thought to permit replication fork progression through damaged DNA.

Another potential role for Dbf4 is that its interaction with Rad53 serves as a signal for downstream checkpoint effectors, consistent with the cell cycle arrest observed when the Dbf4 N-terminus is overexpressed (Duncker *et al.*, 2002). In this scenario, the efficient initial establishment of the checkpoint might maintain the viability of a greater number of cells, which then successfully re-enter the cell cycle following adaptation.

Plasmid-expressed Dbf4ts-FL is more beneficial than plasmid-expressed Dbf4FL for both DY-1 and DY-2 cells exposed to MMS (Figure 3.5 B). Curiously, this is not the case for cells grown on HU medium, as episomal and genomic expression of the same

form of Dbf4 (i.e., episomal Dbf4FL for the DY-1 strain, and episomal Dbf4ts-FL for the DY-2 strain) results in the best growth (Figure 3.5 A). Since Dbf4 and Cdc7 have been shown to form oligomers (Shellman *et al.*, 1998), it is possible that complexes with either Dbf4FL or Dbf4ts-FL are more effective than those with a mix of both at dealing with the consequences of HU-induced fork slowing, while such complexes or their composition may not be important for recovery from MMS-induced fork blockage

### ***3.3.3 Conservation of eukaryotic DDK function.***

The finding that the Dbf4 motif M is required for normal cell cycle progression, while the N-motif is most likely involved in checkpoint responses, adds to the growing body of evidence that DDK function is conserved among eukaryotes (reviewed in Duncker and Brown, 2003; Kim *et al.*, 2003). Studies of Dbf4 ortholog motifs in both fission yeast (Fung *et al.*, 2002; Ogino *et al.*, 2001; Takeda *et al.*, 1999), and humans (Kim *et al.*, 2003; Sato *et al.*, 2003) have shown similar results.. In the present report, the understanding of how Dbf4 fulfills both roles by establishing important functional connections between these motifs and specific interactions with DNA replication and checkpoint factors has been advanced. It will be of considerable interest to determine whether these findings can now be extended to all eukaryotes.

**Chapter 4: Mutagenesis of Dbf4 N-motif and the effect of Dbf4 N-motif mutations  
on Dbf4-Rad53 interactions.**

Figure 4.1 contributed by Julian Weigelmann.

#### **4.1. Introduction**

The *Saccharomyces cerevisiae* protein Dbf4 has three motifs (N, M and C) that are relatively well conserved throughout eukaryotic species (Masai and Arai, 2002). As observed in Chapter 3, of the three motifs, the N-motif has been shown to be important in the checkpoint function of Dbf4 by mediating an association with the checkpoint kinase Rad53. Originally, Duncker *et al.* (2002) showed that the N-terminus of Dbf4 interacts with the FHA1 and FHA2 domains of Rad53 in two-hybrid assays. They also demonstrated that the N-terminus of Dbf4 interacts with Orc2. In the preceding chapter (Chapter 3) of this thesis, two-hybrid analysis was used to show that Dbf4, with the N-motif deleted (Dbf4 $\Delta$ N), has disrupted interactions with Rad53, as well as with Orc2. Interestingly, the interaction between Dbf4 and Mcm2 was maintained for the Dbf4 $\Delta$ N mutant protein. Moreover, it was shown that while the Dbf4 N-motif is dispensable for viability, the *dbf4* $\Delta$ N mutant was sensitive to the genotoxic agents, HU and MMS. This is consistent with what was previously observed in the *Schizosaccharomyces pombe* model, when the N-motif was deleted from the genomic copy of *DFP1* (the *S. pombe* orthologue of *DBF4*) (Fung *et al.*, 2002; Ogino *et al.*, 2001). However, these previous studies, involving the *S. pombe* model, did not investigate the protein-protein interactions that were affected by the Dbf4 N-motif deletion. Thus, these authors were not able to determine, definitively, which molecular mechanisms were affected by the mutations, causing the phenotypes.

A slight growth defect was observed (Figure 3.3 D) for the *dbf4* $\Delta$ N mutant strain relative to an isogenic wild-type strain in the spotting assays, as well as during the initial growth of the tetrads during the construction of the mutant strains. This growth defect

phenotype is examined, in more detail, in this chapter. Since the levels of Dbf4 remain low from the end of mitosis to late G1 phase, any Dbf4 mutant phenotype affecting the cell cycle progression should be evident during S-phase (Cheng *et al.*, 1999). It has been shown that Cdc7 protein interacts with Orc2 (Hardy, 1996). Furthermore, the Cdc7 protein has been shown to remain present on the chromatin in the absence of Dbf4 (Weinreich and Stillman, 1999). Taken together, these results suggest that Cdc7 remains at the origins and Dbf4 complexes with Cdc7 to form an active complex. It is possible that the Dbf4-Orc2 interaction, which was shown (in Chapter 3) to be disrupted as a result of the removal of the Dbf4 N-motif, is contributing to the growth defect phenotype of the *dbf4ΔN* mutant. In this chapter, the growth defect phenotype of the *dbf4ΔN* mutant observed in Chapter 3 was investigated, experimentally.

In addition to a further investigation of the Dbf4 N-motif deletion mutant, the work presented in this chapter also includes a more detailed study of the N-motif by the construction of N-motif point mutants. Other research groups studying the fission yeast, *S. pombe*, have generated *Dfp1* N-motif mutations. More specifically, a precise N-motif deletion mutant and point mutations in a conserved 8 amino acid stretch, were made (Fung *et al.*, 2002; Ogino *et al.*, 2001). These mutants were found to be sensitive to HU and MMS, ionizing radiation (IR) and UV radiation (Fung *et al.*, 2002; Ogino *et al.*, 2001). The molecular mechanisms causing the phenotypes were, however, not studied by these investigators. Thus, it was decided, in the present study, to explore the corresponding amino acids that are conserved in the *S. cerevisiae* Dbf4 (amino acids 168-178). It was hypothesized that equivalent N-motif point mutations might result in phenotypes similar to what was previously observed for the *dbf4ΔN* mutant. This would

imply that the specific Rad53 FHA1 binding site of Dbf4 is contained within this stretch of amino acids within the Dbf4 N-motif. Thus, deletions and point mutations corresponding to amino acids 168-178 were made.

Thus, in this chapter, the Dbf4 N-motif is examined, building upon the findings described in Chapter 3. Firstly, the growth defect observed for the *dbf4ΔN* mutant is investigated. The Dbf4 N-motif is then further dissected and studied, in attempts to further specify the Rad53 FHA1 domain binding site in Dbf4. This was important as it was a means to identify a mutation that specifically abrogates the Dbf4-Rad53 FHA1 domain, and potentially maintains the Dbf4-Orc2 interaction. Any phenotype attributed to such a mutant could be specifically attributed to a disrupted Dbf4-Rad53 FHA1 interaction.

## 4.2. Results

The *dbf4ΔN* mutant (DY-78), created and described earlier in Chapter 3, had exhibited a partial growth defect. The growth defect of the *dbf4ΔN* mutant was of interest because it suggests the N-motif of Dbf4 may be important in the initiation of DNA replication role of Dbf4 in addition to its involvement in the checkpoint response function (by mediating the Dbf4-Rad53 interaction). This is most likely related to the Dbf4-Orc2 interaction that was demonstrated earlier (in Chapter 3) by the two-hybrid analysis. Thus, in an attempt to examine this further, the growth of the mutant *dbf4ΔN* strain was compared to an isogenic wild type control strain by taking cell counts over a period of 6 hours (Figure 4.1A). Clearly, from Figure 4.1A, it is evident that the *dbf4ΔN* mutant strain grows slower than the wild type control strain. The generation time of the *dbf4ΔN* mutant was

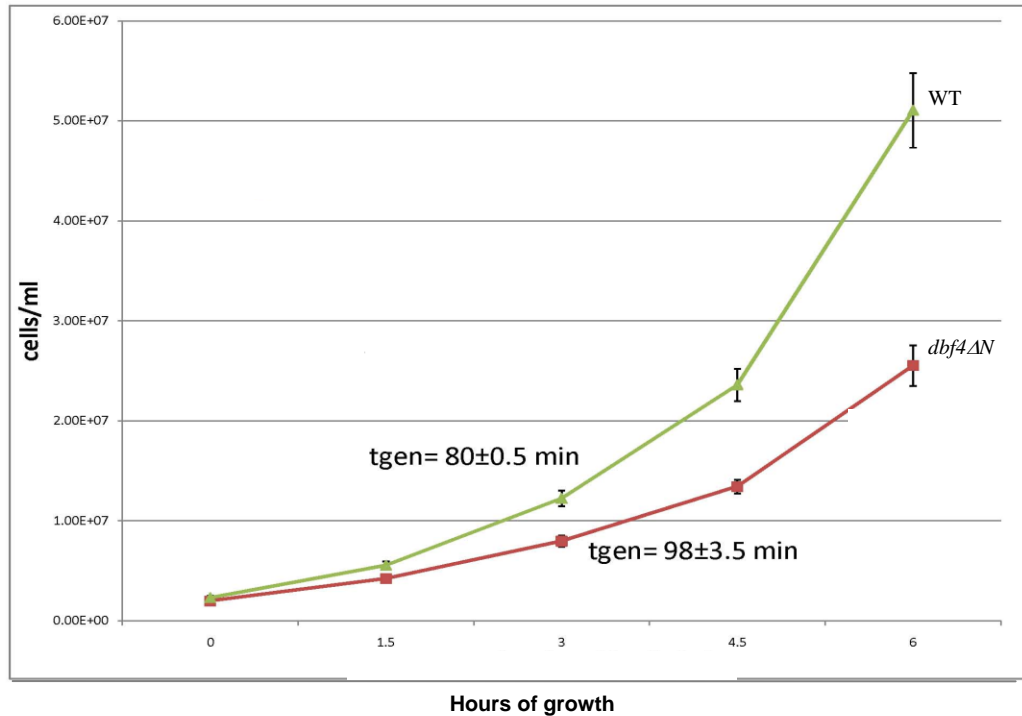
calculated to be  $98 \pm 3.5$  minutes while the generation time of the Dbf4 wild type control strain was found to be  $80 \pm 0.5$  minutes. The S-phase length of the mutant strain was compared to that of the wild type control, through fluorescence activated cell sorting (FACS) profiles of cells progressing through S-phase of the cell cycle, following release from an  $\alpha$ -factor synchronized arrest in G1 phase (Figure 4.1 B). The DNA content for a haploid strain is determined as 1C or 2C. A 2C DNA content indicates that cells have duplicated their DNA. The DNA content of cells in mid-S-phase, are detected, as between 1C and 2C. The *dbf4ΔN* strain completed S-phase approximately 100 minutes after release from alpha-factor arrest, while the wild type strain completed S-phase by 50 minutes, under the same experimental conditions (Figure 4.1 B). It should be noted that for the FACS analysis profiles, strains were grown at 23°C, to facilitate a more detailed analysis of S-phase progression. At this temperature, the entire cell cycle will progress at a slow rate, relative to the normal growth temperature of 30°C. It was relevant to focus on comparing the S-phase length because the levels of Dbf4 remain low from the end of mitosis to G1. Thus, any Dbf4 mutant phenotype would be most prevalent during the G1/S phase transition and during S-phase of the cell cycle (Cheng *et al.*, 1999).

**Figure 4.1. Growth rate of the *dbf4ΔN* mutant (DY-78) relative to an isogenic wild type (DY-77) strain.**

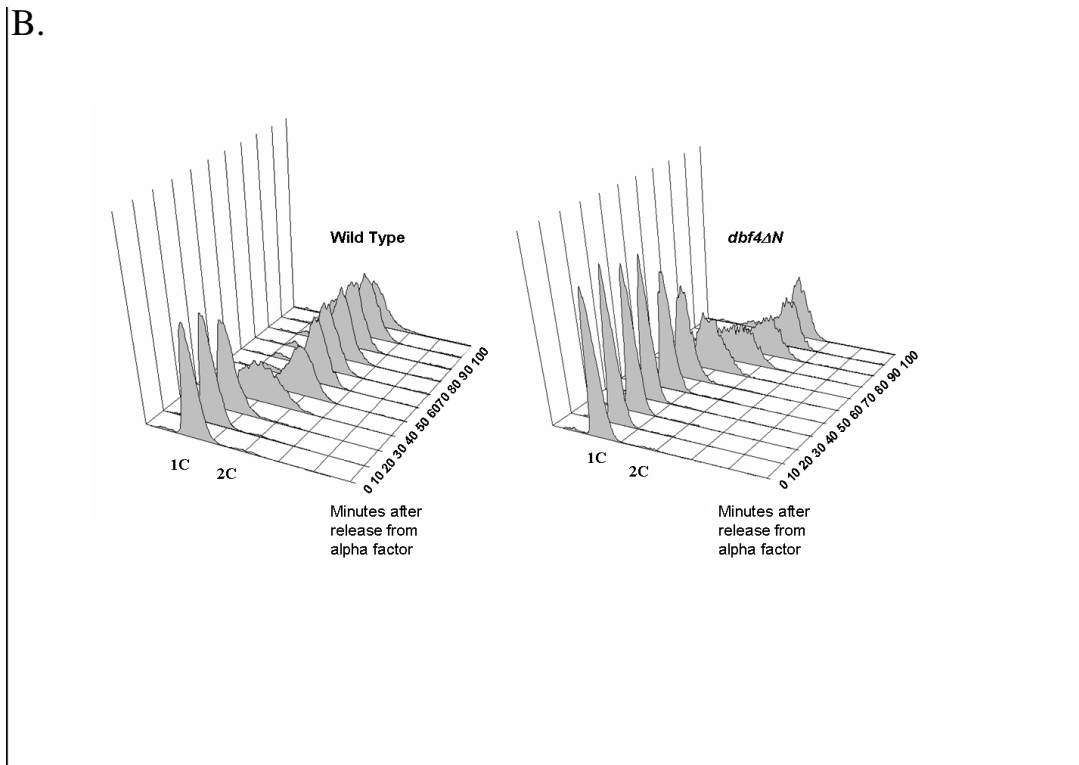
A. Logarithmic growth was determined by direct microscopic counts for each of the two strains and is presented for time points of 0, 1.5, 3, 4.5 and 6 hours after an initial cell concentration of  $2 \times 10^6$  cells/ml. The generation time was calculated for the *dbf4ΔN* mutant ( $80 \pm 0.5$  min) and for the Dbf4 wild type (WT) (DY-77) strain ( $98 \pm 3.5$  min). The cells were grown at 30°C with 200rpm shaking. The cell counts for each of the two strains were done in triplicate and the cell counts presented represent the averages +/- standard deviation.

B. Determination of S-Phase length through FACS analysis. Both the *dbf4ΔN* and wild type strains were synchronized in late G1 phase by alpha-factor and then released into S-phase at 23°C. FACS samples were taken every 10 minutes.

A.



B.



Beyond the study of the entire N-motif as a functional domain, it was of interest to further investigate the N-motif by mutating amino acids that were presumed to be important for the Dbf4-Rad53 interaction. The eleven amino acid stretch (168-178) in Dbf4 corresponding to those residues previously mutated by Fung *et al.* (2002) in *S. pombe* are highlighted in Figure 4.2. It is interesting to note that four threonines are included amongst these eleven amino acids, because fork-head homology (FHA) domains specifically recognize phosphothreonines (Mahajan *et al.*, 2008). The aforementioned eleven amino acids were deleted to form a mutant Dbf4 allele that was tested in two-hybrid assays with full-length Rad53 or its FHA1 domain as prey proteins (Figure 4.3). The FHA1 domain of Rad53 had previously been shown by Duncker *et al.* (2002) to be important in mediating the Dbf4-Rad53 interaction. The Dbf4ts protein was used as an additional control bait protein because in the preceding Chapter 3 the Dbf4-Rad53 interaction was shown to be maintained, in spite of the the temperature-sensitive mutation (Figure 4.3). The two-hybrid assay results indicated that the Dbf4 $\Delta$ 168-178 mutant bait protein had abrogated interactions with both Rad53 and the FHA1 domain as prey proteins (Figure 4.3). This suggests that the Rad53 binding site of Dbf4 is within the amino acid 168-178 stretch of amino acids.

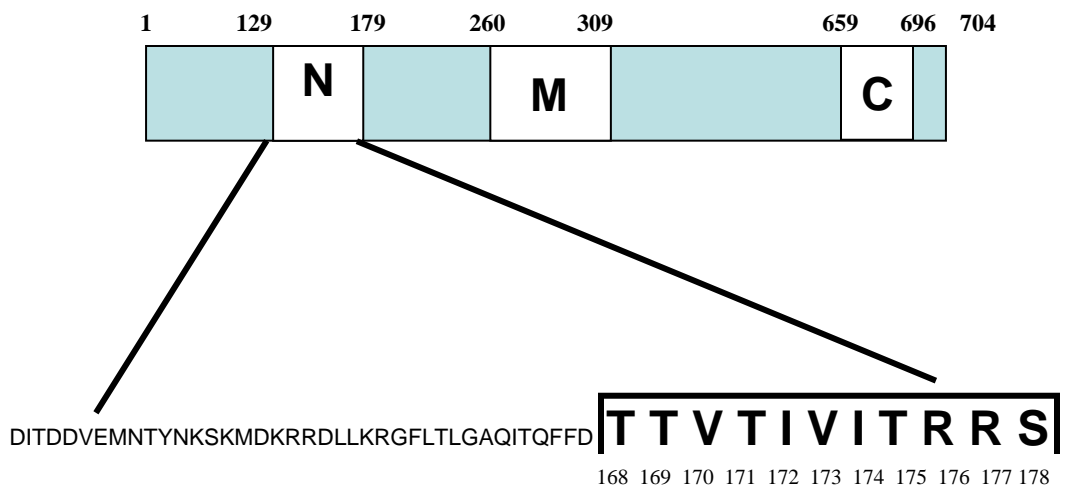


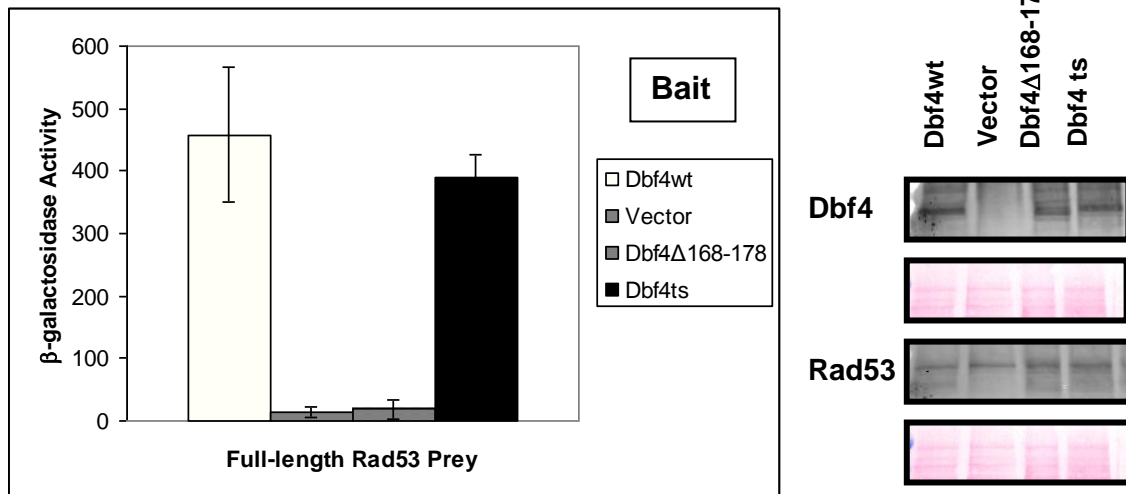
**Figure 4.2. Schematic diagram of Dbf4.** The N, M and C motifs are presented and the entire N-motif amino acid sequence of the Dbf4 is highlighted. Amino acid 168-178 of the Dbf4 N-motif, which were mutated are displayed in a box. The numbers indicate the amino acid residues.

**Figure 4.3. The Dbf4 $\Delta$ 168-178 mutation abrogates interaction with Rad53.**

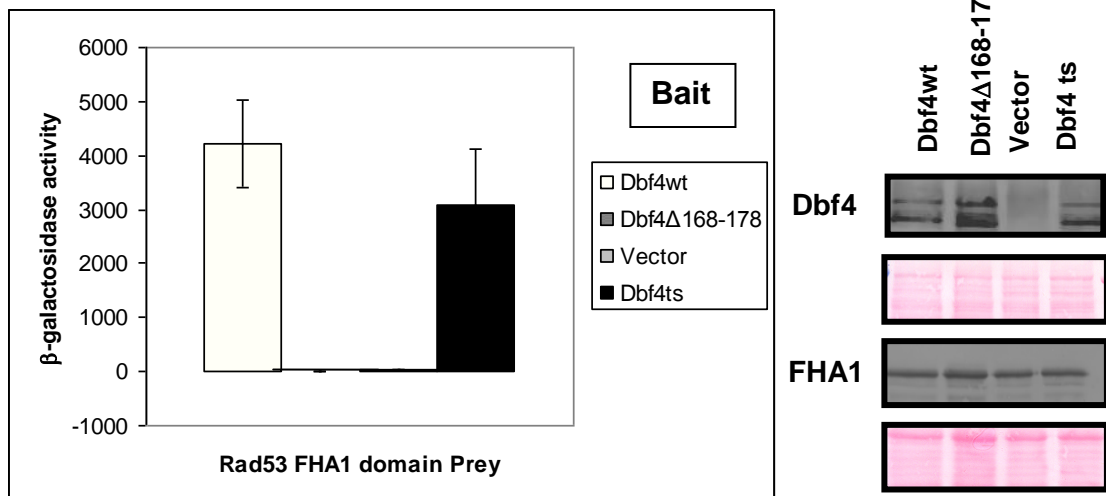
A. Two-hybrid assays using bait constructs pEGDbf4wt, pEG202 (vector only), pEGDbf4ts, and pEGDbf4 $\Delta$ 168-178 and pJGRad53 prey constructs were carried out as described in the Materials and Methods section. Protein expression of bait and prey proteins are presented on the right side of the two hybrid bar graphs. Culture aliquots were removed following the two-hybrid assay induction, whole cell extracts were prepared and western blots were performed as described in Materials and Methods. Bait proteins were detected with rabbit polyclonal anti-LexA antibody (Invitrogen), and prey proteins were detected with mouse monoclonal anti-HA antibody (Sigma). Ponceau-S stain (0.1%) verifying the equal loading of the protein samples are presented below each antibody detection. The  $\beta$ -galactosidase activity values represent the averages of 3 independent experiments, and the error bars indicate standard deviation.

B. Two-hybrid assays using bait constructs pEGDbf4wt, pEG202, pEGDbf4ts and pEGDbf4 $\Delta$ 168-178 and pJG FHA1 prey constructs were carried out as described in the Materials and Methods section. Bait and prey proteins were detected as described above. The  $\beta$ -galactosidase activity values represent the averages of 3 independent experiments, and the error bars indicate standard deviation.

A.



B.



The two-hybrid assay results involving the Dbf4 $\Delta$ 168-178 bait protein were the basis for deciding to create a Dbf4 deletion genomic mutant (*dbf4* $\Delta$ 168-178) strain having the same eleven amino acids deleted from the Dbf4 allele. It was hypothesized that a *dbf4* $\Delta$ 168-178 mutant would be viable and would be sensitive to genotoxic agents similar to the *dbf4* $\Delta$ N mutant. This was attempted using genomic integration in the same way that generated the *dbf4* $\Delta$ N mutant in Chapter 3. A schematic flow diagram depicting the various steps involved in the genomic integration procedure is presented in Figure 4.4. An integrating plasmid vector carrying the *DBF4* $\Delta$ 168-178 allele as well as a *URA3* selective marker gene was transformed into a wild type diploid strain (DY-27). A diploid strain was selected for integration because confirmed integrated transformants could be sporulated resulting in four haploid spores. Two of the four spores would contain wild type *DBF4* alleles and the other two spores would contain the mutant *DBF4* alleles. Thus, if the mutations were lethal, only two wild type spores would grow. The spores were grown on nonselective YPD medium plates. Colonies were grown to saturation and genomic DNA was isolated. A PCR reaction was then set up to determine whether a successful genomic integration had occurred. As a result of a recombination event, the mutant *DBF4* $\Delta$ 168-178 allele should integrate, essentially adjacent, to the *DBF4* wild type allele in the genome, along with plasmid DNA sequence between the two alleles (Figure 4.5 A) The PCR reaction (confirming genomic integration) involved a forward primer at the end of the *DBF4* allele and a reverse primer at the beginning of the *DBF4* allele (see Figure 4.5 B). For a successful integrant, the resulting PCR product consisted of plasmid sequence along with partial sequence of the *DBF4* wild type and mutant *DBF4* alleles, totaling approximately 5.6 kb in size, as determined by gel electrophoresis.

The observation of a 5.6 kb PCR product was indicative of a successfully integrated “pop-in” strains, which are shown in Lane 3 of Figure 4.5 B. This is commonly referred to as the “pop-in” step of the genomic integration procedure. Lanes 1 and 2 of Figure 4.5 B are controls that are PCR products derived from genomic DNA that had previously been confirmed as “pop-ins”.

Following the confirmation of the “pop-in” integration, the “pop-out” procedure was performed by restreaking colonies onto 5’FOA medium plates. The “pop-out” step involves the removal of the plasmid sequence and one copy of the *DBF4* (either the mutant or the wild type) *via* homologous recombination (4.5 A). The 5’FOA selects against the *URA3* marker that is carried by the integrating plasmid. 5’FOA is utilized by the *URA3* gene product as a substrate to produce a toxic compound that is lethal to the cell. Thus, only those cells that have “popped-out” the plasmid sequence (by homologous recombination) along with one copy of *DBF4* would grow on the 5’FOA plates. Thus, cells that have not undergone this recombination event are rendered nonviable.

Colonies from the “pop-out” plates were used to inoculate liquid YPD medium cultures and genomic DNA isolates were prepared. Each colony represents a candidate diploid strain “pop-out” that has one *DBF4* wild type copy and a second copy that is either mutant (*DBF4Δ168-178*) or wild type. It is important to note that only one of the two copies of Dbf4 in the original diploid strain is involved in the integration event. A PCR reaction was performed using the genomic DNA isolated from the candidate diploid “pop-out” strains to determine if they contained either two wild type copies of the *DBF4* allele or a single wild type copy of *DBF4* and a single mutant allele of *DBF4*. The PCR primers used in the PCR reaction flanked the portion of the *DBF4* sequence encoding

amino acids 168-178 (see Figure 4.5 C). The PCR product resulting from the deletion mutant allele would be slightly smaller in size than the PCR product resulting from the *DBF4* wild type allele (Figure 4.5 C). Figure 4.5 C shows a gel electrophoresis image (in Lanes 2 and 3) of double banded PCR products, representing “pop-out” diploid strains that had successfully retained the *DBF4Δ168-178* allele along with one wild type *DBF4* copy.

One of the “pop-out” diploid strains was next induced to sporulate. Sporulation, essentially the induction of meiosis, potentially, allows for the isolation of haploid mutant strains from the diploid mother strain. Upon the observation of tetrads in the sporulated culture by microscopy, several tetrads were dissected using a micromanipulator. Each tetrad should contain 4 haploid spores. Two of the spores were presumed to carry a *DBF4* wild type allele. The other two spores were presumed to be carrying a mutant *DBF4Δ168-178* allele. The dissected spores were grown for four days at 30°C. Following a four-day incubation of the plates, a consistent pattern of only two viable spores was evident for each dissected tetrad based on colony growth (Figure 4.5.D), although one of the tetrads dissected for the *DBF4wt/dbf4Δ168-178* strain yielded only one viable spore. This represents a dissected tetrad in which one of the two presumed wild type spores did not grow. Perhaps it was damaged during the tetrad dissection procedure. For the control plate, in which tetrads derived from a *DBF4wt/DBF4wt* diploid were dissected, a pattern of four viable spores was expected. One of the *DBF4wt/DBF4wt* dissected tetrads yielded three viable spores and one dissected tetrad yielded only one spore that gave rise to a normal size colony and three viable spores that gave rise to much smaller colonies. This demonstrates that some spores that are expected to be viable don’t always grow, as

expected. It is possible that the procedure of tetrad dissection, using the micromanipulator causes damage to some spores. Nonetheless, it was presumed that the *DBF4Δ168-178* mutation was lethal.

It was thought that because the complete N-motif deletion mutation yielded a viable mutant strain (Chapter 3), the apparently less dramatic *DBF4Δ168-178* mutation would also likely be viable. However, this was not the case. It is possible that the lethality of the mutation is caused by the distortion of protein folding.

**Figure 4.4. Schematic flow diagram of attempted construction of a *dbf4ΔI68-178* mutant strain.** The initial step is the cloning of the mutant allele into an integrating plasmid. The plasmid is then transformed into a diploid strain and plated onto SC-URA medium plates. Colonies were used to inoculate liquid cultures as sources of the genomic DNA. The genomic DNA was then used as a template to perform a PCR reaction to confirm that the mutant allele has integrated (“popped -in”), essentially adjacent, to one of the wild type copies of Dbf4 as a result of a recombination event. The same colony that was confirmed as a “pop-in” was then restreaked onto 5-Floroorotic Acid (5’FOA) agar plates to select for “pop-outs”. 5’FOA is used by the *URA3* gene product to produce a toxic compound. The resulting colonies were selected and used to inoculate a liquid culture and genomic DNA was isolated. A PCR reaction, using the genomic DNA as a template, was set up to confirm that the colonies were “pop-outs”. A diploid strain with a single copy of the wild type gene and a single copy of the mutant gene was the desired “pop-out”. The confirmed “pop-out” mutant strain was then used to inoculate a liquid culture followed by the induction of sporulation and tetrad dissection.

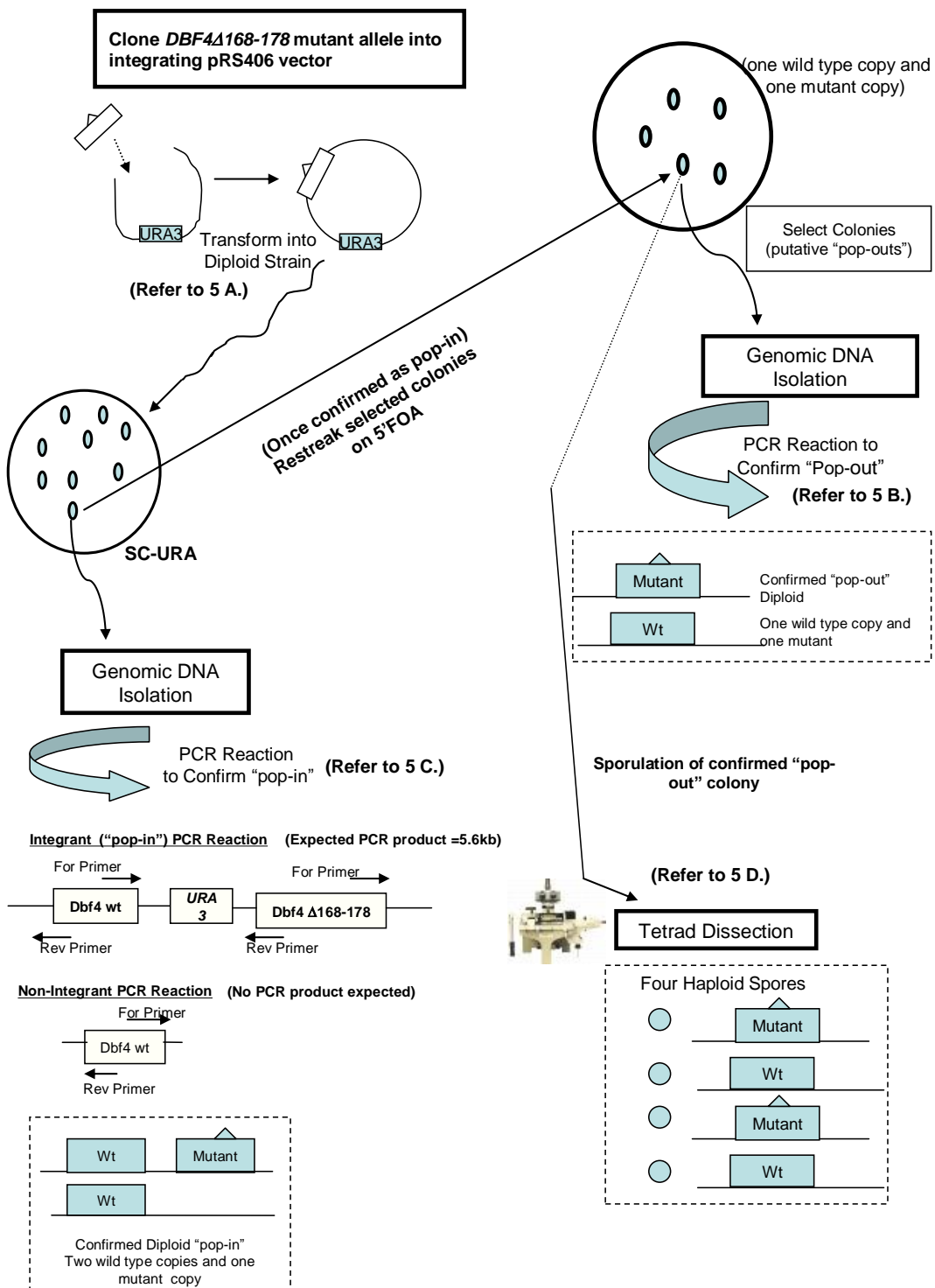
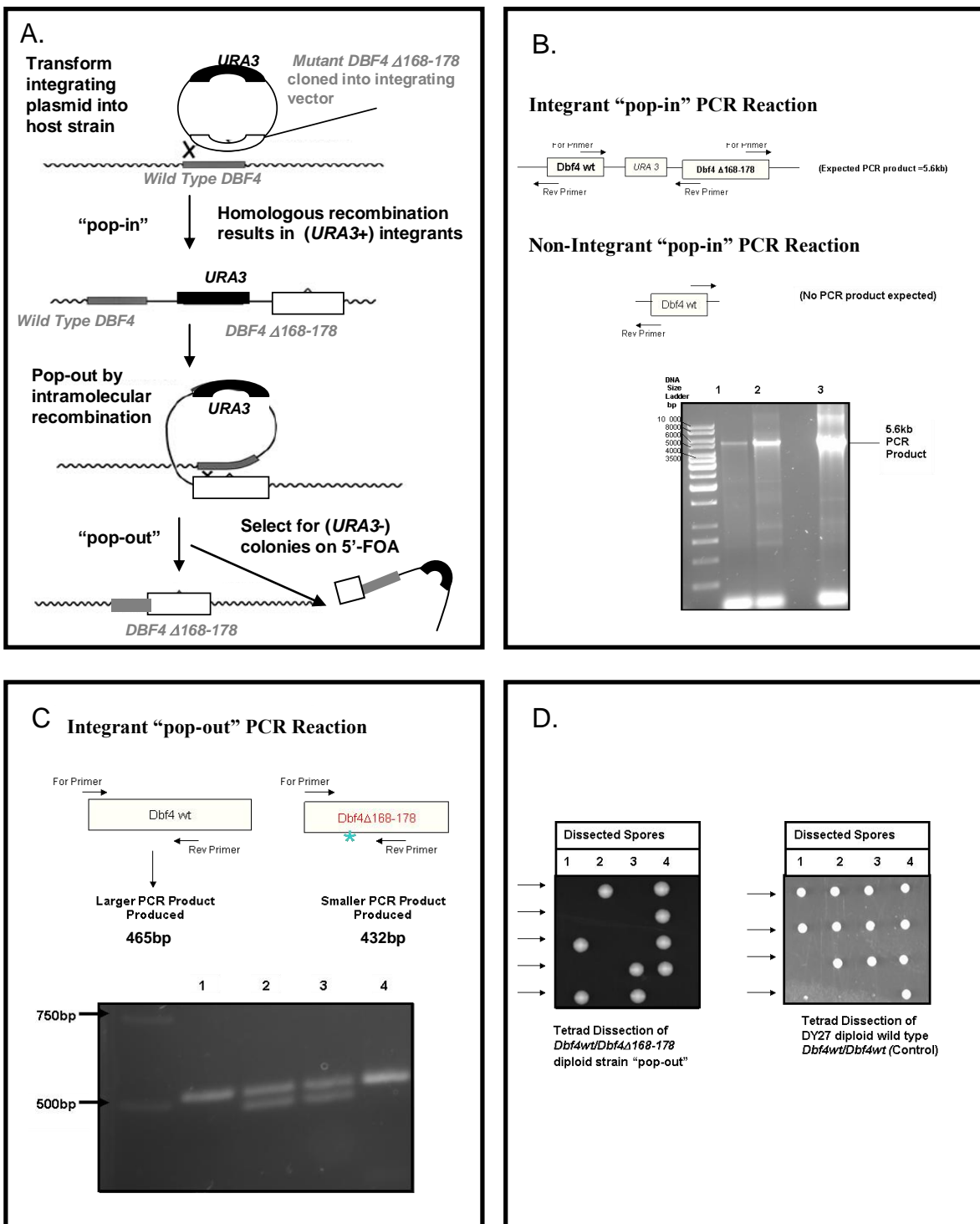


**Figure 4.5. Genomic integration of *Dbf4Δ168-178* mutation.**

- A. Schematic diagram of genomic integration of *DBF4Δ168-178* “pop-in”/“pop-out” strategy. The integrating plasmid (carrying the *URA3* marker) and mutant allele (*DBF4Δ168-178*) was transformed into the host strain and plated on SC-URA medium plates. As a result of a homologous recombination event, the entire integrating plasmid integrates into the genome at the *DBF4* locus, essentially adjacent, to the *DBF4* wild type gene. This is the “pop-in”. Thus, *URA3*+ integrants were selected for on SC-URA medium plates. The “pop-out” occurs by intramolecular recombination, selecting colonies on 5’FOA plates. The *URA3* gene product uses 5’FOA to produce a toxic compound. The intramolecular recombination event causes the complete removal of the integrating plasmid sequence and one of the *DBF4* alleles from the genome (either the mutant or wild type). Adapted from (Allers and Ngo, 2003).
- B. The genomic integration of the *DBF4Δ168-178* allele into the diploid strain DY-27. Agarose gel electrophoresis (0.8%) was carried out to examine the PCR product from a reaction to verify that the integrating plasmid carrying the *DBF4Δ168-178* mutant allele has successfully integrated, as a result of a recombination event. The 5.6kb PCR product is derived from partial Dbf4 sequence from the 3’end of one *DBF4* allele along with the entire integrating plasmid sequence and partial Dbf4 sequence from the 5’end of the second *DBF4* allele. A failed PCR reaction, yielding no PCR product, would indicate that the integration had not occurred. However, it is possible that the PCR reaction could have failed for other reasons. Note that Lanes 1 and 2 represent control PCR products of previously confirmed “pop-ins” (derived from the *dbf4ΔN* mutant construction in previous chapter) and Lane 3 is the experimental PCR product showing a band confirming that the *DBF4Δ168-178* has been integrated.
- C. Agarose gel electrophoresis (0.1%) of PCR products verifying the identity of a diploid integrant strain carrying one *DBF4* wild type allele and one *DBF4Δ168-178* mutant allele. PCR products were derived from a reaction involving primers flanking sequence encoding the Dbf4 amino acids 168-178, using genomic DNA from candidate “pop-out” diploid strains identified is shown. One band represents the *DBF4* wild type allele (465bp) and the second band represents a *DBF4Δ168-178* mutant allele (432bp). A single band indicates that the diploid strain has two copies of the *DBF4* wild type allele. Note that Lane 1 represents control PCR reactions, with two *DBF4* wild type alleles Lane 2 and 3 represent “pop-out” strains that carry one *DBF4* wild type allele and one *DBF4Δ168-178* mutant allele. Lane 4 represents a PCR product from a “pop-out” strain carrying two *DBF4* wild type alleles. Note: the asterisk represents the region where the amino acids were deleted in the *DBF4Δ168-178* mutant allele. It should be noted that the gel bands don’t appear to be running evenly. This is an artifact of the gel electrophoresis conditions.

- D. Tetrad dissection of the diploid *DBF4wt/dbf4Δ168-178* strain. Individual spores derived from tetrads were placed on a YPD plate and grown for 4 days at 30°C. The pattern of two viable spores and two nonviable spores on the tetrad dissection plates suggests that the haploid spores carrying the *DBF4Δ168-178* mutant allele were nonviable. The control plate was the result of sporulation and tetrad dissection of the diploid *DBF4wt/DBF4wt* (DY-27) wild type strain. All four haploid spores derived from the DY-27 control strain were expected to be viable. However, for one row only three spores are viable and for another there are three small spores and one large spore evident. Note: each arrow represents a tetrad that has been dissected.



Since the *dbf4Δ168-178* strain was shown to be nonviable, it was hypothesized that, perhaps, mutating the individual amino acids within the stretch of Dbf4 amino acid residues 168-178 (in various combinations), would potentially yield a viable point mutant that also had a disrupted interaction with Rad53. Data published by Ogino *et al.* (2001) in which the point mutations of critical threonine residues that align with *S. cerevisiae* threonines 171 and 175 resulted in mutants that were sensitive to HU and MMS. Moreover, it was also hypothesized that, *in vivo*, such a point mutant would cause a similar phenotype to that which had been observed for the *dbf4ΔN* strain. That is, perhaps, a Dbf4 N-motif point mutant might be sensitive to genotoxic agents. Thus, a series of two hybrid Dbf4 N-motif point mutant bait vectors was constructed. These were then tested in two-hybrid assays along with a Rad53 FHA1 domain prey vector (Figure 4.6). Amongst the amino acids 168-178 there are four threonines at positions 168, 169, 171 and 175. These threonines seemed to be likely candidates as critical amino acids that may be involved in the interaction with Rad53 FHA1 domain, since FHA domains are known to interact with phosphothreonines (Durocher and Jackson, 2002). In addition to testing various single and combinations of point mutations to the aforementioned threonine residues, two additional point mutants were also included as controls. These were identified by Gabrielese *et al.* (2006) as being sensitive to genotoxic agents. The Dbf4 mutations (GA159LL and W202E) were not, however, characterized in two-hybrid interactions by these researchers. It should be noted that the Dbf4 amino acid 159 does lie within the Dbf4 N-motif and the Dbf4 amino acid 202 does not. Single mutations of Dbf4 T171A and Dbf4 T175A alone were tested in two-hybrid assays (with FHA1) seemed to cause a partial disruption of the Dbf4-FHA1 interaction. However, Dbf4 T175A had a

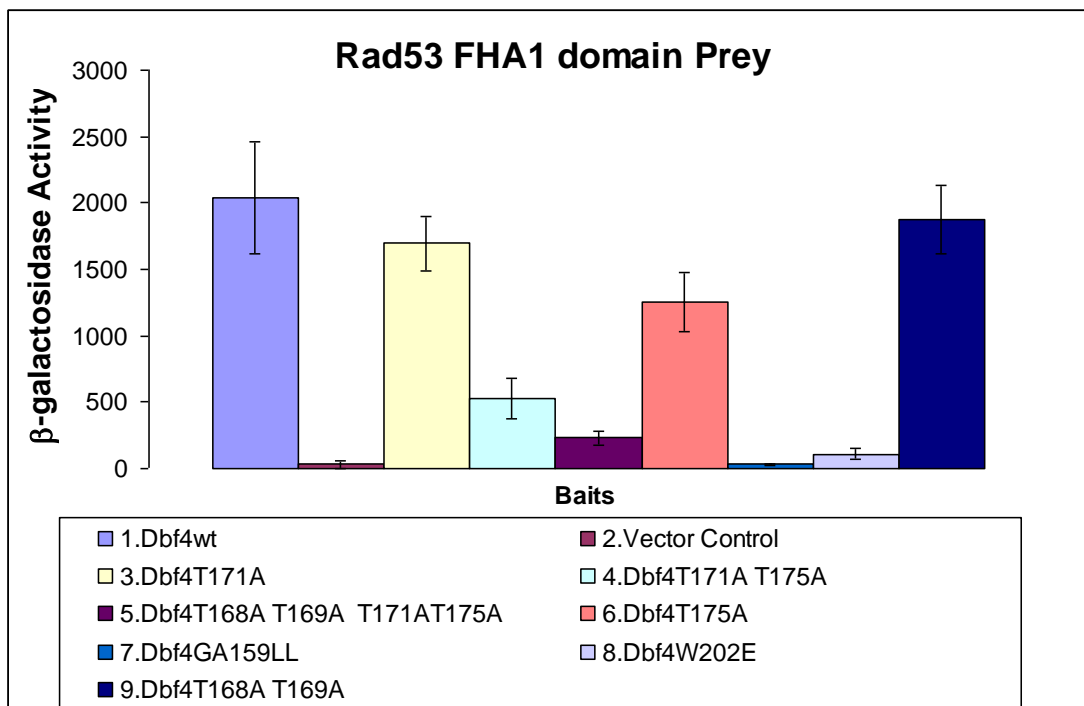
more reduced interaction with FHA1 than Dbf4 T171A. The combination of mutants that were tested included the double mutants: Dbf4 T171A T175A and Dbf4 T168A T169A and the quadruple mutant Dbf4 T168A T169A T171A T175A. The double mutant Dbf4 T171A T175A had a disrupted interaction with the Rad53 FHA1 domain and the quadruple mutant Dbf4 T168AT169A T171AT175A had an even further disrupted interaction with this domain compared to the Dbf4 wild type control interaction (Figure 4.6). Interestingly, the Dbf4 T168AT169A double mutation did not seem to detrimentally affect the Dbf4-Rad53 FHA1 interaction. Thus, it seems that double mutations involving T171A and T175A caused the Dbf4-Rad53 FHA1 interaction to be impaired. That is, the combination of mutations has an effect and single mutations do not. From these results, it can be concluded that it is likely that these same two amino acids (Threonine 171 and Threonine175) together may serve as a binding site for Rad53 in Dbf4. Interestingly, the two mutations (Dbf4GA159LL and Dbf4W202E) examined by Gabrielese *et al.* (2006) also caused disrupted interactions with the FHA1 domain of Rad53.

**Figure 4.6. Two-hybrid analysis of Dbf4 N-motif point mutant and Rad53 FHA1 domain interactions.**

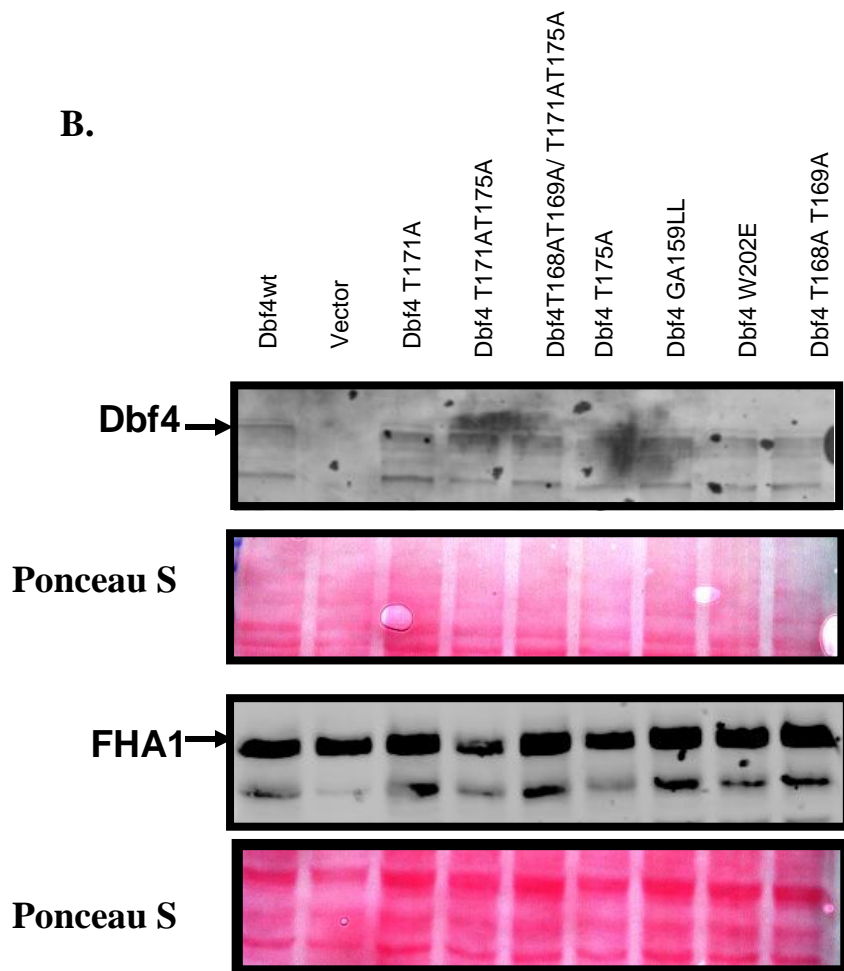
**A.** The following Dbf4 variants were tested in two-hybrid assays as bait constructs pEGDbf4wt, pEGDbf4T171A, pEGDbf4T171AT175A, pEGDbf4T168AT169AT171AT175A, pEGDbf4GA159LL, pEGDbf4W202E, pEGDbf4T168AT169A along with pJGFHA1 as a prey construct. Two-hybrid assays were carried out as described in the Materials and Methods section ( $\beta$ -galactosidase activity values represent the average of two experiments  $\pm$  standard deviation).

**B.** Protein expression of Bait and Prey proteins. Culture aliquots were removed following the two-hybrid assay induction, whole cell extracts were prepared and western blots were performed as described in Materials and Methods. Bait proteins were detected with rabbit polyclonal anti-LexA antibody (Invitrogen), and prey proteins were detected with mouse monoclonal anti-HA antibody (Sigma). Ponceau-S stains (0.1%) verifying the equal loading of the protein samples are presented.

**A.**

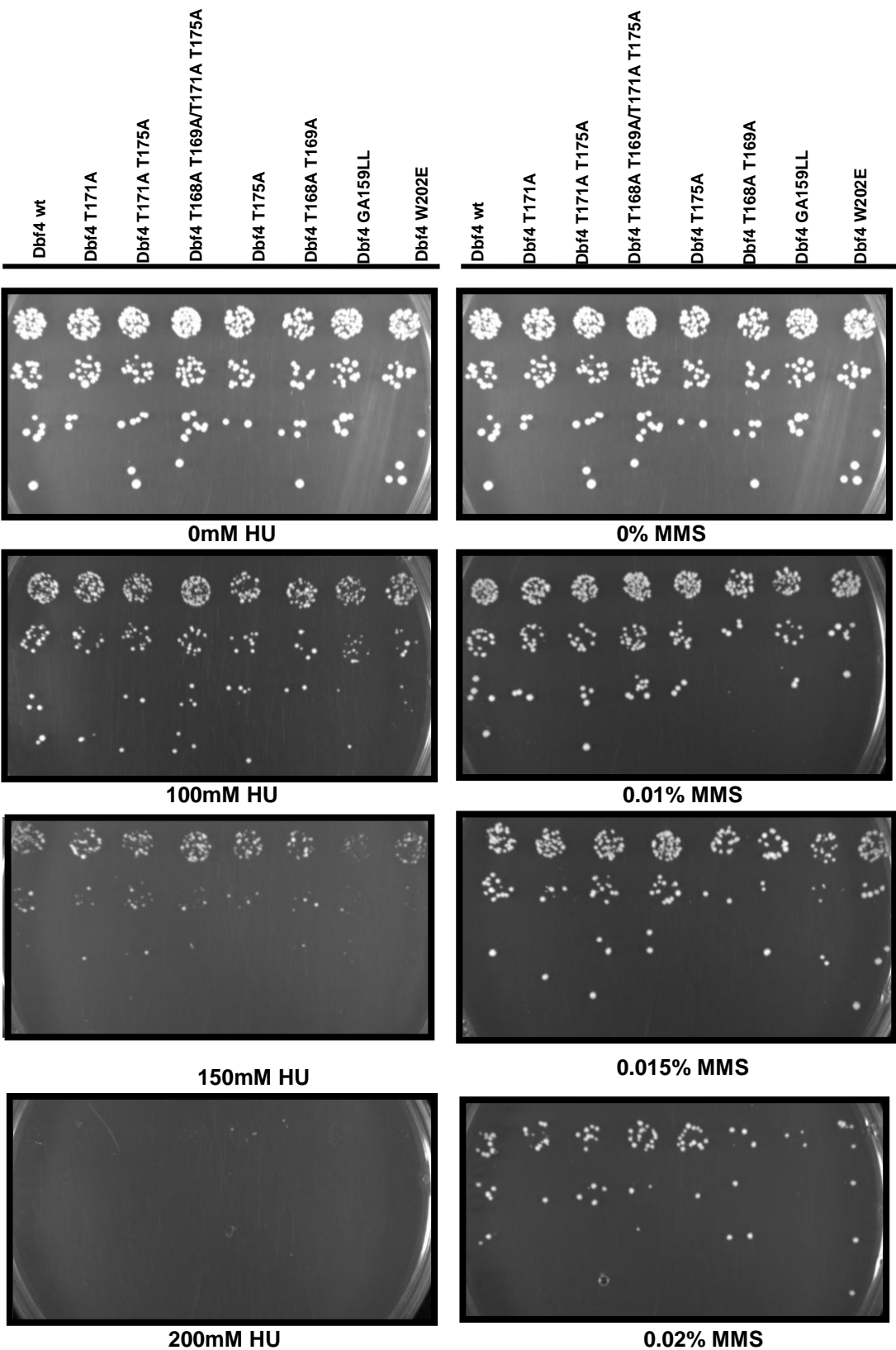


**B.**



The two-hybrid assay results involving the Dbf4 N-motif point mutants and Rad53 FHA1 domain further suggested that these mutations might confer sensitivity to genotoxic agents, *in vivo*. This was hypothesized because the disrupted Rad53-Dbf4 interaction mimics that which was observed for the *dbf4ΔN* mutant strain, which was sensitive to genotoxic agents. Thus, a plasmid shuffle assay was performed testing the same Dbf4 N-motif mutant alleles in a strain lacking the genomic wild type *DBF4* allele (Figure 4.7), as described in Chapter 2. Essentially, the plasmid shuffle strains expressing Dbf4 N-motif point mutants were tested for sensitivity to genotoxic agents, in a growth spotting assay, compared to a control strain expressing wild type Dbf4. In the plasmid shuffle/growth spotting assay, the strain viability was supported by plasmids expressing the Dbf4 N-motif point mutants. These transformant strains were tested for sensitivity to various concentrations of HU and MMS. None of the Dbf4 N-motif point mutants appeared to confer any sensitivity or resistance to HU or MMS. This is somewhat contradictory to the hypothesis that the point mutants would be sensitive to the genotoxic agents, HU and MMS. It is evident, however, that the two mutant strains (Dbf4GA159LL and Dbf4W202E) were slightly sensitive to HU and MMS at concentrations of 150 mM and 0.02%, respectively (Figure 4.7).

**Figure 4.7. Growth spotting assay of N-motif point mutant plasmid shuffle strains.**  
Plasmid shuffle strains expressing pEGDbf4wt or Dbf4 point mutants (pEGDbf4T171A, pEGDbf4T171AT175A, pEGDbf4T168AT169AT171AT175A, pEGDbf4GA159LL, pEGDbf4W202E, pEGDbf4T168AT169A) were grown to saturation in SC-HIS media. A five-fold dilution series was prepared for each culture and the dilutions were spotted onto SC-HIS plates containing 0,100, 150 and 200 mM HU as well as 0, 0.01, 0.015 and 0.02% MMS, as described in the materials and methods chapter. Plates were incubated at 30°C for 4 days.



## 4.3. Discussion

### 4.3.1. Removal of Dbf4 N-motif causes a growth defect

A comparison of the growth rates of the *dbf4ΔN* mutant ( $t_{gen}= 98\pm3.5$ ) relative to the wild type strain ( $t_{gen}= 80\pm0.5$ ) shows that the *dbf4ΔN* mutant grows slower (Figure 4.1) This result does seem to be consistent with the growth defect result observed by Gabrielese *et al.* (2006) for a mutant having the N-terminal 221 amino acids of Dbf4 removed. This N-terminal truncation included the entire Dbf4 N-motif. Interestingly, they also showed that the addition of a Nuclear Localization Signal (NLS) served to rescue the growth defect. The deletion of the N-terminal 221 amino acids of Dbf4 for the mutant described by Gabrielese *et al.* (2006) included a deletion of an NLS. However, the NLS is not disrupted in the *dbf4ΔN* mutant. It would be interesting to see what would happen if an additional NLS was added to the *dbf4ΔN* mutant.

Gabrielese *et al.* (2006) followed up this experiment with a two-dimensional agarose gel analysis of the *dbf4Δ221* mutant, the wild type control strain and the *dbf4Δ221-NLS* strains for two origins of replication (ARS 306 and ARS501). The two-dimensional agarose gel analysis revealed that the *dbf4Δ221* mutant was activating ARS306 less efficiently and the initiation of DNA replication was compromised at ARS501 (Gabrielese *et al.*, 2006). Interestingly, the addition of an NLS to the *dbf4Δ221* mutant strain resulted in a full restoration of the DNA replication defect at ARS306 and a partial restoration of the DNA replication defect at ARS501. It would be very interesting to perform similar two-dimensional agarose gel experiments involving the *dbf4ΔN* strain and compare it to a *dbf4ΔN* strain having the addition of an NLS.

The FACS profile results, obtained from this study, show that the S-phase was slower for the *dbf4ΔN* mutant than the wild type control strain (Figure 3.1.B). A similar result was observed by Gabrielese *et al.* (2006), while comparing the S-phase *dbf4Δ221* mutant to the wild type control, by FACS analysis. Consistent with their other results, the slower S-phase of the *dbf4Δ221* mutant seemed to be restored to wild type levels by the addition of an NLS (Gabrielese *et al.*, 2006).

It is noteworthy that a disrupted Dbf4-Orc2 two-hybrid interaction in the *dbf4ΔN* mutation was observed earlier in Chapter 3 of this thesis. This disrupted interaction could be contributing to the observed growth defect phenotype. It is possible that adding another NLS might enhance the efficiency of importing mutant Dbf4 into the nucleus and, perhaps, compensate for impaired Dbf4-Orc2 interaction.

#### **4.3.2. *The Rad53 binding site of Dbf4 lies within amino acids 168-178 of the N-motif***

It was hypothesized that the deletion of Dbf4 amino acids 168-178 would yield a mutant with a phenotype similar to that of the *dbf4ΔN* strain. The two-hybrid assay results showing the disrupted Dbf4-Rad53 and Dbf4-FHA1 interactions for the Dbf4Δ168-178 mutant were consistent with this hypothesis. The presumed nonviability of the mutant, as judged by the tetrad dissection, was likely due to the distortion of protein folding that resulted from the deletion mutation. Perhaps, attempts to create other deletions that included this region would yield an N-motif deletion mutant that is viable. It should be noted that, in a study published after most of the work included in this chapter had been performed, Gabrielese *et al.* (2006) created a series of Dbf4 N-terminal mutations. Interestingly, some of the deletions resulted in viable mutants and some of

them did not. However, Gabrielse *et al.* (2006) also performed a secondary structure prediction and found that the deletion mutations were predicted to be structurally destabilizing. These mutant alleles were not tested by Gabrielse *et al.* (2006) in two-hybrid assays along with Rad53 as a prey protein, as was done in the present study. Nonetheless, this data further supports the notion that the distortion of protein folding possibly caused the nonviability of the *Dbf4ΔI68-178* mutant. Since deleting the entire N-motif resulted in a viable *dbf4ΔN* deletion mutant, one could logically expect that a partial deletion within the N-motif of Dbf4 would also yield a viable deletion mutant. However, it is quite possible that a different deletion mutation can cause distorted protein folding, rendering the protein non-functional.

The point mutations of Dbf4 N-motif residues showed that combining the mutations of threonines 171 and 175 were important for the Dbf4 interaction with the Rad53 FHA1 domain. However, they did not seem to result in sensitivity to the genotoxic agents, HU or MMS. This could be a result of the fact that a plasmid shuffle assay method was employed to test these mutations. Perhaps, the expression levels of the mutant alleles in the plasmid shuffle strains were above endogenous levels, thereby compensating for the conferred sensitivity. The overexpression of the mutant alleles could possibly force or enhance the interactions with Rad53 that would not have occurred at endogenous levels. Thus, if these mutations were genetically integrated into mutant strains that expressed them at endogenous Dbf4 levels, a different result may have possibly resulted. It is also possible that the disruption of the Dbf4-Rad53 interaction was not severe enough to yield a sensitivity phenotype to the genotoxic agents, HU and MMS, that was observed for the *dbf4ΔN* strain in Chapter 3. It is, however, important to note

that both of the mutant Dbf4 alleles (GA159LL and W202E) originally reported by Gabrielese *et al.* (2006) did seem to have abrogated Dbf4-FHA1 interactions in the two-hybrid assays presented here. As mentioned earlier, one (GA159LL) of these mutations lies within the Dbf4 N-motif and the other one (W202E) does not. It is possible that these mutations are merely causing a conformational change that is not lethal to the cell, but does affect the Dbf4-Rad53 interaction. This is even more of a plausible explanation when one considers the actual structures of the amino acids that have been mutated. For the W202E mutant, the removal of the aromatic ring of tryptophan (W) and replacement with the glutamic acid (E) carboxyl group side chain is likely to be structurally disruptive. The tryptophan side-chain is a bulky, hydrophobic aromatic ring side-chain and the more reactive carboxyl group side-chain of glutamic acid might react with other amino acids causing structural changes. The glycine (G) and alanine (A) mutation to leucine (L) in the GA159LL point mutant is also conceivably structurally disruptive because the Leucine side-chains are more bulky than the glycine and alanine side-chain. Although these possibilities were not addressed by the authors themselves (Gabrielese *et al.*, 2006), it is a reasonable explanation for the two-hybrid assay results presented here in the present study. Nonetheless, these hypotheses could be further investigated when the Dbf4 three-dimensional structure is available.

It is relevant to discuss the Dbf4 N-motif point mutant two-hybrid assay results within the context of a recent model, explaining how FHA domains bind to phosphothreonines. Lee *et al.* (2008) have proposed a model, based on structural, biochemical and genetic evidence, using the Dun1 FHA domain. They have suggested a “pT-pT+3 rule” for the FHA-domain binding substrate preference. This means that the

FHA domain of Dun1 has a binding specificity for double pThr-containing peptides. Lee *et al.* (2008), have suggested that FHA domains have great diversity and versatility and it remains to be determined if the dual-pThr specificity exists in other FHA domains. It is interesting to note that the two critical threonine residues (position 171 and 175) that were identified as being involved (together) as the possible Rad53 FHA1 binding site in Dbf4 in the present study are four positions apart instead of three.

It is also possible that the N-motif point mutations affect the interactions between Dbf4 and other DNA replication protein factors. In particular, it would be interesting to determine if the Dbf4-Orc2 interaction is impaired as it was for the Dbf4 $\Delta$ N mutant protein. Furthermore, the effect of the N-motif point mutations on the Dbf4-Mcm2 interaction would also be of interest. The Dbf4-Mcm2 interaction was maintained, in two-hybrid assays, in spite of the *DBF4* $\Delta$ N mutation (Figure 3.2). A different pattern of two-hybrid assay results from what was observed for the Dbf4 $\Delta$ N mutant protein might also explain why the sensitivity to genotoxic agents was not evident in the spotting assay. That is, possibly, a maintained Dbf4-Orc2 interaction coupled with a maintained Dbf4-Mcm2 interaction would serve to retain conformational states of these proteins that promote the stabilization of replication forks and aid in replication fork recovery following a checkpoint, thereby reducing sensitivity of the cells to genotoxic agents. Furthermore, Segurado and Diffley (2008) have recently proposed that the Mcm 2-7 proteins may be implicated in replication fork stability in association with Mec1, Rad53 and Chk1. Once the three dimensional structure of Dbf4 is obtained, it will be possible, from a structural perspective, to investigate and ascertain as to what extent the N-motif point mutations affect the Dbf4-FHA1 interaction.

## **Chapter 5: Characterization of the Dbf4 C-motif**

Figure 5.4 contributed by Darryl Jones  
Figure 5.5 assisted by Phil Chan.

## **5.1. Introduction**

In the preceding chapters (Chapters 3 and 4), the Dbf4 N and M motifs have been investigated through mutational studies. The Dbf4 N-motif has been shown to mediate the interaction with Rad53 and was found to be dispensable for cell viability. The Dbf4 M-motif was involved in the interaction with Mcm2 and was essential for viability. The data from Chapter 3, showing that *dbf4ΔN* mutant is sensitive to genotoxic agents, highlights the importance of the Dbf4-Rad53 interaction in the intra-S-phase checkpoint response. This interaction serves to regulate late-firing origins of replication during the intra-S-phase checkpoint, by a removal of Dbf4 from late-firing origins. However, this regulation of late-firing origins is not the primary mechanism of importance in the intra-S-phase checkpoint response. A recent proposal has put forth that Rad53 modulates the involvement of Cdc7/Dbf4 in replication fork restart following a checkpoint mediated replication fork arrest (Szyjka *et al.*, 2008).

The Dbf4 C-motif, the most highly conserved of the three motifs, is also the smallest (Masai and Arai, 2000). Very little published data, pertaining to the *Saccharomyces cerevisiae* Dbf4 C-motif, is available. There is, however, a small body of literature investigating the Dbf4 C-motif in other model organisms. Thus, the research described here, in this chapter, was initiated, firstly, to determine if the C-motif is essential for viability in *S. cerevisiae*, and secondly, to determine if mutating the amino acids composing the putative CCHH-type zinc finger, contained within the Dbf4 C-motif, would affect the various protein-protein interactions involving Dbf4. In addition, an attempt was made to determine if such mutations would have any effect on the intra-S-phase checkpoint.

The C-motif has been investigated in *S. pombe* by other research groups, and there is some controversy regarding whether the C-motif is essential for cell viability or not, in this organism. Fung *et al.* (2002) created a viable genomic mutant that lacked the C-motif. However, Ogino *et al.* (2001) published results suggesting that the C-motif is required for viability. The C-motif deletion mutants created by Fung *et al.* (2002) were hypersensitive to the genotoxic agent, MMS, as compared to wild type strains. However, these same mutants were not hypersensitive to the genotoxic agents, HU, UV irradiation or ionizing radiation (Fung *et al.*, 2002). The C-motif deletion mutants that were sensitive to MMS, maintained intact intra-S-phase and mitotic checkpoints, suggesting a role for the C-motif in the recovery from stalled replication forks caused by MMS treatment (reviewed in Duncker and Brown, 2003). This notion is further supported by results from experiments showing increased mitotic recombination and chromosome loss observed for the C-motif mutants, compared to the wild type strain (Fung *et al.*, 2002). However, no investigation of any disrupted or altered protein-protein interactions, resulting from the C-motif deletion mutation, was carried out.

It should be mentioned here that Dowell *et al.* (1994) did test *S. cerevisiae* C-terminally truncated Dbf4 variants in a complementation assay. The truncated mutant Dbf4 was expressed from plasmids in the *dbf4-2* temperature-sensitive strain. This mutant strain carried a point mutation in Dbf4 that rendered the cells nonviable at 37°C. Among the five constructs expressing the C-terminally truncated Dbf4 mutants, tested by Dowell *et al.* (1994), two (Dbf4 amino acids 4 to 416; Dbf4 amino acids 81 to 416) complemented the cell growth of the *dbf4-2* temperature-sensitive (*ts*) strain at 37°C. The other three (Dbf4 amino acids 1 to 320; Dbf4 amino acids 1 to 160; Dbf4 amino acids

241 to 416) did not complement the cell growth of this strain under the same conditions. The same constructs were also tested in one-hybrid assays for their ability to bind to the ARS1 origin of replication and in a two-hybrid assay for their ability to bind to Cdc7. Both of the C-terminally truncated proteins, that did complement growth in the *ts* strain, were able to bind to ARS1 in the one-hybrid assay and also interacted with Cdc7 in a two-hybrid assay. None of the three C-terminally truncated proteins that didn't complement growth of the *ts* strain at 37°C were able to bind to both ARS1 in the one-hybrid assay and to Cdc7, in the two-hybrid assay.

The Dbf4 C-motif, contains a putative CCHH-type zinc-finger. It has been estimated that zinc-finger proteins represent as much as 2-3% of the eukaryotic proteome (Brayer *et al.*, 2008). Zinc-finger proteins have an extremely diverse array of functions and are known to be involved in transcription, DNA recognition, RNA packaging, apoptosis regulation, protein folding and assembly and lipid binding (Laity *et al.*, 2001). The CCHH-type zinc-finger proteins are largely known to be involved in protein-DNA interactions. However, CCHH-type zinc-finger proteins have also been known to be involved in protein-RNA or protein-protein interactions. In fact, Brayer *et al.* (2008), recently, applied an unbiased approach to directly examine the potential for zinc-fingers to facilitate DNA or protein interactions. They concluded that DNA binding is a more restricted function of zinc-finger proteins. It should be noted that the initial approach taken by this group was a bioinformatics analysis to identify sequence features that would predict a DNA or protein-binding function. This attempt was not successful because of several complications, including the uncertainties regarding the full functional capabilities of zinc fingers.

Böhm *et al.* (1997), attempted to classify variations of the CCHH-type zinc-finger motif and zinc-finger proteins in yeast. They grouped the zinc-finger proteins into three subsets. Of the three classifications, one was zinc-fingers with dispersed fingers or with a single zinc-finger. The other two classifications were: zinc-fingers containing clusters with at least two fingers in tandem (linked by two to six residues) and zinc-fingers that occur in arrangements between the other two classifications described. For most zinc-finger proteins in the single zinc-finger classification, no sequence-specific DNA binding sites were found (Böhm *et al.*, 1997). These findings lend further validity to the notion that Dbf4 is a single zinc-finger protein that is involved in protein-protein interactions and may not be involved in DNA binding.

In this chapter, there were two main objectives. The first objective was to determine if the C-motif is essential for viability of *S. cerevisiae*. The approach taken to address this objective was to make a more precise deletion of the C-motif, as well as point mutations of the cysteines and histidines composing the CCHH-type zinc-finger that is contained within the C-motif and test them in complementation assays. The second objective was to investigate any role of the Dbf4 C-motif in the intra-S-phase checkpoint in *S. cerevisiae*. To address the second objective, Dbf4 C-motif mutants were tested in one-hybrid assays and two-hybrid assays with the known Dbf4 binding targets, such as ARS1 origin sequence, Rad53, Mcm2, Cdc7, Orc2. In particular, Rad53 was of interest since it is known to interact with Dbf4 during the intra-S-phase checkpoint response. Earlier work in this thesis (Chapter 3) established that the N-motif mediates the Dbf4-Rad53 interaction and the *dbf4ΔN* mutant is sensitive to genotoxic agents.

## 5.2. Results

The first part of this investigation was focused on determining if the Dbf4 C-motif is essential for viability in *S. cerevisiae*. In order to establish whether the Dbf4 C-motif is essential for cell viability in *S. cerevisiae*, a more precise C-motif deletion mutant allele than those previously tested, was created. The C-motif deletion mutant was tested in a one hybrid assay, along with the Dbf4 $\Delta$ N mutant protein and the Dbf4 $\Delta$ M mutant protein, since they had not been previously tested. A one-hybrid assay is used to measure and quantify the affinity of a protein for a specific DNA sequence, in this case, the ARS1 origin of replication. The Dbf4 $\Delta$ N mutant protein, as expected, did not interact with ARS1 in the one-hybrid assay (Figure 5.1). This was expected because the N-motif falls within a previously determined ARS1 binding region (Dowell *et al.*, 1994). Interestingly, Dbf4 $\Delta$ M had a very robust interaction with ARS1 in the one-hybrid assay. From Figure 5.1, it is also clearly evident that the Dbf4 $\Delta$ C deletion mutant protein does not interact with ARS1 in the one-hybrid assay.

The results presented in Figure 5.1 are definitely interesting. It seems counterintuitive that the Dbf4 $\Delta$ M mutant protein binds robustly to the ARS1 (origin of replication) in the one-hybrid assay and the Dbf4 $\Delta$ N mutant protein did not bind to the ARS1 in the one-hybrid assay. Nonetheless, this result can be corroborated by some of the two-hybrid assay results presented earlier in this thesis (Chapter 3).

Firstly, it is important to discuss the mechanism of the one-hybrid assay, which is an *in vivo* assay that uses a reporter gene linked to the ARS1 (origin of replication) sequence.

The one-hybrid assay can detect proteins that are bound directly to the DNA sequence or, indirectly, through associations with other bound proteins. Since, there is no evidence, to date, indicating that Dbf4 binds directly to DNA, we can assume that the one-hybrid assay involving Dbf4 is detecting indirect binding of Dbf4 to ARS1. Such proteins would include those that compose the pre-replicative complex during the initiation of DNA replication.

It is reasonable to assume that since the M-motif deletion mutation (Dbf4 $\Delta$ M) results in the abrogation of the Dbf4-Mcm2 interaction, the mutant Dbf4 $\Delta$ M is being retained or tethered to the origin by some other protein-protein interaction. The Dbf4-Orc2 interaction is slightly enhanced, as a result of the M-motif deletion (Figure 3.2). Although not tested in the two-hybrid assay, it is possible that the Dbf4-Mcm4 interaction may also be enhanced, as a consequence of the disrupted Dbf4-Mcm2 interaction. Sheu and Stillman (2006) have shown that Mcm4 may also be a target of Dbf4 in the initiation of DNA replication. It is also relevant to discuss this result with reference to Rad53. In fact, the same reporter gene plasmid used in this experiment was also used previously by Dohrmann and Sclafani (2006) demonstrating that Rad53 binds to origins (ARS1) through its kinase domain. This result, in conjunction with other results led the authors to propose a novel role for Rad53 in the initiation of DNA replication that is independent of its checkpoint or dNTP regulation functions. Thus, it is also reasonable to conclude that the Dbf4 $\Delta$ M likely remains bound to the ARS1 origin through associations with Orc2, Rad53, Cdc7 and possibly Mcm4, in spite of the abrogated Dbf4-Mcm2 interaction. However, the *dbf4 $\Delta$ M* mutant is not viable, *in vivo*. Thus, it is not possible to confirm the one-hybrid assay result using another *in vivo* method, such as chromatin binding assay or

chromatin immunoprecipitaiton. Nevertheless, collectively, the one-hybrid assay result, combined with the non-viability of the *dbf4ΔM* mutant, indicates that the Dbf4-Mcm2 interaction must be essential for cell viability; however, it may not be essential for maintaining Dbf4 at ARS1 in the one hybrid assay.

Conversely, the *dbf4ΔN* mutant protein did not bind to the ARS1 origin in the one-hybrid assay. However, the *dbf4ΔN* mutant is viable (although growth defective) and the result could, potentially, be verified using the chromatin binding assay or chromatin immunoprecipitation. Nonetheless, the Dbf4ΔN protein interactions with Orc2 and Rad53 were abrogated in two-hybrid assays (Figure 3.2). Furthermore, the Dbf4ΔN-Mcm2 interaction was reduced to approximately half that of the wild type interaction. Thus, it is possible that the impaired Dbf4-Mcm2 interaction in conjunction with abrogated Dbf4-Orc2 and Dbf4-Rad53 interactions is not sufficient enough to retain Dbf4 at the ARS1 origin such that it is detectable in the one- hybrid assay.

As discussed above, in spite of the fact that the Dbf4ΔN mutant protein does not bind to ARS1 origins, in the one-hybrid assay, the *dbf4ΔN* mutant is still viable *in vivo*. It is, however, growth defective. How then is the *dbf4ΔN* mutant viable? The Dbf4-Mcm2 interaction is retained, despite the removal of the N-motif. Perhaps this is not enough to retain Dbf4 at origins such that it is detectable in a one-hybrid assay. It seems likely that there is a more transient Dbf4-Mcm2 interaction compared to what occurs in wild type cells. This seems likely because Bruck and Kaplan (2009) have shown that Dbf4-phosphorylation of Mcm2 is required for cell growth. Furthermore, Francis *et al* (2009) have demonstrated that the presence of ORC in the pre-RC was not required for the preferential phosphorylation of loaded Mcm2-7, by DDK. They concluded that DDK is

recruited to origin DNA through interactions with the Mcm 2-7 complex. This might explain why the *dbf4ΔN* mutant, is unable to bind Orc2, but maintains an interaction with Mcm2, and is still viable. A mutant isolated by Gabrielse *et al.* (2006) lacking the N-terminus of Dbf4 (the N-motif included), was also viable and growth defective. They suggested that perhaps Cdc7 binds to origins through an association with Orc that is redundant to Dbf4-Orc2 interaction. This redundancy might compensate for the abrogated Dbf4-Orc2 interaction in the *dbf4ΔN* strain, thereby preserving the viability of the strain.

The Dbf4ΔC mutant protein was then tested for its ability to support viability in a complementation assay. A complementation assay was performed in the *dna52-1* Dbf4 temperature sensitive (*ts*) strain, at the non-permissive temperature of 37°C. In addition to the construct having a precise deletion of the Dbf4 C-motif, an additional construct was made in which the C-motif was removed as part of a C-terminal truncation (C-TERM). The Dbf4 C-TERM construct expressed a different C-motif deletion mutant allele that could be compared to the Dbf4ΔC. This was done to ensure that the precise *DBF4ΔC* deletion mutation was not rendered nonfunctional as a result of the fusion of the remaining C-terminal sequence of Dbf4 to the truncated Dbf4, lacking the C-motif. As is evident in Figure 5.2, at 37°C, only the wild type Dbf4 and Dbf4ΔN transformants showed obvious growth. Thus, it is concluded from this result, that both the Dbf4ΔC and the Dbf4 C-TERM mutants are not able to support viability of the Dbf4 *ts* strain *dna52-1* at 37°C. The western blot presenting the protein expression of the Myc-tagged Dbf4 variant is shown in Figure 5.2 and verifies that each of the Dbf4 variants were expressed

in the complementation assay. However, the Dbf4 C-TERM expresses at much lower levels. This result suggests that the Dbf4 C-motif is likely essential for viability.

A further investigation of the Dbf4 C-motif involved the creation of a Dbf4 C-motif point mutant series. The rationale for making point mutations in the C-motif was the fact that the deletion mutations of the C-motif might have caused distorted protein folding. The point mutation of critical amino acids, composing the putative CCHH-type zinc-finger were thought to possibly be functionally disruptive, while maintaining the overall structural integrity of the Dbf4 protein. Strategic point mutations were made to the cysteine and histidine residues that compose the putative CCHH-type zinc-finger (Figure 5.3). These Dbf4 C-motif point mutants were first tested in a complementation assay (Figure 5.4). The complementation assay was carried out analogously to the previous complementation assays. It is clearly evident that all of the Dbf4 C-motif point mutants (Dbf4AAHH, Dbf4CCAA, Dbf4 CCHC and Dbf4 CCHA) were able to complement the Dbf4 temperature sensitive strain at 37°C. The western blot indicates that all of the Dbf4 C-motif point mutants and the wild type Dbf4 are being expressed at equal levels (Figure 5.4).

**Figure 5.1. Analysis of Dbf4 $\Delta$ N, Dbf4 $\Delta$ M and Dbf4 $\Delta$ C in a one-hybrid assay.** One-hybrid assays were carried out using pJGDbf4wt, pJG4-6, pJGDbf4 $\Delta$ N, pJG Dbf4 $\Delta$ M and pJGDbf4 $\Delta$ C as prey constructs along with the pLIARS1 reporter construct, as described in Materials and Methods. Dbf4 $\Delta$ M binds to the ARS1 origin of replication more strongly than wild type (Dbf4). Dbf4 $\Delta$ N and Dbf4 $\Delta$ C do not bind to ARS1. Protein expression of prey proteins were detected by immunoblot analysis with mouse monoclonal anti-HA antibody (Sigma). Ponceau stain (0.1%) verifying the equal loading of the protein samples is also shown. The bar graph represents the average of 2 individual experiments  $\pm$  standard deviation.

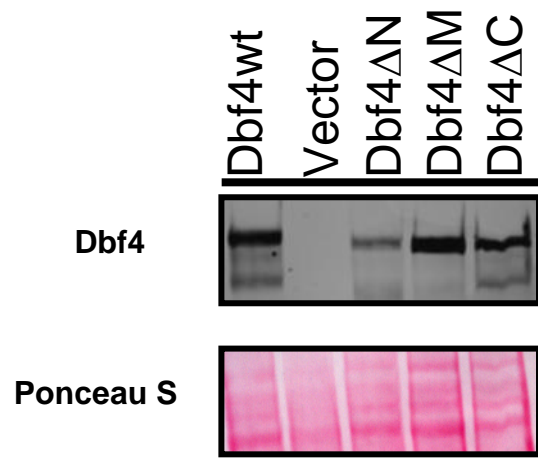
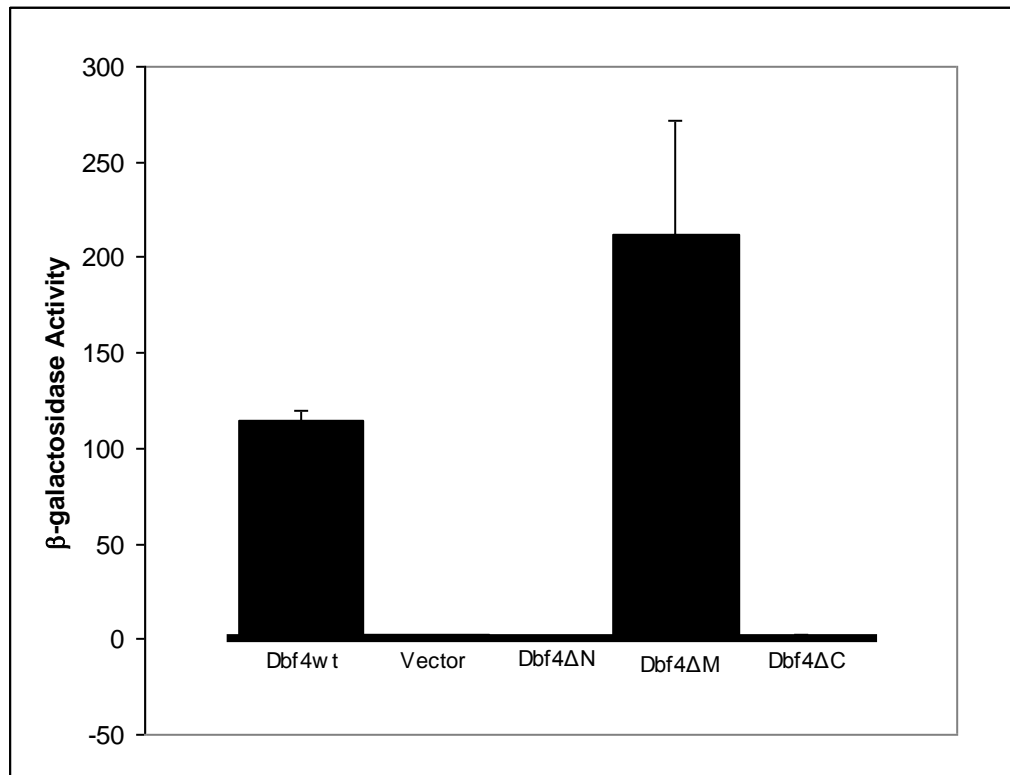
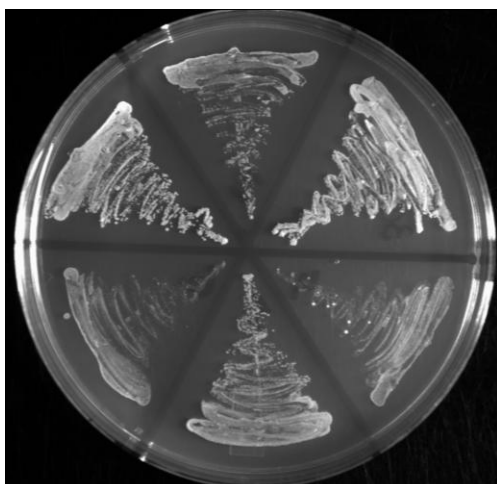
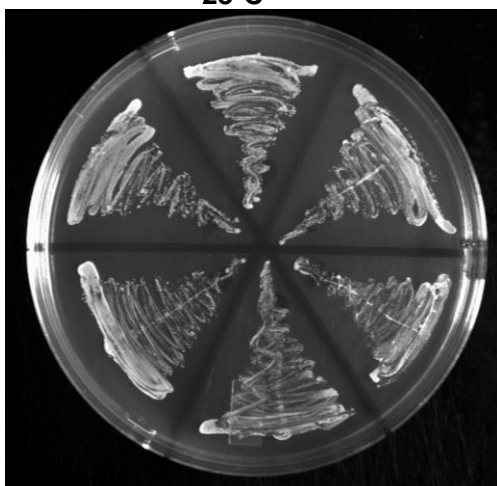


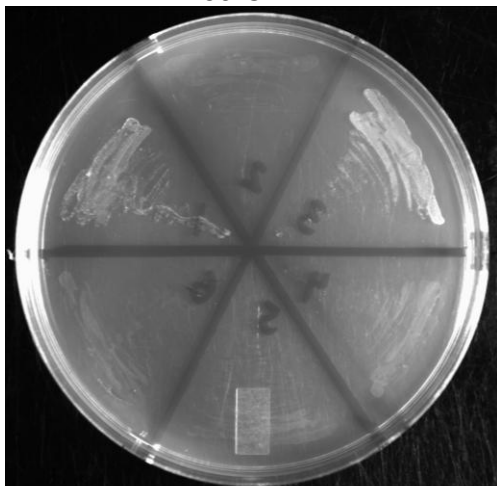
**Figure 5.2. Dbf4 C-motif deletion mutants are not able to complement a Dbf4 temperature sensitive mutant strain at the non-permissive temperature of 37°C.** DY-2 was transformed with pCMDbf4wt, pCM190, pCMDbf4 $\Delta$ N, pCMDbf4 $\Delta$ M, pCMDbf4 $\Delta$ C, pCMDbf4C-TERM constructs and streaked on three SC-URA plates as described in Materials and Methods. The plates were incubated at 23, 30 and 37°C, for 4 days. The protein expression of the constructs were determined by immunoblot analysis with mouse monoclonal anti-Myc (Sigma). Protein was extracted from the same liquid cultures that were used to prepare the streak plates. Ponceau S stain (0.1%) verifying equal loading of the protein samples is also shown.



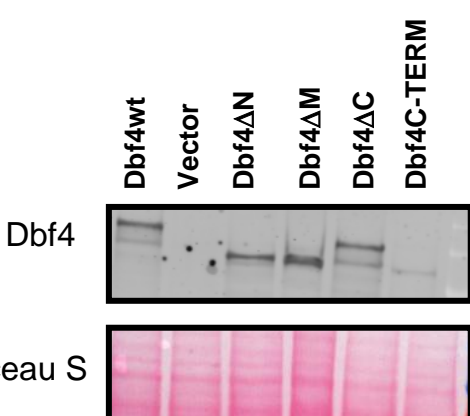
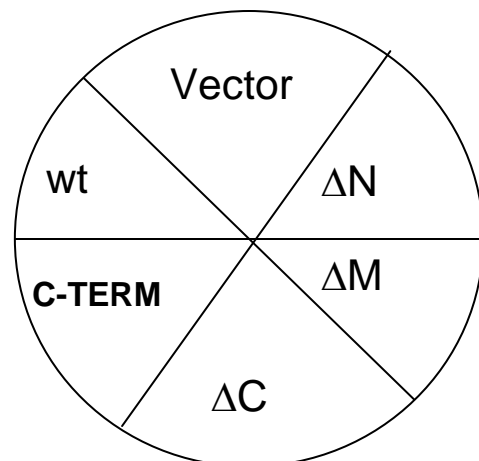
23°C



30°C



37°C



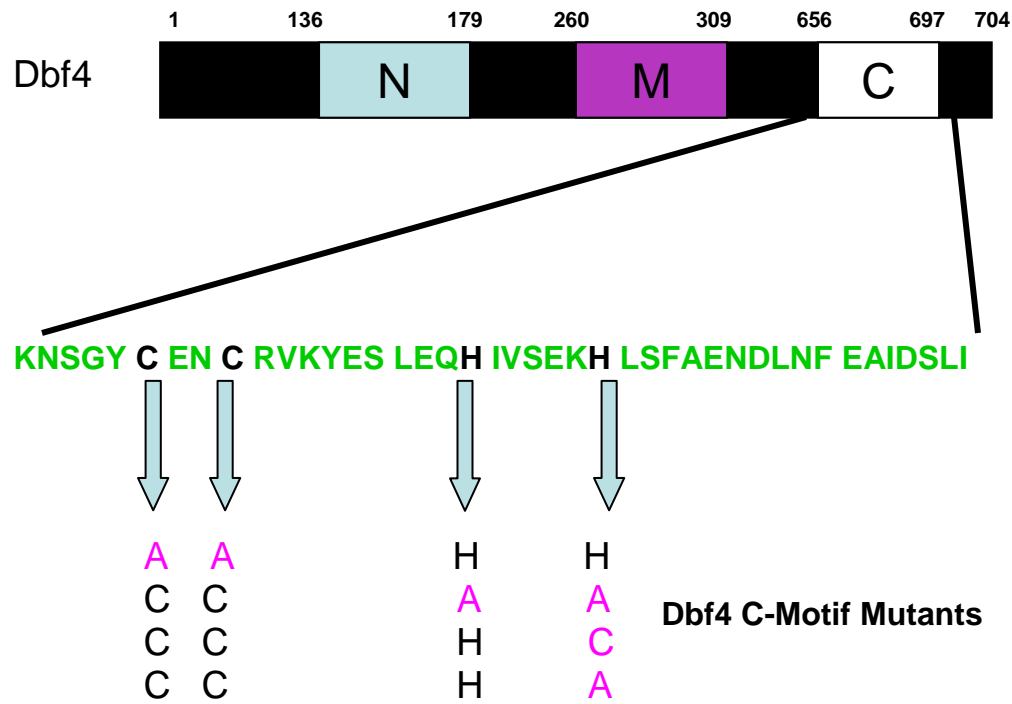
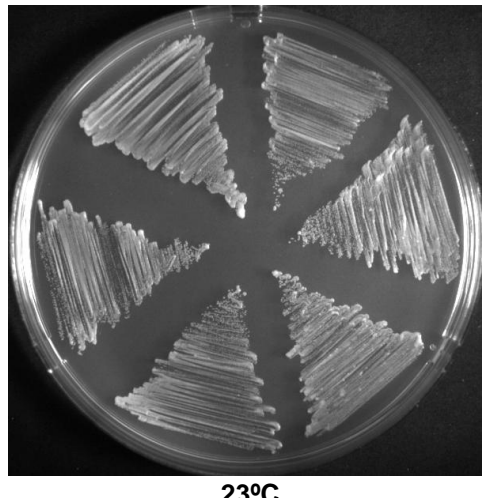
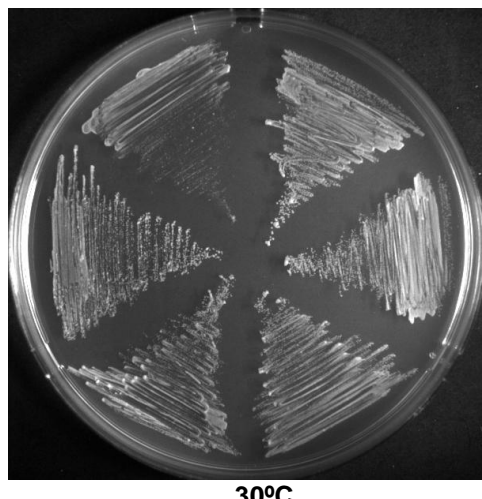


**Figure 5.3. Schematic representation of Dbf4 and its highly conserved motifs (motif N, M and C).** The amino acid sequence of the C-motif is magnified and the cysteines (661 and 664) and histidines (674 and 680) composing the putative zinc-finger are indicated by the arrows. The point mutations that were made are presented in pink text.

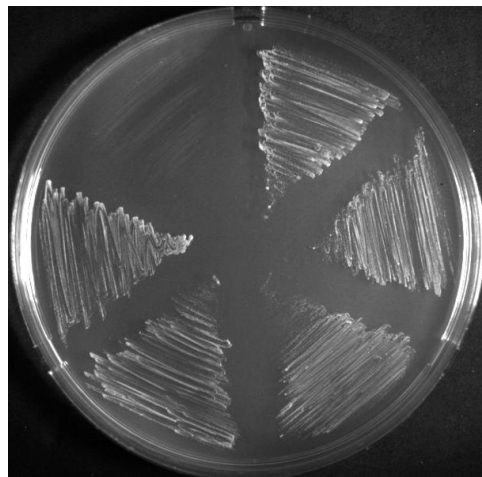
**Figure 5.4. The Dbf4 C-motif point mutants are able to complement the Dbf4 temperature sensitive strain at the non-permissive temperature of 37°C.** The DY-2, Dbf4 temperature sensitive strain was transformed with pCMDbf4wt, pCM190, pCMDbf4AAHH, pCMDbf4CCAA, pCM Dbf4CCHC and pCM Dbf4CCHA constructs and streaked on three SC-URA plates, as described in Materials and Methods. The plates were incubated at 23, 30 and 37°C, for 4 days. The protein expression of the constructs were determined by immunoblot analysis with mouse monoclonal anti-Myc (Sigma). Protein was extracted from the same liquid cultures that were used to prepare the streak plates. Ponceau S stain (0.1%) verifying equal loading of the protein samples is also shown.



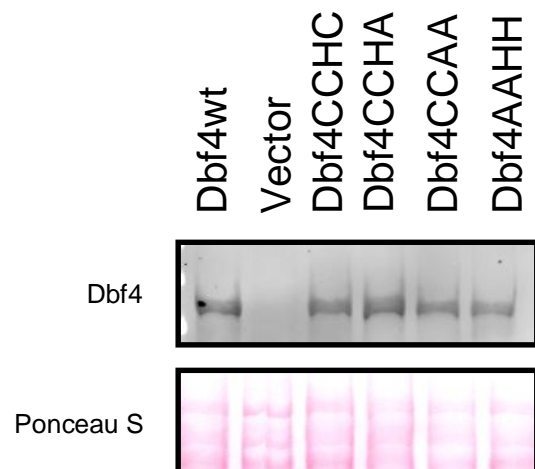
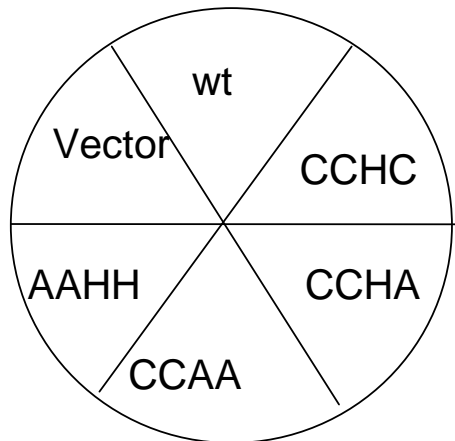
23°C



30°C



37°C



The Dbf4 $\Delta$ C and Dbf4 C-motif point mutants were then tested in a series of two-hybrid assays. A possible function of the Dbf4 C-motif could possibly be derived from a collective assessment of the two-hybrid assay results involving the Dbf4 C-motif mutants and the various known protein binding targets of Dbf4.

The Dbf4 C-motif point mutants seem to have a stronger interaction with Rad53 than the Dbf4 wild type protein in two-hybrid assays (Figure 5.5). Statistical significance was not determined for the differences between the wild type Dbf4-Rad53 interaction and the Dbf4 C-motif point mutant interactions with Rad53. When tested in two-hybrid assays, using Mcm2 as a prey protein, the Dbf4 C-motif point mutants had a reduced interaction with Mcm2 relative to the wild type control interaction. The Dbf4 $\Delta$ C mutant also interacted very weakly with Mcm2 (Figure 5.6). Statistical significance was not determined for the differences between the wild type Dbf4-Mcm2 interaction and the Dbf4 C-motif point mutant interactions with Mcm2. Three of the four Dbf4 C-motif point mutants had an increased interaction with Orc2, in two-hybrid assays, compared to the wild type Dbf4-Orc2 interaction (Figure 5.7). Interestingly, among the Dbf4 C-motif point mutant interactions with Orc2, only the Dbf4CCHA-Orc2 interaction was determined to be statistically significant. These results are interesting because the Dbf4-Rad53 and Dbf4-Orc2 interactions have been shown earlier, in Chapter 3, to be mediated by the Dbf4 N-motif. Furthermore, Mcm2 interaction with Dbf4 has been linked to the M-motif in two-hybrid assays. Thus, it is apparent that the Dbf4 C-motif affects these protein-protein interactions.

The two-hybrid assays, performed with a Cdc7 prey protein and the Dbf4 C-motif point mutants, showed that the mutants interacted with Cdc7 at levels that were

similar to wild type Dbf4. The differences between the Dbf4 C-motif point mutant interaction levels with Cdc7 compared to the wild type Dbf4-Cdc7 interaction were not statistically significant. The Dbf4 $\Delta$ C bait did not interact with Cdc7 (Figure 5.8). This result was statistically significant. The Dbf4-Cdc7 interaction is an important one, in that it forms the active kinase that is involved in the initiation of DNA replication. The Dbf4 C-motif point mutants were also tested in two-hybrid assays using Mcm4, as a prey protein (Figure 5.9). The Mcm4 protein was tested as a prey protein because, in a recent publication, it was reported that Mcm4 is phosphorylated by DDK (Dbf4/Cdc7) (Sheu and Stillman, 2006). The Dbf4 C-motif point mutants showed greatly enhanced interactions with Mcm4, compared to the Mcm4-Dbf4 wild type interaction that interacted only slightly more than the background control. The Dbf4AAHH and Dbf4 CCAA increased interaction levels with Mcm4 were statistically significant when compared to the wild type Dbf4-Mcm4 interaction. This interesting result is, likely, indirectly caused by the impaired Dbf4-Mcm2 interactions that were observed in the two-hybrid assays involving Dbf4 C-motif mutants. That is, the Dbf4 C-motif point mutants bound more tightly to the Mcm4 protein subunit because Dbf4-Mcm2 interaction (Figure 5.6) was weakened, as a result of the C-motif point mutations. The Dbf4 $\Delta$ C mutant protein did not interact with Mcm4 in the two-hybrid assay (Figure 5.9).

Subsequently, the same Dbf4 C-motif point mutants were tested in a one-hybrid assay to bind to ARS1 (origin of replication). The one-hybrid assay detects the direct binding of a protein to ARS1 origin DNA, as well as, indirect binding to ARS1 origin DNA *via* a protein-protein interaction. The one-hybrid assay was performed because, as mentioned previously, the Dbf4 C-motif contains a putative CCHH-type zinc finger

domain. The CCHH-type zinc-finger has been implicated, in other proteins, in mediating protein-DNA interactions. The results of the one-hybrid assay show that the Dbf4 C-motif point mutants had a reduced interaction with ARS1, relative to the wild type (Dbf4) control (Figure 5.10). However, statistical significance was not determined for the Dbf4 C-motif point mutants, in comparison to the wild type (Dbf4).

**Figure 5.5. The Dbf4 C-motif point mutants have an increased interaction with Rad53 relative to wild type (Dbf4), in the two-hybrid assay.** The two-hybrid assay using bait constructs pEGDbf4wt, pEG202, pEGDbf4AAHH, pEGDbf4CCAA, pEGDbf4CCHC, pEGDbf4CCHA and a pJG Rad53 prey construct, was performed as described in Materials and Methods. Protein expression of bait and prey proteins are not shown. Culture aliquots were removed following the two-hybrid assay induction, whole cell extracts were prepared and western blots were performed as described in Materials and Methods. Bait proteins were detected with rabbit polyclonal anti-LexA antibody (Invitrogen) and prey proteins were detected with mouse polyclonal anti-HA antibody (Sigma). Ponceau S stain (0.1%) verifying the equal loading of the protein samples is also not shown. The  $\beta$ -galactosidase activity values represent the averages of 2 independent experiments  $\pm$  standard deviation.

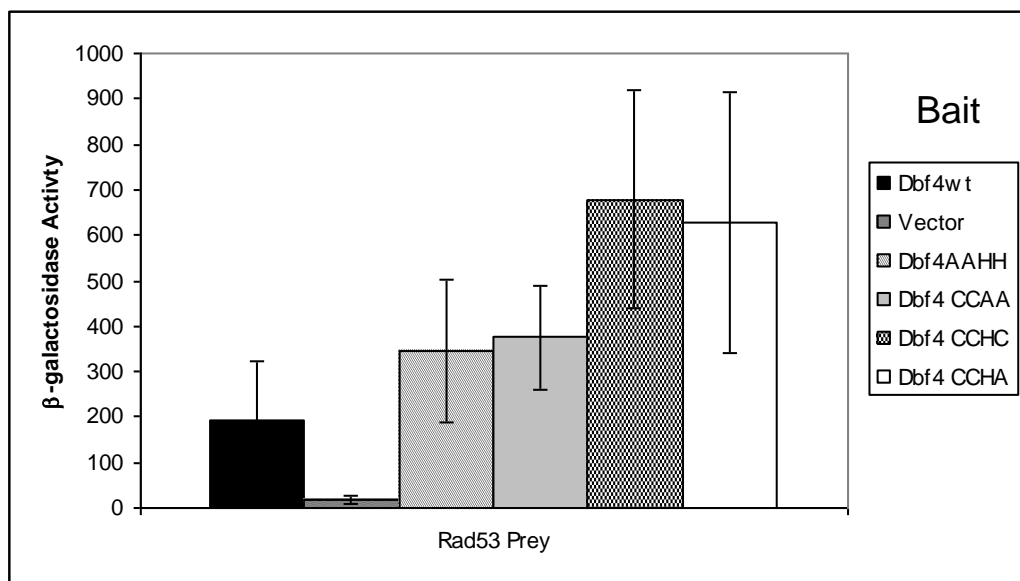


**Figure 5.6. The Dbf4 C-motif point mutants have decreased interactions with Mcm2 relative to the wild type Dbf4-Mcm2 interaction in the two-hybrid assay.** The two-hybrid assay was performed using bait constructs pEGDbf4wt, pEG202, pEGDbf4AAHH, pEGDbf4CCAA, pEGDbf4CCHC, pEGDbf4CCHA and a pJGMcm2 prey construct, as described in Materials and Methods. Protein expression of bait and prey proteins are not shown. Culture aliquots were removed following the two-hybrid assay induction, whole cell extracts were prepared and western blots were performed as described in Materials and Methods. Bait proteins were detected with rabbit polyclonal anti-LexA antibody (Sigma) and prey proteins were detected with mouse polyclonal anti-HA antibody (Sigma). Ponceau S stain (0.1%) verifying the equal loading of the protein samples is also shown. The  $\beta$ -galactosidase activity values represent the averages of 2 independent experiments  $\pm$  standard deviation.

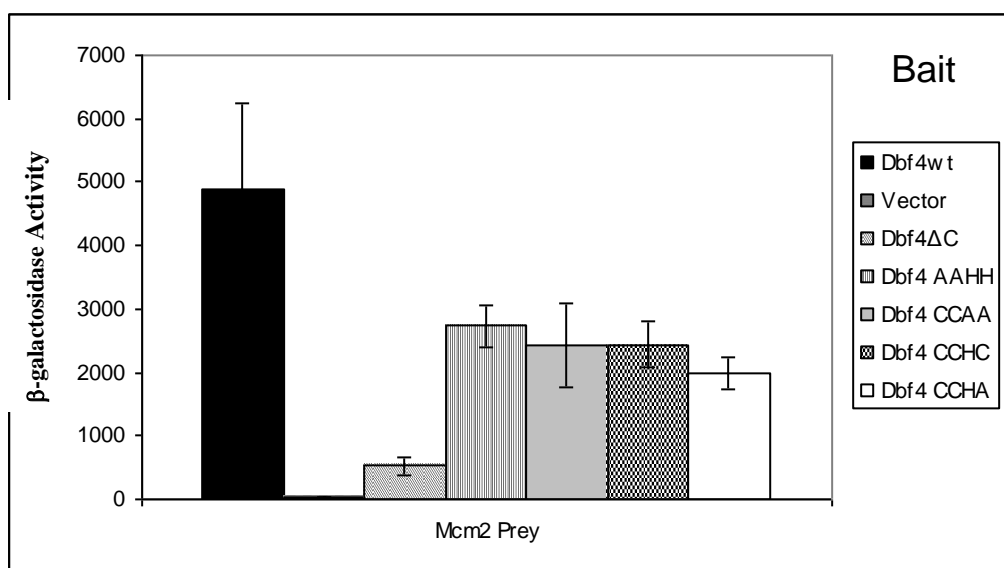


**Figure 5.7. The Dbf4 C-motif point mutants have an increased interaction with Orc2 relative to wild type Dbf4, in the two-hybrid assay.** The two-hybrid assay using bait constructs pEGDbf4wt, pEG202, pEGDbf4AAHH, pEGDbf4CCAA, pEGDbf4CCHC, pEGDbf4CCHA and a pJGOrc2 prey construct, was performed as described in Materials and Methods. Protein expression of bait and prey proteins are not shown. Culture aliquots were removed following the two-hybrid assay induction, whole cell extracts were prepared and western blots were performed as described in Materials and Methods. Bait proteins were detected with rabbit polyclonal anti-LexA antibody (Invitrogen) and prey proteins were detected with mouse polyclonal anti-HA antibody (Sigma). Ponceau S stain (0.1%) verifying the equal loading of the protein samples is not shown. The  $\beta$ -galactosidase activity values represent the averages of 3 independent experiments  $\pm$  standard deviation. Statistical significance was determined using the student's two tailed t-test ( $p \leq 0.05$ ) and is indicated with an asterisks.

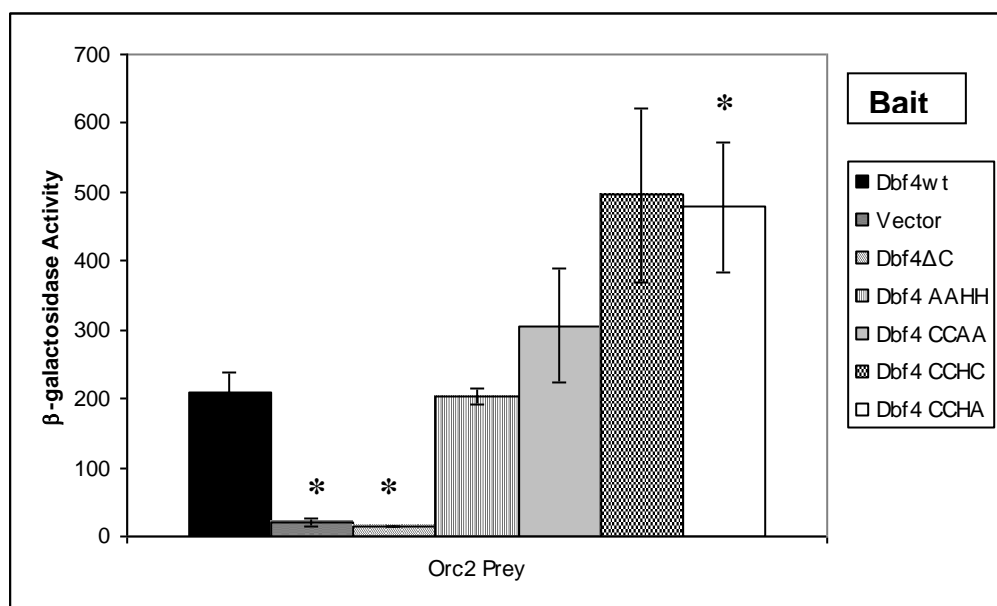


**Figure 5.8. The Dbf4 C-motif point mutants have interactions with Cdc7 that are similar to that with wild type Dbf4 in the two-hybrid assay.** The two-hybrid assay using bait constructs pEGDbf4wt, pEG202, pEGDbf4AAHH, pEGDbf4CCAA, pEGDbf4CCHC, pEGDbf4CCHA and pJGCdc7 prey constructs, as described in Materials and Methods. Protein expression of bait and prey proteins are not shown. Culture aliquots were removed following the two-hybrid assay induction, whole cell extracts were prepared and western blots were performed as described in Materials and Methods. Bait proteins were detected with rabbit polyclonal anti-LexA antibody (Invitrogen) and prey proteins were detected with mouse polyclonal anti-HA antibody (Sigma). Ponceau S stain (0.1%) verifying the equal loading of the protein samples is not shown. The  $\beta$ -galactosidase activity values represent the averages of 3 independent experiments  $\pm$  standard deviation. Statistical significance was determined using the student's two-tailed t-test ( $p \leq 0.05$ ) and is indicated with an asterisks

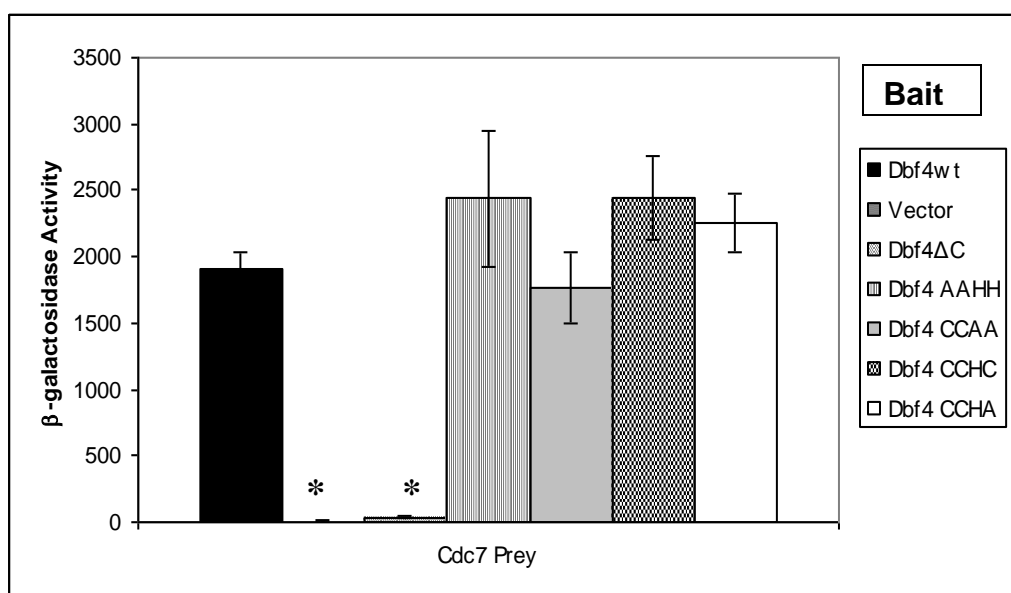


**Figure 5.9. The Dbf4 C-motif point mutants have an increased interactions with Mcm4 in the two-hybrid assay relative to the wild type Dbf4-Mcm4 interaction.** The two-hybrid assay using bait constructs pEGDbf4wt, pEG202, pEGDbf4AAHH, pEGDbf4CCAA, pEGDbf4CCHC, pEGDbf4CCHA and pJGMcm4 prey construct, as described in Materials and Methods. Protein expression of bait and prey proteins are not shown. Culture aliquots were removed following the two-hybrid assay induction, whole cell extracts were prepared and western blots were performed as described in Materials and Methods. Bait proteins were detected with rabbit polyclonal anti-LexA antibody (Sigma) and prey proteins were detected with mouse polyclonal anti-HA antibody (Sigma). Ponceau S stain (0.1%) verifying the equal loading of the protein samples is also not shown. The  $\beta$ -galactosidase activity values represent the averages of 3 independent experiments  $\pm$  standard deviation. Statistical significance was determined using the student's two-tailed t-test ( $p \leq 0.05$ ) and is indicated with an asterisks

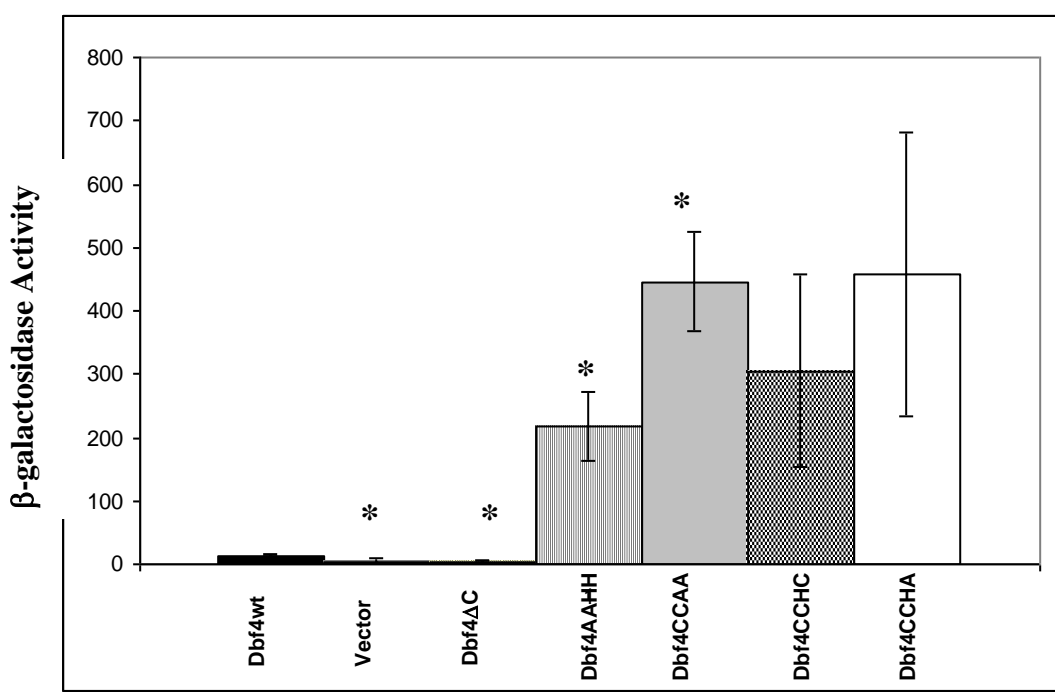
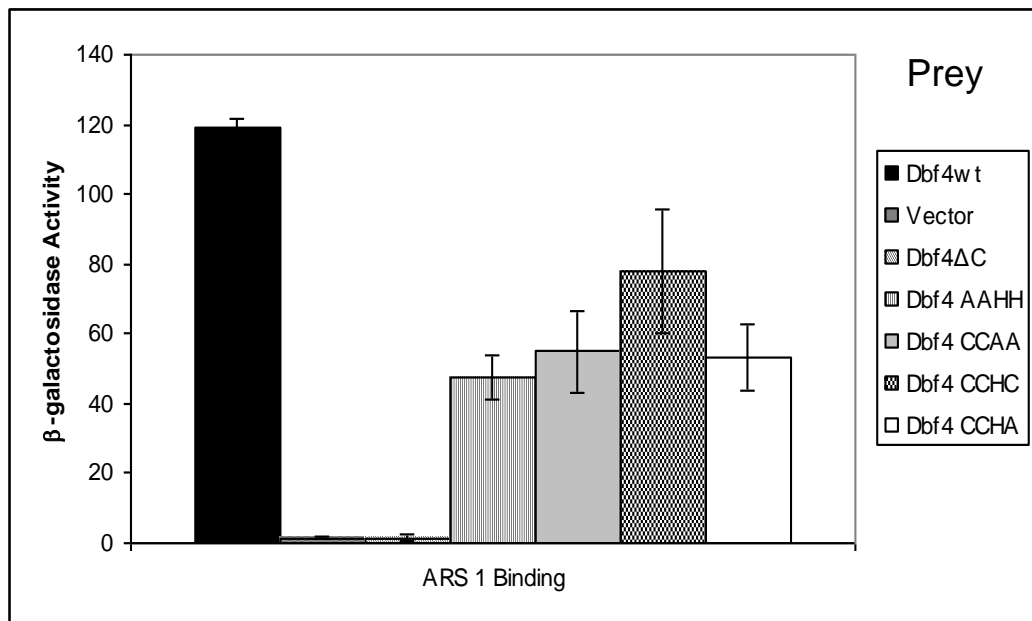


**Figure 5.10. The Dbf4 C-motif point mutants have a decreased interaction with ARS1 in the one-hybrid assay relative to the wild type interaction.** The one-hybrid assays were carried out using prey constructs pJGDbf4wt, pJG4-6, pJGDbf4AAHH, pJGDbf4CCAA, pJGDbf4CCHC, pJGDbf4CCHA and pLIARS1 reporter construct, as described in Materials and Methods. Protein expression of Prey proteins are not shown. Culture aliquots were removed following the two-hybrid assay induction, whole cell extracts were prepared and western blots were performed as described in Materials and Methods. Prey proteins were detected with mouse polyclonal anti-HA antibody (Sigma). Ponceau S stain (0.1%) verifying the equal loading of the protein samples is also not shown. The  $\beta$ -galactosidase activity values represent the averages of 2 independent experiments  $\pm$  standard deviation.



In a series of follow-up experiments, plasmids, expressing Dbf4 C-motif point mutants, were transformed into a *rad53-11* mutant strain. The *rad53-11* mutant is well documented to be checkpoint impaired and is hypersensitive to genotoxic agents, as a result of a single point mutation (G653E) in the Rad53 checkpoint kinase protein. These transformants were tested in growth spotting assays for sensitivity to genotoxic agents (HU, MMS and BLEO) (Figure 5.11). It was expected that the increased Dbf4-Rad53 interactions observed for the Dbf4 C-motif point mutants, in two-hybrid assays, might confer some resistance to the genotoxic agents. The *rad53-11* mutant transformed with plasmids expressing Dbf4 C-motif point mutants conferred some resistance to low concentrations of HU (5mM) in the growth spotting assay (Figure 5.11). Conferred resistance to low concentrations of MMS (0.0075%) and BLEO (1 $\mu$ g/ml) is not clearly evident (Figure 5.11). However, there was not enough definitive colony formation on the bleomycin plates to draw any strong conclusions regarding conferred resistance. The resistance to BLEO was further investigated in a short-term survival assay (Figure 5.12). This short-term survival assay was performed to verify the result from the growth spotting assay. The results from the survival assay indicated that plasmid-based expression of the Dbf4 C-motif point mutants did confer resistance to short-term BLEO exposure at a concentration of 1  $\mu$ g/ml . The growth spotting assay tests for resistance or sensitivity to long-term exposure to genotoxic agents. It also shows a strain's adaptation. The short-term exposure to genotoxic agents tests a strain's resistance or sensitivity to short term exposure, in a liquid culture, relative to a control.

Based upon the finding that the Dbf4 C-motif point mutants conferred resistance to genotoxic agents in the *rad53-11* mutant background, a two-hybrid assay was set-up

using the Rad53-11 mutant protein as a prey protein, along with the Dbf4 C-motif point mutants as bait proteins (Figure 5.13). Increased interactions between the Dbf4 C-motif point mutants and the Rad53-11 mutant protein would lend credibility to the thought that this enhanced interaction was contributing to the conferred resistance to genotoxic agents, as has been described above. As expected, the Dbf4 C-motif point mutants had increased interactions with the Rad53-11 mutant protein compared to the wild type Dbf4-Rad53 interaction (Figure 5.13).

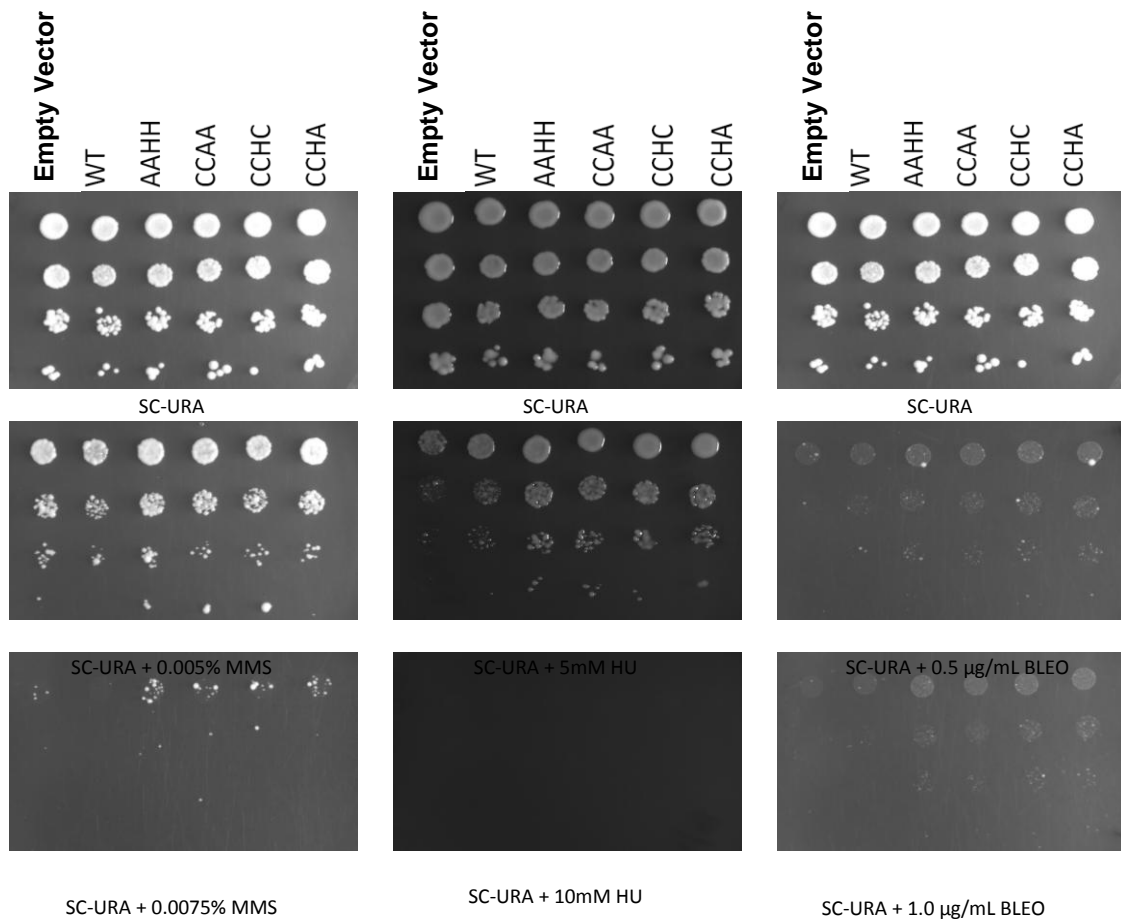


**Figure 5.11. Growth spotting assay testing *rad53-11* Dbf4 C-motif point mutant transformants for sensitivity/resistance to genotoxic agents.** A *rad53-11* mutant strain transformed with plasmids overexpressing Dbf4 C-motif mutants is more resistant than the *rad53-11* mutant strain, empty vector transformant to genotoxic agent: HU. Increased resistance to MMS and BLEO is not clearly evident. Cultures were grown to saturation ( $1 \times 10^8$  cells/mL) and ten-fold dilutions were spotted in  $5\mu\text{L}$  volumes in decreasing concentrations ( $1 \times 10^7$  to  $1 \times 10^4$  cells/mL) from top to the bottom of each plate. Plates were synthetic complete medium lacking uracil to maintain plasmid selection and contain the indicated concentrations of MMS, HU or BLEO. Each plate was incubated at  $30^\circ\text{C}$  for four days. The *rad53-11* mutant strains were transformed with pCMDbf4wt, pCM190 (empty vector), pCMDbf4AAHH, pCMDbf4CCAA, pCMIDbf4CCHC and pCMDbf4CCHA.

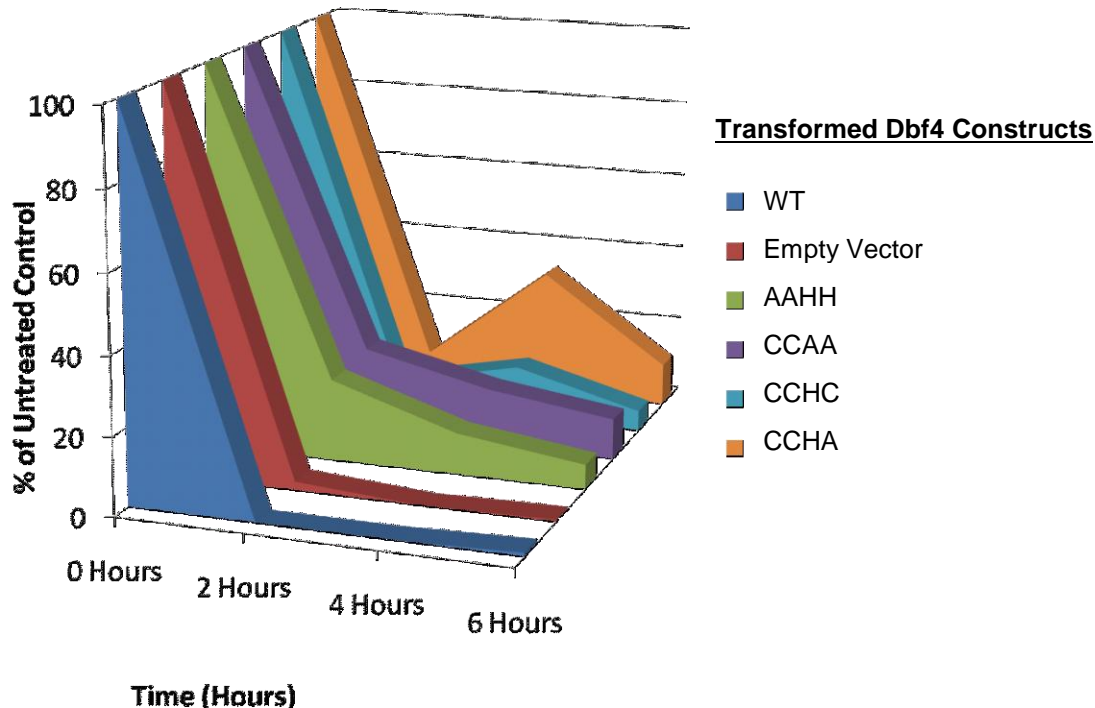
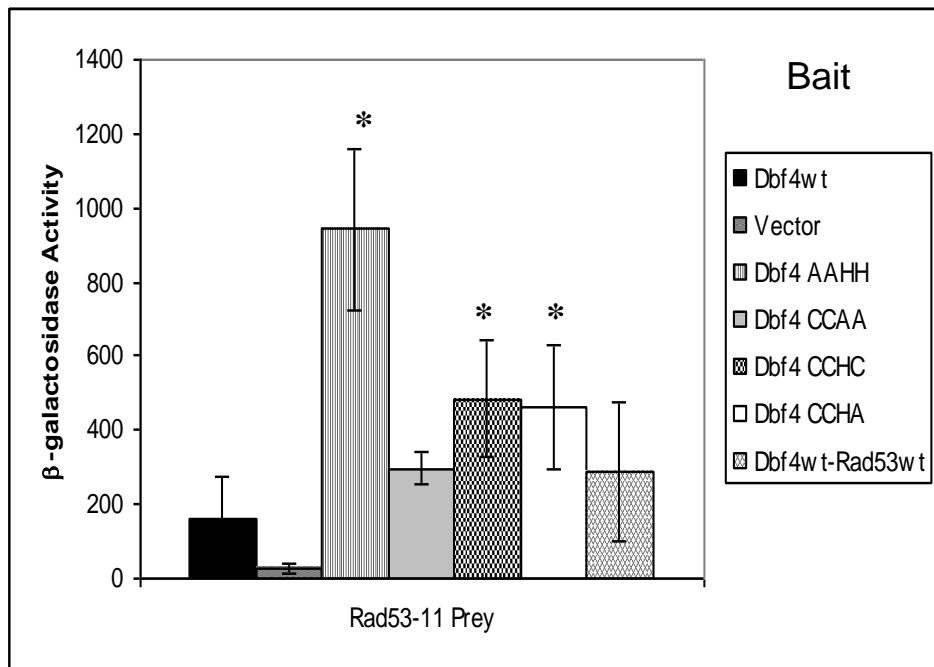


**Figure 5.12. Bleomycin short-term survival assay.** The *rad53-11* strain transformed with Dbf4 C-motif mutants are resistant to short-term exposure to (1 $\mu$ g/ml)bleomycin (BLEO) relative to *rad53-11* strain transformed with wild type (Dbf4) subjected. The transformants used in the spotting assay in Figure 5.11. were tested in a survival assay for testing short term exposure consequences to BLEO. The cells were subjected to bleomycin exposure for up to 6 hours. Aliquots of cells were removed and plated at each time point (0, 2, 4, 6 hours) in parallel with an untreated control. The plates were incubated for 3 days at 30°C and colonies were counted. The percentage of the number of colonies relative to the untreated control for each time point were calculated and graphed.

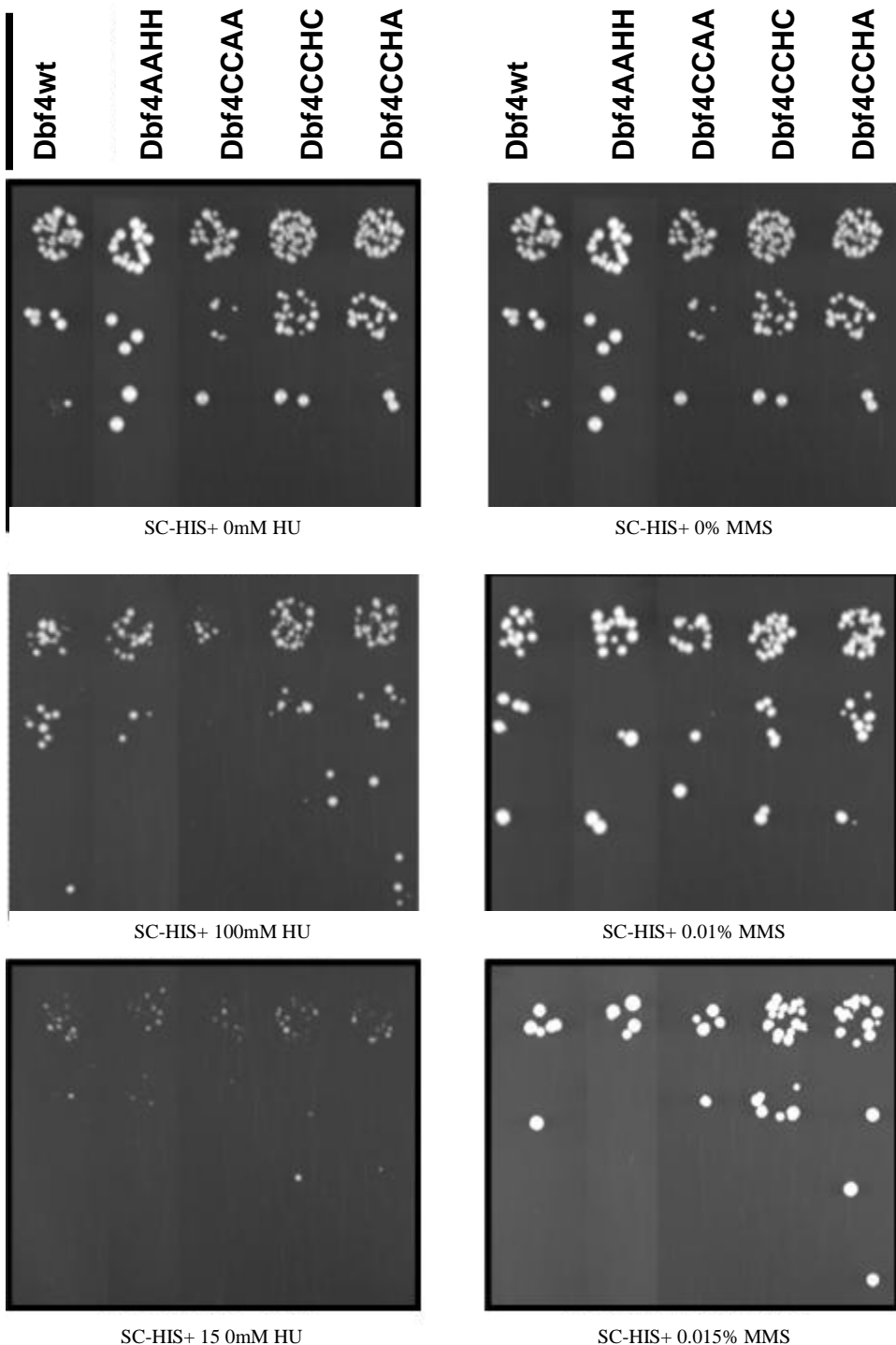
**Figure 5.13. The Dbf4 C-motif point mutants have an increased interaction with the *rad53-11* mutant in the two-hybrid assay.** The two-hybrid assay was performed using bait constructs pEGDbf4wt, pEG202, pEGDbf4AAHH, pEGDbf4CCAA, pEGDbf4CCHC, pEGDbf4CCHA and pJGRad53-11 prey construct, as described in Materials and Methods. Protein expression of Bait and Prey proteins are presented. Culture aliquots were removed following the two-hybrid assay induction, whole cell extracts were prepared and western blots were performed as described in Materials and Methods. Bait proteins were detected with rabbit polyclonal anti-LexA antibody (Sigma) and prey proteins were detected with mouse polyclonal anti-HA antibody (Sigma). Ponceau S stain (0.1%) verifying the equal loading of the protein samples is also shown. The  $\beta$ -galactosidase activity values represent the averages of 3 independent experiments  $\pm$  standard deviation. Statistical significance was determined using the student's two-tailed t-test ( $p \leq 0.05$ ) and is indicated with an asterisks



As a follow-up to the *rad53-11* mutant strain transformant overexpressing the Dbf4 C-motif point mutants, a plasmid shuffle strain assay was set up. Since the *rad53-11* is a mutant strain that is hypersensitive to genotoxic agents, it was of interest to determine if the Dbf4 C-motif point mutants could confer resistance (to genotoxic agents) in a wild type strain background. The plasmid shuffle strains were created to perform a growth spotting assay to determine if expressing only the Dbf4 C-motif point mutants, in an otherwise wild type background, would also confer resistance to genotoxic agents. The plasmid shuffle strain assay was performed, using a series of plasmid shuffle strains that were created, as described in the Methods and Materials section. These transformants expressed the Dbf4 C-motif point mutants from plasmids in a strain where the endogenous wild type *DBF4* allele had been disrupted. The application of these plasmid shuffle strains provided a means to determine if the expression of Dbf4 C-motif point mutant proteins would confer resistance, in a non-mutant, wild type strain, in a growth spotting assay. No obvious resistance or sensitivity to HU or MMS was observed compared to the wild type control (Figure 5.14).

**Figure 5.14. The Dbf4 C-motif point mutants do not confer resistance to genotoxic agents in plasmid shuffle strains, in which the DBF4 allele has been disrupted.** Cells lacking endogenous Dbf4 containing a pEG202 plasmid expressing Dbf4 C-motif mutants or Dbf4 wild type (pEGDbf4AAHH, pEGDbf4CCAA, pEGDbf4CCHC, pEGDbf4CCHA, pEGDbf4wt) were grown to saturation, diluted and spotted onto plates containing 0, 100 and 150 mM HU and 0, 0.01, 0.015% MMS, as described in Materials and Methods. Plates were incubated at 30°C for 4 days.

Transformed  
Expression  
Construct



### 5.3. Discussion

#### 5.3.1. *Deletion of the Dbf4 C-Motif Results in a Loss of Viability.*

The results obtained in this work suggest that the Dbf4 C-motif is essential for viability in *S. cerevisiae*. The complementation assay shows the inability of two Dbf4 constructs, lacking the C-motif, to support growth in a Dbf4 temperature sensitive strain at the non-permissive temperature of 37°C (Figure 5.2). This was further corroborated by the two-hybrid assay results indicating that Dbf4 $\Delta$ C did not seem to interact with Cdc7, Orc2, Mcm4 or Mcm2 (Figures 5.6 through 5.9). The construct tested here was a mutant in which a very precise deletion of the Dbf4 C-motif was made. It is possible that this particular deletion may have caused a distortion in the protein folding that renders the protein non-functional. Gabrielese *et al.* (2006) have demonstrated that when they made a series of N-terminus truncation and deletion mutations, some mutants were nonviable and some were not. They also predicted, based on an analysis of the secondary structure, that some of the nonviable mutants would be structurally unstable. It is stressed here that caution should be taken before claiming, absolutely, that the C-motif is essential for viability. However, the C-terminally truncated mutant (Dbf4 C-TERM) in which the C-motif was also completely removed was also tested in the complementation assay. The Dbf4 C-TERM mutant was used to determine if a different construct that also lacks the C-motif is able to sustain viability or not. The results obtained with the Dbf4 $\Delta$ C were similar to those of the Dbf4 C-TERM in the complementation assay (Figure 5.2). It is possible that the Dbf4 C-TERM mutation also caused distorted protein folding.

At this point, it is important to reflect upon some previously published results. A series of C-terminally truncated Dbf4 mutants was tested by Dowell *et al.* (1994) for their

ability to complement the *dbf4-2* temperature sensitive strain, at 37°C (the nonpermissive temperature). Two of the five constructs expressing the C-terminally truncated Dbf4 mutants (Dbf4 amino acids 4 to 416; Dbf4 amino acids 81 to 416) tested by Dowell *et al.* (1994) complemented the cell growth of the *dbf4-2* temperature-sensitive (*ts*) strain at 37°C. The other three constructs expressing C-terminally truncated Dbf4 mutant proteins (Dbf4 amino acids 1 to 320; Dbf4 amino acids 1 to 160; Dbf4 amino acids 241 to 416) did not complement cell growth of *dbf4-2* at 37°C. These same truncated mutant proteins were also tested in two-hybrid assay for their ability to bind to Cdc7, as well as in one-hybrid assays, for their ability to bind to ARS1 (origin of replication). The two truncated Dbf4 mutant proteins that complemented the *ts* strain at 37°C, were also able to interact with Cdc7 in the two-hybrid assay. They were also able to bind to ARS1 in the one-hybrid assay. However, one of these C-terminally truncated mutants (Dbf4 amino acids 81 to 416) had reduced binding to ARS1, relative to the wild type Dbf4. The other proteins, that Dbf4 is known to interact with, were not tested by Dowell *et al.* (1994) in two-hybrid assays.

In comparison, the Dbf4ΔC mutant tested in the present study, created as the result of a precise deletion of the C-motif, did not complement the *dna52-1 ts* strain (Figure 5.2). The Dbf4ΔC mutant protein was also unable to bind to Cdc7 or ARS1 in the two-hybrid assay and one-hybrid assay, respectively (Figures 5.8 and 5.10). Based on a comparison of the Dowell *et al.* (1994) results to those from the present study, it seems that C-motif mutants required both Cdc7 and ARS1 binding to be able to complement a *ts* strain at the non-permissive temperature. It is possible that the C-motif is involved in Dbf4 binding to Cdc7 and ARS1. It may be that the C-terminally truncated proteins

reported by Dowell *et al.* (1994) were folded such that they were able to bind, anomalously, to Cdc7 and ARS1, despite their lacking a C-motif. This notion is further supported by data published by Jackson *et al.* (1993) in which the removal of the Dbf4 C-terminus caused an increased two-hybrid interaction with Cdc7. The Dbf4 mutant tested by Jackson *et al.* (1993) contained Dbf4 amino acids 52 to 568. It should be noted that Jackson *et al.* (1993) suggested that the removal of PEST sequences in the C-terminus of Dbf4 could affect stability. PEST sequences are small runs of amino acids rich in proline (P), glutamic acid (E), serine (S), threonine (T), and/or aspartic acid (D) amino acid residues located between basic residues and are thought to be specific signals for proteolysis. These PEST sequences were also deleted in the Dowell *et al.* (1994) C-terminally truncated Dbf4 mutants that were able to complement the *dbf4-2 ts* strain. Moreover, there are also two APC/C destruction boxes in the Dbf4 N-terminus which are targeted by the APC/C protease complex for proteolysis (Cheng *et al.*, 1999). It is relevant to mention that both of the Dbf4 C-terminally truncated mutants that complemented the *ts* strain, in the Dowell *et al.* (1994) study, also had partial N-terminal truncations. This could also have affected protein stability. Conversely, the Dbf4ΔC mutant, tested in the present study, retained all Dbf4 amino acid sequence intact, aside from a precise deletion of the C-motif. The Dbf4 C-TERM protein in the present study, which also failed to complement the *dna52-1 ts* strain at 37°C, also retained all Dbf4 amino acid sequence N-terminal to the C-motif of Dbf4. This is relevant because a less stable protein might be less efficient at complementing a *ts* strain at its nonpermissive temperature.

It is important to note that the in western blot displayed in Figure 5.2, the Dbf4 $\Delta$ C protein seems to be as stable as the wild type Dbf4 control protein at 30°C. However, the Dbf4 C-term protein seems to be less stable. It is also important to note that protein stability was not compared at 37°C, which was the non-permissive temperature for the strain. Thus, a mutant protein that is less stable at that temperature might be unable to complement and facilitate growth of the *ts* strain at non-permissive temperature of 37°C.

In the present study, a special attempt was made to create a Dbf4 C-motif deletion mutant that was more precise than those used in previously published studies. It was thought that creating a precise deletion mutant would lend more validity to the eventual result. That is, if only the C-motif was deleted, then the phenotype resulting from the deletion mutant could be more accurately applied to the function of the C-motif. Nonetheless, despite the precisely deleted C-motif of the mutants tested here, it cannot be determined, absolutely, that the C-motif is essential for cell viability. As discussed above, the truncations made by Dowell *et al.* 1994, could also affect protein stability compared to the Dbf4 $\Delta$ C mutants. The two-hybrid results, showing that the Dbf4 $\Delta$ C mutant did not bind to any of the known Dbf4 binding targets, suggested that this mutant may have been rendered functionally disabled. It is reasonable to think that the deletion mutation may have caused distorted protein folding.

It should be noted that there were some experimental differences between the present study and the work published by Dowell *et al.*, (1994). These authors used a different temperature sensitive strain for the complementation assay. The *dbf4-2 ts* mutant strain used, had a point mutation: Proline (P) to Leucine (L) point mutation at Dbf4 amino acid residue 308. The *dna52-1* temperature sensitive strain, which was used

for the complementation assay in the present study, had a Proline to Leucine point mutation at amino acid residue 277 of Dbf4. It is possible that the Dbf4P308L mutant protein expressed by the *dbf4-2 ts* mutant strain was more stable at 37°C, thereby better facilitating a complementation by the C-truncated mutant plasmid constructs. In the present study, for the complementation assay, the mutant Dbf4ΔC protein was expressed from the pCM190 plasmid. In the Dowell *et al.* (1994) study, the mutant proteins were expressed from pACT plasmid. It is possible that there were different plasmid copy numbers resulting in different protein expression levels. This factor could also have possibly affected whether a mutant protein was able to complement a *ts* strain at its nonpermissive temperature. Nonetheless, a genomically integrated mutant strain expressing mutant Dbf4 lacking the C-motif would be the best proof of the C-motif being nonessential for cell viability.

There were also some experimental differences in one-hybrid and two-hybrid assays that were performed by Dowell *et al.* (1994) compared to those carried out in the present study. Dowell *et al.* (1994) reported qualitative plate one-hybrid assay results. Two of the Dbf4 mutants described by Dowell *et al.* (1994) had the C-terminus of Dbf4 truncated, resulting in a complete removal of the Dbf4 C-motif. Both of these mutants did interact with ARS1 in the one-hybrid assay. The reporter plasmid used by Dowell *et al.* (1994) is the same plasmid that was used in the experiments reported in the present study. However, the prey plasmid used by Dowell *et al.* (1994) was different from the one used in the present study. Dowell *et al.* (1994) expressed Dbf4 derivatives that were fused to a GAD (Gal Activational Domain). In the present study, the pJG4-6 prey plasmid expressing the Dbf4 C-motif mutants fused to a B42 activational domain, derived from

the SV40 T-antigen was used. The different activational domains could possibly result in different sensitivity levels of detection of the ARS1 interaction when comparing the Dowell *et al.* (1994) results to those from the present study. Thus, it is possible that an ARS1 interaction might be detected in one assay system and not in the other. Unfortunately, the plate one-hybrid assay is not quantitative and it is difficult, from the pictures published by Dowell *et al.* (1994), to determine if the truncated Dbf4 mutants had any (slight) reduction or enhancement of the interaction with ARS1, compared to the wild type control. The same problem holds true for interpreting and comparing the qualitative plate two-hybrid assay results from the Dowell *et al.* (1994) study to the qualitative liquid two-hybrid assays performed in the present study. Thus, it is concluded that the disparity between this and the previous study could be due to the use of differences in experimental procedures used which could have affected protein stability and protein levels.

It is also important to note that two research groups working with *S. pombe* have published contradictory results regarding the essentiality of the C-motif in Dfp1 (the Dbf4 orthologue) (Fung *et al.*, 2002; Ogino *et al.*, 2001). It is also relevant to keep in mind that *S. pombe*, and some other organisms (i.e. *Xenopus laevis*, humans), have both a Dbf4 orthologue and also a Dbf4 related protein (Drf1). The Dbf4-related proteins also have sequence similarity to Dbf4, but are distinct from the Dbf4 orthologues. To date, there has been no Dbf4-related protein found in *S. cerevisiae*. It is conceivable to think that, perhaps, there is some redundancy of function. Thus, in other organisms, if the Dbf4 C-motif is absent, it is possible that a redundant Dbf4-related protein could perform the essential function, thereby sustaining viability.

It should also be noted that the Dbf4 $\Delta$ M mutant protein had an apparent increased interaction with ARS1 in the one-hybrid assay reported in the present study (Figure 5.1). It is possible that the M-motif deletion causes the ARS1 binding site to be exposed without any interference resulting in an enhanced one-hybrid assay result.

Since, the investigation of the Dbf4 C-motif by deletion mutation analysis was not definitive, it was decided to generate point mutations resulting in changes to the critical amino acids composing the CCHH-type zinc-finger contained within the C-motif. When tested in two-hybrid assays, these point mutations did influence Dbf4's ability to bind to various known binding targets. Interestingly, some of these binding targets have been previously shown to bind to Dbf4 through the N or M-motif. Thus, these results first bring into question the absolute specificity of the binding sites, within Dbf4, for the various binding targets. The fact that both Rad53 and Orc2 had increased interactions with the Dbf4 C-motif point mutants is interesting, since both of these were found to interact with the N-motif in Chapter 3. Thus, there is something about the C-motif point mutations that causes these interactions to be enhanced compared to the wild type interactions. It would be of great interest to assess this from a structural perspective when the three-dimensional physical structure of Dbf4 is available.

It is also relevant to note that Mcm2, which was found to bind to the M-motif (Chapter 3), has reduced interactions with the C-motif point mutants. Thus, the protein-protein interaction that is mediated by the M-motif is negatively affected by the C-motif point mutations. In contrast, the Dbf4-Cdc7 interaction does not seem to be affected by the C-motif point mutations. The previously identified Cdc7 binding site in Dbf4 includes part of the M-motif and part of the C-motif. This result would, however, suggest that the

DDK (Dbf4/Cdc7) complex remains active and functional, in spite of the Dbf4 C-motif point mutations.

### ***5.3.2. Point Mutations to the Dbf4 C-Motif Zinc-Finger Confer Resistance to Genotoxic Agents.***

By combining the data showing that expressing the Dbf4 C-motif point mutants from plasmids transformed into the *rad53-11* mutant strain confers resistance to genotoxic agents, with the mutation that induced altered protein-protein interactions detected by the two-hybrid assay, a model of the mechanism can be proposed (Figure 5.15).

The model in Figure 5.15, provides a hypothesis for how the plasmid-based overexpression of the Dbf4 C-motif point mutants confers resistance to genotoxic agents; however, the two-hybrid assay interactions between the Dbf4 C-motif point mutants and Mcm4 and Orc2, might be construed as contradictory to this model. Since Mcm4 and Orc2 are origin bound, their increased interaction with Dbf4 as a result of the C-motif point mutations should serve to retain Dbf4 at origins. When one looks at the relative intensity of the interactions between Dbf4 and these respective proteins, it is clearly evident that the interactions are much weaker than the Dbf4-Mcm2 interaction. Thus, it seems likely that the impaired Dbf4-Mcm2 interaction results in a shift of Dbf4 towards Mcm4 and Orc2, at the origin. This shifting did not fully compensate for the reduced Dbf4-Mcm2 interaction, which ultimately results in a pre-RC in which mutant Dbf4 is more weakly bound than wild type. When the checkpoint is triggered, the enhanced Dbf4-Rad53 interactions further facilitates a removal of Dbf4 from the late-firing origins,

enhancing the checkpoint response. Thus, removal of Dbf4 from late-firing origins prevents the late origins from firing until the DNA damage is repaired. Furthermore, it is also possible that, in addition to the regulation of late-firing origins, there is also a stabilization of replication forks that originated from early origins. It is possible that the impaired Dbf4-Mcm2 interaction is involved in a mechanism resulting in conferred resistance to genotoxic agents. Seguarado and Diffley (2008) have suggested that the Mcm2-7 proteins are candidates as functionally relevant substrates by Mec1, Rad53 and Chk1. This association suggests a role for Mcm2-7 in replication fork stability. Labib *et al.* (2000) demonstrated that a loss of Mcm2-7 from stalled replication forks causes an irreversible arrest similar to that seen in checkpoint mutants. Thus, it is possible that the disrupted Dbf4-Mcm2 interaction allows for Mcm2 to be unimpeded in its involvement in replication fork stability at early origins.

Very recently, Francis *et al.* (2009) proposed a model in which loading of Mcm2-7 onto the DNA facilitates their subsequent activation by enhancing their recruitment of and further phosphorylation by Dbf4/Cdc7. They showed that interfering with the docking of Dbf4 with Mcm2-7 also eliminates preferential targeting of pre-RC Mcm2-7. Thus, the impaired Dbf4-Mcm2 interaction observed by the Dbf4 C-motif point mutants might be causing a reduced targetting of Dbf4/Cdc7 to the Mcm2-7 complex. Therefore, it is possible that the Mcms retain a conformational shape that inhibits their helicase activity, resulting in replication fork stability.

Recently, Szyjka *et al.* (2008) have proposed a model whereby Cdc7/Dbf4 is required for replication fork restart, following replication fork arrest. They propose that Rad53 modulates the involvement of Cdc7/Dbf4 in replication fork restart through the

translesion synthesis pathway (TLS). This hypothesis could possibly explain why the Dbf4 C-motif point mutants conferred resistance to genotoxic agents in the *rad53-11* mutants. The two-hybrid assay results, from the present study, showing enhanced Dbf4-Rad53 interaction observed for the Dbf4 C-motif point mutants coupled with the maintained Dbf4-Cdc7 interaction are compatible with this proposal. Presumably, the enhanced Dbf4-Rad53 interactions are facilitating a more efficient replication fork restart by Cdc7/Dbf4. It is believed that Rad5-mediated replication fork restart is preceded by a replication fork regression. Cdc7/Dbf4 mediated TLS acts in replication fork restart without a regression step. The Rad5 and Cdc7/Dbf4 mediated TLS are thought to act in parallel pathways. Szyjka *et al.* (2008) have proposed that Rad53 may regulate which of the two parallel pathways is activated. It is possible that the increased Dbf4-Rad53 interaction, observed for the Dbf4 C-motif point mutants in the present study, may serve to favour the Cdc7/Dbf4 replication fork restart through the TLS pathway.

The plasmid shuffle strain experiments made it possible to test if the same conferred resistance by the Dbf4 C-motif point mutants would be detectable in a wild type background. It is evident from the spotting assay results that when the Dbf4 C-motif mutants were expressed in the plasmid shuffle strains lacking endogenous Dbf4 expression, increased resistance to genotoxic agents (relative to the wild type control) was not observed. It is possible that a different result could be obtained if short term exposure to genotoxic agents was tested in a survival assay. An enhanced Dbf4-Rad53 interaction, facilitating a robust intra-S-phase checkpoint response, would likely be detectable in an assay testing resistance/sensitivity to short-term exposure to genotoxic

agents. An improved replication fork recovery following the checkpoint should improve cell survival following short term exposure to genotoxic agents.

In contrast, long-term exposure to genotoxic agents can result in the cells undergoing checkpoint adaptation, which is, essentially, an extended cell cycle arrest (lasting 12-24 hours), caused by a checkpoint response induced by DNA damage. Eventually, the cells re-enter the cell cycle and continue to divide, in spite of residual DNA damage (Harrison and Haber, 2006; Bartek and Lukas, 2007). The DNA residual damage could affect cell survival. Nonetheless, conferred resistance to genotoxic agents was definitely observed for the *rad53-11* transformants. The *rad53-11* mutants are hypersensitive to genotoxic agents. It is possible that the effect of the proposed mechanism is not detectable as resistance to genotoxic agents in the wild type background of the plasmid shuffle strain. This result could be a reflection of the plasmid-based expression levels of the protein. Overexpression of proteins could serve to force protein-protein interactions that might be disrupted at endogenous levels. Perhaps, the inherent hypersensitivity of the *rad53-11* mutant strain allows for the enhanced Dbf4-Rad53 interactions to be detectable as a phenotype of conferred resistance to genotoxic agents. The phenotype, observed here, was the result of overexpression of the Dbf4 C-motif point mutants in a mutant background (*rad53-11*) that is hypersensitive to genotoxic agents. It is possible that the phenotype is only detectable as a result of the extreme hypersensitivity of the *rad53-11* mutant. The Dbf4-Rad53-11 protein-protein interaction, in the *rad53-11* mutant background is already weaker than the wild type interaction. This weakened interaction is also possibly contributing to the hypersensitivity to genotoxic agents phenotype of the *rad53-11* mutant. As a consequence of the enhanced

Dbf4-Rad53-11 protein-protein interaction, caused by the Dbf4 C-motif point mutants, a detectable phenotype of conferred resistance to genotoxic agents in the *rad53-11* mutant background was observed. The same phenotype may not have been detectable in a wild type background because the increased Dbf4-Rad53 protein-protein interaction (caused by the Dbf4 C-motif point mutations) may not have been prominent enough to cause such a phenotype. One might also expect a genetically integrated double mutant, carrying both the *rad53-11* and Dbf4 C-motif point mutations, to be more resistant to genotoxic agents than the *rad53-11* mutant strain itself.

The above discussion suggests that the Dbf4 C-motif, a putative CCHH-type zinc-finger motif, is likely involved in protein-protein interactions. This is further supported by a recent study suggesting that CCHH-type zinc-finger proteins are more likely to be involved in protein-protein interactions than previously thought (Brayer *et al.*, 2008). It is, however, still possible that the Dbf4 C-motif CCHH-type zinc-finger is involved in DNA binding. Many zinc-finger proteins are transcription factors that bind to DNA at recognized sequences (Laity *et al.*, 2001). They can also serve to unwind the DNA, influencing the protein-protein interactions of factors around the DNA helix (Shi and Berg, 1996). It has been shown that, as a result of mutations, changes in protein-induced DNA unwinding can alter the protein-protein interactions of surrounding protein factors (Shi and Berg, 1996). However, there is no direct evidence suggesting that Dbf4 also acts as a transcription factor. Moreover, within the context of its known role in the initiation of DNA replication, Dbf4 is not known to have helicase activity. It is, however, known to interact with Mcm2 and Mcm4 and Cdc45, which do have helicase activity. Nevertheless, it is possible that the Dbf4 C-motif mutations are indirectly affecting protein-protein

interactions, as a result of the DNA distortions caused by an altered protein-DNA interaction involving Dbf4. It is relevant to mention that Gabrielese *et al.* (2006) concluded that some of the nonviable BRDF (N-motif) deletion mutants that they attempted to construct were predicted to be unstable based on the secondary protein structures. The evidence, however, points towards a more likely scenario of the Dbf4 C-motif CCHH-type zinc-finger mutations directly affecting the protein-protein interactions involving Dbf4.

In summary, the results presented here lead one to believe that the Dbf4 C-motif may be an essential domain for viability. It is possible that the results showing Dbf4 $\Delta$ C and Dbf4C-TERM do not complement the Dbf4 temperature sensitive strain at the nonpermissive temperature are a reflection of the deletion mutations causing a distortion in the protein folding, resulting in a non-functional protein. It is also evident from the results presented here that point mutations to the Dbf4 C-motif CCHH-type zinc-finger are likely directly affecting the interactions of Dbf4 and most of its known binding partners. The Dbf4 C-motif point mutants, created in the present study, seemed to cause increased Dbf4-Rad53 interactions and decreased Dbf4-Mcm2 interactions, thus conferring upon the *rad53-11* mutants, resistance to genotoxic agents. The likely mechanism is the more efficient regulation of late-firing origins (*via* the Dbf4-Rad53 interaction) coupled with the enhanced stabilization of replication forks at early origins as a result of the impaired Dbf4-Mcm2 interaction, making Mcm2 more available as a substrate for the checkpoint protein factors (Figure 5.15). Moreover, a novel model (Szyjka *et al.*, 2008) proposing that Rad53 regulates Dbf4/Cdc7 involvement in replication fork restart following replication fork arrest through the translesion synthesis

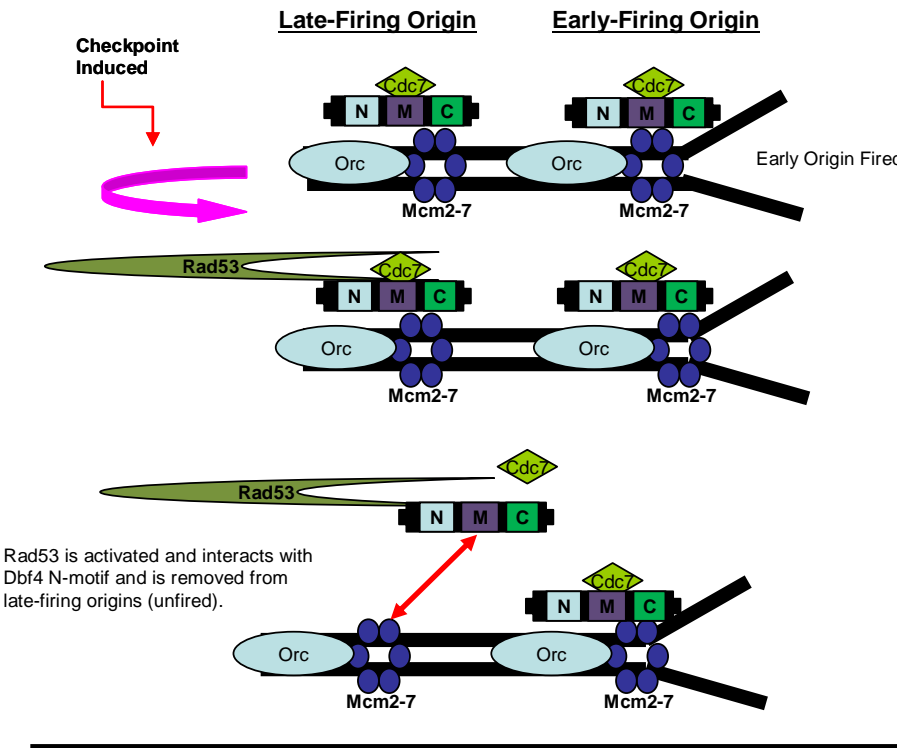
pathway is also consistent with results presented here. The Dbf4 C-motif point mutants have enhanced interactions with Rad53 and maintained interactions with Cdc7. This data is consistent with the proposal suggesting that the C-motif point mutants were conferring resistance to the *rad53-11* mutant strain by a more efficient replication fork restart following replication fork arrest.

**Figure 5.15. Model proposing the mechanism by which Dbf4 C-motif mutants confer resistance to genotoxic agents.**

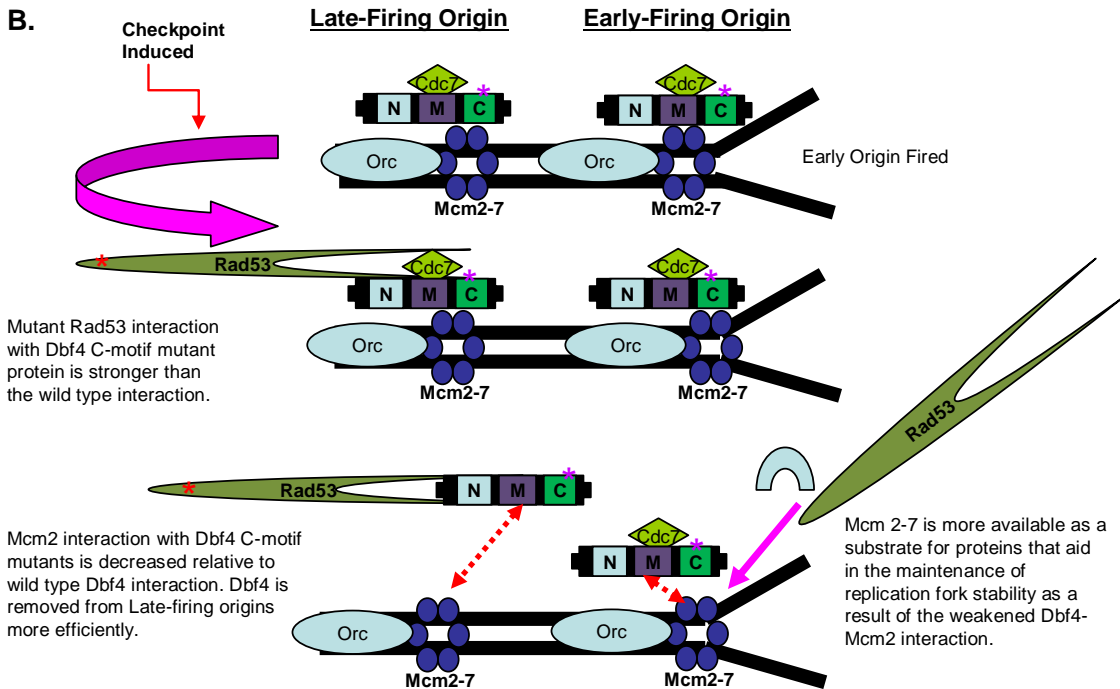
**A.** Intra-S-phase checkpoint response in a wild type strain. The pre-replicative complex assembles at early and late-firing origins, consisting of Orc, Mcm2-7 and other factors (not shown). The Dbf4/Cdc7 function as a kinase complex triggering the initiation of DNA replication. When a checkpoint is induced by DNA damage or some other perturbation, Rad53 interacts with Dbf4 and removes it from the late-firing origins.

**B.** Intra-S-phase checkpoint response in a *rad53-11* mutant strain transformed with plasmids expressing mutant Dbf4 C-motif protein. The Intra-S-phase checkpoint response is induced, as described above for the wild type strain. However, increased Rad53-Dbf4 interactions and decreased Mcm2-Dbf4 interactions lead to more efficient regulation of late-firing origins. Furthermore, the Mcm2-7 complex is more available as a substrate for proteins (i.e. Rad53 and other unknown factors) that may be involved in replication fork stabilization during checkpoint response resulting in resistance to genotoxic agents. Note: the Rad53-11 mutant protein is indicated by a red asterisk and Dbf4 C-motif mutant protein is indicated by a pink asterisk.

A.



B.



## **CHAPTER 6: X-Ray Crystallography of the Dbf4 N-Motif**

Figures 6.3. and 6.4. assisted by Melanie Gloyd.  
Figure 6.5. assisted by Monica Pillon and Melanie Gloyd.

## **6.1. Introduction**

The role of Dbf4 in the initiation of DNA replication and in the Intra-S-phase checkpoint response has been established by the results detailed in previous chapters (Chapters 3,4, and 5) and by those of other authors (Duncker *et al.*, 2002; reviewed in Duncker and Brown, 2003; Pasero *et al.*, 1999, reviewed in Sclafani, 2000). However, no successful attempts to obtain the structure of Dbf4 or its orthologs have been published. Information on the three-dimensional structure of Dbf4 is needed to complement the work presented in the previous chapters. With this in mind, the study described in this chapter was initiated. The Dbf4 crystallography project was carried out in collaboration with Dr. Alba Guarné's Laboratory, Department of Biomedical Sciences and Biochemistry, McMaster University, Hamilton, Ontario.

Three-dimensional structure of a protein can reveal insights into the evolutionary relationships of a protein to orthologues in other organisms (Teichmann *et al.*, 2001). The structure of a protein can help in identifying its function, oligomerization state or potential binding partners. Also, researchers are benefited greatly from structural data pertaining to proteins that have been well studied because mechanistic models can be proposed and subsequently tested.

*Saccharomyces cerevisiae* Dbf4 has three highly conserved motifs (N, M and C). However, overall, there is a low degree of conservation among Dbf4 orthologs, and no structural data is available for Dbf4 from any species. Three-dimensional structural data for Dbf4 would nicely complement the work presented in previous chapters, wherein a thorough mutational investigation of the three conserved Dbf4 motifs was carried out. Special attention was placed on linking individual motifs of Dbf4 to the protein-protein

interactions involving Dbf4 with specific DNA replication or checkpoint factors. Thus, the structure of Dbf4 would be useful in further characterizing these interactions. Moreover, when the three-dimensional structure is available, the various mutations resulting in disrupted protein-protein interactions could possibly be studied from a structural perspective. In particular, the Dbf4-Rad53 interaction, well characterized in previous chapters, is believed to be involved in the intra-S-phase checkpoint response. It should be noted that Rad53, an effector checkpoint kinase, consists of a kinase domain flanked by two forkhead homology associated (FHA) domains. The FHA domains of Rad53 have been well studied and the three dimensional structure has been published (Byeon *et al.*, 2001). In Chapter 3, the Dbf4 N-motif has been identified as mediating interaction with Rad53 FHA domains. Furthermore, the availability of extensive data characterizing the three motifs allows for a more intelligent and strategic approach to the truncation of the Dbf4 protein.

In addition to the thorough characterization of the Dbf4 N-motif presented here, Masai and Arai (2000) originally proposed that the Dbf4 N-terminus contains a BRCT-like motif. Subsequently, Gabrielese *et al.* (2006) have proposed that at the N-terminus of Dbf4 lies a BRDF (BRCT and Dbf4 similarity) domain. The proposed BRDF domain included the N-motif, a BRCT-like motif, and also a stretch of amino acids that encoded a Dbf4-specific secondary structure. The assertion of a BRDF domain, however, remains questionable in the absence of three-dimensional structural data. It is relevant to note that it is possible for two proteins that have no evolutionary relationship to have very similar major secondary structures and chain topology which can result in similar folding patterns (Teichmann *et al.*, 2001). Thus, it has been suggested, that in order to confirm if

two proteins, that bear the same folding patterns have an evolutionary relationship, it is necessary to identify detailed structural and/or functional similarities (Teichmann *et al.*, 2001). To accurately assess the validity of the proposed BRCT and BRDF domains, the complete or partial three-dimensional structure of Dbf4 is required.

Methods available to obtain the biological structure of a protein include X-ray diffraction, Nuclear Magnetic Resonance (NMR), Electron diffraction, Electron Microscopy, Neutron Diffraction and Molecular Modelling. Approximately 80% of all protein structures have been obtained by X-ray crystallography, while, about 15-20% of new protein structures have been determined by NMR. However, NMR is only appropriate for studying proteins that have less than 30,000 Daltons (Da) molecular weight (Winecek, 1999). Electron diffraction and electron microscopy are limited to very large protein assemblies (~ 1 MDa). In the present study, X-ray crystallography methods were used in attempts to obtain the partial structure of Dbf4.

The complete procedure of X-ray crystallography involves a number of steps. A very brief summary is presented below. Firstly, the desired gene or DNA sequence is cloned into an appropriate plasmid expression vector. The cloned expression plasmid is then transformed into various *Escherichia coli* hosts. Recombinant protein expression is then induced in the transformants and the solubility of the recombinant protein is assessed. This is followed by an extensive protein purification and concentration procedure. The purified, concentrated protein is then induced to crystallize. If and when crystals are observed, their ability to diffract X-rays to high resolution is assessed. Structure determination can be then pursued by several methods (molecular replacement, multiple isomorphous replacement or multiple anomalous diffraction). The employment

of these various methods depends on the availability of a protein with a structure similar to that of the studied protein or lack thereof.

Prior to any crystallization, it is essential to prepare a highly purified protein sample (Abola *et al.*, 2000). Obtaining enough homogenous and monodisperse (all proteins of the same size) protein material is a major barrier for crystallographers (Stevens, 2000). The crystallization of a protein is contingent upon many factors. Buffer conditions can be optimized by manipulating several variables including pH, temperature, ionic strength, salt concentration, organic additives and detergents (Stevens, 2000). It has been suggested that only 10% of the proteins cloned and expressed have led to high-resolution structures (Pusey *et al.*, 2005).

The first critical parameter for protein crystallization is the purity of the sample. Proteins are usually purified by chromatography methods that exploit particularities of the sample such as the presence of expression tags, charge of the protein or its molecular weight. Sodiumdodecyl sulfate-polyacrylamide gel electrophoresis (SDS-PAGE) is used at each purification step to assess the degree of purity achieved and the yield of protein. Once a pure sample (>98%) is available, sparse sampling matrix screening kits, including a variety of precipitants and pH conditions, are used to assess the ability of the sample to form crystals (reviewed in Winecek, 1999). The availability of these kits, along with the technical improvement of radiation sources and computer power, have greatly increased the number of protein structures determined in the last decade (Pusey *et al.*, 2005).

Initial crystals are improved by fine-tuning the amounts of precipitant agent (i.e. polyethelyne glycol, salt or an organic solvent), pH in the crystallization solution, as well as the temperature. The variables affecting the crystallization process are often presented

in a phase diagram (Figure 6.1). In a phase diagram, the state of the material (i.e. solid and liquid) is presented as a function of the ambient conditions (i.e. temperature; buffer concentration) (Asherie, 2004). The basis of crystallization experiments is that a protein will stay in solution up to a certain concentration. Beyond this concentration, a new state or phase will appear (Asherie, 2004). A crystallographer will attempt to change the solution conditions such that the solubility limit of the protein is exceeded, thereby producing crystals (Asherie, 2004). The manipulation of solution conditions does not always result in the production of protein crystals that are appropriate for the determination of protein structure. It is possible that the protein will remain in solution. It is also possible for crystals to appear that do not yield a good quality X-ray diffraction pattern and are, therefore, not appropriate for structure determination (Asherie, 2004). This could be caused by a less ordered or irregular pattern of molecules that make up the crystal. Nonetheless, it is possible to overcome some of these problems by attempting many different solution conditions (Asherie, 2004).

The phase diagram depicts the solubility curve that separates the undersaturated conditions from the saturated conditions (Figure 6.1). The diagram also depicts three zones: “metastable” zone; “labile” or “crystallization” zone and the “precipitation” zone. The “metastable” zone represents conditions in which the supersaturation is too small resulting in a slow nucleation rate, which will not yield crystals in a reasonable timeframe. Nucleation is the process of forming a nucleus of a crystal. The “labile” or “crystallization” zone is large enough to facilitate spontaneous nucleation (Asherie, 2004). The “precipitation” zone is unfavourable for crystal formation, often yielding aggregation and precipitation. Aggregation is the assembly of proteins into amorphous

clusters. Aggregates can, occasionally, rearrange to form crystals. However, aggregation is usually avoided by crystallographers (Asherie, 2004).

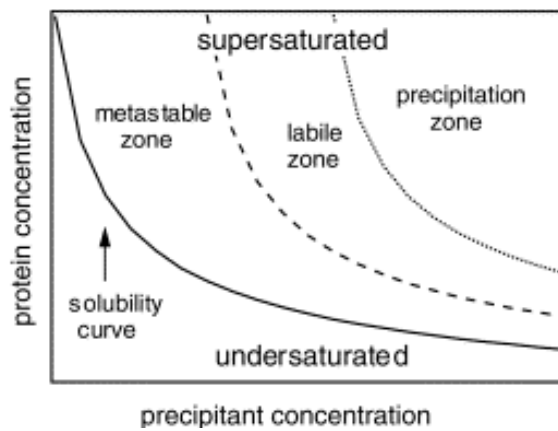


**Figure 6.1. Phase diagram for protein crystallization.** (from Asherie, 2004, reproduced with permission).

If one is unable to obtain crystals after several attempts, it is possible to attempt crystallization of a homologous protein from another source. Crystallization of one or more proteolytic fragments of the protein or engineering the protein (i.e. by mutating surface amino acid residues or removing flexible parts) is also a possible approach.

In the present study, the goal was to determine the three-dimensional structure of Dbf4. Since, the complete structure of a protein is often difficult to obtain, the structure of truncated N-terminal Dbf4 variants was also examined. Truncations were made based on an assessment of the secondary structure, with an attempt to retain the N and/or M motifs intact. In addition to the full-length Dbf4 protein, the first 396 amino acids of the Dbf4 N-terminus were attempted and, subsequently, the first 248 amino acids of the N-terminus were also attempted.

## 6.2. Results

The initial approach taken in this part of the project was to create a plasmid vector that expressed full-length recombinant Dbf4 protein. The solubility of the protein was then assessed and a determination was made regarding its suitability for a larger-scale protein purification and crystallization. Since Dbf4 is known to be a highly labile protein, it was predetermined that if the resulting recombinant Dbf4 was not suitable for crystallization, a variant of Dbf4 that was truncated at the C-terminus would be tested.

My main contributions to this work include involvement in the strategic planning for the cloning of the plasmid expression constructs, using my knowledge and experience working with Dbf4. Furthermore, I created the plasmid expression constructs that were tested. I also carried out some of the solubility assays that were used to determine if a

protein was suitable for large-scale purification and crystallization. Protein purification and crystallization was carried out by the Guarné laboratory members, because of their expertise with the relevant techniques.

The pET15b plasmid expression vector (Novagen) was used as the vector backbone for the constructs that were made. pET15b is an expression plasmid that is compatible with the Novagen pET system (Figure 6.2). The Novagen pET system is a T7 promoter-system that was originally developed by Studier and colleagues (Moffatt and Studier, 1986, Rosenberg *et al.*, 1987; Studier *et al.*, 1990). The pET15b expression vector carries the T7 lac promoter, encodes a cleavable N-terminal histidine (His) tag (with 6 repeats of His) and has an ampicillin expression marker. The recombinant protein that is expressed from the pET15b vector has a His-tag which is at the N-terminus of the protein. The His-tag can be cleaved from the recombinant protein at a thrombin digestion site. The His-tag sequence facilitates the purification of the recombinant protein by binding to a nickel column. The  $\text{Ni}^{2+}$  ions of the column will selectively retain proteins if a His-tag is exposed on the surface of the protein. The His-tagged proteins can be desorbed from the column with buffers containing imidazole. It is essential to maintain a balance between the amount of imidazole needed to prevent non-specific binding of contaminants and the amount of imidazole needed to elute the His-tagged protein.

In the present study, the *DBF4* (full-length) gene was cloned into the pET15b vector at the restriction sites: *NdeI* and *BamHI*. The T7 lac promoter contains a 25 base-pair lac operator. Transcription is controlled by the binding of the lac repressor to the lac operator which inhibits T7 RNA polymerase activity. pET plasmids with the T7 lac promoter also carry their own copy of *lacI* repressor gene which encodes for the lac

repressor. The cloned pET15b expression vectors were sequenced and then transformed into a series of *E. coli* derived host strains, as described in Materials and Methods.

It is important to note that the host *Escherichia coli* cells that were used (BL21 (DE3) and STAR) have a second lacI-based mechanism that suppresses basal expression of the recombinant protein. STAR cells, which are a derivative of BL21 (DE3) cells, were also tested as host cells. STAR cells are identical to BL21(DE3) cells, but also carry the rnaseE mutation. The rnaseE mutation reduces endogenous levels of RNAses and consequently reduces mRNA degradation.

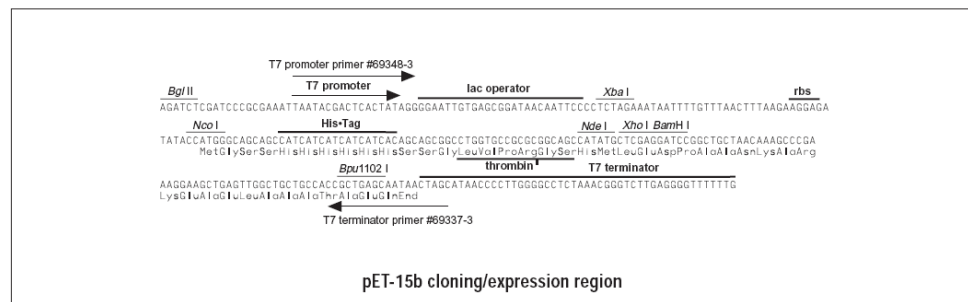
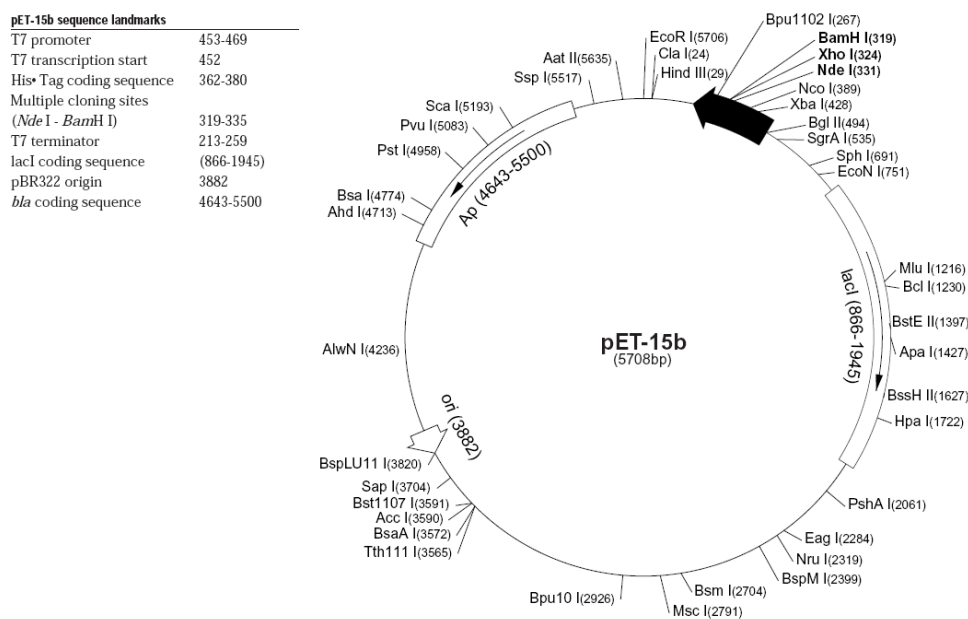


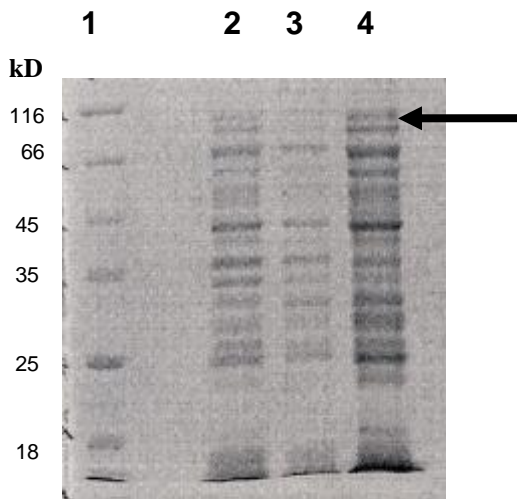
**Figure 6.2. Plasmid map of pET15b expression vector. (Novagen).**

Both the BL21 (DE3) and STAR cells were transformed with plasmids, as additional variables, that could possibly improve expression of the recombinant protein. The pLySs plasmid encodes for T7 lysozyme gene which lowers the background expression level of target genes under the control of the T7 promoter. However, the pLysS does not interfere with the level of expression achieved following induction by Isopropyl  $\beta$ -D-1-thiogalactopyranoside (IPTG). The pRARE plasmid was also used to potentially enhance expression of the recombinant protein. Therefore, the pRARE plasmid encodes several tRNAs that are infrequently used by *E. coli*, but are common in eukaryotes and, therefore, enhances the expression levels of recombinant proteins otherwise limited by codon usage. Thus, the following cells and cell transformants were tested: BL21 (DE3); BL21 (DE3) pLySs; BL21 pRARE, STAR, STAR pLySs, STAR pRARE.

The protein solubility assay allows for a comparison of protein expression and protein solubility at different induction temperatures and times. Initially, for each of the constructs tested, a solubility assay was performed. The results of the protein solubility assay were used to determine which, if any, of the strains and induction conditions were appropriate for a scale-up protein purification procedure. The induction was initiated by the addition of IPTG. Following a lysis procedure, the soluble fraction was also collected for a comparison to the pellet fraction.

The STAR pRARE transformant host was determined to have appropriate expression and solubility of the full-length Dbf4 (Figure 6.3). The other solubility assays for other host cell transformants are shown in the Appendix. The suitable induction conditions were determined to be 30°C for 5 hours. Unfortunately, persistent protein

degradation was observed during the solubility assay and initial attempts at large-scale protein purification. The protein degradation is evident in the western blots (shown in Figures A-1 through A-5 in Appendix). It was, therefore, concluded that pET15b Dbf4-FL was unsuitable for crystallization and was not pursued any further.



#### LANES

- |                              |                                       |
|------------------------------|---------------------------------------|
| <b>1. Pre-Stained Marker</b> |                                       |
| <b>2. IPTG-</b>              | <b>STAR pRARE</b>                     |
| <b>3. IPTG+</b>              | <b>STAR pRARE      30°C (5 hours)</b> |
| <b>4. IPTG+ (soluble)</b>    | <b>STAR pRARE      30°C (5 hours)</b> |

**Figure 6.3. SDS-PAGE of Protein Solubility Assay for the pET15b Dbf4FL construct in STAR pRARE cells.** The molecular weight marker is labeled as kilodaltons (kD). The construct was tested at 30°C for 5 hours with 200rpm shaking. Soluble fractions were prepared as described in Materials and Methods. Samples were prepared as described in the Materials and Methods section by mixing them with 2X SDS-loading dye. A 15 µl volume of each prepared sample was loaded in the 12% SDS-PAGE lanes. Lane 2 represents a pellet fraction before induction with IPTG. Lane 3 represents a pellet fraction following an 5 hour induction (with IPTG) at 30°C. Lane 4 represents a soluble fraction obtained after a 5 hour induction (with IPTG) at 30°C.

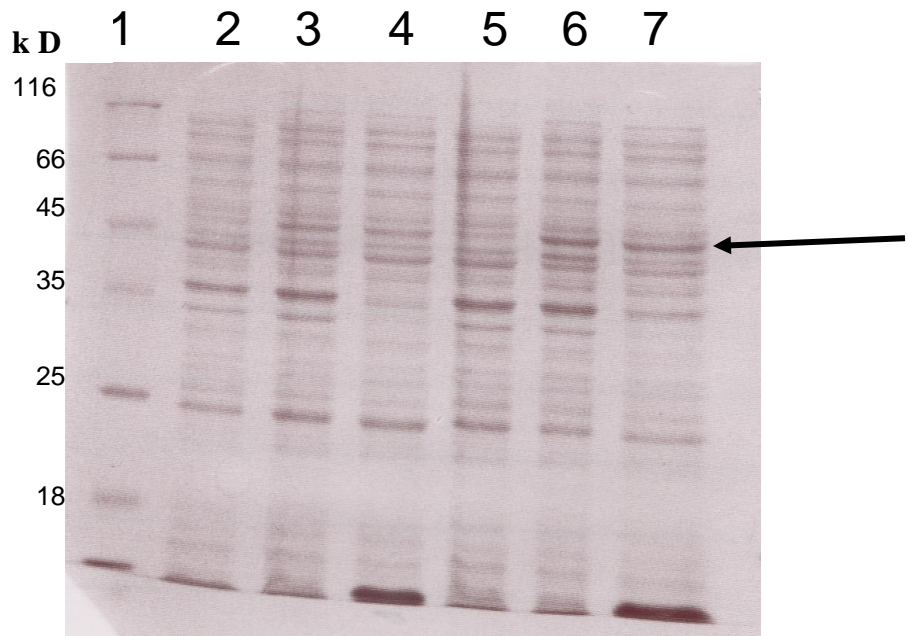
As mentioned above, since the full-length Dbf4 protein is highly labile, it was foreseen that if it was unsuitable for crystallization, a C-terminally truncated variant of Dbf4 would be tested. pET15bDbf4-396 was constructed to include amino acids 1 to 396 of Dbf4. It was important to make the truncations strategically and, ideally, maintain the Dbf4 conserved motifs intact. Since, much of the initial work in this study was focused on the Dbf4 N-motif and also the M-motif, it was desirable to clone a construct that would retain an intact Dbf4 N-motif and ideally an intact M-motif. Structural data for the Dbf4 N and M motifs would nicely complement the genetic data presented in the previous chapters. The truncation at 396 was chosen based on two criteria. Firstly, it retained both the Dbf4 motifs N and M and, secondly, it did not disrupt any secondary structure elements. The BL21(DE3) pRARE cell line was selected as an appropriate host for recombinant expression, based on the results of the protein solubility assay (Figure 6.4). The appropriate induction conditions were determined to be 30°C for 5 hours. These induction conditions, in a BL21(DE3) pRARE host, resulted in the best recombinant protein induction and protein solubility for the Dbf4-396 truncated protein. This is indicated by the arrow pointing to the relevant protein bands in the SDS-PAGE gel shown in Figure 6.4. The results for the other induction conditions are shown in Figure A-6 in the Appendix. These SDS-PAGE results show a comparatively inferior recombinant protein induction and protein solubility banding pattern. Unfortunately, during the protein purification procedure, the His-tag would not bind to the Nickel column on repeated attempts, suggesting a protein misfolding problem and, hence, the pET15bDbf4-396 construct was not pursued any further.

The next construct that was tested was pET15bDbf4-248, encoding amino acids 1 to 248. This truncated protein was tested because it was previously observed to be stable by Duncker *et al.* (2002). Furthermore, it retains the Dbf4 N-motif intact. However, the Dbf4 M-motif is not included in this construct. The solubility assay results determined that the STAR pRARE strain was most appropriate for the Dbf4-248 construct (Figure 6.5). Good protein expression and solubility were observed with STAR pRARE cells, as a host, and an induction period 5 hours at 30°C (Figure 6.5). This is indicated by the arrow pointing to the relevant protein bands in the SDS-PAGE shown in Figure 6.5. The results for the other cell line that was tested (BL21 (DE3) pRARE) are shown in Appendix Figure A-7. The arrow points to bands on the SDS-PAGE that indicate recombinant protein induction and solubility (Figure A-7). However, the STAR pRARE cells (Figure 6.5) were determined to be better.

A large-scale protein purification was performed by Melanie Gloyd in the Guarne Lab. A purified, concentrated protein sample of Dbf4-248 was sent to the Hauptman-Woodward Institute, Centre for High throughput Structural Biology, Buffalo, New York, for high throughput crystallization screening. It was tested at the Hauptman-Woodward Institute in 1500 buffer conditions for a period of 4 weeks. This large-scale screening effort did not yield any obvious crystallization.

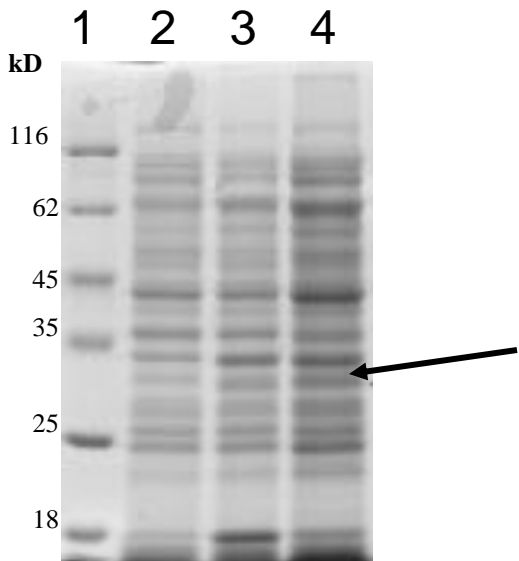
A schematic diagram, comparing full-length Dbf4 to the two truncated Dbf4 variants Dbf4-396 and Dbf4-248, is given in Figure 6.6.

**Figure 6.4. SDS-PAGE of Protein Solubility Assay for the pET15b Dbf4-396 construct in BL21 (DE3) pRARE cells.** The molecular weight marker is labeled with the units Kilodaltons. The lanes are numbered corresponding to the samples listed below the SDS-PAGE. The construct was tested at 37°C for 3 hours induction and at 30°C for 5 hours, 200rpm shake. Soluble fractions were prepared as described in Materials and Methods. Loaded samples were prepared by mixing with 2X SDS-loading dye as described in Materials and Methods. A 15 µl volume of each sample was loaded in the lanes of the SDS-PAGE (12%). The induced Dbf4-396 recombinant protein is indicated by the arrow



LANES

- |                         |             |
|-------------------------|-------------|
| 1.Prestained Marker     |             |
| 2. BL21pRARE IPTG-      |             |
| 3. BL21 pRARE IPTG+     | (37°C,3hrs) |
| 4. BL21 pRARE (SOLUBLE) | (37°C,3hrs) |
| 5.BL21 pRARE IPTG-      |             |
| 6.BL21 pRARE IPTG+      | (30°C,5hrs) |
| 7.BL21 pRARE (SOLUBLE)  | (30°C,5hrs) |



### LANES

1. Prestained Marker
2. STAR pRARE pETDbf4-248 IPTG-
3. STAR pRARE pETDbf4-248 IPTG+ (30°C,3hrs)
4. STAR pRARE pETDbf4-248 (SOLUBLE) (30°C,3hrs)

**Figure 6.5. SDS-PAGE for the pET15b Dbf4-248 construct in STAR pRARE cells.** The molecular weight marker is labeled with the units kilodaltons (kD). The lanes are numbered corresponding to the sample listed below the SDS-PAGE. The construct was tested 30°C for 5 hours induction at 200rpm shake. Soluble fractions were prepared as described in Materials and Methods. Loaded samples were prepared as described in the Materials and Methods. A 15µl volume of each sample was loaded in the lanes. Arrow points to the induced protein: Dbf4-248.

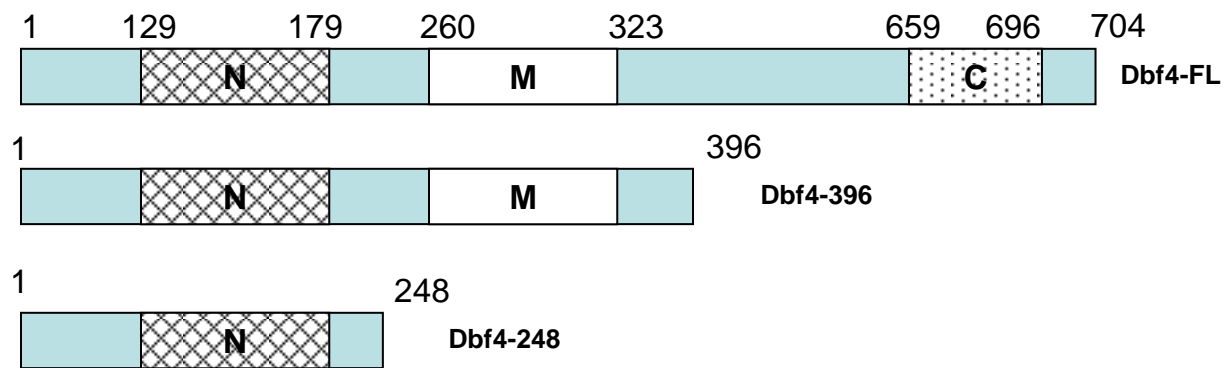


**Figure 6.6. Comparison of Dbf4 truncations that were cloned into pET15b expression vector and tested for solubility.** The numbers represent the numbers of the amino acid residues. The Dbf4 conserved motifs N, M and C are labeled at the appropriate position.

### **6.3. Discussion**

It is clear, from the data presented here, that trial and error is the key to obtaining success in protein crystallization. However, the strategic approach to the cloning is also important in, ultimately, achieving crystals. It is evident that the full-length Dbf4 protein was not suitable for crystallization, since it was not stable enough to purify on a large scale. Nonetheless, because the three Dbf4 motifs (N, M and C) were so well defined, it was possible to create a series of truncated Dbf4 variants that would possibly reveal the partial structure of Dbf4 and retain the N and M motifs intact. Retaining the complete N and/or M motif intact was crucial in obtaining a structure that would provide good information about the function of the domains and complement the existing data.

Observing the solubility of the Dbf4-248 construct, perhaps, the cloning of various lengths within the first 250 amino acids of Dbf4 N-terminus will lead to a stable, soluble and crystallizable truncated protein fragment. It seems a relevant and promising future direction beyond this research to further narrow down the N-terminus in an attempt to clone a fragment that includes the N-motif but possibly excludes the two destruction boxes that are located within the first 70 amino acids of the N-terminus of Dbf4 (Ferreira *et al.*, 2000).

If the physical structure of the Dbf4 N-motif is obtained, it may be possible to determine how the structure is altered as a result of specific point mutations. In Chapter 4, the region of the Dbf4 N-motif amino acids 168 to 178 was subjected to a series of point mutations. These point mutants were tested in two-hybrid assays. Specifically, the threonine residues 171 and 175 were identified as being critical in maintaining the interaction with the Rad53 FHA1 domain. Once the physical structure of Dbf4 is

available, it will be interesting to analyze these mutations within the context of a computer model to assess how these mutations might affect the structure of Dbf4. If the physical structure is determined, it may also be possible to co-crystallize this peptide with the FHA domains of Rad53.

It would also be worthwhile to attempt to crystallize the C-terminus (i.e. including the C-motif). This truncated protein fragment would, ideally, contain the C-motif and possibly the M-motif. This could possibly facilitate the eventual elucidation of the entire Dbf4 full-length structure. Moreover, the C-motif point mutations that were tested in Chapter 5 could be further investigated from a structural perspective. It would be interesting to determine how the C-motif point mutations, that compose the putative zinc-finger, alter the structure. This would possibly explain the results of the two-hybrid assays that were performed showing altered interactions between Dbf4 and its various known binding partners. Alternatively, the M and C-motifs could be crystallized, separately, as parts of two different truncated Dbf4 protein fragments.

If the structure of the Dbf4 M-motif is determined, it may be possible to investigate the *dna52-1* point mutation in Dbf4 proline residue at position 277 to a leucine (P277L) causing it to be a temperature-sensitive mutant that was studied in Chapter 3 of this thesis. Furthermore, there are other similar mutations to Dbf4 that cause a temperature-sensitive phenotype (Kihara *et al.*, 2000). It would be interesting to explore how these mutations cause structures that diverge from the wild type Dbf4 protein. Thus, eventually, in time, the entire three-dimensional physical structure of Dbf4 could be solved. All of this would nicely complement the data presented in the preceding chapters of this thesis.

## **Chapter 7: General Discussion and Conclusions**

## **7.1. Dbf4 Motifs (N,M and C)**

At the start of this research, little information was available on the Dbf4 protein in *S. cerevisiae*, with respect to its three conserved motifs. After the identification of the Dbf4's three highly conserved regions, referred to as the N, M and C motifs (Masai and Arai, 2000), two studies were conducted with the *S. pombe* model, placing an emphasis on *in vivo* phenotypes of various strains bearing mutations to the motifs (Fung *et al.*, 2002; Ogino *et al.*, 2001). Although, they isolated mutants, they did not investigate any disrupted molecular mechanisms or attribute mutant phenotypes to any altered protein-protein interactions. Thus, a study emphasizing the functional importance of the three motifs was needed. The present study is novel in that, firstly, the *S. cerevisiae* model organism was employed to study the functional importance of the three highly conserved motifs. Secondly, mutant phenotypes were correlated to altered protein-protein interactions involving Dbf4 and various known DNA replication and checkpoint factors. It should be noted that putative binding sites of Dbf4's various protein binding targets (DNA replication protein factors and checkpoint factors) were identified and attributed to specific motifs (N, M or C) of the Dbf4 protein. Subsequently, a more precise identification of the Rad53 binding site in Dbf4 was made by mutational studies, in conjunction with two-hybrid assay methods.

## **7.2. Essentiality of Motifs N, M and C for Cell Viability**

### **7.2.1. *Dbf4 N-Motif***

This work has shown that removing the Dbf4 motif-N did not affect the essential function of the Dbf4 protein, indicating that it is nonessential for cell viability. This is

consistent with the results observed in earlier studies with the *S. pombe* model (Fung *et al.*, 2002; Ogino *et al.*, 2001). However, in a study with mouse embryonic stem (ES) cells, the N-motif was found to be essential for cell viability (Yamashita *et al.*, 2005). These results, however, are questionable in view of the fact that the N-motif deletion mutant tested in their study retained an incomplete portion of the N-motif and had an additional 32 N-terminal amino acids that were not part of the N-motif deleted. Nonetheless, the above results prompt the conclusion that the N-motif of Dbf4 is not essential for cell viability in unicellular eukaryotes (yeasts), while it is essential for cell viability in multicellular eukaryotes (i.e. mice). Further work on the effects of the deletion of the N-motif on cell viability in other model organisms is desirable to validate the above conclusion.

The deletion of the N-motif also resulted in a growth defect that was attributed to a slower S-phase, as determined by FACS analysis. It is likely that the impaired Dbf4-Orc2 interaction contributed to this phenotype. A similar growth defect has been observed by Gabrielese *et al.* (2005) for a *S. cerevisiae* mutant in which the N-terminal 221 amino acids (including N-motif) were deleted.

In addition, the deletion of Dbf4 N-motif preserves the Dbf4-Mcm2 association, disrupts Dbf4 interaction with Rad53 and renders the cells hypersensitive to genotoxic agents. Furthermore, the deletion of the 11 amino acids (168 to 178) of the Dbf4 N-motif was found to cause an abrogation of the Dbf4-Rad53 interaction. Point mutations amongst the 11 amino acids (168 to 178) revealed that, threonine residues 171 and 175 were important for mediating the Dbf4-Rad53 interaction, which when mutated together to alanines, also caused a disruption of the Dbf4-Rad53 interaction.

### **7.2.2. Dbf4 M-Motif**

In contrast to the N-motif, removing the M-motif impairs the ability of Dbf4 to support normal cell cycle progression. That is, the M-motif was found to be essential for cell viability. This finding is consistent with what has been observed in *S. pombe* (Fung *et al.*, 2002; Ogino *et al.*, 2001) and in mouse ES cells (Yamashita *et al.*, 2005). Importantly, it was revealed that the M-motif is responsible for mediating the Dbf4-Mcm2 interaction. Deletion of the M-motif did not affect the Dbf4 interaction with Rad53 or Orc2.

It should also be noted that a temperature-sensitive mutant carrying a proline to leucine point mutation at amino acid 277 of the Dbf4 M-motif was found to confer resistance to genotoxic agents. This mutation caused impaired Dbf4-Mcm2 and Dbf4-Orc2 interactions and resulted in a maintained Dbf4-Rad53 interaction. This will be discussed later in this chapter.

### **7.2.3. Dbf4 C-Motif**

The Dbf4 C-motif was found to be essential for cell viability. This finding is consistent with what has been observed in *S. pombe* (Ogino *et al.*, 2001), *Aspergillus nidulans* (James *et al.*, 1999) and mouse ES cells (Yamashita *et al.*, 2002). However, contradictory results have been obtained in another study involving the *S. cerevisiae* (Dowell *et al.*, 1994) and also in a study using the *S. pombe* model, which indicate that the C-motif is nonessential for cell viability. It should be pointed out that there are several reasons for the discrepancy between the results from the present study and those from the Dowell *et al.* (1994) study, involving *S. cerevisiae*, which have been discussed in detail,

earlier (Chapter 5). The precise deletion of the Dbf4 C-motif, in the present study, resulted in disrupted interactions between Dbf4 and Mcm2, Orc2, Rad53 and also with Cdc7.

Since, the Dbf4 C-motif is the most highly conserved of the three motifs and represents a putative CCHH-type zinc-finger, it was investigated further in the present study, by creating point mutations to the critical cysteine and histidine residues (composing the zinc-finger motif). Interestingly, the point mutation of the cysteine and histidine residues (composing the zinc-finger) to alanines resulted in stronger protein-protein interactions between Dbf4 and some of its known protein binding targets (Rad53, Orc2, Mcm4), as detected by two-hybrid assays. The same point mutations also caused reduced interactions between Dbf4 and Mcm2 and also with ARS1, as detected with the two-hybrid assay and one-hybrid assay, respectively. These data indicate that point mutations made to the putative zinc-finger (histidines and cysteines) of the C-motif can affect the protein-protein interactions that are presumed to be mediated through the two other Dbf4 motifs (N and M). In affecting the protein-protein interactions, the molecular mechanisms that are orchestrated by Dbf4, in association with other proteins, were presumed to be altered as a result of the Dbf4 C-motif point mutations. By this logic, the C-motif point mutantions were tested, *in vivo*, in a *rad53-11* mutant background, which is hypersensitive to genotoxic agents, as a result of an impaired intra-S-phase checkpoint response. This series of experiments was designed to test the effect of increased Dbf4-Rad53 interaction caused by the C-motif point mutations on the intra-S-phase checkpoint response. The Dbf4 C-motif point mutant proteins were overexpressed from plasmids, in transformed *rad53-11* mutant cells. The resulting transformants were tested in growth

spotting assays for sensitivity to genotoxic agents and discovered to be more resistant to HU and BLEO when compared to a wild type control. This resistance, that was observed, is discussed later in this chapter. The mutant Rad53-11 mutant protein was also tested in a two-hybrid assay and an increased interaction with Dbf4 C-motif point mutants was observed.

From the above discussion, as expected, the essentiality of these motifs of Dbf4 in *S. cerevisiae* is similar to some organisms, but differs from others. Care must be taken not to overgeneralize the application of these conclusions, until data from future studies can be similarly analyzed and the reproducibility of these conclusions is established in *S. cerevisiae* and other organisms. Obviously, more work is desirable.

### **7.3. *Saccharomyces cerevisiae* Does Not Have a Dbf4-Related Protein**

As discussed earlier, Dbf4 and several other cell cycle DNA replication and checkpoint factors are conserved throughout the species, as are some of their molecular mechanisms and processes. From an evolutionary perspective, although the overall conservation of Dbf4 is low, the high degree of conservation of the three motifs (N, M and C) leads one to believe that Dbf4 is involved in the important fundamental mechanisms that allow for the species to perpetuate and proliferate. In other species (*S. pombe*, *X. laeveus*, *Homo sapiens*) that have Dbf4 orthologues, Dbf4-related proteins have also been identified (Montagnoli *et al.*, 2002; Yanow *et al.*, 2003; Nakamura *et al.*, 2000). That is, in addition to having a Dbf4 orthologue, these other organisms also have a second protein (Dbf4-related protein) with sequence similarity to Dbf4. To date, no such Dbf4-related protein has been identified in *S. cerevisiae*. It is possible that there is a

Dbf4-related protein in *S. cerevisiae* that has not been discovered yet. Assuming it does not exist in *S. cerevisiae*, it is relevant to comment on this from an evolutionary perspective. Firstly, the evolution of a Dbf4-related protein in other eukaryotes is a testament to the importance of this essential protein. The presence of a Dbf4-related protein in other organisms (in addition to having a Dbf4 orthologue) might also explain why a lethal mutation in *S. cerevisiae* Dbf4 may not be lethal in other organisms. It is possible that the Dbf4-related protein, in other organisms, performs a compensatory role when the Dbf4 orthologue protein function is impaired by mutation. This is an important consideration when one looks to extrapolate the experimental findings obtained from these studies with *S. cerevisiae* to other eukaryotes.

#### **7.4. The Role of Dbf4 in the Intra-S-Phase Checkpoint Response**

At the outset of this study, the role of Dbf4 in the intra-S-Phase checkpoint was a fairly novel concept (Jares *et al.*, 2000; Duncker and Brown, 2003). Essentially, the Dbf4-Rad53 interaction had been implicated as a means by which late-firing origins of replication are regulated by the removal of Dbf4, preventing the firing of these origins (Duncker *et al.*, 2002). This mechanism was not well characterized, but appeared to be as a result of a physical interaction between Dbf4 N-terminus (amino acids 1 to 296) and Rad53 (Duncker *et al.*, 2002). However, it had also been shown that this mechanism did not contribute, greatly, to cell survival in response to genotoxic stress (Tercero *et al.*, 2003). Additional mechanisms, involving Dbf4 and/ or Rad53, were proposed to be acting in the intra-S-phase checkpoint response, which contribute to cell viability in response to genotoxic stress. Although not yet proven, experimentally, the stabilization of

replication forks during a checkpoint response and the recovery of replication forks following a checkpoint arrest were both proposed as possible mechanisms by which Rad53 and/or Dbf4 could be contributing to cell survival in response to genotoxic stress.

In order to prove, experimentally, that Dbf4 and/or Rad53 were acting in intra-S-phase checkpoint mechanisms, in addition to the function of late-firing origin regulation (*via* the Rad53 mediated removal of Dbf4 from late origins), it was deemed necessary to create a mutant strain in which the Dbf4-Rad53 interaction was disrupted, while retaining an intact wild type Rad53 protein. Removal of the Dbf4 N-motif caused an abrogated Dbf4-Rad53 interaction. Importantly, that the *dbf4ΔN* mutant strain was sensitive to genotoxic agents (HU and MMS) (Figure 3.3), suggested that Dbf4 and Rad53 likely act in another way to promote cell viability in the intra-S-phase checkpoint response, aside from the regulation of late-firing origins mechanism. Here a mechanism of impaired replication fork restart following the intra-S-phase checkpoint as a result of the disrupted Dbf4-Rad53 interaction in the *dbf4ΔN* mutant is proposed. This could be studied using two-dimensional agarose gel electrophoresis methods. It then follows that in wild type cells, the Dbf4-Rad53 is implicated in a mechanism aiding in the recovery and restart of replication forks following the intra-S-phase checkpoint response. More work is required to fully elucidate exactly how this occurs. However, in view of recent proposals (Szjyka *et al.*, 2008; Ogi *et al.*, 2008) along with the results reported here, the role of Dbf4 in the intra-S-phase checkpoint response can be better defined. Szjyka *et al.*, (2008) have also proposed that Rad53 regulates replication fork restart after DNA damage. They suggest that Rad53 may inhibit Dbf4/Cdc7 activity in normal replication, at origins, while stimulating Dbf4/Cdc7 activity in replication fork restart following DNA damage. This

would explain why the *dbf4ΔN* mutant would be sensitive to genotoxic agents (HU and MMS), since the Dbf4-Rad53 interaction mediating this mechanism would be disrupted.

In addition, the proposal of Ogi *et al.* (2008) is somewhat helpful in supporting an explanation as to why the *dbf4ΔN* mutant strain was more sensitive to genotoxic agents (HU and MMS) than wild type cells. Ogi *et al.* (2008) have proposed that *S. cerevisiae* Cdc7/Dbf4 is required for the full activation of Rad53, together with the autophosphorylation of Rad53, after Mec1 phosphorylation of Rad53 in the S-phase checkpoint. They have also suggested that the Cdc7/Dbf4 hyperphosphorylation of Rad53 may be involved in inducing transcription of genes involved in DNA repair or in the coordination of dNTP pool levels. Although, this mechanism needs to be more fully characterized (with experimental data) a disruption of the Dbf4-Rad53 interaction, according to this model, as is the case with the *dbf4ΔN* mutant, could result in a phenotype of sensitivity to genotoxic agents.

From the above discussion, a more clearly defined picture of the mechanisms involved in the intra-S-phase checkpoint response has emerged. The question then arises, as to whether these mechanisms of origin regulation and replication fork restart occur in higher eukaryotes. Recent work with frog (*Xenopus laevis*) egg extracts and mammalian cells has shown that the Dbf4/Cdc7 complex is not removed from chromatin during a DNA-damage induced S-phase checkpoint (Tsuji *et al.*, 2008). This indicates that in higher eukaryotes, origin regulation is not occurring as it does in yeast. However, a role for Dbf4/Cdc7 in checkpoint recovery does seem to be present in *S. cerevisiae*, as in higher eukaryotes. They propose a model, in which, Cdc7 modulates the S-phase checkpoint signaling and triggering DNA replication re-initiation during the S-phase

checkpoint recovery. Thus, the mechanism of Rad53-Dbf4 mediated regulation of origins does not seem to be conserved in higher eukaryotes. However, a role for Dbf4/Cdc7 in checkpoint recovery does seem to be present in *S. cerevisiae*, as well as in higher eukaryotes. Nonetheless, further research is necessary to fully explore the details of the role of Dbf4 and Rad53 in the intra-S-phase checkpoint response in *S. cerevisiae* and in higher eukaryotes.

Thus, the role of Dbf4 in the intra-S-phase checkpoint has been further characterized beyond the starting point of this research. The role of the Rad53-Dbf4 interaction in the intra-S-phase checkpoint response, regulating late-firing origins, seems to be complemented by another mechanism that appears to be replication fork recovery and restart. The regulation of late-firing origins seems to be a fitness advantage for unicellular yeasts, but does not appear to have been conserved, as a mechanism, in the higher, multicellular eukaryotes. This evolutionary distinction suggests that it is not a fitness advantage for multicellular organisms. It will be of interest to utilize the *dbf4ΔN* mutant to further characterize the means by which Dbf4 and Rad53 are involved in the checkpoint replication fork recovery.

The work in the present study has shown that mutations in both the Dbf4 M and C motifs also seemed to affect the intra-S-phase checkpoint response. The P277L mutation of the *dna52-1* mutant strain conferring resistance to genotoxic agents points to the M-motif as being involved in the intra-S-phase checkpoint response. Furthermore, point mutations in the Dbf4 C-motif resulted in increased interactions with Rad53. Thus, although the primary focus of the intra-S-phase checkpoint response mechanism involving the Dbf4-Rad53 interaction was centered on the Dbf4 N-motif, some M and C

motif mutations also had an effect on the intra-S-phase checkpoint response; that will be discussed below.

### 7.5. Resistance To Genotoxic Agents

Resistance to genotoxic agents was observed with the *dna52-1* mutant, which carried the P277L mutation, in the M-motif of Dbf4. The Dbf4-Rad53 interaction was preserved in this mutant, but the Dbf4-Mcm2 interaction was disrupted, as shown by two-hybrid assay interactions. Interestingly, when the Dbf4 C-motif point mutants were overexpressed in the *rad53-11* mutant background, a conferred resistance to genotoxic agents was observed, as well. The Dbf4-Rad53 interaction was enhanced in this case and the Dbf4-Mcm2 interaction was impaired. Taken together, these results suggest that the disrupted Dbf4-Mcm2 interaction, as a result of mutation, may contribute to the phenotype of resistance to genotoxic agents.

It is important to place these results and interpret them within a context of some new developments in the field. As discussed above, the regulation of late-firing origins is a mechanism of the intra-S-phase checkpoint that is not as important for cell survival as previously thought (reviewed in Jares *et al.*, 2000; reviewed in Duncker and Brown, 2003). It seems that early-origin replication fork stability is also important in the intra-S-phase checkpoint response. Segurado and Diffley (2008) have demonstrated that the sensitivity to DNA damaging agents can be almost completely suppressed, in *rad53* mutants, by the deletion of the *EXO1* gene, which encodes an enigmatic flap endonuclease. Importantly, deletion of the *EXO1* gene seems to cause a suppression of the replication fork instability in *rad53* mutants. This effect is independent of Mec1,

since *mec1* mutants are still sensitive to the DNA damaging agents when *EXO1* is deleted. Although the actual mechanism by which the Exo1 protein disrupts the integrity of replication forks is not known, the most likely explanation is that Exo1 is being directly regulated by Rad53 (Segurado and Diffley, 2008). There is evidence of a Rad53-dependent phosphorylation of Exo1 (Smolka *et al.*, 2007). In the *mec1* mutants, the Mec1 protein is not able to act with Chk1 to stabilize replication forks. Nonetheless, the target substrates and precise mechanisms by which Rad53, Mec1, Chk1 and Exo1 are acting are not fully known, at this time.

It is possible that the results demonstrating resistance to genotoxic agents, conferred by the Dbf4 P277L and C-motif point mutations, in the present study, were caused by an efficient stabilization of early-firing origin replication forks, by the mechanism described above. The impaired Dbf4-Mcm2 interaction observed for both mutations may be allowing Mcm2 to be more available to be involved in replication fork stability. It has been suggested by Segurado and Diffley (2008), that the Mcm2-7 proteins are candidates, as functionally relevant substrates by Mec1, Rad53 and Chk1, which would implicate them in replication fork stability, perhaps, through a physical interaction or a phosphorylation event. This notion is further supported by the results presented by Labib *et al.* (2000) which demonstrated that the loss of Mcm2-7 from stalled replication forks causes an irreversible arrest similar to that seen in checkpoint mutants.

Recently, Francis *et al.* (2009) have published results indicating that Dbf4/Cdc7 activation by phosphorylation of the Mcm2-7, requires a stable interaction between Mcm2-7 and Dbf4/Cdc7. Thus, Dbf4 mutations causing an impaired Dbf4-Mcm2

interaction could result in an inhibition of the Mcm helicase activity, which could contribute to replication fork stability.

To sum up: the phenotype of resistance to genotoxic agents, displayed by the mutants in this study, are likely caused by a more efficient stabilization of replication forks at origins as a result of an impaired Dbf4-Mcm2 interaction. The regulation of late-firing origins by the removal of Dbf4 *via* Rad53 during the intra-S-phase checkpoint as reviewed by Duncker and Brown (2003) may also be a contributing factor. However, more work is required to fully determine the mechanism by which this occurs.

## 7.6. Relevance to Cancer

The experiments pursued in the present study were carried out in *S.cerevisiae*. Can the results obtained be applied to higher eukaryotes? Although, the research, presented here, was carried out from a curiosity-driven basic research perspective, it is still of interest to retrospectively attempt to analyze the results with reference to biomedical sciences. Ultimately, the aim of any biomedical research is to achieve results that can be used for medical applications in humans. Such an analysis could potentially influence the future directions and applications of the work presented here. It is of particular interest when one considers recent reports that indicate that there is an upregulation of Dbf4 in cancer cells and tumours (Nambiar *et al.*, 2007; Bonte *et al.*, 2008).

Nambiar *et al.* (2007) have reported that Dbf4 is upregulated in primary melanoma, melanoma metastasis and melanoma cell lines. Moreover, Bonte *et al.* (2008) found that approximately 50% of 62 human tumour cell lines had increased Cdc7-Dbf4

expression levels compared to normal cell lines. They also observed that 5 of 14 tumour cell lines and one primary cell line had multiple copies of the *DBF4* gene. Furthermore, a high correlation, between p53 loss and increased Cdc7 and Dbf4 expression in primary breast cancers and in the cancer cell lines, studied, was also observed (Bonte *et al.*, 2008). Thus, in light of this new data, it is of interest to further explore the effects of Dbf4 overexpression in the *S.cerevisiae* model and to possibly test various drugs to reduce the overexpression.

It is known that the intra-S-phase checkpoint response is active in normal (unperturbed) S-phase which suggests that there is some replication stress in a normal S-phase (Grallert and Boye, 2008). Interestingly, precancerous cells are under selective pressure to inactivate the checkpoint mechanism. Thus, checkpoint mutations are selected for in the early stages of cancer (Grallert and Boye, 2008). Most oncogenic mutations affect a cell's commitment to the cell cycle and genes involved in G1 progression are often mutated in human cancers (Grallert and Boye, 2008). In view of the work carried out in the present study in *S. cerevisiae*, one could determine which of the three conserved motifs of Dbf4 is affected by the mutations in cancer cells. It would be interesting to determine if any human Dbf4 N-motif mutations are affecting the interaction with Chk2 (the human Rad53 orthologue) in human cancers. It is likely that a disrupted Dbf4-Chk2 interaction, caused by a mutation, would result in a faulty S-phase checkpoint response that could lead to an increase rate of mutations leading to cancer. One would expect to possibly see such Dbf4 mutations in combination with other more common oncogenic mutations. It should be noted that *CHK2* is a multi-organ cancer

susceptibility gene that seems to act in synergy with other genes or factors to cause cancer (reviewed in Antoni *et al.*, 2007).

The *dbf4ΔN* mutant strain, created and tested in the present study, yielded some interesting results having a phenotype that is hypersensitive to genotoxic agents and a growth defect that was studied in the work presented here. It is relevant to note the an N-motif deletion was lethal in mouse embryonic stem cells (Yamashita *et al.*, 2005). It would be interesting to determine if the *DBF4ΔN* mutation could be introduced into some other model mammalian cell lines or model organisms. It would also be most interesting to develop a transgenic rodent (or another mammal) mutant carrying the *DBF4ΔN* mutation. The resulting phenotype, if viable, would put into perspective the importance of the Dbf4-Rad53 interaction in a multicellular organism. This is even more interesting when one considers the study by Marchetti *et al.* (2006), in which *S. pombe* N-motif deletion mutants were shown to produce increased levels of Reactive Oxygen Species (ROS). ROS is a term describing any mixture of molecules, ions and free radicals which contain derivatives of molecular oxygen that are more reactive than oxygen itself. Studies have shown that replication stress can trigger apoptosis-like cell death, accompanied by the production of ROS in *S. cerevisiae* and mammalian cells (Marchetti *et al.*, 2006). Thus, one would expect a *dbf4ΔN* mutant rodent, if viable, to be more prone to cancer, given this result. Although ROS levels were not measured in the *S. cerevisiae dbf4ΔN* mutant strain in the present study, it is reasonable to expect increased ROS levels, as observed in *S. pombe*. It is possible that N-motif mutations are present in cancer cell lines and tumours. This could be determined by identifying Dbf4 mutations in various cell lines and tumour samples.

Interestingly, Chaudhuri *et al.* (2005) tested the effects of aqueous cigarette smoke extract exposure (CSE) on *S. pombe*. They observed an increase in the accumulation of ROS and an S-phase checkpoint induced cell cycle arrest *via* a Rad3-Cds1 pathway. John *et al.* (2005) studied the effects of aqueous CSE in *S. cerevisiae*. They observed that, as a result of aqueous CSE exposure, cell growth was inhibited and there were changes in gene expression in many classes of genes, including genes involved in oxidative stress response which were upregulated (John *et al.*, 2005). They also observed an accumulation of ROS (John *et al.*, 2005). The observed effects of the cigarette smoke exposure were reversible by treating the cells with anti-oxidants (John *et al.*, 2005).

As discussed above, *dbf4ΔN* mutants have also been shown to have an increase in ROS accumulation in *S.pombe* (Marchetti *et al.*, 2006). Since this phenotype is similar to the observed effects of CSE exposure, it is worthy of further examination. Firstly, ROS levels will have to be tested in the *S. cerevisiae dbf4ΔN* mutant, experimentally, before proceeding. Nonetheless, if the *S. cerevisiae dbf4ΔN* mutant does prove to have increased ROS levels, this mutant could possibly serve as a model that mimics the effect of CSE on cells. The *S. pombe* mutant strain described above could also be used for this purpose. It is reasonable to presume that oxidative stress response genes would be upregulated in *dbf4ΔN* mutant cells. It would be very interesting to determine if the addition of anti-oxidant treatment has any other effects on the *dbf4ΔN* phenotype with respect to the growth defect or sensitivity to genotoxic agents. One could also determine the effect of CSE on the *dbf4ΔN* mutant, relative to a wild type control. If in fact, an even greater accumulation of ROS is observed, this would be a good example of a genetic mutation in

combination with an environmental toxin creating a synergy, having a detrimental effect. Furthermore, one could also test ROS levels in other Dbf4 mutants such as *dna52-1* (Dbf4 temperature-sensitive mutant), which has exhibited resistance to genotoxic agents, in the present study.

Thus, the Dbf4 protein has, in recent years, shown itself to be a potentially useful biomarker for the study of cancer, and perhaps, the basis for the development of a diagnostic assay. Moreover, the fact that Dbf4 is conserved and that the three motifs (N, M and C) are highly conserved lend relevance to research based in *S. cerevisiae*. Clearly, the data obtained in this work is relevant to biomedical sciences; and can contribute, further, to our understanding of molecular mechanisms that may be disrupted in some forms of cancer.

## 7.7. Future Directions

Of the future directions of the project, further characterization of the *dbf4ΔN* mutant is an obvious one. The observed growth defect could be further investigated by using a two-dimensional agarose gel electrophoresis methods. This will allow the comparison of the replication fork progression relative to the Dbf4 wild type, as well as, comparing the effect of genotoxic agents on the *dbf4ΔN* strain compared to the Dbf4 wild type. It will provide insight into whether the replication fork stability or the replication fork recovery following a checkpoint is impaired in *dbf4ΔN* strain as a result of treatment with genotoxic agents. Furthermore, it may be worthwhile to pursue, experimentally, the phenomenon of reactive oxygen species accumulation in the *dbf4ΔN* mutant, as well as its potential application as a model for the effect of cigarette smoke extract exposure.

It would be interesting to further investigate the Dbf4 M-motif. The Dbf4 M-motif proved to be essential for cell viability and mediated the Dbf4-Mcm2 interaction. Furthermore, a single point mutation in the Dbf4 M-motif caused an interesting *in vivo* phenotype of resistance to genotoxic agents. Perhaps, in addition to the *dna52-1* P277L mutant tested in the present study, a series of partial M-motif deletion and point mutants could be made to further isolate the Mcm2 binding site in Dbf4. This could also, potentially, lead to the creation of and characterization of a viable Dbf4 M-motif mutant that is not temperature sensitive (as is the *dna52-1* P277L mutant). Moreover, a possible role for Mcm2 being involved in replication fork stability of early-firing origins should also be investigated further.

Another future direction is to continue with the study of the Dbf4 C-motif. In addition to the point mutants created and tested in the present study, similar methods could be applied to test triple and quadruple mutations, in which both cysteine and both histidine residues that compose the putative zinc-finger are mutated to alanines. Various triple point mutation combinations could also be tested in which either both histidines and one cysteine is mutated to alanines or both cysteines and one histidine is mutated to alanine. Also, it will be very important to introduce the C-motif point mutations into the genome and determine the phenotypes with respect to growth and sensitivity to genotoxic agents. Creating a series of integrated double mutants, carrying the Dbf4 C-motif point mutants and the *rad53-11* mutation would be interesting to determine if a similar phenotype (conferred resistance to genotoxic agents) to what has been observed with plasmid-based overexpression of the Dbf4 C-motif point mutants in the *rad53-11* mutant background, would result. The creation of a double mutant, carrying the *DBF4ΔN* allele

and the Dbf4 C-motif point mutants could also be created and tested *in vivo* and in two hybrid assays. The phenotypes of these double mutants, if viable, would indicate if the resistance phenotype of one mutation could possibly cancel out the sensitivity phenotype of the other mutation. The two-hybrid results in conjunction with the *in vivo* data testing sensitivity to genotoxic agents will indicate which protein-protein interactions are critical for replication for stabilization and/or recovery from replication fork arrest.

It will also be beneficial to continue the Dbf4 X-ray crystallography collaboration. Hopefully, continued efforts will lead to the successful elucidation of the three-dimensional structure of the Dbf4 N-terminus. Furthermore, it will be interesting to follow-up with attempts to crystallize the Dbf4 C-terminus, which would ideally contain an intact Dbf4 C-motif and also the M-motif. Such efforts could eventually result in the determination of the complete three-dimensional physical structure of the Dbf4 protein. A comparison of the three-dimensional physical structures of mutants to the wild type Dbf4 protein would nicely complement the data obtained in the present study. The effects of the various mutations that have been studied by two-hybrid assay could be analyzed from the perspective of how they affect the structure of the mutated proteins and how any altered protein structures influence their interactions with other proteins.

Finally, it will also be relevant to investigate the mechanism by which Rad53-Exo1 pathway is involved in replication fork stability. This could be pursued by setting up two-hybrid assays to determine if there is a physical interaction between Rad53 and Exo1. If in fact Rad53 and Exo1 interact physically, various Rad53 mutant proteins could be tested and compared to the wild type Rad53-Exo1 interaction, using two-hybrid assay

methods. The results from these experiments could possibly indicate how Rad53 mutations cause sensitivity to genotoxic agents.

## 7.8. Summary

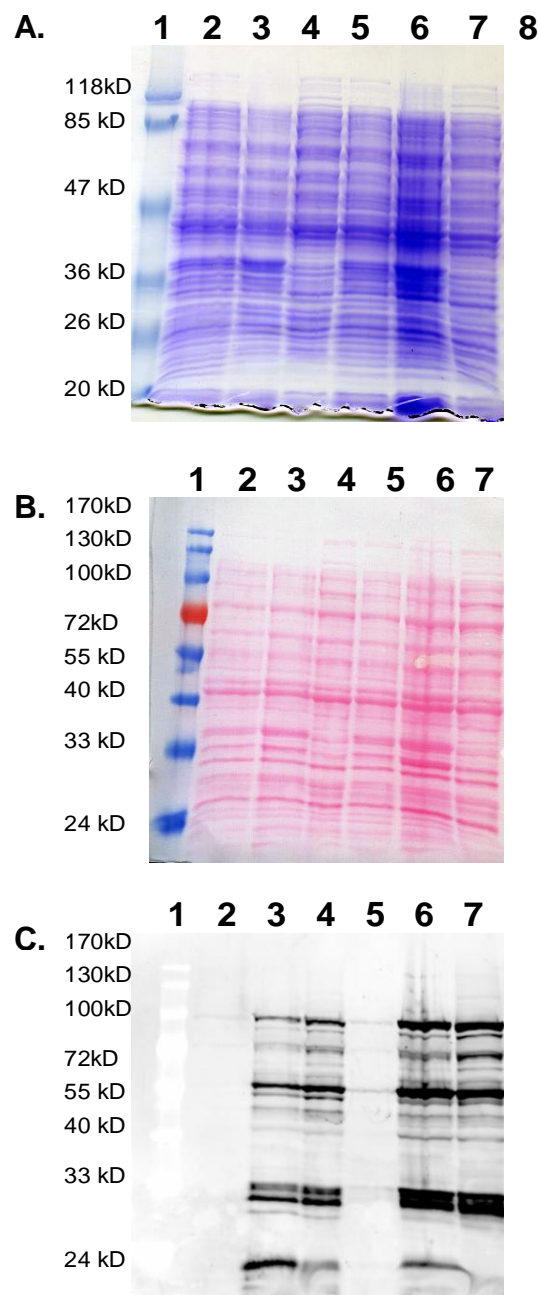
In summary, the roles of Dbf4 conserved motifs (N, M and C) have been characterized from a functional and mechanistic perspective. A series of two hybrid assays were carried out using Dbf4 and various DNA replication protein factors Cdc7, Mcm2 and Orc2, as well as the effector checkpoint kinase Rad53. The Dbf4 N-motif was determined to be non-essential for viability, and was involved in the Dbf4-Rad53 and Dbf4-Orc2 protein-protein interactions. The Dbf4 M motif was determined to be essential for viability and was involved in the Dbf4-Mcm2 protein-protein interaction. The Dbf4 C-motif, which resembles a putative CCHH-type zinc finger, has been shown to be essential for viability in the present study. A series of four Dbf4 C-motif point mutants were constructed in which the critical two cysteines and two histidines were mutated in various combinations. These point mutations were able to support viability in complementation assays and in plasmid shuffle strains and when overexpressed in *rad53-11* mutant cells, they conferred resistance to genotoxic agents. This is likely due to an increased Dbf4-Rad53 interaction and a decreased Dbf4-Mcm2 interaction, as demonstrated in two hybrid assays. Attempts were also made to obtain the three-dimensional structure of Dbf4, using X-ray crystallography methods.

Recent developments involving studies focused on the human orthologue of Dbf4 overexpression in various cancer cell lines have served to emphasize the importance of and relevance of the present study that was carried out in the *S. cerevisiae* model. It is

possible that the research presented here could eventually lead to the use of the human orthologue of Dbf4 as a cancer biomarker which could be utilized as a basis for the development of a diagnostic test or as a therapeutic target.

## **APPENDIX**

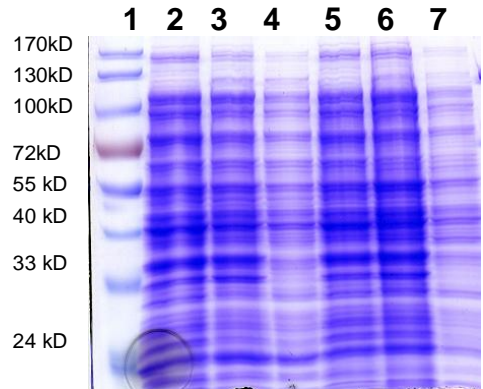
**Figure A-1. SDS-PAGE and Western Blot for BL21 (DE3) pET15bDbf4-FL.** The molecular weight marker is labeled, representing Kilodaltons as units. The lanes are numbered corresponding to the samples listed below. The construct was tested, in the BL21 (DE3) host, under induction conditions of 25°C for 5 hours and 37°C for 3 hours, 200rpm shake. Soluble fractions were prepared as described in Materials and Methods section. A. SDS-PAGE (12%) corresponded to a protein solubility assay. Samples were prepared as described in the Materials and Methods section by mixing them with 2X SDS-loading dye. A 15 ul volume of each prepared sample was loaded in the SDS-PAGE lanes. B. Ponceau S (0.1%) stain of the nitrocellulose membrane indicates how equal the lanes were loaded and corresponded to the western blot C. Western blot. A nitrocellulose membrane was probed with anti-Dbf4 antibody (Santa Cruz) 1:100 concentration. The secondary antibody used was Alexa Fluor 488 (donkey anti-goat) (Invitrogen) at a concentration of 1:1500.



**LANES**

- 1. Pre-Stained Marker
- 2. IPTG-
- 3. IPTG+  $37^{\circ}\text{C}$  (3 hours)
- 4. IPTG+(soluble)  $37^{\circ}\text{C}$ (3hours)
- 5. IPTG-
- 6. IPTG+  $25^{\circ}\text{C}$  (5 hours)
- 7. IPTG+ (soluble)  $25^{\circ}\text{C}$  (5 hours)
- 8. Unstained Marker

**Figure A-2. SDS-PAGE and Western Blot for BL21 (DE3) pLySs pET 15bDbf4-FL.** The molecular weight marker is labeled, representing Kilodaltons as units. The lanes are numbered corresponding to the samples listed below. The construct was tested, in the BL21 (DE3) pLySs host under conditions of 25°C for 5 hours and 37°C for 3 hours, 200rpm shake. Soluble fractions were prepared as described in Materials and Methods section. A. SDS-PAGE (12%) corresponding to the protein solubility assay. Samples were prepared as described in the Materials and Methods section by mixing them with 2X SDS-loading dye. A 15 ul volume of each prepared sample was loaded in the SDS-PAGE lanes. B. Ponceau S (0.1%) stain of the nitrocellulose membrane indicates how equal the lanes were loaded and corresponded to the western blot C. Western blot. A nitrocellulose membrane was probed with anti-Dbf4 antibody (Santa Cruz) 1:100 concentration. The secondary antibody used was Alexa Fluor 488 (donkey anti-goat) (Invitrogen) at a concentration of 1:1500.



LANES

1. Pre-Stained Marker
  2. IPTG-
  3. IPTG+ 37°C (3 hours)
  4. IPTG+(soluble) 37°C(3hours)
  5. IPTG-
  6. IPTG+ 25°C (5 hours)
  7. IPTG+ (soluble) 25°C (5 hours)

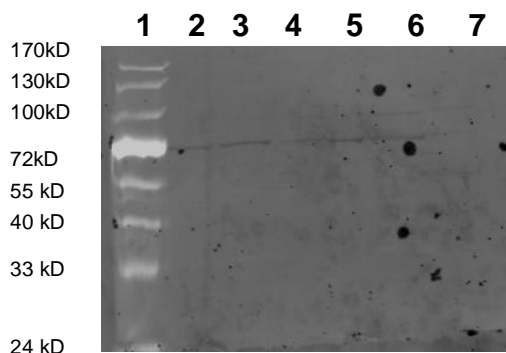
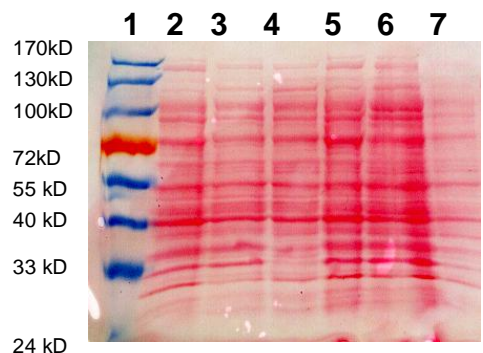
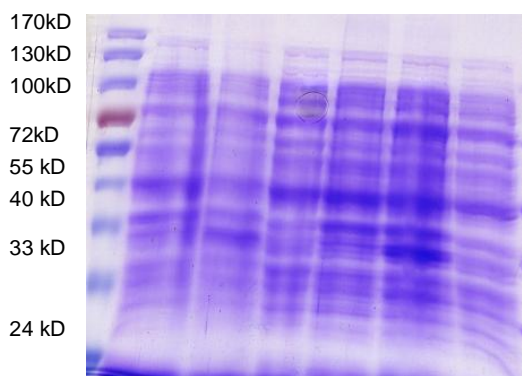


**Figure A-3. SDS-PAGE and Western Blot for STAR pET 15bDbf4-FL.** The molecular weight marker is labeled, representing Kilodaltons as units. The lanes are numbered corresponding to the samples listed below. The construct was tested in the STAR host, under induction conditions of 25°C for 5 hours and 37°C for 3 hours, 200rpm shake. Soluble fractions were prepared as described in Materials and Methods section. A. SDS-PAGE (12%) corresponded to the protein solubility assay. Samples were prepared as described in the Materials and Methods section by mixing them with 2X SDS-loading dye. A 15 ul volume of each prepared sample was loaded in the SDS-PAGE lanes. B. Ponceau S (0.1%) stain of the nitrocellulose membrane indicates how equal the lanes were loaded and corresponded to the western blot C. Western blot. A nitrocellulose membrane was probed with anti-Dbf4 antibody (Santa Cruz) 1:100 concentration. The secondary antibody used was Alexa Fluor 488 (donkey anti-goat) (Invitrogen) at a concentration of 1:1500.

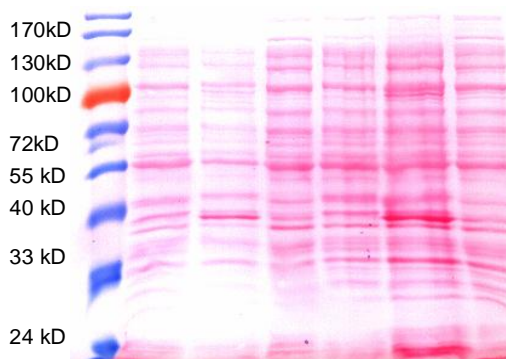
**A.** 1 2 3 4 5 6 7



**LANES**

- |                             |                       |
|-----------------------------|-----------------------|
| <b>1.Pre-Stained Marker</b> |                       |
| <b>2. IPTG-</b>             |                       |
| <b>3. IPTG+</b>             | <b>37°C (3 hours)</b> |
| <b>4. IPTG+(soluble)</b>    | <b>37°C(3hours)</b>   |
| <b>5. IPTG-</b>             |                       |
| <b>6. IPTG+</b>             | <b>25°C (5 hours)</b> |
| <b>7. IPTG+ (soluble)</b>   | <b>25°C (5 hours)</b> |

**B.** 1 2 3 4 5 6 7



**C.** 1 2 3 4 5 6 7

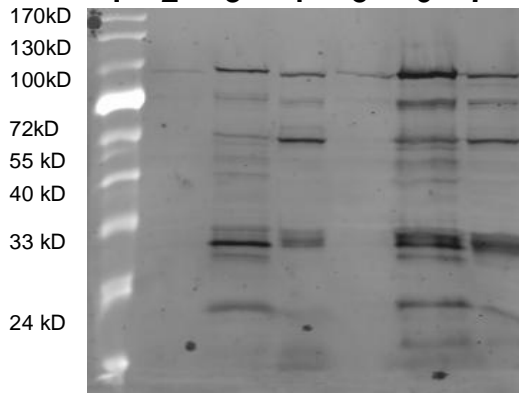


**Figure A-4. SDS-PAGE and Western Blot for STAR pLySs pET15b Dbf4-FL.** The molecular weight marker is labeled, representing Kilodaltons as units. The lanes are numbered corresponding to the samples listed below. The construct was tested in the STAR pLySs host under conditions of 25°C for 5 hours and 37°C for 3 hours, 200rpm shake. Soluble fractions were prepared as described in Materials and Methods section. A. SDS-PAGE (12%) corresponding to the protein solubility assay. Samples were prepared as described in the Materials and Methods section by mixing them with 2X SDS-loading dye. A 15 ul volume of each prepared sample was loaded in the SDS-PAGE lanes. B. Ponceau S (0.1%) stain of the nitrocellulose membrane indicates how equal the lanes were loaded and corresponded to the western blot C. Western blot. A nitrocellulose membrane was probed with anti-Dbf4 antibody (Santa Cruz) 1:100 concentration. The secondary antibody used was Alexa Fluor 488 (donkey anti-goat) (Invitrogen) at a concentration of 1:1500.

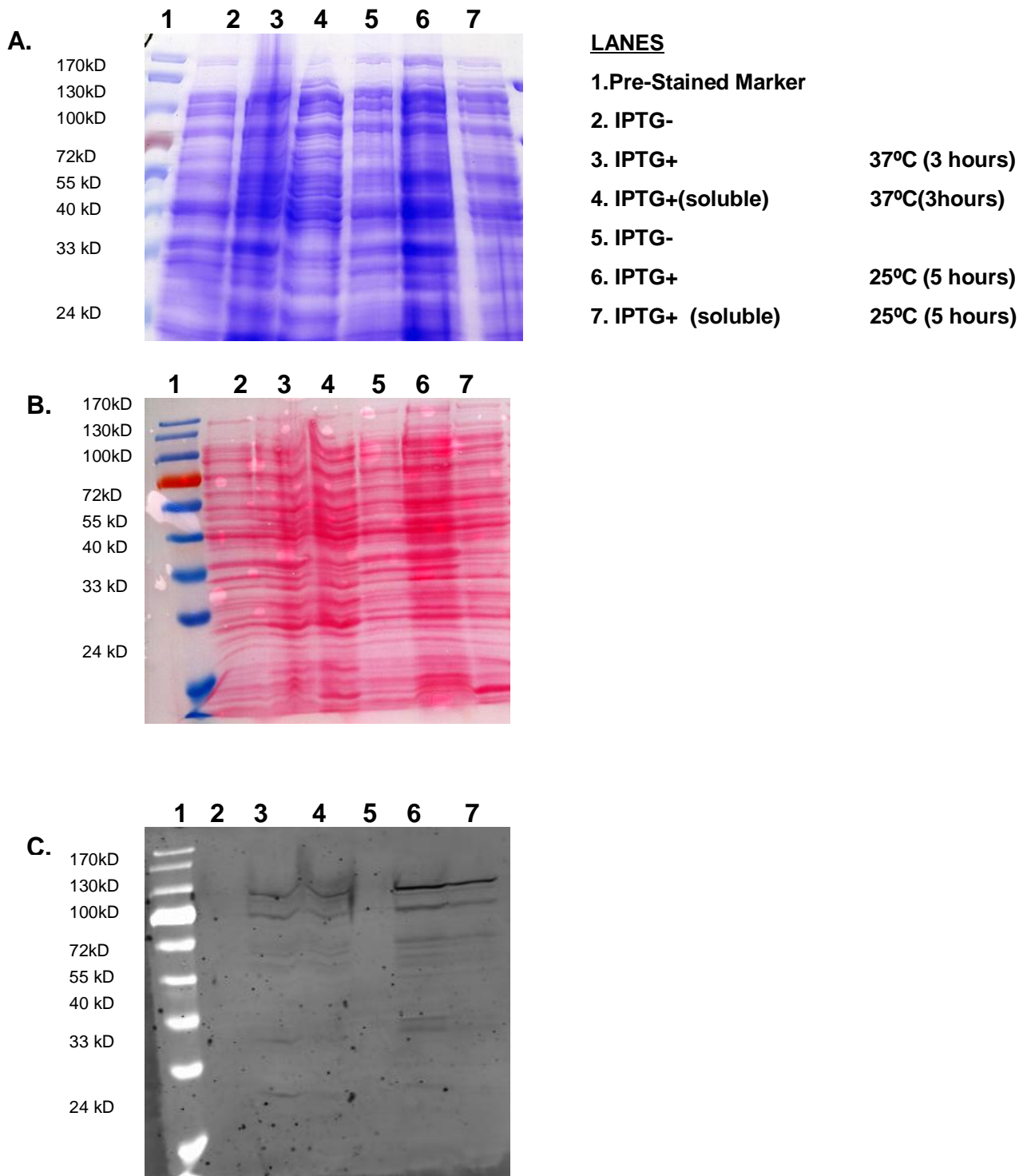


**Figure A-5. SDS-PAGE and Western Blot for STAR pRARE pET 15bDbf4-FL.** The molecular weight marker is labeled, representing Kilodaltons as units. The lanes are numbered corresponding to the samples listed below. The construct was tested in the STAR pRARE host under conditions of 25°C for 5 hours and 37°C for 3 hours, 200rpm shake. Soluble fractions were prepared as described in Materials and Methods section. A. SDS-PAGE (12%) corresponding to the protein solubility assay. Samples were prepared as described in the Materials and Methods section by mixing them with 2X SDS-loading dye. A 15 ul volume of each prepared sample was loaded in the SDS-PAGE lanes. B. Ponceau S (0.1%) stain of the nitrocellulose membrane indicates how equal the lanes were loaded and corresponded to the western blot C. Western blot. A nitrocellulose membrane was probed with anti-Dbf4 antibody (Santa Cruz) 1:100 concentration. The secondary antibody used was Alexa Fluor 488 (donkey anti-goat) (Invitrogen) at a concentration of 1:1500.

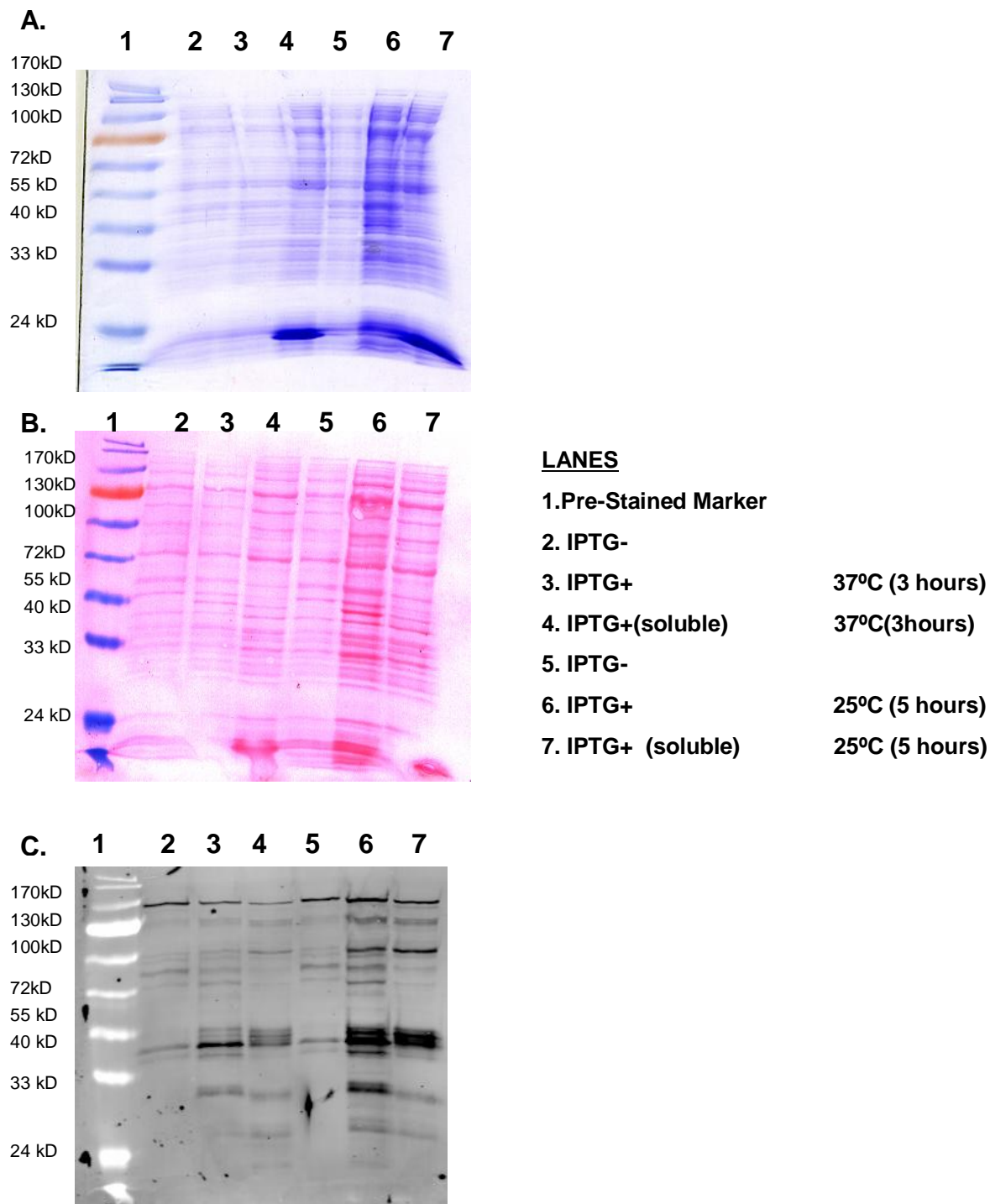
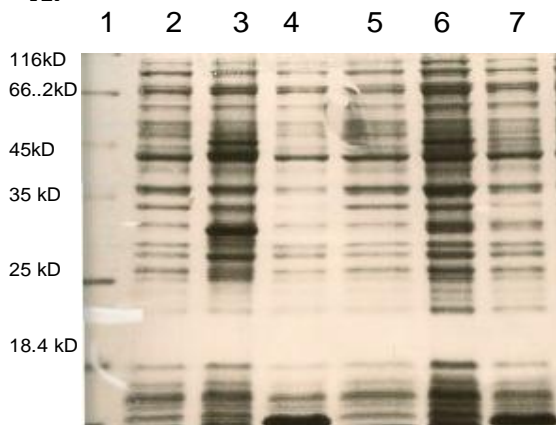


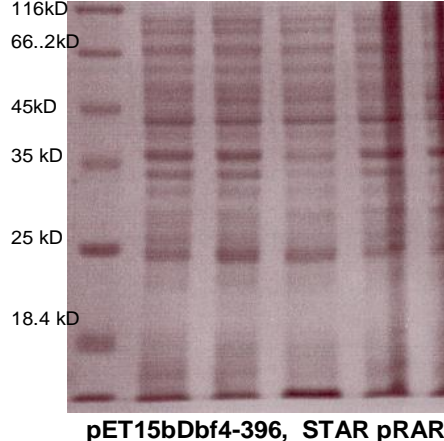
**Figure A-6. SDS PAGE for A. STAR, pET15b Dbf4-396 15bDbf4-FL. B. STAR pRARE, pET15b Dbf4-396. C. STAR pLySs, pET15b Dbf4-396.** For each of the cell hosts, the molecular weight marker is labeled with the units Kilodaltons. The lanes are numbered corresponding to the sample listed below the SDS-PAGE. The construct was tested under conditions of 25°C for 5 hours and 37°C for 3 hours induction at 200rpm shake. Soluble fractions were prepared as described in Materials and Methods. Loaded samples were prepared as described in the Materials and Methods. A 15ul volume of each sample was loaded in the lanes.

**A.**



pET15bDbf4-396, STAR

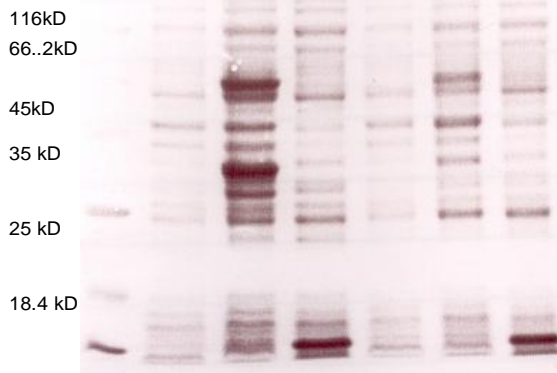
1 2 3 4 5 6 7



pET15bDbf4-396, STAR pRARE

1 2 3 4 5 6 7

**C.**

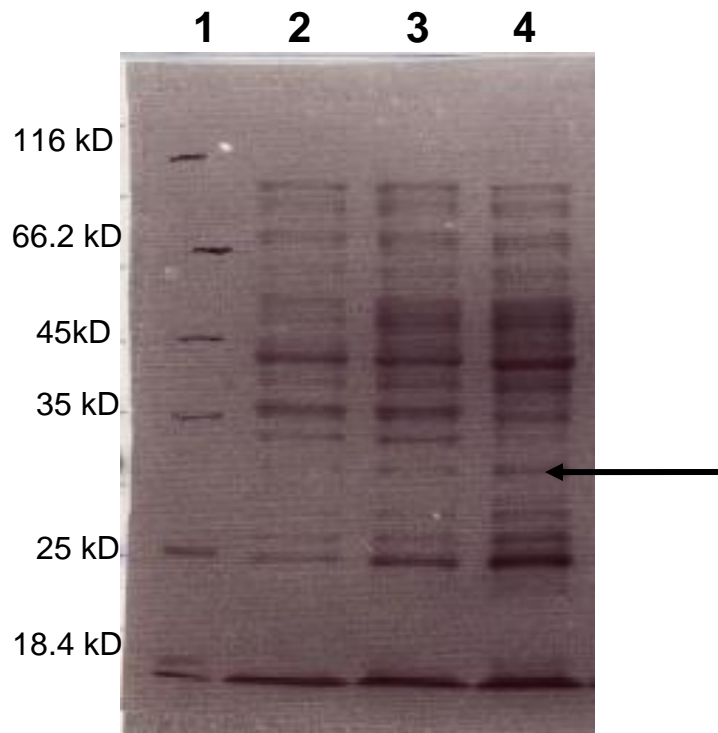


pET15bDbf4-396, STAR pLySs

LANES

- 1. Pre-Stained Marker
- 2. IPTG-
- 3. IPTG+ 37°C (3 hours)
- 4. IPTG+ (soluble) 37°C(3hours)
- 5. IPTG-
- 6. IPTG+ 25°C (5 hours)
- 7. IPTG+ (soluble) 25°C (5 hours)

**Figure A-7. SDS PAGE for BL21 (DE3) pET15b Dbf4-248.** The molecular weight marker is labeled with the units Kilodaltons. The lanes are numbered corresponding to the sample listed below the SDS-PAGE. The construct was tested under conditions of 30°C for 5 hours induction at 200rpm shake. Soluble fractions were prepared as described in Materials and Methods. Loaded samples were prepared as described in the Materials and Methods. A 15ul volume of each sample was loaded in the lanes. Arrows point to the induced proteins: Dbf4-248.



# **LANES**

- |                              |                   |                       |
|------------------------------|-------------------|-----------------------|
| <b>1. Pre-Stained Marker</b> |                   |                       |
| <b>2. IPTG-</b>              | <b>BL21 pRARE</b> |                       |
| <b>3. IPTG+</b>              | <b>BL21 pRARE</b> | <b>30°C (5 hours)</b> |
| <b>4. IPTG+ (soluble)</b>    | <b>BL21 pRARE</b> | <b>30°C (5 hours)</b> |

## **REFERENCES**

## REFERENCES

- Abola, E., Kuhn, P., Earnest, T. and Stevens, R.C. (2000). Automation of X-ray crystallography. *Nature Struc. Biol.* **7**: 973-97.
- Antoni, L., Sodha, N., Collins, I. and Garrett, M.D. (2007). CHK2 kinase: cancer susceptibility and cancer therapy- two sides of the same coin? *Nat. Rev. Cancer* **7**:925-936.
- Alexopoulos, C.J., and Bold, H.C. (1967). *Algae and fungi*. The Macmillan Company, New York, NY.
- Allers, T. and Ngo, H.-P. (2003) Genetic analysis of homologous recombination in Archaea: *Haloferax volcanii* as a model organism. *Biochem. Soc.Trans.* **31**:706-709.
- APHA. (1995). *Standard methods for the examination of water and wastewater*, 19<sup>th</sup> edition, American Public health Association, Washington, D.C.
- Asherie, N. (2004). Protein crystallization and phase diagrams. *Methods* **34**:266-272.
- Ausubel, F., Brent, R., Kingston, R.E., Moore, D.D., Seidman, J.G., Smith, J.A., and Struhl, K. (1995). *Short protocols in molecular biology*, 3<sup>rd</sup> edition. Wiley Press, New York, NY.
- Bahler, J. (2005). Cell-cycle control of gene expression in budding and fission yeast. *Annu.Rev.Genet.* **39**:69-94.
- Ballatori, N. and Villalobos, A.R. (2002). Defining the molecular and cellular basis of toxicity using comparative models. *Tox. Appl. Pharmacol.* **183**:207-220.
- Barnett, J.A. (2007). A history of research on yeasts 10: foundations of yeast genetics. *Yeast* **24**:799-845.
- Bartek, J., Lukas, C. and Lukas, J. (2004). Checking on DNA damage in S-phase. *Nature Reviews, Mol.Cell. Biol.* **5**:792-804.
- Bartek, J. and Lukas, J. (2007). DNA damage checkpoints: from initiation to recovery or adaptation. *Curr.Opin.Cell Biol.* **19**:238-245.
- Bell, S.P and Dutta, A. (2002). DNA replication in eukaryotic cells. *Annu.Rev.Biochem.* **71**:333-374.
- Bi, E. (2001). Cytokinesis in budding yeast: the relationship between actomyosin ring function and septum formation. *Cell. Struct. Funct.* **26**:529-537.

- Bjornsti, M. (2002). Cancer therapeutics in yeast. *Cancer Cell* **2**: 267-273.
- Böhm, S., Frishman, D., and Mewes, H.W. (1997). Variations of the C2H2 zinc finger motif in the yeast genome and classification of yeast zinc finger proteins. *Nucleic Acids Res.* **25**:2464-2469.
- Bonte, D., Lindvall, C., Liu, H., Dykema, K., Furge, K. and Weinreich, M. (2008). Cdc7-Dbf4 kinase overexpression in multiple cancers and tumor cell lines is correlated with p53 inactivation. *Neoplasia* **10**:920-931.
- Bousset, K., and Diffley, J.F.X. (1998). The Cdc7 protein kinase is required for origin firing during S-phase, *Genes Dev.* **12**:480-490.
- Branzei, D. and Foiani, M. (2006). The Rad53 signal transduction pathway: Replication fork stabilization, DNA repair, and adaptation. *Exp. Cell Res.* **312**:2654-2659.
- Brayer, K.J., Kulshreshtha, S. and Segal, D.J. (2008). The protein-binding potential of C2H2 zinc finger domains. *Cell Biochem. Biophys.* **51**:9-19
- Brott, B.K. and Sokol, S.Y. (2005). A vertebrate homologue of cell cycle regulator Dbf4 is an inhibitor of Wnt Signalling required for heart development. *Dev. Cell* **8**:703-715.
- Brown, G. W. and Kelly, T.J. (1999). Cell cycle regulation of Dfp1, an activator of the Hsk1 protein kinase. *Proc. Natl. Acad. Sci. U. S. A.* **96**:8443-8448.
- Byeon, I.L., Yongkiettrakul, S., and Tsai, M. (2001) Solution structure of yeast Rad53 FHA2 complexed with a phosphothreonine peptide pTXXL: comparison with the structures of FHA2-pTXXD complexes. *J. Mol.Biol.* **314**:577-588.
- Cann, K.L. and Hicks, G.G. (2007). Regulation of the cellular DNA double-strand break response. *Biochem.Cell Biol.* **85**:663-674.
- Carlile, M.J., Watkinson, S.C. and Gooday, G.W. (2001). *The Fungi*. Academic Press, San Diego, CA.
- Chaudhuri, S.P., Sundaram, G., Bhattacharya, A., Ray, P., Ray, A., Chatterjee, I.B. and Chattopadhyay, D. (2005). Activation of S-phase checkpoint by cigarette smoke extract in *Schizosaccharomyces pombe*. *Yeast* **22**:1223-1238.
- Cheng, L., Collyer, T., and Hardy, C.F. (1999). Cell cycle regulation of DNA replication initiation factor Dbf4p, *Mol. Cell. Biol.* **19**:4270-4278.
- Codon, A.C., Gasent-Ramirez, J.M. and Benitez, T. (1995). Factors which affect the frequency of sporulation and tetrad formation in *Saccharomyces cerevisiae* baker's yeasts. *Appl. and Environ. Micro.* **61**:630-638.

Considine, P.E. and Considine, G.D., eds. (1983). Van Nostrand's Scientific Encyclopedia, 6<sup>th</sup> Edition, Van Nostrand Company, Inc. New York, NY.

Corbett, M., Xiong, Y., Boyne, J.R., Wright, D.J., Munro, E., Price, C. (2006). IQGAP and mitotic exit network (MEN) proteins are required for cytokinesis and re-polarization of the actin cytoskeleton in the budding yeast *Saccharomyces cerevisiae*. *Eur. J. Cell Biol.* **85**:1201-1215.

Costanzo, V., Shechter, D., Lupardus, P.J., Cimprich, K.A., Gottesman, M., and Gautier, J. (2003). An ATR- and Cdc7-dependent DNA damage checkpoint that inhibits initiation of DNA replication. *Mol. Cell* **11**:203-213.

Cvetic, C. and Walter, J.C. (2005). Eukaryotic origins of DNA replication: could you please be more specific? *Seminars in Cell and Dev. Biol.* **16**:343-353.

DePamphilis, M.L. (2005). Cell cycle dependent regulation of the origin recognition complex. *Cell Cycle* **4**:70-79.

Deshpande, A. M. and Newlon, C.S. (1996). DNA replication fork pause sites dependent on transcription1. *Science* **272**:1030-1033.

Dhillon, N. and Hoekstra, M.F. (1994). Characterization of two protein kinases from *Schizosaccharomyces pombe* involved in the regulation of DNA repair. *EMBO J.* **13**:2777-2788.

Dohrmann, P.R., Oshiro, G., Tecklenburg, M., and Sclafani, R.A. (1999). RAD53 regulates DBF4 independently of checkpoint function in *Saccharomyces cerevisiae*. *Genetics* **151**:965-977.

Dohrmann, P.R. and Sclafani, R.A. (2006). Novel role for checkpoint Rad53 protein kinase in the initiation of chromosomal DNA replication in *Saccharomyces cerevisiae*. *Genetics* **174**:87-99.

Dolinski, K. and Botstein, D. (2005). Changing perspectives in yeast research nearly a decade after the genome sequence. *Genome Res.* **15**:1611-1619.

Donaldson, A. D., Fangman, W.L., and Brewer, B.J. (1998). Cdc7 is required throughout the yeast S-phase to activate replication origins. *Genes Dev.* **12**:491-501.

Dowell, S.J., Romanowski, P, and Diffley, J.F. (1994). Interaction of Dbf4, the Cdc7 protein kinase regulatory subunit, with yeast replication origins *in vivo*. *Science* **265**:1243-1246.

Dumas, L.B., Lussky, J.P., McFarland, E.J., and Shampay, J.(1982). New temperature-sensitive mutants of *Saccharomyces cerevisiae* affecting DNA replication. *Mol. Gen. Genet.* **187**:42-46.

- Duncker, B.P., Shimada, K., Tsai-Pflugfelder, M., Pasero, P., and Gasser, S. (2002). An N-terminal domain of Dbf4p mediates interaction with both origin recognition complex (ORC) and Rad53p and can regulate late origin firing. *Proc. Natl. Acad. Sci. USA.* **99**:16087-16092.
- Duncker, B.P. and Brown, G.W. (2003). Cdc 7 kinases (DDKs) and checkpoint responses: lessons from two yeasts. *Mutat. Res.* **532**:21-27.
- Durocher, D. and Jackson, S.P. (2002). The FHA domain. *FEBS Lett.* **513**:58-66.
- Elledge, S.J. (1996). Cell cycle checkpoints: preventing an identity crisis. *Science.* **247**:1664-16672.
- Ferreira, M.F., Santocanale, C., Drury, L.S. and Diffley, J.F. (2000) Dbf4p, an essential S phase-promoting factor, is targeted for degradation by the anaphase-promoting complex. *Mol. Cell. Biol.*, **20**:242-248
- Fiorani, S., Mimun, G., Caleca, L., Piccini, D., Pellicioli, A. (2008). Characterization of the activation domain of the Rad53 checkpoint kinase. *Cell Cycle* **4**:493-499.
- Foiani, M., Pellicioli, A., Lopes, M., Lucca, C., Ferrari, M., Liberi, G., Muzi Falconi, M., and Plevani 1, P. (2000). DNA damage checkpoints and DNA replication controls in *Saccharomyces cerevisiae*. *Mutat. Res.* **451**:187-96.
- Forsburg, S.L. and Nurse, P. (1991). Cell cycle regulation in the yeasts *Saccharomyces cerevisiae* and *Schizosaccharomyces pombe*. *Annu. Rev. Cell Biol.* **7**:227-56
- Francis, L.I., Randell, J.C., Takara, T.J., Uchima, L., and Bell, S.P. (2009). Incorporation into the prereplicative complex activates the Mcm2-7 helicase for Cdc7-Dbf4 phosphorylation. *Genes Dev.* **23**:643-54.
- Friedman,K.L.,Driller, J.D.,Ferguson,B.M., Nyland,S.V.,Brewer,B.J., and Fangman,W.L. (1996). Multiple determinants controlling activation of yeast replication origins late in S-phase. *Genes Dev.* **10**:1595-1607.
- Fung, A.D., Ou, S., Bueler, S., and Brown, G.W. (2002). A Conserved domain of *Schizosaccharomyces pombe* dfp1+ is uniquely required for chromosome stability following alkylation damage during S-phase. *Mol. Cell. Biol.* **22**:4477-4490.
- Gabrielse, C., Miller, C.T., McConnell, H., DeWard, A., Fox, C.A. and Weinrich, M. (2006). A Dbf4p BRCA1 C-Terminal-like domain required for the response to replication fork arrest in budding yeast, *Genetics* **173**:541-555.
- Game, J.C. (2002). New genome-wide methods to bring more power to yeast as a model organism. *TRENDS in Pharmacol. Sci.* **23**:445-447.

Garg, P. and Burgers, P.M. (2005). DNA polymerases that propagate the eukaryotic DNA replication fork. *Crit.Rev. Biochem. Mol. Biol.* **40**:115-128.

Gari, E., Piedrafita, L., Aldea, M. and Herrero, H. (1997). A set of vectors with a tetracycline-regulatable promoter system for modulated gene expression in *Saccharomyces cerevisiae*. *Yeast* **13**:837-848.

Grallert, B. and Boye, E. (2008). The multiple facets of the intra-S checkpoint. *Cell Cycle* **7**:2315-2320.

Guthrie, C. and Fink, G.R. (2002). *Methods in enzymology volume 350, guide to yeast genetics and molecular and cell biology*. Academic Press. Inc. San Diego, CA.

Hakem, R. (2008). DNA-damage repair; the good, the bad, and the ugly. *EMBO J.* **27**:589-605.

Hammet, A., Pike, B.L., McNees, C.J., Conlan, L.A., Tenis, N., Heierhorst, J.(2003). FHA domains as phospho-threonine binding modules in cell signaling. *IUBMB Life.* **55**:23-27.

Hardy, C. F. (1996). Characterization of an essential Orc2p-associated factor that plays a role in DNA replication. *Mol. Cell Biol.* **16**:1832-1841.

Harris, S.D., Turner, G., Meyer, V., Espeso, E.A., Specht, T., Takeshita, N., and Helmstedt, K. (2009). Morphology and development in *Aspergillus nidulans*: A complex puzzle. *Fungal Gen. Biol.* **46**:S82-S92

Harrison , J.C. and Haber, J.E.(2006). Surviving the breakup: the DNA damage checkpoint. *Annu. Rev. Genet.* **40**:209-235.

Hartwell, L., Culotti, L.H. and Reid, B. (1970). Genetics of control of the cell-division cycle in yeast, I. detection of mutants. *Proc. Nat. Acad. Sci.* **66**:352-359.

Herskowitz, I. (1988). *Life cycle of the budding yeast Saccharomyces cerevisiae*. *Microbiol. Rev.* **52**: 536-553.

Hoang, M.L., Leon, R.P., Pessoa-Brandao, L., Hunt, S., Raghuraman, M.K., Fangman, W.L., Brewer, B.J., Sclafani, R.A. (2007). Structural Changes in Mcm5 Protein Bypass Cdc7-Dbf4 Function and Reduce Replication Origin Efficiency in *Saccharomyces cerevisiae*. *Mol. Cell. Biol.* **27**: 7594-7602.

Hoffman, R.C., Horvath, S.J., and Klevit, R.E. (1993). Structures of DNA-binding mutant zinc finger domains: Implications for DNA-binding. *Protein Sci.* **2**:951-965

Hohmann, S. (2005). The yeast systems biology network: mating communities. *Curr.Opin.Biochem.* **16**:356-360.

- Homesley, L., Lei, M. and Kawasaki, Y., Sawyer, S., Christensen, T., and Tye, B.K. (2000). Mcm10 and the Mcm2-7 complex interact to initiate DNA synthesis and to release replication factors from origins. *Genes Dev.* **14**:913-926.
- Honey, S. and Futcher, B. (2007) Roles of CDK phosphorylation sites of yeast Cdc6 in chromatin binding and rereplication. *Mol. Biol. Cell* **18**:1324-1336.
- Ishimi, Y. (1997). A DNA helicase activity is associated with an MCM4, -6, and -7 protein complex. *J. Biol. Chem.* **272**:24508-24513.
- Ismail, I.H, Nyström S., Nygren, J. and Hammarsten, O. (2005). Activation of ataxia telangiectasia mutated by DNA strand break-inducing agents correlates closely with the number of DNA double strand breaks. *J.Biol. Chem.* **280**:4649-4655.
- Jackson, A.L., Pahl, P.M., Harrison, K., Rosamond, J., and Sclafani, R.A. (1993). Cell cycle regulation of the yeast Cdc7 protein kinase by association with the Dbf4 protein. *Mol. Cell. Biol.* **13**:2899-2908.
- James, S.W., Bullock, K.A., Gygax, S.E., Kraynack, B.A., Matura, R.A., MacLeod, J.A., McNeal, K.K., Prasauckas, K.A., Scaheri, P.C., Shenefield, H.L., Tobin, H.M., and Wade, S.D. (1999). *nimO*, an *Aspergillus* gene related to budding yeast Dbf4, is required for DNA synthesis and mitotic checkpoint control. *Cell Sci.* **112**:1313-1324.
- Jares, P., Donaldson, A., and Blow, J. (2000). The Cdc7/Dbf4 protein kinase: target of the S-phase checkpoint? *EMBO Reports* **1**:319-322.
- Jares, P., Luciani, M.G., and Blow, J.J. (2004). A *Xenopus* Dbf4 homolog is required for Cdc7 chromatin binding and DNA replication. *BMC. Mol. Biol.* **5**:5.
- John, L., Sharma, G., Chaudhuri, S.P., and Pillai, B. (2005). Cigarette smoke extract induces changes in growth and gene expression of *Saccharomyces cerevisiae*. *Biochem. Biophys. Res. Commun.* **338**:1578-1586.
- Kelly, T.J. and Brown, G.W. (2000). Regulation of chromosome replication. *Annu. Rev. Biochem.* **69**:829-880.
- Kihara, M., Nakai, W., Asano, S., Suzuki, A., Kitada, K., Kawasaki, Y., Johnston, L.H., and Sugino, A. (2000). Characterization of the yeast Cdc7p/Dbf4p complex purified from insect cells. Its protein kinase activity is regulated by Rad53p. *J. Biol. Chem.* **275**:35051-35062.
- Kim, J.M., Yamada, M., and Masai, H. (2003). Functions of mammalian Cdc7 kinase in initiation/monitoring of DNA replication and development. *Mutat. Res.* **532**:29-40.

- Koc, A., and Merril, G.F., (2007). Checkpoint deficient rad53-11 yeast cannot accumulate dNTPs in response to DNA damage. *Biochem. Biophys. Res. Commun.* **353**:527-530.
- Kockova-Kratochvilova, A. (1990). *Yeasts and yeast-like organisms*. VCH Publishers, New York, NY.
- Kolodner, R.D., Putnam, C.D., and Myung, K. (2002). Maintenance of genome stability in *Saccharomyces cerevisiae*. *Science* **297**:552-557.
- Labib, K., Tercero, J.A., and Diffley, J.F. (2000). Uninterrupted MCM2-7 function required for DNA replication fork progression. *Science* **288**:1643-1647.
- Laity, J.H., Lee, B.M. and Wright, P.E. (2001). Zinc finger proteins: new insights into structural and functional diversity. *Curr. Opin. Struct. Biol.* **11**:39-46.
- Landis, G. and J. Tower, J. (1999). The Drosophila chiffon gene is required for chorion gene amplification, and is related to the yeast Dbf4 regulator of DNA replication and cell cycle. *Development* **126**:4281-4293.
- Landry, C.R., Townsend, J.P., Hartl, D.L. and Cavalieri, D. (2006). Ecological and evolutionary genomics of *Saccharomyces cerevisiae*. *Mol. Ecology* **15**:575-591.
- Lebedeva, L.I., Fedorova, S.A, Trunova, S.A. and Omel'ianchuk, L.V. (2004). Mitosis: regulation and organization of cell division. *Genetika*. **40**:1589-1608.
- Lee, J. K. and Hurwitz, J. (2001). Processive DNA helicase activity of the minichromosome maintenance proteins 4, 6, and 7 complex requires forked DNA structures. *Proc. Natl. Acad. Sci. U. S. A* **98**:54-59.
- Lee, H., Yuan, C., Hammet, A., Mahajan, A., Chen, E.S., Wu, M.R., Su, M.I., Heierhorst, J., and Tsai, M.D. (2008). Diphosphothreonine-specific interaction between an SQ/TQ cluster and an FHA domain in the Rad53-Dun1 kinase cascade. *Mol. Cell* **30**:767-778.
- Lei, M., Kawasaki, Y., Young, M.R., Kihara, M., Sugino, A., and Tye, B.K. (1997). Mcm2 is a target of regulation by Cdc7-Dbf4 during the initiation of DNA synthesis. *Genes Dev.* **11**:3365-3374.
- Li, A. and Harris, D.A. (2005). Mammalian prion protein suppresses bax-induced cell death in yeast. *J. Biol. Chem.* **290**:17430-17434.
- Liao, H., Yuan, C., Su, M.I., Yongkiettrakul, S., Qin,, D., Li, H., Byeon, I.J., Pei, D., and Tsai, M.D. (2000). Structure of the FHA1 domain of yeast Rad53 and identification of binding sites for both FHA1 and its target protein Rad9. *J. Mol. Biol.* **304**:941-951.

Lillard-Wetherell, K., Combs, K.A., and Groden, J. (2005). BLM helicase complements disrupted type II telomere lengthening in telomerase-negative *sgs1* yeast. *Cancer Res.* **65**:5520-5522.

Lindegren, C.C. (1949). *The yeast cell: its genetics and cytology*. Education Publishers, St.Louis, MO.

Lindegren, C.C. and Lindgren, G. (1951). Tetraploid *Saccharomyces*. *J. Gen. Microbiol.* **5**:885-893.

Lindegren, C.C., Lindegren G., Shult, E.E. and Deesborough, S. (1959). Chromosome maps of *Saccharomyces*. *Nature* **183**:800-802.

Lindon, C. (2008). Control of mitotic exit and cytokinesis by the APC/C. *Biochem. Soc. Trans.* **36**:405-410.

Liu, J.S., Kuo, S.R., and Melendy, T. (2003). Comparison of checkpoint responses triggered by DNA polymerase inhibition versus DNA damaging agents. *Mutat. Res.* **532**:215-226.

Longtine, M.S., McKenzie, A. 3rd, Demarini, D.J., Shah, N.G., Wach, A., Brachet, A., and Philippsen, P., and Pringle, J.R. (1998). Additional modules for versatile and economical PCR-based gene deletion and modification in *Saccharomyces cerevisiae*. *Yeast* **10**:953-961.

Longhese, M.P., Clerici, M., and Lucchini, G. (2003). The S-phase checkpoint and its regulation in *Saccharomyces cerevisiae*. *Mutat.Res.* **532**:41-58.

Longhese, M.P., Foiani, M.M, Luccini, G., and Plevani, P. (1998). DNA damage checkpoint in budding yeast. *EMBO J.* **17**:5525-5528.

Lukas, J., and Bartek, J. (2004). Cell division: the heart of the cycle. *Nature* **432**:564-567.

Mahajan, A., Yuan, C., Lee, H., Chen, E.S., Wu, P.Y., Tsai, M.D. (2008). Structure and function of the phosphothreonine-specific FHA domain. *Sci. Signal.* **1**:re12.

Marchetti, M.A., Weinberg, M., Murakami, Y., Burhans, C. and Huberman, J.A. (2006). Production of reactive oxygen species in response to replication stress and inappropriate mitosis in fission yeast. *J.Cell Sci.* **119**:124-131.

Masai, H. and Arai, K. (2000). Dbf4 motifs: conserved motifs in activation subunits for Cdc7 kinases for S-phase. *Biophys. Res. Commun.* **275**:228-232.

Moffatt, B.A. and Studier,F.W. (1986). Use of bacteriophage T-7 RNA polymerase to direct selective high-level expression of cloned genes. *J. Mol.Biol.* **189**:113-130.

Montagnoli, A., Bosotti, R., Villa, F., Rialland, M., Brotherton, D., Mercurio, C., Berthelsen, J. and Santocanale, C. (2002). Drf, a novel regulatory subunit for human Cdc7 kinase. *EMBO J.* **21**:3171-3181.

Moyer, S.E., Lewis, P.W., and Botchan, M.R. (2006). Isolation of the Cdc45/Mcm2-7/GINS (CMG) complex, a candidate for the eukaryotic DNA replication fork helicase. *Proc. Natl. Acad. Sci. U.S.A.* **103**: 10236-10241.

Nakamura, T., Kishida, M. and Shimoda, C. (2000). The *Schizosaccharomyces pombe* spo6+ gene encoding a nuclear protein with sequence similarity to budding yeast Dbf4 is required for meiotic second division and sporulation. *Genes Cells.* **5** :463-479.

Nambiar, S., Mirmohammadsadegh, A., Hassan, M., Hegemann, J.H. and Hengge, U.R. (2007). Transcriptional regulation of ASK/Dbf4 in cutaneous melanoma is dependent on E2F1. *Exp. Dermatol.* **17**:986-991.

Nguyen, V.Q., Co, C., Irie, K., and Li, J.J. (2000). Clb/Cdc28 kinase promotes nuclear export of the replication initiation proteins Mcm2-7. *Curr. Biol.* **10**:195-205.

Nougarede, R., Della, S.F., Zarzov, P., and Schwob, E. (2000). Hierarchy of S-phase-promoting factors: yeast Dbf4-Cdc7 kinase requires prior S-phase cyclin-dependent kinase activation. *Mol. Cell. Biol.* **20**:3795-3806.

Novak B., Sible J.C., and Tyson, J.J . (2002). Checkpoints in the cell cycle. In: *Encyclopedia of life sciences*. Macmillan Publishers Ltd., Nature Publishing Group.

Ogi, H, Wang,C.Z., Nakai, W., Kawasaki, Y., and Masumoto, H.(2008). The role of the *Saccharomyces cerevisiae* Cdc7-Dbf4 complex in the replication checkpoint. *Gene.* **414**:32-40.

Ogino, K., Takeda, T., Matsui, E., Iiyama, H., Taniyama, C., Arai, K., and Masai, H. (2001). Bipartite binding of a kinase activator activates Cdc7-related kinase essential for S phase. *J. Biol. Chem.* **276**:31376-1387.

Oshiro, G., Owens, J.C., Shellman, Y., Sclafani, R.A., and Li, J.J. (1999). Cell cycle control of Cdc7p kinase activity through regulation of Dbf4p stability. *Mol. Cell. Biol.* **19**:4888-4896.

Pacek, M., Tutter, A., Kubota, Y., Takisawa, H., Walter, J. (2006). Localization of MCM2-7, Cdc45, and GINS to the site of DNA unwinding during eukaryotic DNA replication. *Mol. Cell* **21**:581-587.

- Pasero, P., Duncker, B.P., Schwob, E., and Gasser, S.M.(1999). A role for the Cdc7 kinase regulatory subunit Dbf4p in the formation of initiation-competent origins of replication. *Genes Dev.* **13**:2159-2176.
- Pasero, P., Shimada, K., and Duncker,B.P. (2003). Multiple roles of replication forks in S- phase checkpoints. *Cell Cycle* **2**:568-572.
- Pessoa-Brandao, L. and Sclafani, R.A. (2004). CDC7/DBF4 functions in the translesion synthesis branch of the RAD6 epistasis group in *Saccharomyces cerevisiae*. *Genetics* **167**:1597-1610.
- Pelczar, Jr., M.J., and Chan, E.C.S. (1981). *Elements of microbiology*. McGraw-Hill Inc., New York, NY.
- Pesin, J.A. and Orr-Weaver, T.L. (2008). Regulation of APC/C activators in mitosis and meiosis. *Annu. Rev. Cell. Dev. Biol.* **24**:475-499.
- Pike, B.L., Yongkiettrakul,S., Tsai, M., and Heierhorst, J. (2003). Diverse but overlapping functions of the two forkhead-associated (FHA) domains in Rad53 checkpoint kinase activation. *J. Biol. Chem.* **28**:30421-30424.
- Pusey, M.L., Liu, Z., Tempel, W., Praissman, J., Lin, D., Want, B., Gavira J.A. and Ng, J.D. (2005). Life in the fast lane for protein crystallization and X-ray crystallography. *Prog.Biophys.Mol.Bio.* **88**:359-386.
- Raghuraman, M.K., Winzeler, E.A., Collingwood, D., Hunt, L., Wodieka,A.,Conway,D.J., Lockhart,D.J.,Davis,R.W., Brewer,B.J., and Fangman,W.L. (2001).Replication dynamics of the yeast genome. *Science* **194**:115-121.
- Ratledge, C. (1991). Yeast physiology – A microsynopsis. *Bioproc. Biosyst. Engin.* **6**: 1615-7591.
- Raveendranathan, M., Chattopadhyay, S., Bolon, Y., Haworth, J, Clark, D.J., and Beliensky A. (2006). Genome-wide replication profiles of S-phase checkpoint mutants reveal fragile sites in yeasts. *EMBO J.* **25**:3627-3639.
- Rosenberg, A.H., Lade, B.N., Chui, D., Lin, S., Dunn, J.J., and Studier, F.W. (1987) Vectors for selective expression of cloned DNAs by T7 RNA polymerase. *Gene* **56**:125–135.
- Sancar, A., Lindsey-Boltz, L.A., Unsal-Kacmaz, K., and Linn, S. (2004). Molecular mechanisms of mammalian DNA repair and the DNA damage checkpoints. *Annu. Rev. Biochem.* **73**:39-85.
- Santocanale, C. and Diffley , J.F. (1998). A Mec1- and Rad53-dependent checkpoint controls late-firing origins of DNA replication. *Nature* **395**:615-618.

Sato, N., Sato, M., Nakayama, M., Saitoh, R., Arai, K. and Masai, H. (2003) Cell cycle regulation of chromatin binding and nuclear localization of human Cdc7-ASK kinase complex. *Genes to Cells* **8**:451-463.

Sclafani, R.A. (2000). Cdc7-Dbf4 becomes famous in the cell cycle. *J. Cell Sci.* **113**:2111-2117.

Sclafani, R.A. and Holzen, T.M. (2007). Cell cycle regulation of DNA replication. *Annu. Rev. Genet.* **41**:237-280.

Schlect, U., Erg, I., Demougin, P., Robine, N., Borde, V., van Nimwegen, E., Nicolas, A. and Primig, M. (2008). Genome-wide expression profiling, in vivo DNA binding analysis, and probabilistic motif prediction reveal novel Abf1 target genes during fermentation, respiration and sporulation in yeast. *Mol. Biol. Cell* **19**:2193-2207.

Segurado, M. and Diffley J.F. (2008). Separate roles for the DNA damage checkpoint protein kinases in stabilizing DNA replication forks. *Genes Dev.* **22**:1816-1827.

Shellman, Y. G., Schauer, I. E., Oshiro, G., Dohrmann, P., and Sclafani, R.A. (1998). Oligomers of the Cdc7/Dbf4 protein kinase exist in the yeast cell. *Mol. Gen. Genet.* **259**:429-436.

Sheu, Y.J. and Stillman, B. (2006). Cdc7-Dbf4 phosphorylates MCM proteins via a docking site-mediated mechanism to promote S-phase progression. *Mol. Cell* **24**:101-113

Shi, Y. and Berg, J.M. (1996). DNA unwinding induced by zinc finger protein binding. *Biochemistry* **35**:3845-3848.

Shirahige, K., Hori, Y., Shiraishi, K., Yamashita, M., Takahashi, K., Obuse, C., Tsurimoto, T., and Yoshikawa, H. (1998). Regulation of DNA-replication origins during cell-cycle progression. *Nature* **395**:618-621.

Sidorova, J.M. and Breeden, L.L. (2003). Rad53 checkpoint kinase phosphorylation site preference identified in the Swi6 protein of *Saccharomyces cerevisiae*. *Mol. Cell. Biol.* **23**:3405-3416.

Smolka, M.B., Albuquerque, C.P., Chen, S.H. and Zhou, H. (2007). Proteome-wide identification of *in vivo* targets of DNA damage checkpoint kinases. *Proc. Natl. Acad. Sci. U S A* **104**:10364-10369.

Smolka, M.B., Chen, S.H., Maddox, P.S., Enserink, J.M., Albuquerque, C.P., Wei, X.X., Desai, A., Kolodner, R.D., and Zhou, H. (2006). An FHA domain-mediated protein interaction network of Rad53 reveals its role in polarized cell growth. *J. Cell Biol.* **175**:743-745.

Stanier, R., Doudoroff, M. and Adelberg, E.A. (1965). *Microbial world*. Prentice-Hall, Inc. Englewood Cliffs, NJ.

Stevens, R.C. (2000). High-throughput protein crystallization. *Curr. Opin. Struc. Biol.* **10**:558-563.

Straight, A.F., Marshall, W.F., Sedt, J.W., Murray, A.W. (1997). Mitosis in Living Budding Yeast: Anaphase A But No Metaphase Plate. *Science* **277**:574-578.

Studier, F.W., Rosenberg, A.H., Dunn, J.J., and Dubendorff, J.W. (1990). Use of T7 RNA polymerase to direct expression of cloned genes. *Meth. Enzymol.* **185**:60–89.

Szyjka, S.J., Aparicio, J.G., Viggiani, C.J., Knott, S., Xu, W., Tavaré, S., and Aparicio, O.M. (2008). Rad53 regulates replication fork restart after DNA damage in *Saccharomyces cerevisiae*. *Genes Dev.* **22**:1906-1920.

Takeda, T., Ogino, K., Matsui, E., Cho, M.K., Kumagai, H., Miyake, T., Arai, K., and Masai, H. (1999). A fission yeast gene, him1(+)/dfp1(+), encoding a regulatory subunit for Hsk1 kinase, plays essential roles in S-phase initiation as well as in S-phase checkpoint control and recovery from DNA damage. *Mol. Cell. Biol.* **19**:5535-5547.

Takeda, D.Y. and Dutta, A. (2005). DNA replication and progression through S-phase. *Oncogene* **24**:2827-2843.

Tam, A.T., Pike, B.L., and Hierhorst, J. (2008). Location-specific functions of the two forkhead-associated domains in Rad53 checkpoint kinase signaling. *Biochem.* **47**:3912-3916.

Tanaka, S., Umemori, T., Hirai, K., Muramatsu, S., Kamimura, Y. and Araki, H. (2007) CDK-dependent phosphorylation of Sld2 and Sld3 initiates DNA replication in budding yeast. *Nature* **445**:328-332.

Teichmann, S.A., Murzin, A.G. and Chothia, C.(2001). Determination of protein function, evolution and interactions by structural genomics. *Curr. Opin. Struct. Biol.* **11**:354-363.

Tercero, J.A., Longhese, M.P., and Diffley, J.F. (2003). A central role for DNA replication forks in checkpoint activation and response. *Mol. Cell* **11**:1323-1336

Theis, J.F. and Newlon, C.S. (1997). The ARS309 chromosomal replicator of *Saccharomyces cerevisiae* depends on an exceptional ARS consensus sequence. *Proc. Natl. Acad. Sci .U S A.* **94**:10786-10791

Travesa, A., Duch, A. and Quintana, D.G. (2008). Distinct phosphatases mediate the deactivation of the DNA damage checkpoint kinase Rad53. *J.Biol.Chem.* **283**:17123-17130

- Trotter, P.J. (2001). The genetics of fatty acid metabolism in *Saccharomyces cerevisiae*. *Annu. Rev. Nutr.* **21**:97-119.
- Tsuji, T., Lau, E., Chiang, G.G., and Jiang, W. (2008). The role of Dbf4/Drf1-dependent kinase Cdc7 in DNA-damage checkpoint control. *Mol. Cell* **32**:862-869.
- Tully, G.H., Nishihama, R., Pringle, J.R., and Morgan, D.O. (2009) The Anaphase-promoting Complex Promotes Actomyosin-Ring Disassembly during Cytokinesis in Yeast. *Mol. Cell. Bio.* **20**:1201-1212.
- Varrin, A.E., Prasad, A.A., Scholz, R.P., Ramer, M.D. and Duncker, B.P. (2005). A mutation in Dbf4 motif M impairs interactions with DNA replication factors and confers increased resistance to genotoxic agents. *Mol. Cell. Biol.* **25**:7494-7504.
- Walker, G.M. (1998). *Yeast physiology and biotechnology*. Wiley Press, New York, NY.
- Wang, Y., Vujcic, M. and Kowalski, D. (2001). DNA replication forks pause at silent origins near the HML locus in budding yeast. *Mol. Cell. Biol.* **21**:4938-4948.
- Webster, J. and Weber, R. (2007). *Introduction to fungi*, Cambridge University Press, Cambridge, U. K.
- Weinreich, M. and Stillman, B. (1999). Cdc-Dbf4 kinase binds to chromatin during S-phase and is regulated by both the APC and the RAD53 checkpoint pathway. *EMBO J.* **18**:5334-5346.
- Winecek, J.M. (1999). New strategies for protein crystal growth. *Annu. Rev. Biomed. Eng.* **1**:505-534.
- Wolfe, B.A. and Gould, K.L. (2005). Split decisions: coordinating cytokinesis in yeast *Trends Cell Biol.* **15**:1510-1518.
- Yamashita, N., Kim, J.M., Koiwai, O., Arai, K., and Masai, H. (2005). Functional analyses of mouse ASK, an activation subunit for Cdc7 kinase, using conditional ASK knockout ES cells. *Genes Cells* **10**:551-563.
- Yanow, S.K., Gold, D.A., Yoo, H.Y. and Dunphy, W.G. (2003). Xenopus Drf1, a regulator of Cdc7, displays checkpoint-dependent accumulation on chromatin during an S-phase arrest. *J. Biol. Chem.* **278**:41083-41092.
- Yeong, F.M. (2005) . Severing all ties between mother and daughter: cell separation in budding yeast *Mol. Microbiol.* **55**:1325-1331.

Yongkiettrakul, S., Byeon, I.L., and Tsai, M. (2004). The ligand specificity of yeast Rad53 FHA domains at the +3 position is determined by nonconserved residues. *Biochemistry* **43**:3862-3869.

Zegerman, P. and Diffley, J.F. (2007). Phosphorylation of Sld2 and Sld3 by cyclin-dependent kinases promotes DNA replication in budding yeast. *Nature* **445**:281-285.